D I S S E R T A T I O N

Impact of Exoskeletons on Life Cycle Primary Energy Consumption and CO$_2$e Emissions of Tall Buildings

ausgeführt zum Zwecke der Erlangung des akademischen Grades eines
Doktors der Technischen Wissenschaften Architektur unter der Leitung von

Assoc. Prof. Dipl.-Ing. Dr.techn. Alireza Fadai
E259-02 Forschungsbereich Tragwerksplanung und Ingenieurholzbau
Institut für Architekturwissenschaften
Fakultät für Architektur und Raumplanung, TU Wien

Begutachtung durch

Univ.-Prof. i.R. Dipl.-Ing. Dr.techn. Andreas Kolbitsch
E210-02 Forschungsbereich Hochbau und Gebäudeerhaltung
Institut für Hoch- und Industriebau
Fakultät für Bau- und Umweltingenieurwesen, TU Wien

Univ.-Prof. i.R. Dipl.-Ing. Dr.techn. Ardeshir Mahdavi
Institut für Bauphysik, Gebäudetechnik und Hochbau
Fakultät für Bauingenieurwissenschaften, TU Graz

eingereicht an der Technischen Universität Wien
Fakultät für Architektur und Raumplanung

von

Aryan Shahabian MSc MSc

Wien, am Datum   Unterschrift

Abstract

Tall buildings (synonymous with high-rise buildings) generally refer to buildings with an architectural height of $\geq$ 50 m. The taller the buildings are, the longer their average lifespan; e.g., the lifespan of tall buildings with a height of over 150 m is arguably infinite, as only very few of them have ever been demolished. The primary structural system in tall buildings is constructed earlier and demolished later than other building systems, e.g., Heating, Ventilation, and Air Conditioning (HVAC) and electric lighting, which require periodic renewal during the operational phase. Primary structural elements typically remain untouched, requiring minimal maintenance throughout the entire lifespan of tall buildings. Therefore, the design of the high-rise structural system is a pivotal decision with long-lasting consequences.

The entire skeleton of most tall buildings is positioned within the interior space, defined as the endoskeleton. However, in some tall buildings, parts of their skeleton are placed outside the thermal envelope, forming an exoskeleton. It has been claimed that exoskeletons, by casting shadows on the thermal envelope, offer an environmentally friendly solution for tall buildings in warmer climates, by reducing the need for cooling. However, despite their use in renowned tall buildings, the environmental impact of exoskeletons compared to endoskeletons, particularly in terms of life cycle energy consumption and CO_2e emissions, remained understudied and lacked sufficient scientific evidence prior to this research. Despite the potential advantage of exoskeletons reducing cooling needs by shading the facade, they may impact the electric lighting system by blocking or reflecting sunlight. They can also create thermal bridges, as they connect to interior structural elements, potentially affecting the conditioned space. Choosing exoskeletons over endoskeletons may alter other parts of the structural system, as structural components interact, and changes to one part may affect the rest. Moreover, contextual variations over time, like neighboring tall buildings affecting sunlight, technological advancements in building systems and energy generation, and climate change impacting HVAC needs, can influence tall buildings' environmental performance during operation. Architectural engineers cannot control contextual factors during the early design stages of tall buildings. However, it is essential to consider how these uncontrollable factors interact with design and material parameters. While controllable factors shape design choices, uncontrollable factors define the contextual conditions.

Thus, in addition to the main variable of interest (exoskeletons vs endoskeleton), various factors at different levels were considered for assessment. These factors were studied in the short-term (pre-operational phase) and over the medium- and long-term (up to 30 and 60 years of operation, respectively). In the short term, three additional factors related to structural materials and thermal bridge control were analyzed. Over the medium- and long-term, scenarios addressing contextual changes over time were explored. Each factor's levels represented potential scenarios. Applying scenario planning and a full factorial Design of Experiments (DoE), this study assessed over

1400 scenarios through computer simulation and analysis. The computer experiments involved cylindrical 40-story office building digital prototypes situated in a hot desert climate (Dubai, UAE), featuring a reinforced concrete diagrid frame and a service core as the primary structural system. Through statistical analysis with generalized linear models (GLMs), the researcher addressed the first research question: *What is the impact of exoskeletons (vs endoskeletons) on the life cycle primary energy consumption and CO_2e emissions of tall buildings? I.e., how effective and desirable is it compared to and in interaction with some other controllable and uncontrollable factors from the perspective of architectural engineers in the early stage of design?*

The answer to the first research question measured in detail the main effects and the interactions of the aforementioned factors during the life cycle phases. However, as certain uncontrollable factors proved remarkably more effective than the controllable ones (including the main variable of interest), it gave rise to the following concluding research question: *What would be the optimal decision or decisions about the controllable factors, made objectively (based on quantitative data), by architectural engineers considering such uncontrollable circumstances?*

The researcher applied three objective decision analysis methods: maximax, maximin, and minimax regret, which correspond to optimistic, conservative/robust, and cautious perspectives, respectively, to address the second research question. In conclusion, respecting the second question, the study found that in the short term, endoskeletons outperformed exoskeletons in conserving primary energy and reducing carbon footprints for tall buildings. In medium- and long-term periods, endoskeletons remained the optimal choice for optimistic criteria, while exoskeletons proved optimal when prioritizing conservative/robust or cautious perspectives in the hot desert climate. The significant original contribution of this research to the interdisciplinary field of architectural engineering is that it represents the first comprehensive scientific study of its own kind, dedicated to illuminating the impact of utilizing exoskeletons vs endoskeletons on the life-cycle primary energy consumption and CO_2e emissions of tall buildings; by employing a replicable quantitative methodology, without oversimplifying critical interacting factors (including multiple controllable factors influencing design choices and uncontrollable factors associated with urban, technological, and climatic contexts that evolve over time).

Zusammenfassung (Abstract in German)

Hochhäuser beziehen sich im Allgemeinen auf Gebäude mit einer architektonischen Höhe von ≥ 50 m. Je höher die Gebäude sind, desto länger ist ihre durchschnittliche Lebensdauer. Zum Beispiel ist die Lebensdauer von Hochhäusern mit einer Höhe von mehr als 150 m möglicherweise unendlich, da nur sehr wenige von ihnen jemals abgerissen wurden. Das primäre Tragwerk in Hochhäusern wird früher errichtet und später abgerissen als andere Gebäudesysteme, wie Heizung, Lüftung und Klimatisierung (HLK) und elektrische Beleuchtung, die während der Betriebsphase regelmäßig erneuert werden müssen. Die primären Strukturelemente bleiben in der Regel unberührt und erfordern während der gesamten Lebensdauer von Hochhäusern nur minimalen Wartungsaufwand. Daher ist die Gestaltung des Hochhaus-Tragwerks eine entscheidende Entscheidung mit lang anhaltenden Konsequenzen.

Das gesamte Gerüst der meisten Hochhäuser ist im Innenraum positioniert und wird als Endoskelett definiert. In einigen Hochhäusern sind jedoch Teile ihres Skeletts außerhalb der thermischen Hülle positioniert und bilden ein Exoskelett. Es wurde behauptet, dass Exoskelette, indem sie Schatten auf die thermische Hülle werfen, eine umweltfreundliche Lösung für Hochhäuser in wärmeren Klimazonen bieten, indem sie den Kühlbedarf reduzieren. Trotz ihrer Verwendung in renommierten Hochhäusern blieb die Umweltauswirkung von Exoskeletten im Vergleich zu Endoskeletten, insbesondere in Bezug auf den Energieverbrauch im Lebenszyklus und die CO_2-Äquivalent-Emissionen, vor dieser Forschung untersunders und mangelte an ausreichend wissenschaftlichen Beweisen. Trotz des potenziellen Vorteils von Exoskeletten, den Kühlbedarf durch Beschattung der Fassade zu reduzieren, können sie das elektrische Beleuchtungssystem beeinflussen, indem sie das Sonnenlicht blockieren oder reflektieren. Sie können auch thermische Brücken erzeugen, da sie mit inneren Tragelementen verbunden sind und den konditionierten Raum beeinflussen können. Die Wahl von Exoskeletten gegenüber Endoskeletten kann auch andere Teile des Tragwerkssystems verändern, da Bauteile miteinander interagieren und Änderungen an einem Teil die anderen Teile beeinflussen können. Darüber hinaus können zeitliche Veränderungen im Kontext, wie benachbarte Hochhäuser, die das Sonnenlicht beeinflussen, technologische Fortschritte in Gebäudesystemen und der Stromerzeugung sowie der Klimawandel, der den Bedarf an HLK-Systemen beeinflusst, die Umweltleistung von Hochhäusern während des Betriebs beeinflussen. Architektonische Ingenieure können während der frühen Entwurfsphasen von Hochhäusern keine Einfluss auf Kontextfaktoren nehmen. Es ist jedoch wichtig zu berücksichtigen, wie diese nicht steuerbaren Faktoren mit Design- und Materialparametern interagieren. Während steuerbare Faktoren Designentscheidungen beeinflussen, definieren nicht steuerbare Faktoren die Kontextbedingungen.

Daher wurden neben der Hauptvariable (Exoskelette vs. Endoskelette) verschiedene Faktoren auf verschiedenen Ebenen zur Bewertung herangezogen. Diese Faktoren wurden kurzfristig (vor der Betriebsphase) und mittel- bis langfristig (bis zu

30 und 60 Jahren Betriebszeit) untersucht. Kurzfristig wurden drei zusätzliche Faktoren im Zusammenhang mit Baustoffen und thermischer Brückenkontrolle analysiert. Mittel- und langfristig wurden Szenarien zur Berücksichtigung von Veränderungen im Kontext im Laufe der Zeit untersucht. Die Level jedes Faktors repräsentierten potenzielle Szenarien. Durch Anwendung von Szenarioplanung und einem vollständigen faktoriellen Design von Experimenten (DoE) wurden in dieser Studie über 1400 Szenarien durch Computersimulation und Analyse bewertet. Die Computerexperimente umfassten zylindrische 40-stöckige Bürogebäude-Digitalprototypen in einem heißen Wüstenklima (Dubai, VAE) mit einem verstärkten Beton-Diagrid-Rahmen und einem Servicekern als primäres Tragwerksystem. Durch statistische Analysen mit verallgemeinerten linearen Modellen (GLMs) beantwortete der Forscher die erste Forschungsfrage: *Welchen Einfluss haben Exoskelette (gegenüber Endoskeletten) auf den Primärenergieverbrauch und die CO_2e-Emissionen im Lebenszyklus von Hochhäusern? Das heißt, wie effektiv und wünschenswert ist es im Vergleich zu und in Wechselwirkung mit einigen anderen steuerbaren und nicht steuerbaren Faktoren aus der Sicht von Architekturingenieuren zu Beginn des Entwurfs?*

Die Antwort auf die erste Forschungsfrage maß im Detail die Haupteffekte und die Wechselwirkungen der oben genannten Faktoren während der Lebenszyklusphasen. Da jedoch einige nicht steuerbare Faktoren sich als deutlich wirksamer erwiesen als die steuerbaren (einschließlich der Hauptvariable), gab es die folgende abschließende Forschungsfrage auf: *Welche wäre die optimale Entscheidung oder die Entscheidungen über die steuerbaren Faktoren, die objektiv getroffen werden (basierend auf quantitativen Daten), von Architekturingenieuren unter Berücksichtigung solcher nicht steuerbarer Umstände?*

Der Forscher wandte drei objektive Entscheidungsanalysemethoden an: Maximax, Maximin und Minimax-Regret, die optimistischen, konservativen/robusten und vorsichtigen Perspektiven entsprechen, um die zweite Forschungsfrage zu beantworten. Abschließend, in Bezug auf die zweite Frage, stellte die Studie fest, dass Endoskelette in kurzer Zeit im Hinblick auf die Einsparung von Primärenergie und die Reduzierung des CO_2-Fußabdrucks von Hochhäusern Exoskelette übertrafen. In mittel- und langfristigen Zeiträumen blieben Endoskelette die optimale Wahl für optimistische Kriterien, während Exoskelette sich als optimal erwiesen, wenn konservative/robuste oder vorsichtige Perspektiven in einem heißen Wüstenklima priorisiert wurden. Der signifikante originelle Beitrag dieser Forschung zum interdisziplinären Bereich des architektonischen Ingenieurwesens besteht darin, dass es sich um die erste umfassende wissenschaftliche Studie ihrer Art handelt, die sich der Aufklärung des Einflusses der Verwendung von Exoskeletten gegenüber Endoskeletten auf den Primärenergieverbrauch im Lebenszyklus und die CO_2e-Emissionen von Hochhäusern widmet; durch die Anwendung einer replizierbaren quantitativen Methodik, ohne wichtige interagierende Faktoren zu vereinfachen (einschließlich mehrerer steuerbarer Faktoren, die Designentscheidungen beeinflussen, und nicht steuerbarer Faktoren, die mit städtischen, technologischen und klimatischen Kontexten verbunden sind, die sich im Laufe der Zeit verändern).

Dedication

I dedicate this dissertation to my parents.

Acknowledgments

First and foremost, I would like to express my sincere gratitude to my supervisor, Prof. Alireza Fadai. He compassionately and diligently supported my doctoral dissertation with his exemplary motivation, patience, and deep knowledge. Without his precious support, it would not be possible to finalize this research.

Besides my advisor, I would like to thank some professors, researchers, and other academic staff members of the Faculty of Architecture and Planning, and the Faculty of Civil Engineering at TU Wien, as well as the Institute of Architecture at the University of Applied Arts Vienna (where I started my doctoral studies) for their encouragement, insightful comments and feedback, but also for their questions and criticisms during meetings and reviews, colloquiums and symposia that helped me to enrich my research from various perspectives (names in alphabetical order): Prof. Peter Bauer, Prof. Klaus Bollinger, Prof. Georg Franck, Prof. Rudolf Giffinger, Prof. Andreas Kolbitsch, Prof. Iva Kovacic, Dr. Wolfgang E. Lorenz, Prof. Ardeshir Mahdavi, Dr. Joachim Nathanael Nackler, Prof. Wolf D. Prix, Dr. Clemens Preisinger, Prof. Karin Raith, Dr. Marijana Sreckovic, Prof. Georg Suter, Prof. Wolfgang Winter, Dr. Gabriel Wurzer, and †Prof. Reiner Zettl.

Likewise, I would like to express my sincere thanks to many professors, scholars, and experts from universities, research centers, organizations, companies, etc. around the world (namely Australia, Austria, Canada, Cyprus, Germany, Iran, Italy, the Netherlands, the UAE, and the USA) who have contributed in one way or another to my research by providing comments, answering my questions, sharing their knowledge, providing data and authorizing the use of their creative properties (images, photos, etc.) in my dissertation. Some of the experts who dedicated part of their time to answering to my various inter-/multi-disciplinary inquiries did not even know me in person. The following list cannot possibly cover all the names of the people that I wish to include, but I hope it will suffice to mention some of the most helpful ones. Their areas of expertise include architectural engineering and related disciplines (i.e., aero-/acoustics; architecture; building information, energy, and performance modeling and simulation; building physics and building services engineering; computer programming and data science; daylighting, electrical and power engineering; engineering mathematics and statistics; life-cycle assessment, and technological innovation; mechanical engineering; research methods; structural and civil engineering; urban planning, strategies, and design, etc.). Here is the list: Prof. Bassam Abu-Hijleh, Prof. Mir M. Ali, Prof. Yashar Ahmadian, Prof. Hassan Azad, Dr. Araz Azarnejad, Malin Berden, Prof. Terri Meyer Boake, Benjamin Brannon, Prof. Ben Bolker, Prof. David Eugene Booth, Dr. Matthew Dahlhausen, Prof. Juliana Felkner, David Goldwasser, Dr. Idin Karuei, Chris Mackey, Prof. Ali Mehran, Dr. Zahra Moussavi, Dr. Neumann Lukas, Prof. Kyoung Sun Moon, Prof. Farshad Nasrollahi, Prof. Michael Oberguggenberger, Prof. Philip Oldfield, Dr. Laya Parviz Sedghy, Thomas Peruzzi, Bernard Plattner, Prof. Jesse Reiser, Prof. Amir

Table of Contents

List of Abbreviations

- aA: Position of the Flow Separation
- ACI: American Concrete Institute
- AESS: Architecturally Exposed Structural Steel
- AIC: Akaike Information Criterion
- $amin$: Position of the Minimum Pressure
- ANOVA: Analysis of Variance
- ASCE: American Society of Civil Engineers
- ASHRAE: American Society of Heating, Refrigerating and Air-Conditioning Engineers
- AVr: (Building-Envelope-) Area to (Building-) Volume Ratio (m^2/m^3)
- BIC: Bayesian Information Criterion
- BIM: Building Information Modeling
- BS: British Standards
- C: Base Shear Coefficient
- CAD: Computer-Aided Design
- CCWorldWeatherGen: Climate Change World Weather file Generator
- Cd: Dynamic Amplification Factor
- CEM I: Pure (100%) Ordinary Portland Cement
- $Ce(z)$: Height-Dependent Surface Friction Coefficients
- CFD: Computational Fluid Dynamics

- Cfr: Friction Coefficient
- COP: Coefficient of Performance
- $Cp0$: Pressure Coefficient without End-Effect
- $Cp0A$: Base Pressure Coefficient
- $Cp0min$: Minimum Pressure Coefficient
- Cpe: External Pressure Coefficient
- CPU: Central Processing Unit
- CR: Cement Replacement
- Cs: Load Correlation Coefficient
- CT: Topography Coefficient
- Ct: Empirical Factor for the Calculation of Predominant Period in the Earthquake Direction
- CTBUH: Council on Tall Buildings and Urban Habitat
- d: Height of the Location from the Sea Level
- DARPA: (USA) Defense Advanced Research Projects Agency
- DEWA: Dubai Electricity and Water Authority
- DGI: Discomfort Glare Index
- DGNB : German Sustainable Building Council/Deutsche Gesellschaft für Nachhaltiges Bauen
- DoE: Design of Experiments
- DOE: (US) Department of Energy

- DOAS: Dedicated Outdoor Air System
- DSF: Double Skin Facade
- DXF: Drawing Exchange Format
- ECB: European Central Bank
- EHL: Efficient Height Limit
- EN: European Norm (in German: Europäische Norm)
- EPD: Environmental Product Declaration
- EPW: EnergyPlus Weather (-file)
- ETABS: Extended 3D (Three-Dimensional) Analysis of Building Systems
- EUI: Energy Use Intensity
- F: Total Wind Loads
- FA: Fly Ash
- FAR: Floor Area Ratio
- FCU: Fan-Coil Units
- F_{ex}: Forces on External Surfaces
- F_{fr}: Friction Forces
- F_{in}: Forces on Internal Surfaces
- g: Acceleration of Gravity
- GFA: Gross Floor Area
- GGBFS: Ground-Granulated Blast-Furnace Slag
- GH: Grasshopper
- GHG: Greenhouse Gas
- GLM: Generalized Linear Model
- GWP: Global Warming Potential
- h: Height of the Structure
- HadCM3: Hadley Centre Coupled Model, Version 3
- HB: Honeybee
- HDD: Hard Disk Drive

- HN: Total Height of Structure
- HVAC: Heating, Ventilation, and Air Conditioning
- I: Building Importance Factor
- IBC®: International Building Code®
- ICC: International Code Council
- ICE: Inventory of Carbon and Energy
- IECC: International Energy Conservation Code
- IN: Inside; i.e., skeleton kept inside the building thermal envelope (endoskeleton)
- IPCC: Intergovernmental Panel on Climate Change
- ISO: International Organization for Standardization
- $IW(z)$: Turbulence Intensity
- l: Slenderness
- kr: Terrain Factor
- LB: Ladybug
- LBNL: Lawrence Berkeley National Laboratory
- LCA: Life Cycle Assessment
- LCI: Life Cycle Inventory
- LCIA: Life Cycle Impact Assessment
- LED: Light-Emitting Diode
- LEED: Leadership in Energy and Environmental Design
- LOD: Level of Development
- LOI: Level of Information
- LP: Lighting Power
- LPW: Lumens Per Watt (unit of efficacy of light sources)
- LSP: Lighting Set Point
- MID: Middle; i.e., skeleton partly inside (endoskeleton) and partly penetrating outside

- the building thermal envelope (exoskeleton)
- MIGD: Million Imperial Gallons per Day
- MSF: Multi-Stage Flesh
- NA: Not Applicable/Available
- NFA: Net Floor Area
- NRA: Net Rentable Area
- NREL: (USA) National Renewable Energy Laboratory
- NRMCA: (USA) National Ready Mixed Concrete Association
- *NS*: Sufficient Number of Vibration Modes
- NYC: New York City
- ÖNORM: Austrian Standard (in German: Österreichische Norm)
- OFAT: One-Factor-At-a-Time
- OS: Operating System
- OUT: Outside; i.e., skeleton penetrating outside the building thermal envelope (exoskeleton)
- ÖGNI : Austrian Sustainable Building Council/Österreichische Gesellschaft für Nachhaltige Immobilienwirtschaft
- PARL: Parallel
- PDWPRC: Percentage of Desalinated Water in Production of Reinforced Concrete
- PEF: Primary Energy Factor
- *ph*: Solidly Ratio
- PIF: Public Investment Fund
- PSEs: Primary Structural Elements
- *psl*: End-Effect Factor
- PTC: Placement of (outer) Tube with Respect to Curtain Wall

- PTSAU: Percentage of Transported Sand from Australia
- PV: photovoltaic
- q: Behavior Factor
- *qp(ze)*: Peak Pressure at External Height *ze*
- *qR_T*: Seismic Load Reduction Factor
- RAM: Random-Access Memory
- RC: Reinforced Concrete
- RO: Reverse Osmosis
- *ro*: Density of the Air
- *S1D*: 1.0 Second Elastic Spectral Acceleration
- *SAE_T*: Elastic Spectral Acceleration
- *SAR_T*: Design Spectral Acceleration
- *SC*: Soil Class
- SCM: Supplementary Cementitious Material
- SEI/ASCE: Structural Engineering Institute/ American Society of Civil Engineers
- SOM: Skidmore, Owings, and Merrill
- *SSD*: Short Period (0.2 Second) Elastic Spectral Acceleration *T1*: Natural Period of Predominant Mode (First Mode)
- TBC: Thermal Bridge Control
- *TL*: Transition Period of Response Spectrum to Long-Period Range
- *TN*: Terrain Number
- *To*: Response Spectrum Short Corner Period
- *TS*: Response Spectrum Long Corner period

- TY: Technology Year
- TYP: Technology Year Pattern
- UAE: United Arab Emirates
- UHI: Urban Heat Island
- UD: Urban Density
- UWG: Urban Weather Generator
- VAV: Variable Air Volume
- *Vb*: Basic Wind Velocity
- W: With (with thermal bridge control / with thermal insulation)
- WDY: Weather Data Year
- WDYP: Weather Data Year Pattern
- *WER*: Wind Envelope Radius
- WO: Without (without thermal bridge control / without thermal insulation)
- *z0*: Surface Friction Length
- *zmin*: Minimum Friction Height
- ZHA: Zaha Hadid Architects

1   Chapter No. 1

Introduction

This chapter serves as a brief introduction to the research, covering its background, problem, target audience, research questions, objectives, and scope. Additionally, an outline of the conceptual framework, experiments, and results are also provided. A more detailed introduction and explanation of the significance of each factor and response variables being studied, along with the specific background information related to each factor, are presented in the next chapter.

1.1   Background and Problem

Although global living conditions have significantly improved in many economic and social dimensions over the past couple of centuries, these enhancements have been achieved at the expense of the natural environment. Buildings, while necessary for settlement and development of societies, are proven to consume a massive share of natural resources of materials and energy, and emit large amounts of Greenhouse Gases (GHGs) to the atmosphere throughout their life cycle. Emissions recognize no borders between countries; no matter where they come from, they affect the whole Earth [1].

A crucial step in the early stage of design of tall buildings is informed decision making about the placement and design of cross sections of Primary Structural Elements (PSEs). These elements incorporate relatively larger amount of materials than those of mid-rise or low-rise buildings—mainly because the PSEs of lower levels should also carry the loads applied from above. PSEs are usually kept inside the thermal envelope and designed to withstand only the structural loads caused by gravity, wind and earthquake. However, in some buildings, a group of outer PSEs penetrate the thermal envelope and directly interact with the outdoor environment. A network or layer of PSEs when exposed to the outdoor environment is often called as exoskeleton. O-14 Tower in the hot desert climate of Dubai, UAE (completed in 2009, designed by Reiser + Umemoto, aka RUR Architecture, see Figure 1), and Shenzhen Rural Commercial Bank Headquarters in the subtropical climate of Shenzhen, China (2020, by Skidmore, Owings and Merrill, aka SOM, see Figure 4) are examples where the exoskeleton (outer tube) functions as a large exterior shading device as well. It has been claimed that applying this integrated architectural design strategy resulted in a major reduction of operational (cooling-) energy consumption despite the thermal bridging effect of structural connections between the tube and floor slabs [2][3]. Needless to say that changing the size and placement of the outer tube elements with respect to boundaries of floor slabs and curtain walls may affect the behaviour of the structure under lateral and gravity loads and thus might also affect the total amount of structural materials.

While incorporation of exoskeletons in architecture of tall buildings is not uncommon in practice (as seen in Figure 1), the review of the scientific literature on Life Cycle Assessment (LCA) of tall buildings reveals a methodological gap: the most relevant existing research works tend to focus either on (1) structural systems/elements, regardless of their interaction with other systems such as heating, ventilation and air conditioning (HVAC), electric lighting, microclimate of urban fabrics during the operational phase [4][5][6][7]; or (2) the so-called "whole building (energy) modeling", in which only the effect of the thermal mass of slabs and shear walls on the operational thermal energy consumption is usually taken into account, but exoskeletons which can provide shading are not included in the studies [8][9][10]; or (3) they take into account the shading/reflecting effect of exoskeleton frames but do not estimate the building's life cycle primary energy consumption and CO_2e emissions [11][12]; or (4) do not compare the environmental impact of exoskeletons with endoskeletons of similar type (i.e., the logical problem of confounding factors, as an apples to apples comparison is missing) [13].

Another aspect of the gap in the relevant studies is the lack of notion to develop and apply "future scenarios" in LCAs of tall building PSEs [14]. The taller the buildings are, the longer their average lifespan; e.g., the lifespan of tall buildings with +150 m height is arguably infinite as only a very few of them have ever been demolished in entire world [15][16] (see Table 1). PSEs are the first to build and the last parts of buildings to demolish. They usually remain untouched during the whole operational phase whereas other systems (e.g., HVAC, lighting) have relatively much shorter lifespans and are progressively replaced by newer technologies. It is important to take into consideration not only the evolution of those building systems (e.g., HVAC, lighting) but also the variation of uncertain context factors that are influential on the actual primary energy use and carbon footprint of buildings throughout their life cycle. These uncertain context factors are weather (climate change), energy mix in electricity production, and shading effect of emerging adjacent buildings on each other—variation of Urban Density (UD)/Floor Area Ratio (FAR)— just to name a few.

Table 1. The world's tallest demolished buildings (with architectural height of over 150 m, list updated in 2023). Source: CTBUH [15]

Rank	Name	Location	Completion-Demolished	Height (m)	Floors
1	One World Trade Center	New York City (NYC), USA	1972-2001	417	110
2	One World Trade Center	NYC, USA	1973-2001	415.1	110
3	AXA Tower	Singapore	1986-2023	234.7	52
4	JPMorgan Chase Tower	NYC, USA	1960-2020	215.5	52
5	Singer Building	NYC, USA	1908-1968	186.6	41
6	Seven World Trade Center	NYC, USA	1987-2001	173.7	47
7	CPF Building	Singapore	1976-2018	171	45
8	Fuji Xerox Tower	Singapore	1986-2023	164.9	40
9	Morrison Hotel	Chicago, USA	1925-1965	160.3	45
10	Sekaiboeki Center Building	Tokyo, Japan	1970-N/A (Under Demolition)	158	40
11	Deutsche Bank	NYC, USA	1974-2011	157.6	39
12	Qilu Hotel	Jinan, China	1997-2022	157	39
13	UIC Building	Singapore	1974-2013	152	40
14	Crowne Plaza Mutiara KL	Kuala Lumpur, Malaysia	1973-2013	150.3	36
15	Old St. Paul's Cathedral	London, England	1240-1666	150.3	N/A

The aforementioned interconnected aspects of the gap in the literature end up in an unsolved complex architectural engineering problem: the impact of using exoskeletons on the life cycle primary energy consumption and CO_2e emissions of tall buildings has remained unclear! Consequently, this ambiguity in quantitative information makes it unfeasible to make unbiased, informed and optimal decision whether to expose the skeleton elements to the outdoor environment or not (or maybe place them somewhere between indoor and outdoor space).
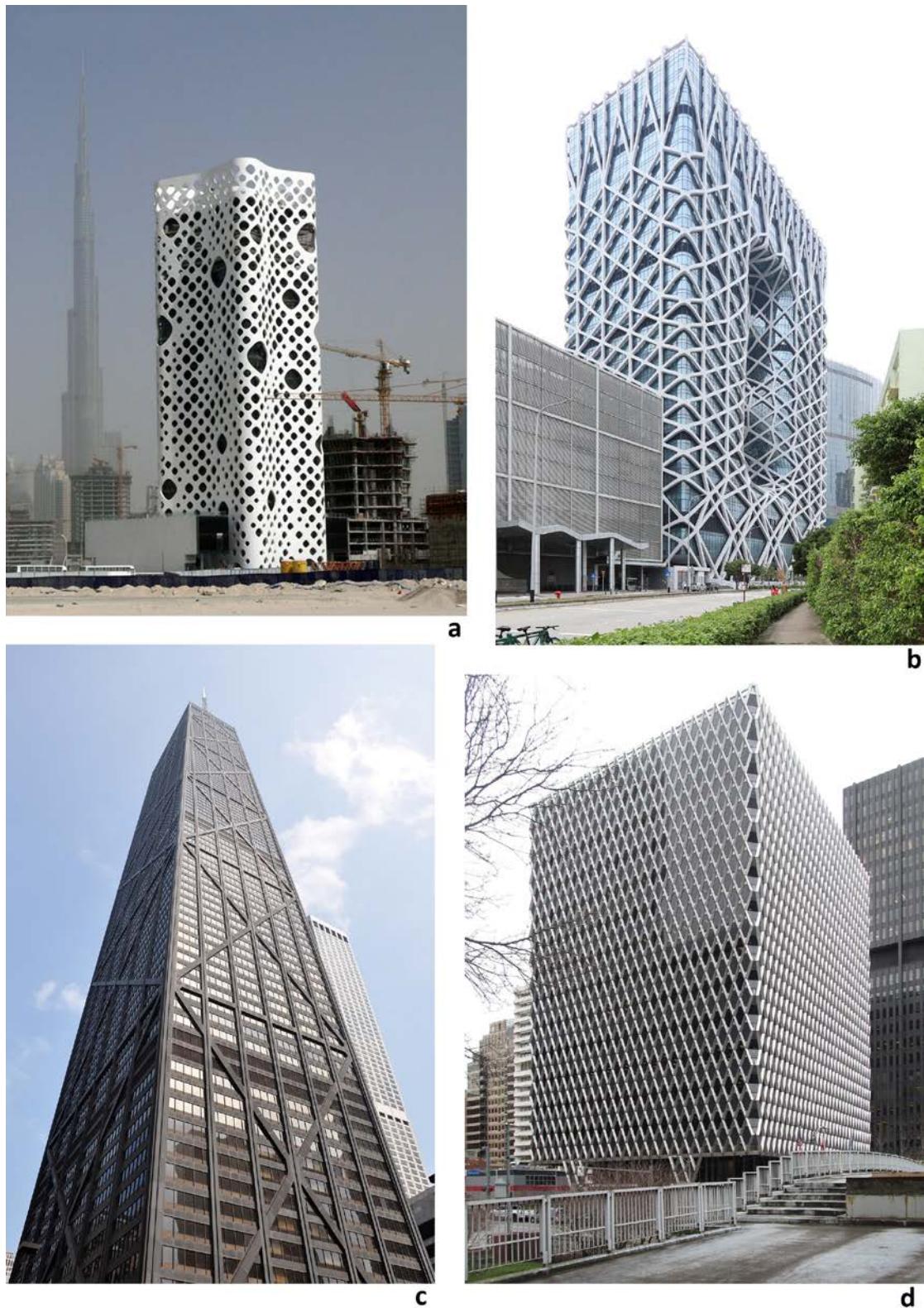
Figure 1. Examples of tall buildings with exoskeleton structures; from top left to bottom right: (a) O-14 Tower, Dubai, UAE, completed in 2009, designed by Reiser + Umemoto (RUR Architecture); (b) Morpheus Hotel, Macau, 2018, by Zaha Hadid Architects (ZHA); (c) John Hancock Center, Chicago, USA, 1969, by Fazlur Rahman Khan, Skidmore, Owings and Merrill (SOM); and (d) United Steelworkers Building (originally named the IBM Building), Pittsburgh, USA, 1964, by Curtis and Davis. Sources/Credits (©): photographs by (a) Joe Wolf via Flickr, licensed under CC BY-ND 2.0 [17]; (b) Störfix via Wikimedia, licensed under CC BY-SA 3.0 DE [18]; (c) Joe Ravi via Wikimedia, licensed under CC BY-SA 3.0 [19]; and (d) Cbaile19 via Wikimedia, licensed under CC0 1.0 [20].

1.2 Audience/Perspective

This research essentially looks at the problem from the perspective of architectural engineers (in research and practice) dealing with the early stage of the design of tall buildings. They are assumed as the main audience of the current study.

A note regarding the audience and definitions of the scientific terms presented in this dissertation (next chapter): due to the complex inter/multidisciplinary and multi-parametric nature of the topic, and the limited capacity of a doctoral dissertation, it has not been possible to introduce all interrelated parameters and methods presented and applied in the study at hand one by one at a basic/undergraduate level; therefore, a considerable level of prior knowledge, expertise and experience in sustainable (tall) building design or architectural engineering seems to be necessary to relate to the concepts presented in this research.

1.3 Research Questions

1. What is the impact of exoskeletons (vs endoskeletons) on the life cycle primary energy consumption and CO_2e emissions of tall buildings? I.e., how effective and desirable is it compared to and in interaction with some other controllable and uncontrollable factors from the perspective of architectural engineers in the early stage of design? This question will be followed by:

2. What would be the optimal decision or decisions about the controllable factors, made objectively (based on quantitative data), by architectural engineers considering such uncontrollable circumstances?

1.4 Scope, Aim and Objectives

The present investigation aims to shed light upon the impact of using exoskeletons (vs endoskeletons) on the life cycle primary energy and carbon footprint of tall buildings from the perspective of architectural engineers involved in the early stage of design. At its core, this research provides a comparative assertion LCA, evaluating the choices between endoskeleton and exoskeleton alternatives under various design and contextual scenarios (whose specifications, variables, and boundaries are briefly presented in this chapter, and introduced in detail in the second and third chapters). Alternatives or design scenarios refer to controllable factors from the perspective of architectural engineers. On the contrary, contextual scenarios refer to uncontrollable factors from that same perspective. This study evaluates only the superstructures, i.e., above-grade structural systems, which is common in similar holistic studies on tall buildings, e.g., see [4][5][11][6][13], as substructures/foundations depend on specific cases and locations (e.g., number and area of basement floors, soil type). All the simulated superstructures in this study are ideally

located in the hot desert climate of Dubai, UAE, having 40 stories and reinforced concrete (RC) diagrid structural systems. In terms of life cycle stages, this study predominantly focuses on the most crucial/decisive/impactful stages with respect to structural systems (which are the cradle-to-gate phase), and with respect to the HVAC and electric lighting systems (which is the operational phase); the scientific evidence based on the literature sources will be explained later to justify these selections (see 2.3.9 Response Variables and Scope). However, the deliberate constraint in selecting the above parameters and stages enabled the researcher to expand the scope and analyze multiple interacting factors from diverse disciplines, building systems, as well as urban, climate and technological conditions varying over time. These aspects are frequently overlooked in comparable studies within the literature.

On the other hand, due to the multitude of potential interacting factors (from architectural, structural, mechanical and electrical parameters to urban, climatic, technological and contextual ones) that could influence the environmental performance of tall building exoskeletons, addressing them all would exceed the limits of any single investigation. Therefore, this study attempts to strike a balance between avoiding overcomplexity and oversimplification (i.e., to keep it understandable while not sacrificing the natural complexity of the subject matter). Various longitudinal and cross-sectional scenarios are discussed regarding the issue of changes in building systems and context circumstances over time. This research answers to the research questions within the boundaries of an exemplary case study and it is expected that its results as well as its extensible conceptual and methodological framework will also pave the way for future researchers and practitioners in architectural engineering to reply to similar questions, and make scientifically informed decisions in other cases (i.e., other types of structural systems and materials, climates, locations, etc.).

This is an early-stage-design-related, holistic and big-picture-oriented research serving architectural engineers and building designers, but it should not be confused with a design project itself. The purpose of the study at hand is neither to design a particular building, with all details of all its building systems, on a particular lot/urban parcel (as if it were in the last stages of the design phase, i.e., the preparation of construction documents, bid specifications, applying for green certificates, etc.), nor to do a complete LCA of such a building by going through all building materials, details, and items of relevant standards (be it international, European, local, etc.).

On the contrary, this research intends to obtain a holistic view of the subject matter which is an understudied topic in relation to the early stage of the design of tall buildings via bringing an example (or a set of examples) of fictitious generic tall building prototypes with variables which are set to common, conventional, or well-known optimal values so that relatively a more significant number of audience and projects can relate to (why fictitious generic and not specific actual buildings? Simply because it is impossible to find many tall buildings being precisely the same except for the value of one variable at a time or combination of some variables, to measure, analyze, and detect the effects of all variables of interest). So in contrast to design projects that in many cases designers use creativity and try to create something unique and different to stand out from other buildings, an objective here is to generate generic fictitious building prototypes so that a larger of projects can relate to it and use it as a reference point for comparison).

'Early stage' is also a keyword here. LCA can be integrated with Building Information Modeling (BIM) and performance simulation to enrich the decision-making process, even at the early stage of design [21]. A fundamental difference between the early and the late stages of design is that in the former, due to its very nature, most of the details of the final building simply either do not exist or are subject to change, while the design team, namely the architectural engineers, have to make important decisions that greatly affect the building performance—including the decision on the type of structural system (e.g., see [22][23, Pt. 18:00]) and thus also the decision on the use of an exoskeleton. During the design process, and for various purposes, several building prototypes (either digital or physical) are often made to represent the appearance, function, or performance of particular parts, systems, aspects, or combinations thereof in projects.

In early computer prototyping, designers and engineers—based on their previous knowledge and experience and/or by referring to acceptable or conventional technical standards or parameters, coefficients, details or other standards-based prerequisites—try to simplify the building models as much as possible and focus on the specific aspects of the project on which they want to make a decision or an analysis; in other words, a "full detail" prototype can no longer be called an early phase prototype, but a final building prototype. In BIM, this concept of including a certain level of detail on building elements depending on the phase or milestone the model is intended to present is called Level of Development (LOD) for graphical content and Level of Information (LOI) for non-graphical content [24][25]; and a similar concept applies to the initial prototyping phase of any other design-related project in various industries and engineering disciplines (for more information on prototyping in general, see [26]). Figure 2 presents examples comparing prototypes in early stage of design and final products in building and automotive industries.
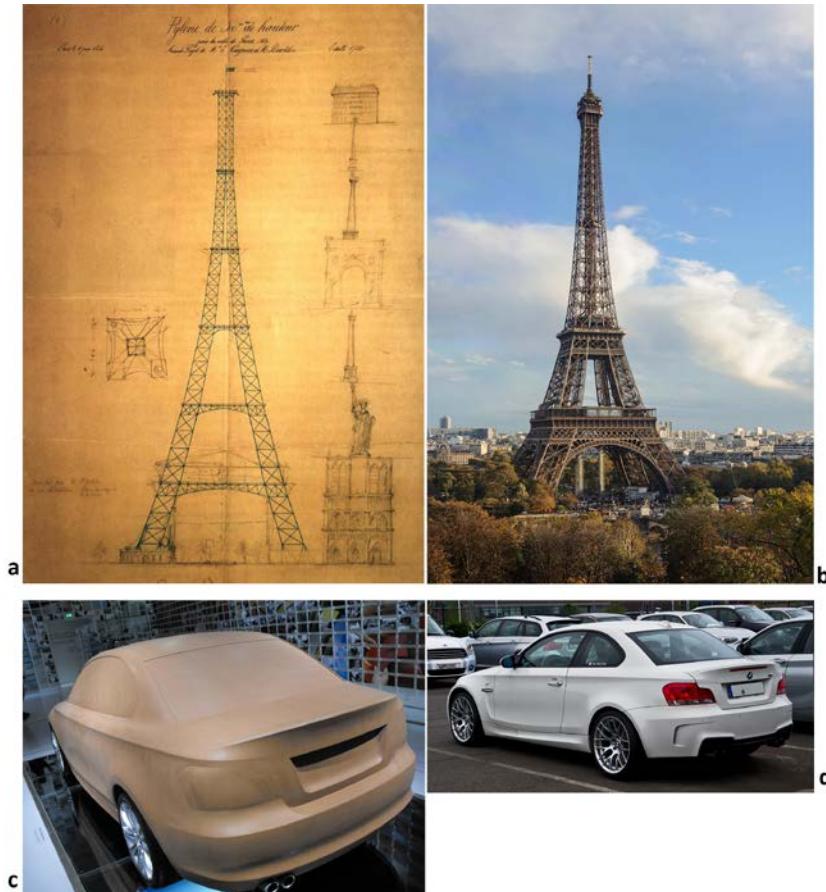
Figure 2. Examples of prototypes developed in early stage of design compared to final products in building and automotive industries; from top left to bottom right: (a) an early sketch of Eiffel Tower by Maurice Koechlin (structural engineer) in 1884; (b) Eiffel Tower, Paris, France, completed in 1889; (c) a clay (industrial plasticine) model of BMW 1 Series in 2009; and (d) a BMW 1er M Coupé (E82) produced in 2011-2012. Sources/Credits (©): photographs by (a) Public Domain via Wikimedia [27]; (b) Myrabella via Wikimedia, licensed under CC BY-SA 3.0 [28]; (c) Biso vis Wikimedia, licensed under CC BY 3.0 [29]; and (d) M 93 via Wikimedia, licensed under CC BY-SA 3.0 DE [30].

Therefore, one of the objectives of the present investigation is to intentionally avoid going into detail (i.e., high LOD/LOI) whenever possible, and to seek out and highlight key players (who may interact with the main variable of interest) and key sub-phases/stages of the life cycle; focus simply on the topic dealing with the environmental impact of a particular design decision (i.e., the use of exoskeletons), in a particular phase that is the initial phase of tall building design (where there are simply not yet many details in the design, but many major design decisions must be made), with respect to two main environmental impact metrics (i.e., primary energy consumption and CO_2e emissions) that are routinely calculated and announced in adjacent studies.

Another objective of this research (in relation to the above) is to include in the experiments and analyses, at least one factor from each of the major disciplines that are (or are expected to be) involved due to the inter/multidisciplinary nature of the architectural engineering issue; i.e., structural/civil engineering, HVAC/mechanical engineering, electrical/energy engineering, and urban planning/design/strategies. It is hoped that by meeting this objective, not only will the subject matter be better understood from different points of view, but also that the thesis will become an exemplary scientific module that highlights and reinforces the interconnections

8

between various disciplines through the analysis and resolution of an architectural engineering phenomenon/problem.

1.5 Outline of variables (Conceptual Framework)

The main independent/explanatory variable/factor of interest is the placement of skeleton elements with respect to the thermal envelope (thermal envelope in tall buildings typically refers to curtain walls or window walls separating the interior and exterior space). The researcher set up a skeleton adjacent to the thermal envelope in interior space of a high-rise prototype building as a baseline level or control group for comparison with exoskeleton setups in which parts of the skeleton are positioned in the exterior space.

The dependent/response variables are primary energy consumption and CO_2e GHG emissions.

Mediating/intervening variables which connect the independent variable to the dependent ones are: operational primary energy and carbon footprint of fuel and/or electricity required for HVAC and electric lighting systems; and embodied primary energy and carbon of structural materials and insulation materials (for thermal bridge reduction).

Other independent/explanatory variables whose interactions with the main independent variable is subject to test in the study at hand are listed below. If the statistical analysis confirms significant interactions, these would be called moderator variables:

Density of urban neighbourhood (i.e. FAR), structural material—in case of RC: different types and percentage of Cement Replacement (CR), i.e., use of fly ash, GGBFS; use of desalinated water, etc.—, thermal bridging control; time-dependent variables, e.g.: climate change, development of environment-friendly technologies such as improvement of insulation materials, energy mix, Coefficient of Performance (COP) of HVAC system, efficacy of electric lighting sources.

The researcher did the delimitation of factors and their levels by reasoning and in accordance with sources of literature and valid databases. Review of these sources show many other explanatory variables may also have the potential to moderate the impact of the main independent variable on the response ones. The researcher set them as control variables with constant values due to the limited capacity and scope of one dissertation. However, the conceptual and methodological frameworks remain extensible to facilitate future studies. In depth explanation why certain selection of variables or levels was made are reflected in the next chapter one by one. Below is a **brief list of the control variables and their constant values in this research**. Constant values of some variables are written between parentheses:

Location (Dubai; it the has hottest climate among the 5 cities with greatest number of buildings taller than 150m [31]**), Building Program (office), Overall Architecture (Overall Form: vertical extrusion, cylindrical; 40-story, Typical floor-to-floor height: 4.08 m), Type of structural system and material (Diagrid, RC, C40/50 MPa Concrete), Type of HVAC System–Fan Coil Units (FCU) +**

Dedicated Outdoor Air System (DOAS)–, Lighting System (high performance LED), Type of Skin (Single-Skin, Glazing Ratio 2/3), thermal envelope's U-value and Visible Light Transmission, etc. These are introduced in more detail in the second and third chapters.

Figure 3 illustrates a simplified version of the conceptual framework of this study. More comprehensive versions can be found in the next chapter.
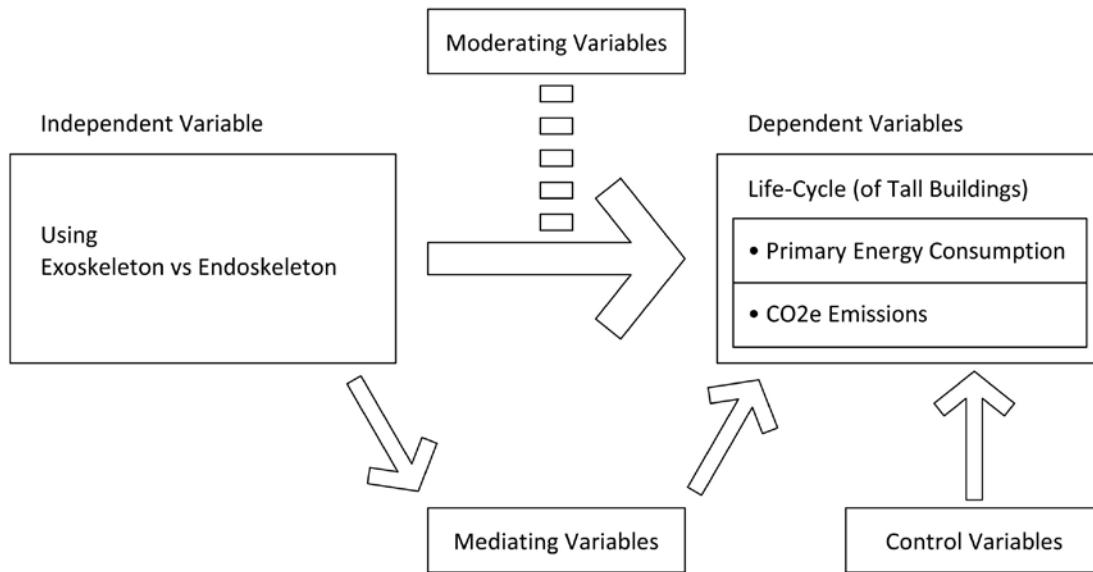
Figure 3. A simplified version of the Conceptual Framework of this study. Source: the researcher

1.6   Outline of Experiments and Results

Chapter No. 3 presents the experiments on a 40-story office building prototype with diagrid RC structure [32] and FCU+DOAS HVAC system in the hot desert climate of Dubai as the baseline scenario for computer-simulation-based case-studies. By applying the principles of factorial Design of Experiments (DoE) [33][34] the researcher simulated all possible combinations of different levels of independent/explanatory variables (factors) of interest, and calculated and collected the dependent variables (responses). This procedure was done on three time steps; years 2020, 2050 and 2080. The researcher assumed the operational phase of the prototype building to begin in 2020. Therefore the response data of this year represents the embodied primary energy and carbon footprint of structural and insulation materials. Factors in this step are either controllable or uncontrollable by the architectural engineers involved in the design process.

The data from 2020 to 2080 represents 60 years of operational phase with respect to the future scenarios. None of the factors in this phase are controllable by the architectural engineers. The researcher packaged and assumed as one scenario some variables whose individual effects were not in the focus area of the present investigation but their collective effect could be influential on the association of the variables of interest (this is a common practice in scenario planning).

Die approbierte gedruckte Originalversion dieser Dissertation ist an der TU Wien Bibliothek verfügbar.

The approved original version of this doctoral thesis is available in print at TU Wien Bibliothek.

TU Bibliothek
Your knowledge hub
WIEN

The researcher fit Generalized Linear Models (GLMs) for each phase of life cycle separately as well as cumulatively to see the magnitude of influence and desirability (negative or positive) of each factor and two-way interactions between factors. The final results of this stage, replies to the first research question. It can also reply to the second question where there are no significant large interactions between the controllable and uncontrollable factors contradicting the decision.

The next part is to apply objective decision analyses (i.e., optimistic, conservative, and cautious). Maximax criterion targets optimistic decisions, maximin targets conservative ones, and minimax regret method targets the cautions ones. With this method, different alternatives (combinations of controllable factors) are compared to rank and find the ones which minimize the maximum loss of opportunity in different states of the world/nature (combinations of uncontrollable factors) [35]. The results of this part answer to the second research question.

2   Chapter No. 2

State-of-the-Art Review, and Factorial Design of

Experiments

This chapter consists of three sections, which are briefly introduced below.

The **first section** (2.1 Definitions) defines several important terms related to this research in alphabetical order. Some key words in this section that are worth highlighting here are the definition of exoskeletons (vs endoskeletons) and the general definition of tall buildings (aka high-rise buildings). However, there are other terms used in this study that will be defined in the body of other sections of this chapter, as well as in subsequent chapters.

The **second section** (2.2 Review of Tall Buildings; Structural Systems, Exoskeletons, and LCA) presents a broad background knowledge and reviews some of the most important literature sources related to the topic of this dissertation. The structure of this section is like a funnel that starts with a relatively broader scope presenting general knowledge about tall buildings and their characteristics and functions in today's world and then gradually, after a few steps in its subsections, focuses its attention on the most important state-of-the-art literature sources that are relatively more relevant to this research, as they partially address the life cycle environmental impacts of tall building exoskeletons. However, there remains a significant gap in the literature due to limitations of existing literature sources that will be discussed and highlighted in this section, and this thesis aims to fill the gap by addressing those limitations to the extent possible. The subsections of this section are briefly presented below:

The subsection 2.2.1 presents the general advantages and disadvantages of tall buildings in the current global and urban planning context. It is a summary of the findings of comprehensive studies reflected in two reference papers [36] (by K. Al-Kodmany) and [37] (by M. M. Ali and K. Al-Kodmany), updated with further information and additional references. Next, subsection 2.2.2 presents a brief history of tall buildings focusing on the evolution of their form, envelope, and design with respect to energy and environmental aspects, mainly reflecting a summary of two papers by P. Oldfield et al. [38][39] and a study by K. Al-Kodmany [40]. In addition, the researcher updated the content with additional examples and specifications for contemporary trends. Then, the typology of conventional structural systems for tall buildings will be introduced in two main categories of interior and exterior structures, each with multiple categories and sub-categories. This classification by M. M. Ali and K S Moon [41][42]

is widely accepted and cited by researchers on tall building studies. Subsequently, in subsection 2.2.4, multiple studies by K S Moon et al. focusing on geometric optimization of the layouts of various types of structural systems in the preliminary design of tall buildings will be briefly presented. The reviewed studies specifically help to establish some of the control variables, e.g., they highlight the diagrid structural system with certain geometric arrangements as a suitable type of exterior structural system for tall buildings with potential for the purpose of comparing exoskeletons versus endoskeletons. Many other implications of the above studies will be discussed in each subsection.

Subsection 2.2.5 briefly introduces the international and European standards on LCA of buildings. After this point, the literature review funnel will narrow further to focus on some important LCA studies relevant to the topic of the study at hand, and each subsection will not only present the lessons learned from each study but also discuss their limitations in addressing the research questions of this dissertation. A comprehensive LCA of tall building structural systems by Trabucco et al. [4][5] will be discussed in subsection 2.2.6. This study, although not focused on the comparison of exoskeletons and endoskeletons, sheds some light on the effect of different structural types, materials, and life cycle phases on the full life cycle primary energy and CO_2e emissions of tall building structural systems. It will be followed by the study of Foraboschi et al. [6], which focuses especially on floor systems in the structure of tall buildings. In subsection 2.2.8, a paper by Z. Moussavi, and A. Akbarnezhad [8] will be discussed as an example of research that took into account the interactions of structural systems with heating, cooling, and electrical lighting systems when performing LCA of structural systems. However, they did not particularly investigate exoskeletons (vs endoskeletons). Finally, two important state-of-the-art research papers focusing on the life cycle impacts of tall building exoskeletons will be discussed, which are relatively the most relevant literature sources for this thesis. Subsections 2.2.9 and 2.2.10 discuss these two papers by Felkner et al. [11], and Weber et al. [13], respectively. The research process, results, and limitations of each paper will be discussed in detail from the perspective of this dissertation and its research questions, and the existing gap in the literature that the present study aims to fill as far as possible will be highlighted.

The **third section** (2.3 Factorial DoE and Scenario Planning) thoroughly outlines the conceptual framework and research design of this dissertation. The full factorial DoE forms the backbone of this study. It encompasses the various independent variables (aka factors, each with different levels) that are hypothesized to interact with each other, particularly with the main variable of interest, influencing the response variables. The main variable interest in this study is the utilization of exoskeletons (vs endoskeletons) in tall buildings. The response variables include the life cycle primary energy and CO_2e emissions. The introduction and rationale for the selection of different levels of several independent variables, which are assumed to be controllable (i.e., design factors) or uncontrollable (i.e., context factors) from the perspective of architectural engineers involved in the early design stage of tall buildings, will be elaborated in the subsections of this section.

The combination of all possible permutations of factors at various levels in the DoE results in a total of 1440 compound scenarios, forming the basis for computer simulation experiments detailed in the next chapter. These experiment results will be

compiled and further analyzed to address the research questions. The next chapter will also introduce statistical analysis using GLMs to address the first research question and mathematical decision analysis methods of maximax, maximin, and minimax regret to answer the second research question. The final two chapters will provide answers to the research questions, along with discussions and conclusions.

2.1 Definitions

This section includes definitions of some of the terms and concepts used throughout the thesis in alphabetical order. It should be noted that many other definitions are integrated into the body of the text in the following sections and chapters and, to avoid repetition, are not included in this section.

■ Allocation
Partitioning or subdividing the input or output flows of a process between one or more product systems.

■ Architectural Engineering
Architectural engineering, also known as building engineering or architecture engineering, is an engineering discipline that deals with the technological aspects and a multi-disciplinary approach to the planning, design, construction, and operation of buildings. This includes the analysis and integrated design of environmental systems (such as energy conservation, HVAC, plumbing, lighting, fire protection, acoustics, vertical and horizontal transportation), structural systems, behavior and properties of building components and materials, and construction management [43][44]. From reducing GHG emissions to constructing resilient buildings, architectural engineers are at the forefront of addressing several major challenges of the 21st century. They apply the latest scientific knowledge and technologies to building design. Architectural engineering is a relatively new licensed profession that emerged in the 20th century due to rapid technological developments. Architectural engineers are at the forefront of two major historical opportunities that today's world is immersed in: (1) the rapidly advancing computer technology, and (2) the parallel revolution arising from the need to create a sustainable planet [45]. Distinguished from architecture as an art of design, architectural engineering is the art and science of engineering and construction as practiced in respect of buildings [46].

■ Carbon emissions
In this research, unless otherwise stated, carbon emissions refer to GHG emissions; here, 'carbon' briefly refers to 'CO_2e'.
For more information on ' CO_2e', see 'Global Warming Potential'.

■ Carbon footprint
In the study at hand, unless otherwise stated, carbon footprint refers to all GHGs emitted during one or more life cycle stages of something; here, 'carbon' briefly refers to 'CO_2e'.
For more information on 'CO_2e', see 'Global Warming Potential'.

14

■ Cradle
Resource extraction or material deposits within the ground/earth.

■ Cradle-to-cradle
Unlike 'cradle-to-grave', 'cradle-to-cradle' involves extensive reuse, recovery, and recycling to support the next generation of products, services, and processes (Stages A1-D; see Table 5).

■ Cradle-to-gate
Covers the pre-use/pre-operational stage of a life cycle, including all input and output flows from the 'cradle' up to the factory gate of the final manufacturing factory (Stages A1-A3; see Table 5).

■ Cradle-to-grave
A complete study that equals the sum of cradle-to-gate, use/operation, and end-of-life processes (Stages A1-C4; see Table 5).

■ Cradle-to-site
Equals the sum of cradle-to-gate and delivery to the site of use/operation, i.e., construction site, installation site, etc. (Stages A1-A4; see Table 5).

■ Delivered energy
The energy that is delivered to the site (building)/the point of use (e.g. electricity, natural gas).

■ Feedstock energy
The energy obtained from fuel inputs that have been used as a material rather than a fuel; e.g., petrochemicals to produce plastics and rubber. The energy is not released but retained, and therefore the energy can be recovered at the end of the life of products, e.g., by incineration.

■ Functional Unit
A quantified definition of a product's function used for comparative purposes in assessments, such as kWh or $kgCO_2e$ per square meter area of a reference building.

■ Embodied Carbon (EC)
In this research, unless stated otherwise, EC refers to the sum of carbon emissions related to fuel (the combusted embodied energy) and additional process-related emissions (non-fuel related carbon emissions arising in processes such as chemical reactions). It does not include the 'feedstock energy' that is retained within materials. EC can be measured within different boundaries, such as cradle-to-gate or cradle-to-grave. In the study at hand, unless otherwise specified, it refers to the cradle-to-gate boundary [47][48].
Also, see 'Embodied Energy'

■ Embodied Energy (EE)
EE is the total primary energy consumed from direct and indirect processes for the extraction, processing, manufacturing, and delivery of a material, product, or service. It is used within the cradle-to-gate boundaries, including all activities from material extraction, manufacturing, transportation, and fabrication processes until the

product is ready to leave the factory gate. EE does not include the operation/use or disposal/recycling/end-of-life stages, as opposed to the complete LCA that deals with all life stages [47][48].

Also, see 'Embodied Carbon'

■ Endoskeleton

See 'Exoskeleton' (also see 'Skeleton')

■ Environmental Product Declaration (EPD)

An EPD is a document that describes the environmental impacts associated with the production of a specific set of products or services. It includes information about energy and raw material consumption, waste generation, atmospheric emissions, and discharges into bodies of water. EPDs must be verified by an independent third party before publication. Only accredited certification bodies can carry out checks to validate the EPD and apply uniform methods. Publishing an EPD enables companies to communicate the environmental impact of a product or service clearly and transparently to the market. However, an EPD for a product is a voluntary declaration of environmental life cycle effects and does not necessarily mean that the declared product is ecologically superior to alternatives. The minimum phases taken into account range from the extraction of raw materials through their transport to the production site and production itself (i.e., "cradle-to-gate") to the disposal of the product itself (i.e., "cradle-to-grave"). The results are presented in summarized form using a series of environmental indicators, such as the amount of carbon dioxide emitted or the GWP (Global Warming Potential) per declared product unit, e.g., per kg.

■ Exoskeleton (vs Endoskeleton)

(also see 'Skeleton')

A skeleton (or parts of a skeleton) placed outside the interior space of a (tall) building, i.e. exposed to the exterior space/surrounding environment, is called an exoskeleton. An example is shown in Figure 4.

Figure 4. A tall building with a diagrid frame utilized as exoskeleton; Shenzhen Rural Commercial Bank Headquarters, Shenzhen, China, 2020, by SOM. Source/Credit (©): photograph by Lhzss8 via Wikimedia, licensed under CC BY-SA 4.0 [49] (brightness adjusted, right: cropped).

An endoskeleton is the opposite of an exoskeleton; it refers to a skeleton (or parts of a skeleton) positioned inside the interior space of a (tall) building. Figure 5 illustrates an example of a tall building with an endoskeleton. The term "endoskeleton" used in this dissertation is borrowed from biology, which is explained below. The "default" type of skeleton is endoskeleton, as most buildings merely have endoskeletons. That is why even when only parts of the skeleton of a building are exposed to the environment, it is called a building with an exoskeleton.

Figure 5. A tall building with an endoskeleton; European Central Bank (ECB), Frankfurt am Main, Germany, 2014, by Coop Himmelb(l)au; left: the endoskeleton is being covered by curtain walls during construction; right: after the construction phase, the endoskeleton is completely covered by curtain walls. Sources/Credits (©): photographs from left to right by Simsalabimbam [50], and Norbert Nagel [51], respectively, via Wikimedia, licensed under CC BY-SA 3.0 (both photographs cropped).

A tall building with an exoskeleton usually has partially an endoskeleton in combination with the exoskeleton; i.e., the beams that support the floors and are located inside, as well as the interior columns that support the beams, are parts of the endoskeleton.

The above definitions of exoskeleton and endoskeleton refer to architectural and construction engineering terms. Similar terms with similar meanings exist in other (scientific) fields, such as biology [52][53][54][55][56] and the interdisciplinary fields between industrial design and medical, robotic, and military sciences [57][58]. In biology, exoskeletons are animal skeletons located outside the body. Exoskeletons cover and protect all or part of an animal's body; for example, the entire skeleton of a crab [52][53], a lobster [54], a grasshopper [55], or a cockroach [56] is exposed to the environment. Endoskeletons are not found outside the body, such as the skeleton of a human being or a horse [53]. Some animals have both exoskeletons and endoskeletons, for example, a tortoise's shell is an exoskeleton, but its hands and legs have an endoskeleton [59]—similar to buildings with exoskeletons mentioned earlier. Figure 6 presents examples of animals' skeletons (exoskeleton vs endoskeleton). Figure 7 shows examples of exoskeletons in military and personal assistance applications where the

additional exoskeleton is a wearable device to support and enable humans to carry heavy objects or to walk or move easily. These devices can be active (supported by electric motors, hydraulic systems, etc.) or passive (moved purely and directly by humans).
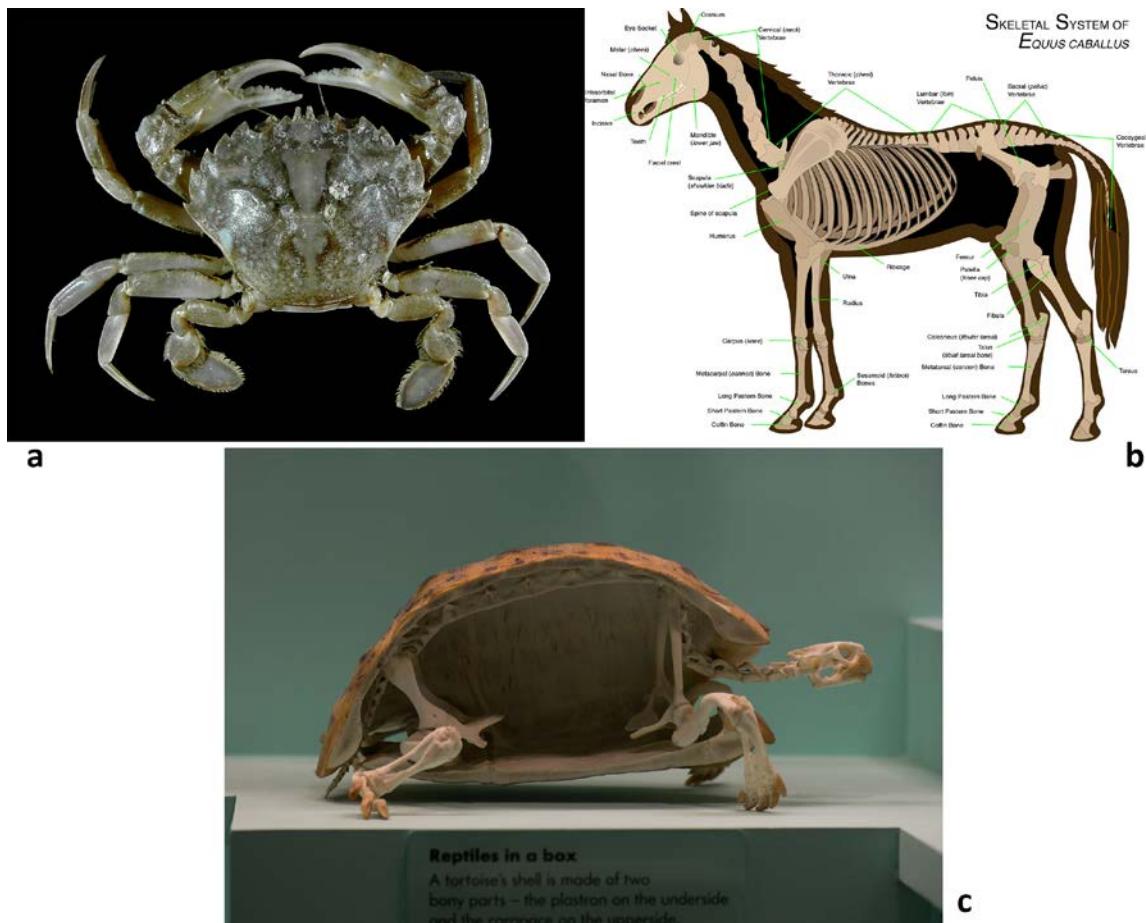
Figure 6. Examples of animal skeletons (exoskeleton vs endoskeleton); from top left to bottom: (a) a grey swimming crab (Liocarcinus vernalis) has an exoskeleton that is clearly visible in the photograph and covers its body parts; (b) a diagram including the skeleton of a horse (Equus ferus caballus), which is an endoskeleton, that is not directly visible from outside; and (c) a cross-section of the skeleton of a tortoise consisting of its shell as the exoskeleton, and other parts (hands, legs, neck, and head) as the endoskeleton. Sources/Credits (©): (a) photograph by Hans Hillewaert via Wikimedia, licensed under CC BY-SA 4.0 [60]; (b) illustration by Wikipedian Prolific, and Wilfredor via Wikimedia, licensed under CC BY-SA 3.0 [61] ; and (c) photograph by Thomas Quine via Wikimedia, licensed under CC BY 2.0 [62].
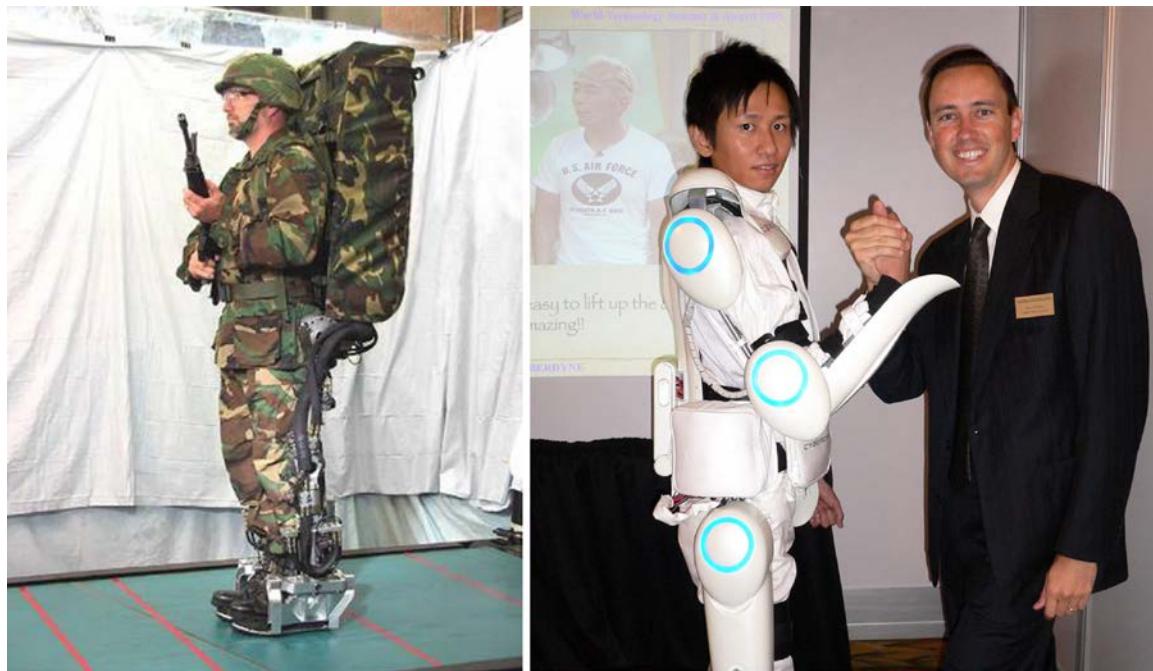
Figure 7. Examples of wearable exoskeletons; from left to right: (a) An electrically powered exoskeleton developed by the (USA) Defense Advanced Research Projects Agency (DARPA) [57]; and (b) a (prototype of a) powered exoskeleton suit intended to aid and expand its users' physical skills, particularly people with disabilities, named the Hybrid Assistive Limb (aka HAL) [58], created by Tsukuba University in Japan and the robotics company Cyberdyne. Sources/Credits (©): photographs by (a) DARPA via Wikimedia, licensed under Public Domain [63]; and (b) Steve Jurvetson via Wikimedia, licensed under CC BY 2.0 [64].

■ Global Warming Potential (GWP)

GWP, also known as the 'greenhouse effect', is an index representing the combined effect of the relative effectiveness of well-mixed greenhouse gases (GHGs) in absorbing the outgoing infrared radiation. Its unit approximates the time-integrated global warming effect of 1 kg of a particular GHG, such as nitrous oxide (N_2O) and methane (CH_4), in today's atmosphere relative to that of carbon dioxide (CO_2). This unit is also known as 'CO_2e', 'CO_2eq', or ' CO_2 equivalent'.

■ Height of tall buildings (measuring)

According to the Council on Tall Buildings and Urban Habitat (CTBUH) [65], the height of a tall building can refer to several items. In this dissertation, unless otherwise stated, it refers to the 'architectural height'. The different types of heights are described below and also presented in Figure 8:

(1) To-Tip: To-tip height is the height to the highest point of the building measured from the lowest significant outdoor pedestrian entrance. The material or function of the highest element is not critical; it can be any functional-technical equipment, such as signs, antennas, flagpoles, etc.

(2) Architectural: Architectural height is the height to the architectural top of the building measured from the lowest significant outdoor pedestrian entrance. An architectural top may include spires but does not include functional-technical equipment such as signs, antennas, flagpoles, etc.

(3) Occupational: Occupational height is the height to the highest occupied floor within the building measured from the lowest significant outdoor pedestrian entrance.

Figure 8. Tall building height categories: To-Tip vs Architectural vs Occupied; the example shows Commerzbank Tower, Frankfurt am Main, Germany, 1997, designed by Foster and Partners. Source: the image was redrawn by the researcher based on an illustration available online on CTBUH's database of skyscrapercenter.com (for the original image and its credits ©, see [66]).

■ High-rise building

A high-rise building is the same as a 'tall building' (see 'tall building'; also see Figure 9).

■ Life Cycle Assessment (LCA)

LCA (which is further introduced in 2.2.5 LCA; ISO and European Norms), is a tool and methodology for evaluating the performance of products, services, or the consequences of decisions. It may address different dimensions of sustainability, including environmental, economic, and social aspects over time. However, this research (unless otherwise stated), specifically refers to LCA of environmental performance. LCA is a multi-step procedure for calculating and evaluating the short-term to long-term or lifetime environmental impacts of materials, products, activities, processes, or services. It quantifies and interprets energy and materials consumed, waste generated, pollutants, and emissions released into the environment at different stages of the life cycle (for the list of stages/phases, see Table 5). The four components of a complete LCA process are goal and scope definition, inventory analysis, impact assessment, and interpretation.

21

■ Life Cycle Impact Assessment (LCIA)

In LCIA, the goal is to analyze the inventory for environmental impact, answering the question "What does this mean?" For example, the production of a product may involve the consumption of natural gas, which is recorded in the inventory; the LCIA phase would calculate the impact of the combustion of this fuel on global warming. However, different methods exist around the world to categorize and characterize the effects of flows entering and leaving the environment, which can make it difficult to compare different LCA studies. Other variables of LCIA include the system boundaries (i.e., how far upstream, downstream, and sidestream the analysis runs), the functional unit (i.e., the volume/mass/purpose of the object being assessed), and specific LCIA methods such as allocation (i.e., how the effects are attributed to the product and by-products). When comparing two LCA studies, these factors are critical to understanding whether the comparison is fair (i.e., apples to apples).

■ Life Cycle Inventory (LCI)

LCI involves the direct count of everything involved in the system of interest. It is the data acquisition part of the life cycle analysis. LCI involves detailed monitoring of all flows entering and exiting the product system, including resources or raw materials, energy by type, water, and emissions to air, water, and soil by specific substance. This type of analysis can be extremely complex and involve dozens of individual processes in a supply chain, such as raw material extraction, various primary and secondary production processes, transportation, tracking hundreds of processes and substances, etc.

■ Low-rise building
A building typically with 1-3 stories (see Figure 9).

■ Megatall building
A tall building 600 meters or taller (see Figure 9).
Also see the definition of 'tall building'.

■ Mid-rise building

A mid-rise building is taller than a low-rise and shorter than a high-rise/tall building, usually ranging from 4 stories up to less than 50 meters in height (see Figure 9).

■ Primary energy

Primary energy refers to the energy not yet exploited or used that is stored in natural resources that have not yet been extracted or transformed into other forms of energy. This is in contrast to secondary energy sources, also known as energy carriers, such as electricity and hydrogen that are the results of the conversion of other sources. Primary energy can be non-renewable, such as nuclear, oil, coal, etc., or renewable, such as geothermal, wind, solar, etc.

■ Product Category Rules (PCRs)

A Product Category refers to a group of products that can perform equivalent functions, such as "insulation" or "double-pane windows". PCRs are particularly useful for comparing the environmental impact of products within a category group, as part of a product specification process. These rules ensure that products with similar functions

Die approbierte gedruckte Originalversion dieser Dissertation ist an der TU Wien Bibliothek verfügbar.
The approved original version of this doctoral thesis is available in print at TU Wien Bibliothek.

TU Bibliothek
Your knowledge hub
WIEN

are compared fairly, and that apples are compared to apples, or rather, insulation with insulation and window with window. Product Category Rules are a natural step in providing standardized information for a group of products or materials with similar functions. The EPD publisher has defined PCRs for each product type, which contain the rules for carrying out the LCA and the EPD itself. It is important to note that these PCRs must comply with ISO 14025:2006 [67] (reviewed and confirmed in 2020) and EN 15804+A2:2019 [68] for construction products.

■ Renewable energy

Renewable energy is derived from sources that are not depleted when used, such as solar, wind, and hydroelectric power.

■ Supertall building

A tall building 300 meters or taller (see Figure 9).

Also, see the definition of 'tall building'.

■ Skeleton

(also see 'Exoskeleton')

A skeleton, also known as a skeleton frame, is a network of columns and beams in a superstructure that supports floors, facades, and other building elements. It carries gravity and lateral loads, including wind and seismic forces, and transfers them to the substructure, which is the foundation.

■ System boundaries

The set of criteria that defines which unit processes to include within the boundaries of an assessment. System boundaries are initially set subjectively during the scoping phase.

■ Tall Building

(Also see the definition of 'supertall building' and 'megatall building')

Equivalent to a 'high-rise building'.

According to the CTBUH [65] (also see [36]), there is no universal absolute definition for a tall building; it is subjective and is usually classified based on one or more of the following categories:

(1) Height relative to context: In a high-rise city such as Hong Kong, Shenzhen, New York City (NYC), or Dubai, a 14-story building may not be considered a tall building, but it may be noticeably taller than the urban norm in a provincial European city or a suburb.

(2) Proportion: There are many slender buildings that are not particularly high but give the appearance of a high-rise building, and on the contrary, many large-footprint buildings are tall but are not classified as high-rise buildings due to their appearance.

(3) Embracing technologies relevant to tall buildings: Buildings that contain and showcase the critical technologies found in high-rise buildings, such as wind bracing or vertical transportation systems.

(4) General definition based on the number of floors and/or overall height: A building of 14 or more stories or more than 50 meters in height is considered a high-rise building (although the number of floors is a poor indicator of

defining a high-rise building due to the changing floor-to-floor height between usages, e.g., office vs. residential).

In this research, unless stated otherwise, the definition of a tall building/high-rise building refers to categories number 1 and number 4. Figure 9 presents simplified definitions of low-rise, mid-rise, high-rise/tall-, supertall and megatall buildings.
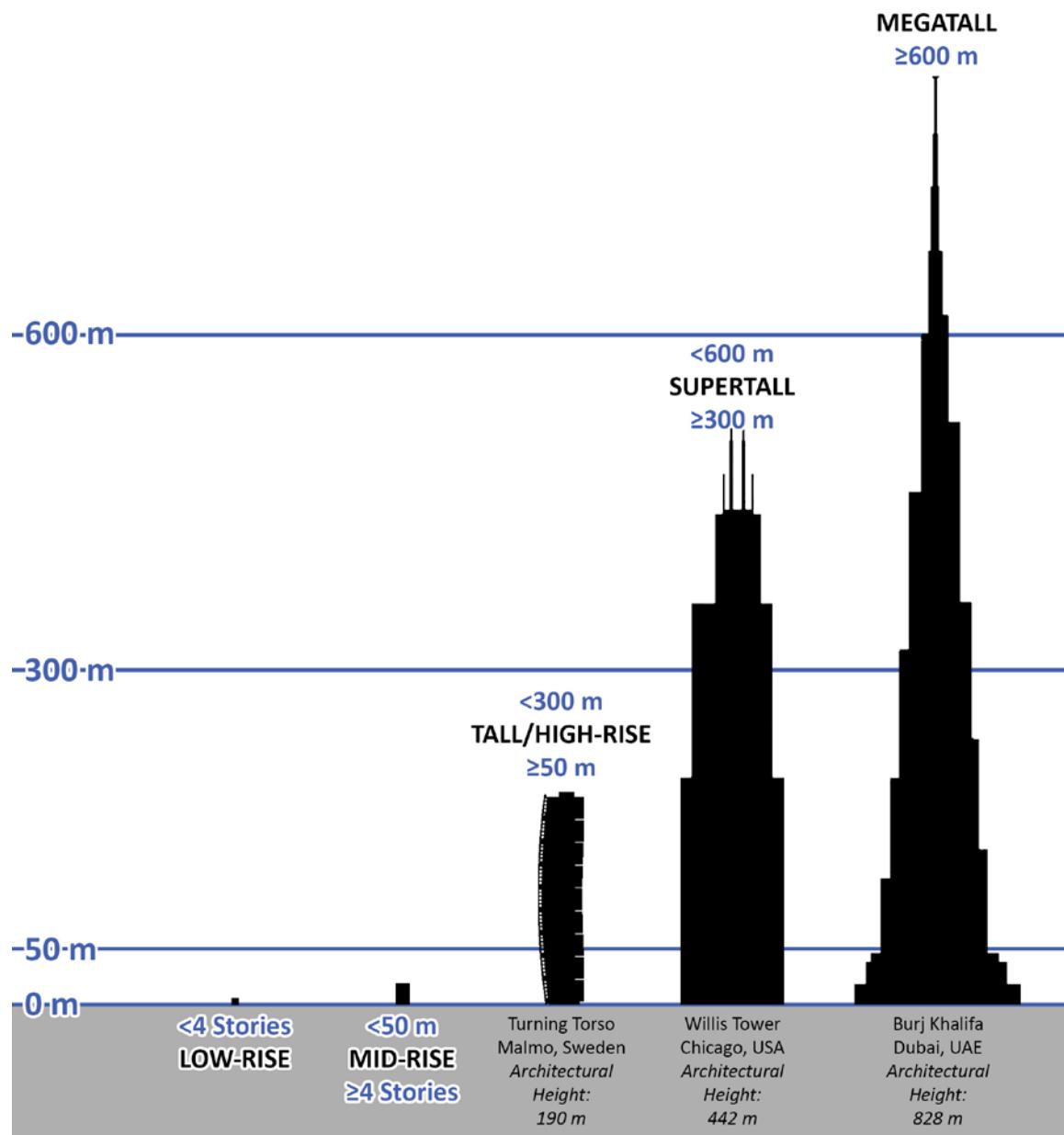
Figure 9. Simplified definitions of low-rise, mid-rise, high-rise/tall-, supertall, and megatall buildings. Source: the researcher

■ Tall Structure
(Also see 'tall building')

The terms 'Tall Structure' and 'Tall Building' are sometimes used interchangeably in the literature. However, to distinguish between the two when necessary, 'Tall Buildings' are structures with relatively large indoor spaces, such as office, commercial, residential, or mixed-use towers. On the other hand, 'Tall

Structures' are those with relatively smaller indoor functions, such as telecommunication towers, water storage towers, air traffic control towers, etc.

■ Tower
(Also see the definition of 'tall building', and 'tall structure')
A tower can be a 'tall building' or a 'tall structure'.

■■   Endnote: In   this   dissertation,   unless   otherwise   stated, "structural"/"structure"/etc. refer to "primary structural"/"primary structure"/etc. For brevity, the word "primary" is not mentioned.

2.2 Review of Tall Buildings; Structural Systems, Exoskeletons, and LCA

2.2.1 Pros and Cons of Tall Buildings: Why Tall Buildings Matter

For decades, researchers, practitioners and policy makers have deliberated on the advantages and disadvantages of erecting tall buildings. Compelling arguments have emerged both for and against their impact on the quality of human life and the sustainable development of urban societies around the world, especially in comparison to low-rise buildings. Although Table 1 briefly presents some of these arguments, one undeniable reality remains constant: tall buildings, whether considered "good" or "bad," play an integral role in the ongoing evolution of urban areas. Moreover, their construction is expected to increase in the future, driven by global population growth and rural-to-urban migration (both of which are significant contributors to the sustainability crisis but are beyond the control of architects or engineers). As available horizontal space ('xy' terrain) decreases, vertical expansion ('z' direction) through skyscrapers becomes a tempting solution, encouraging agglomeration and densification. This transformation reframes the 'why tall buildings' inquiry into a central question: 'how can we enhance their relative sustainability?'. The current study delves into an understudied facet of this overarching query (i.e., specifically examining the impact of exoskeletons vs endoskeletons on the life cycle environmental performance of tall buildings).

Table 2. Summary of arguments highlighting advantages (pros) and disadvantages (cons) of tall buildings. Source: Compiled and summarized primarily from references [36] (by K. Al-Kodmany) and [37] (by M. M. Ali and K. Al-Kodmany), incorporating updated information and additional references.

Pros/ Cons	Aspect	Description
Con -	Economic Considerations	Tall buildings carry additional construction costs due to complex foundations and extensive structural systems that must support significant gravity and lateral loads. They also require service cores, elevators and mechanical systems, which reduce the Net Rentable Area (NRA) of the floors. High energy and maintenance costs, especially for elevators and emergency preparedness, are common [36][37].
Con -	Environmental Impact and Civic Infrastructure	Tall buildings, when built too close together, leave little space for vegetation and sunlight in urban environments. Poorly designed tall structures can create wind turbulence that affects pedestrians. Their reliance on HVAC, electric lighting, and elevator systems can increase energy consumption and carbon footprint (yet, at the urban scale, they reduce per capita grid length, travel distances, and the energy and emissions associated with traffic). Infrastructure planning oversights can lead to problems such as traffic congestion, power grid, sewerage and water supply challenges, and social discomfort [36][37][69][70][71].

Con -	Socio-Cultural Factors, Historic Context, and Placemaking	Residents of traditional low-rise cities may initially resist high-rise development. High-rise living can lead to isolation and disconnection from nature, with potential cultural, psychological and social consequences. Tall buildings can also affect the skyline of historic sites, requiring careful planning. However, there are arguable exceptions, such as the proximity of Mecca's Royal Clock Tower to the Kaaba, which highlights its location despite its height [36][37][72].
Con -	Public Safety and Perception	Events such as the September 11 attacks raised concerns about the safety of high-rise buildings. Statistically, tall buildings are relatively safe, thanks to measures such as smoke control systems, compartmentalization, fire-resistant materials, and detailed evacuation plans. Poorly designed tall structures can damage a city's image, but they have been improved by the incorporation of public spaces and green areas [36][37][73].
Con -	Virtual World	With technological advancements and the growth of the virtual world, debates arise about the need for physical office spaces. While some argue for reduced demand in the future, opposing arguments suggest that internet interactions primarily occur between physically close individuals [36][37].
Pro +	Population and Migration Trends	Urbanization is a global trend, with more than two-thirds of the world's population expected to reside in urban areas by 2050. Tall buildings are essential to accommodate this urbanization, especially in regions such as Asia, Africa and Latin America. E.g., China's rapid urban migration illustrates the need for tall buildings [36][37][74][75][76].
Pro +	Glocal Competition and Economy	Local governments strategically invest in super/mega-tall buildings to draw global attention and attract investors and tourists. These iconic landmarks transform cities into world-class centers, justifying their economic and environmental challenges. Examples include the Petronas Towers and the Burj Khalifa [36][37][77][78].
Pro +	Urban Regeneration and Agglomeration	Tall buildings contribute to urban regeneration by reversing suburban migration. They offer higher quality of life, accessibility to services and lower property maintenance costs. Agglomeration in business districts fosters innovation, increases productivity and improves urban comfort [36][37][79][80][81][82].
Pro +	Land Prices	The price of land has a strong influence on the development of tall buildings. High land prices drive demand for tall buildings, especially in geographically constrained cities such as Singapore, New York and Hong Kong. Tall buildings maximize land use, which makes them economically viable in those locations. Cass Gilbert's quote, "A skyscraper is a machine that makes the land pay," underscores this concept [36][37][83].
Pro +	Land Preservation	Tall buildings mitigate the removal of trees and vegetation, improving air quality and reducing flooding. They take up less natural land through dense development, leaving more green space unbuilt. This is in line with sustainable urban development models [36][37][84][85].
Pro +	Transportation, Infrastructure, Energy Conservation, and Climate Change	Tall buildings minimize energy waste due to reduced heat loss and smaller façade and roof areas compared to shorter buildings. They use fewer resources such as power grids, gas lines, and road networks. Dense development reduces travel distances, saving time and lowering emissions [36][37].
Pro +	Symbols of Collective Greatness and Emerging Technologies	Tall buildings symbolize human potential, modernity, and economic prosperity. They serve as sources of collective pride and identity for citizens where modernization is considered a value. Tall structures also reflect a society's commitment to technological advancement and global recognition [36][37][86].

2.2.2 A Brief History of Tall Buildings; Evolution of Form, Envelope, and Design Concerning Energy and Environment

The researcher wrote this subsection primarily by reflecting and reviewing a paper by Oldfield et al. (originally published in 2009 [38], and revised in 2019 [39]) about the historical categories of five generations of tall buildings from the perspective of primary operational energy consumption and other environmental aspects, with an emphasis on and with respect to the overall shape of buildings and characteristics of their facades among other factors. The five generations are: (1) early tall buildings; (2) from the Zoning Resolution in NYC to the development of glazed curtain walls; (3) from the development of glazed curtain walls to the energy crisis in the early 1970s; (4) from the energy crisis in the early 1970s to the present time; and (5) from the environmental crisis awareness in the late 1990s to the present time. The most recent two of the five generations/categories overlap, and the borderline between them is not clear-cut, as many newly built distinguished tall buildings can fall into both. The researcher added examples and specifications for contemporary trends in accordance with other sources, namely a study by K. Al-Kodmany [40]. Descriptions and examples of these five historical generations are provided below:

2.2.2.1 Before the Energy and Environmental Crisis

■ **Early tall buildings**

The first generation of tall buildings began with the birth of tall buildings in 1885 to the Zoning Resolution in 1916 in NYC. A series of technological innovations, particularly the advent of the steel skeleton and the invention of modern elevators, coupled with urban population growth, particularly in large USA cities such as Chicago and NYC in the mid-19th century, and rising land prices in the centers of those cities justified technologically and economically the increase in the number of stories and led to the first generation of tall buildings, arguably the first of which was the Home Insurance Building in Chicago completed in 1885 (see Figure 10). By using a steel structural system, cladding load-bearing walls were no longer necessary; although these walls were still thick and of masonry materials, they required less thickness than before on the lower floors. Compared to today's curtain walls/window walls, these walls provided a large amount of thermal mass that coped with summer heat and winter cold peaks despite the absence of thermal insulation materials. Their facades had a U-value of 2-3 W/m^2K and a transparency of 20-40%. Examples of buildings from this period include 90 West Street, 195 Broadway, Equitable Building (sketched in Figure 12, left), Municipal Building, Woolworth Building (all in NYC), and Fine Arts Building in Chicago (see Figure 11). They had compact forms; the average building-envelope-Area to the building-Volume ratio (AVr) of these buildings was about 0.1 m^2/m^3. They were relying on natural daylighting and were naturally ventilated by opening windows (they were later renovated into fully air-conditioned buildings). Elevators and heating were the main primary energy consumers [38][39]. Typical office lighting levels in this period were approximately 20-90 lux [87] (which were much lower than contemporary standards, e.g., 200-400 lux [88, p. 53][89]).

Figure 10. Home Insurance Building, Chicago, USA, completed in 1885, demolished in 1931, designed by William Le Baron Jenney, often considered the world's first modern tall building due to its pioneering use of iron frame skeleton with that height. Source/Credit (©): photograph by Chicago Architectural Photographing Company via Wikimedia, licensed under Public Domain [90].

Figure 11. Examples of the first generation of tall buildings; from left to right: (a) Fine Arts Building (previously known as the Studebaker Building), Chicago, completed in 1885, designed by Solon Beman; and (b) Municipal Building, Manhattan, NYC, completed in 1914, designed by William M. Kendall. Sources/Credits (©): photographs by (a) AlexanderUtz via Wikimedia, licensed under CC BY-SA 4.0 [91], cropped; and (b) Tony Hisgett via Wikimedia, licensed under CC BY 2.0 [92].

■ **From the Zoning Resolution in NYC to the development of glazed curtain walls**

This period took place between the years 1916 and 1951. The construction of many tall, bulky buildings, especially the Equitable Building in NYC, which occupied an entire urban block and 'stole' the view and natural light from the urban neighborhood [93], generated controversy and discontent among many citizens. This finally led to the development of the landmark Zoning Resolution by the authorities of NYC in 1916. This law restricted the bulk of tall buildings gradually with setbacks on the upper floors (also known as the 'wedding cake' style of skyscraper), and was followed by similar decisions made in other major North American cities that were home to the majority of tall buildings in that era [38][39]. Figure 12 is a schematic diagram representing the envelope of tall buildings before and after the Zoning Resolution. Examples of this generation in NYC include: 500 5th Avenue, 1931; 570 Lexington Avenue (aka General Electric Building), 1931; Chrysler Building, 1930; and Mercantile Building, 1929. Examples in other cities include: Penobscot Building in Detroit, 1928; Chicago Board of Trade, 1930; Palmolive Building, 1929, in Chicago; and Carew Tower, 1930, in

Cincinnati [38][39]. A couple of tall buildings from the second generation are shown in Figure 13.
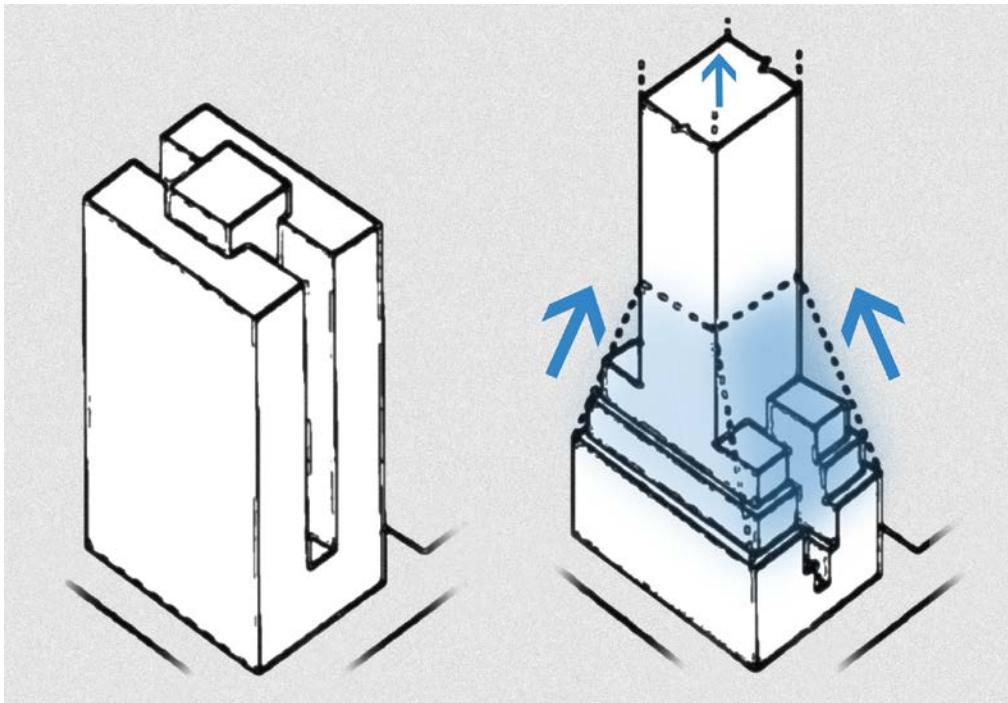

Figure 12. Influence of the 1916 Zoning Resolution on the mass and structure of tall buildings; showcasing pre- and post-Zoning Resolution examples (resembling the Equitable Building and the Chrysler Building in NYC, from left to right). Source: sketch adapted by the researcher, from the original diagram in (source/credits ©) 'P. Oldfield, D. Trabucco, and A. Wood, "Five energy generations of tall buildings: An historical analysis of energy consumption in high-rise buildings," *J. Archit.*, 2009' [38]. Courtesy of Philip Oldfield.

Figure 13. Examples of tall buildings after the Zoning Resolution; from left to right: (a) Chrysler Building, NYC, completed in 1930, designed by William Van Alen; and (b) Chicago Board of Trade Building, Chicago, 1930, by Holabird & Root. Sources/Credits (©): photographs by (a) Rolf Obermaier via Wikimedia, licensed under CC BY-SA 4.0 [94]; and (b) Joe Ravi via Wikimedia, licensed under CC BY-SA 3.0 [95].

The AVr during this period significantly increased from about 0.1 m^2/m^3 to 0.15 m^2/m^3, resulting in a greater need for space heating. However, the taller and more slender volumes, allowed more natural light to enter buildings, reducing the need for electrical lighting [38][39]. Nevertheless, there was a remarkable increase in the illumination levels recommended by the health authorities for offices, from about 90 lux in 1916 to 120 lux in 1920, and some experts, influenced by the power companies, even advocated reaching 270 lux in 1930 [96].

These were general trends but there were exceptions to the rule; the AVr of the Flatiron Building, belonging to the first generation (constructed in 1902), was 0.17 m^2/m^3, whilst the AVr of the Empire State Building, belonging to the second generation (constructed in 1931), was 0.09 m^2/m^3. The triangular shape of the Flatiron Building's

site increased its envelope area, and the Empire State Building (which remained the world's tallest building for about 40 years) was exceptionally massive. The use of air-conditioning was initiated in the second generation of tall buildings to improve comfort. The Milam Building in Texas (1928) was the first fully air-conditioned office tower. It was followed by some towers using retrofitting air-conditioning, e.g., the Chicago Tribune Tower, built in 1925 and retrofitted air-conditioning in 1933 [97][98]. It was around 1950-1960 when air-conditioning became a standard feature in tall buildings. Primary energy consumption increased due to higher demand for heating and electric lighting but the high-rise buildings still benefited from the large amounts of thermal mass in their facades (which were made similarly to the first generation, typically: stone, brick, and dense plasterwork) that reduced the impact of extreme heat and cold of the surrounding environment on the interior space; transparency and U-value of the facades were also similar to those of the previous generation [38][39].

■ From the development of glazed curtain walls to the energy crisis in the early 1970s

As mentioned before, even in the first generation of tall buildings the perimeter walls were no longer built as PSEs but they were still made of masonry materials, and it took decades until modern curtain wall and window wall systems developed and became popular. Before describing the third generation of tall buildings, this paragraph briefly highlights the similarities and differences between these two facade systems for the audience who may not be familiar with them. Both curtain walls and window walls are designed and constructed to separate the interior (often conditioned) space and exterior environment, to control exterior/natural light, solar heat, and atmospheric hygrothermal loads, typically by preventing unwanted rainfall, snowfall, moisture, water vapor, wind, etc., from entering the interior space. Both systems only carry their own local structural loads and apply the loads to the primary structure. The main difference between these two systems is that window walls structurally apply their loads to the primary structure on top/bottom of slabs as they are located in between the slabs, while curtain walls are hung off the slab edges (see Figure 14). Curtain walls do not occupy interior space, typically have better hygrothermal performance and are typically more expensive, and have more complex local structural elements (mullions and joints). Window walls are cheaper and require less expertise to build and maintain, but they occupy some interior perimeter space and usually lack esthetics quality compared to curtain walls. However, they are economically more justifiable and nowadays also provide similar quality of performance as curtain walls [99]. Due to the holistic perspective of the research and intentional avoidance of focusing on details, and for the sake of brevity, only the term 'curtain wall' is mentioned throughout the dissertation, but it is worth noting that in most cases, it could fairly be replaced with 'curtain wall/window wall'. While fully glazed/transparent curtain walls are commonly used in building facades, there are also many old and contemporary designs that incorporate translucent or opaque panels/surfaces, either in combination with transparent glass or on their own (see Figure 15).

Figure 14. Left: a schematic drawing showing the difference in where the loads of a window wall vs a curtain wall apply to primary structure/slabs; right: an example of a curtain wall in the AKH building, Vienna. Source: the researcher

Figure 15. Ribbons of opaque panels separate ribbons of transparent glass windows in curtain wall facades of a contemporary tall building; Millennium Tower, Vienna, completed in 1999, designed by Gustav Peichl, Boris Podrecca and Rudolf Weber. Source: photographs by the researcher

Mies van der Rohe's proposal for the Friedrichstrasse Tower in Berlin in 1921 was arguably the first for a tall building with a fully glazed facade, but this design was not realized as it went far beyond the building technologies commonly used at the time. After World War II, technological advances in the construction industry made it possible to build entirely curtain wall facades for tall buildings, and it gradually became a popular feature and a symbol of modernity, especially for office buildings of large international corporations. One of the first tall buildings using curtain walls was the Lever House building built in 1951 in Midtown Manhattan, NYC. Figure 16 shows photos and a section drawing of the facade of the Lever House building; concrete upstands for fire legislation purposes were covered by dark opaque spandrel panels, and tinted single-glazed curtain walls that covered the entire height of the tower [100]. Tall buildings in the form of black or bronze glass boxes became very popular around the world. The transparent area of facades significantly increased to about 50% to 75%, and due to the usage of single-pane glazing with poor thermal isolation properties, the

35

U-value of facades also increased to around 3.5-4 W/m²K. Air-conditioning became very popular in tall buildings, and in many cases, buildings were highly dependent on them due to the low performance of their facades and also higher expectations of people for comfort. Dark colors of facades absorbed more heat in summer and reduced the penetration of natural light. Typical office lighting levels in this period increased to around 1000-1500 lux, which is higher than all generations. Low-cost energy and extravagant consumption regardless of the long-term environmental impact are among the characteristics of this generation. Typical AVr decreased to less than 0.1 m²/m³, buildings were compact, however, a new version of the NYC Zoning Resolution in 1961 granted a compromise that allowed a 20% density bonus for buildings that created a public plaza on part of their property. Examples of this generation of tall buildings include (the first three buildings designed by Mies van der Rohe): Drive Apartments (Chicago, 1951), the Seagram Building (NYC, 1958), and the Toronto Dominion Bank Tower (1967), Shinjuku Mitsui Building (Tokyo, 1974) and Tour Fiat (Paris, 1974) [38][39][93] (see Figure 17).
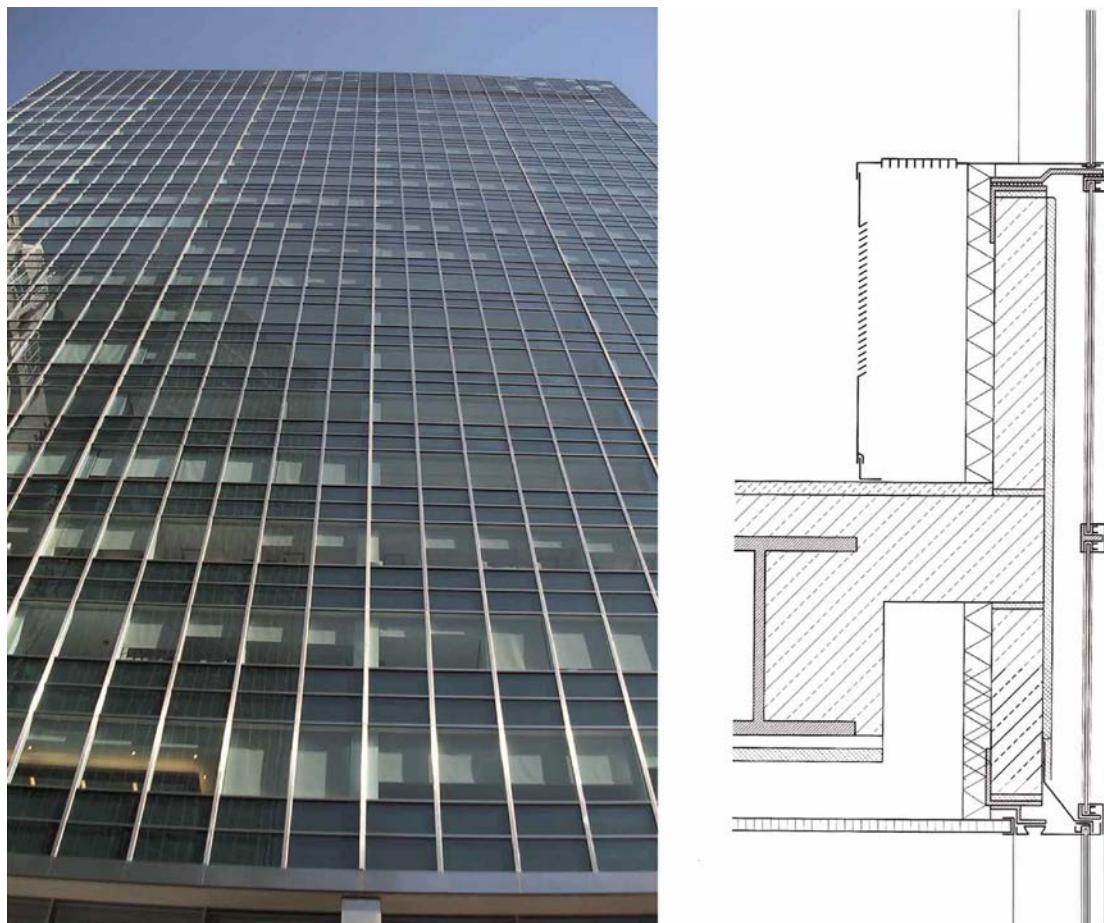

Figure 16. Lever House, NYC, 1952, designed by Gordon Bunshaft and Natalie de Blois of SOM. The left side of the figure shows a photograph of the tower's fully glazed curtain wall facade, while the right side displays a section drawing of the curtain wall detail, including the dark opaque spandrel panels covering the concrete upstands required for fire safety. Sources/Credits (©): 'P. Oldfield, D. Trabucco, and A. Wood, "Five energy generations of tall buildings: An historical analysis of energy consumption in high-rise buildings," *J. Archit.*, 2009' [38]. Courtesy of Philip Oldfield.

Figure 17. Examples the third generation of tall buildings, which spanned from the introduction of glazed curtain walls to the energy crisis in the early 1970s; from left to right: (a) Seagram Building, NYC, completed in 1958, designed by Ludwig Mies van der Rohe, Philip Johnson, Ely Jacques Kahn, and Robert Allan Jacobs; and (b) Shinjuku Mitsui Building, Tokyo, Japan, 1974, by Nihon Sekkei. Sources/Credits (©): photographs by (a) Ken Ohyama via Wikimedia, licensed under CC BY-SA 2.0 [101], cropped; and (b) Rs1421 via Wikimedia, license under CC BY-SA 3.0 [102].

2.2.2.2   During the Ongoing Energy and Environmental Crisis

■ **From energy crisis in the early 1970s to the present**

Rising oil prices and the occurrence of energy crises in 1973 and 1979 led to a sudden decline in public interest in high-rise buildings with dark/colored/mirrored single-pane glass facades, which required large amounts of (mostly fossil fuel) primary energy consumption for the operation of air-conditioning and artificial lighting, This led to a trend of using transparent double glazing with argon-filled cavities, low-emissivity (Low-E) coatings, and other technologies to improve building facade performance. For example, curtain wall U-values were reduced from 3-4.5 W/m^{2}K to 1-1.5 W/m^{2}K to reduce primary energy consumption [103][38][39][100]. Transparency of facades usually ranges between 40-80%, and the overall form of these buildings that basically aim for operational energy efficiency remained compact (AVr near and less than 0.1 m^2/m^3) [38][39]. In this period even building codes let some reduction in standard office lighting levels (to around 400 lux) but at the same time due to the dramatic rise of using computers, monitors, and other electronic devices, increased the

demand for electricity, and it also resulted in additional heat gain (e.g., 17 W/m^2 in 2003 [104]).

Given the substantial overlap between this generation and the next, more details are explained in the next part. Some examples of tall buildings of this generation are: UOB Plaza (Singapore, two towers completed in 1973 and 1995), First Canadian Place (Toronto, 1975), Wells Fargo Plaza (Houston 1983), One Canada Square (London, 1991), Cheung Kong Centre (Hong Kong, 1999) [38][39].

■ From environmental crisis awareness in the late 1990's to the present

As mentioned earlier, due to the direct impact of operational primary energy consumption on the operational costs borne by building users, efforts to reduce these costs have become common practice since the energy crises in the 1970s. Long before that, since the beginning of the Industrial Revolution, with the widespread use of fossil fuels and the indiscriminate exploitation of natural resources, a process began that posed a threat to the environment, with one of the most critical dimensions being global warming and the climate crisis, which was not taken seriously for a long time.

Scientists and certain organizations, notably the Intergovernmental Panel on Climate Change (IPCC), the United Nations body responsible for assessing climate change science, initiated a wave of environmental awareness. They warned of a projected temperature increase of around 1.8-4 degrees Celsius by the end of the 21st century. Ignoring these warnings could lead to irreversible global-scale human disasters [105].

Although most high-rise buildings worldwide still only meet basic energy-saving standards and can be considered fourth-generation buildings, a new generation of high-rise buildings, albeit a small but significant minority, has emerged in recent decades. These buildings symbolically prioritize sustainability and the environment by adopting new technologies and strategies, often in experimental stages.

The Commerzbank Tower in Frankfurt am Main, designed by Foster and Partners and completed in 1997 (see Figure 18), is often considered the first high-rise building to receive widespread recognition as an exemplary building for the environmentally conscious generation. However, there were earlier modern buildings that also paid close attention to bio-climatic and ecological issues, such as the Price Tower in Oklahoma (designed by Frank Lloyd Wright and completed in 1956), which featured exterior shading devices that respect solar orientations, and used the thermal mass of the structural system to tackle weather temperature peaks [38][39][106][40]; or the Mesiniaga Tower in Selangor, Malaysia, completed in 1995 and designed by Ken Yeang, one of the pioneers in academic research and design on sustainable tall buildings in recent decades (see Figure 18). Some of the features of the Commerzbank Tower that can be found in some other tall buildings of the fifth generation include plenty of natural light and ventilation through a 'Klima-facade' with operable windows, a large central atrium, sky gardens, and a shallow office area plan. Other examples of this generation include the GSW Headquarters in Berlin, 1999; Deutsche Post Building in Bonn, 2002; Hearst Tower in NYC, 2006; and Bank of America Tower in NYC, 2009. The overall form of these buildings was less bulky, with an AVr of over 0.1 m^2/m^3 up

to around 0.2 m²/m³, which reduced the demand for electric lighting but increased thermal transmission with the exterior environment, and thus increased the primary energy consumption for space heating and cooling [38][39].

Figure 18. Two tall buildings widely cited as notable early examples of bio-climatic design; from left to right: (a) Mesiniaga Tower, Selangor, Malaysia, completed in 1992, designed by Ken Yeang; and (b) Commerzbank Tower, Frankfurt am Main, Germany, 1997, by Foster and Partners. Sources/Credits (©): photographs by (a) Cmglee via Wikimedia, licensed under CC BY-SA 4.0 [107], cropped; and (b) Thomas Wolf via Wikimedia, licensed under CC BY-SA 3.0 DE [108], cropped.

Various passive and active strategies, along with different innovations to reduce environmental impacts, have been promoted and experimented with in this generation. Examples include high-performance curtain walls with low U-values and thermal breaking profiles, double-pane or triple-pane glazing, low-E glass with suitable visible light transmission based on climate type, passive naturally ventilated Double Skin Facades (DSFs), on-site energy generation, reduced structural material consumption, integrated structural systems with solar-climatic functions, and optimal orientations in overall form design and elements, among others. It is important to note that these categories are not entirely distinct from one another, and a building or technique can fall into more than one of them.

● **Bio-climatic design**

Both Yeang's Mesiniaga Tower and Foster's Commerzbank Tower fall into the category of bio-climatic design. Paying attention to local climate as the basis of departure in design and applying passive measures and being humane (i.e., human comfort and health-oriented) are principles that Ken Yeang's research and practice were shaped around. In Mesiniaga Tower: sky gardens provide massive shading (that's desirable in the local climate of Malaysia at the equator), the core is not in the center and blocks undesirable sunlight and reduces operational cooling energy demand (however, the efficiency of this strategy over the life cycle of the building can be questionable due to possible extra EE caused by reduction in rentable area and additional building materials [109][110]; protrusion of the facade and sunscreens control sunlight on (operable-) curtain walls; circular plan shape provides daylight to office areas, service areas and core are naturally ventilated [40][111][112].

Likewise, a 'climate facade' is used in the Commerzbank Tower; it is a DSF with a 16.5 cm cavity between the inner double glazing layer with operable windows and an outer layer of glass panels with acoustically controlled gaps that let the fresh air in while blocks the outside noise. A layer of Venetian blind with a 5cm depth controls the sunlight entering the interior space. The DSF and the sky gardens activity trap the air during winter to avoid loss of thermal energy [113][114].

Vertical landscaping including vertical courtyards or sky decks, vertical farms, and using balconies and terraces are among new trends in the design of tall buildings with environmentally friendly purposes. Vertical landscaping can reduce the Urban Heat Island (UHI) effect caused by the substitution of plants and green areas with massive buildings. It can also bring more vitality and improve the quality of air and sense of place for humans, and add to the biodiversity of the urban ecosystems. Some examples of vertical landscaping, vertical courtyards, or sky decks are: Mesiniaga Tower, ParkRoyal on Pickering (2013, Singapore), CapitaGreen (2014, Singapore), Bosco Verticale (2014, Milan), and Oasia Hotel Downtown (2016, Singapore).

Balconies and terraces as a feature for residential buildings particularly in mild and warm climates where the outside temperature is pleasant in noticeable periods of time and seasons can make desirable spaces between interior and exterior environment and can provide passive shading on the facade during summertime if properly designed in accordance to the local sun-path diagram and neighborhood building volumes. Some practice examples are: Marina City twin towers (1964, Chicago, USA), Bosco Verticale (2014, Milan, Italy), and Beirut Terraces (2016, Lebanon) [40].

● **On-site renewable energy generation**

One of the new trends among the 21st-century high-rise building designs aiming at reducing GHGs and the use of fossil fuels is the integration of renewable energy harvesting tools into the building. Photovoltaic (PV) panels or wind turbines are typically placed somewhere on the facade or roof of these buildings. However, given that these techniques are currently only implemented in a very small percentage of buildings and are spreading at a slow rate compared to population growth and environmental problems, experts and researchers have doubted their generalizability as

a solution to the global environmental crisis with respect to buildings and the construction industry [115][116]. In many cases, these measures and innovations, which are done targeting the 'zero energy' or even 'positive energy' horizons to be reached in the future, have shown little effectiveness and are facing problems related to efficiency, such as the difficulty of maintenance on the facades and roofs of tall buildings, noise generation of wind turbines, as well as overshadowing of PVs by buildings volumes or climates with insufficient sunlight [40][117][113]. In other words, at a similar cost, much more electricity can be generated, for example, on sites outside the cities and/or on the ground level. This has been particularly suggested by Adrian Smith, the architect of the world's tallest building (Burj Khalifa in Dubai, UAE) with regards to mega-/super-tall buildings (in desert climates with lots of sunlight—and dust) that the use of PVs can supply only a minuscule portion of the operating energy, which does not make it cost-effective to maintain. They have found a more effective alternative approach; the conversion of the mechanical kinetic energy of downward motion of elevators to generate electricity that is going to be used in future mega-/super-tall buildings [78].

Among buildings incorporating PV panels are: the 11-floor TU Wien's Plus-Energy Office High-Rise Building/"Plus-Energie-Bürohochhaus" (2015, Vienna, Austria) that is known as a successful example [118][119], and in contrast to that, the 46-floor Heron Tower in London generates merely 2.5% of the building energy demand by its PV panel mounted facade mainly due to the predominantly cloudy weather of the city (2011, London, England) [113] (this building also incorporates an exoskeleton structural system).

● **Passive and active solar shading devices**

○ **Heat gain and glare**

Shading devices, when designed to achieve optimal solar orientations, reduce heat gain in the interior space of buildings during the summer, resulting in human thermal comfort and HVAC efficiency, and decrease glare (meaning excessive light at high contrast with the surroundings that could harm people's eyes; it often occurs due to the direct sunlight or unwanted concentration of the reflection of direct or indirect sunlight from non-convex highly glazed or metallic facades) [120][121][12]. Architectural engineers have developed creative forms of passive and active shading devices and integrated them into tall buildings, some of which are presented here (passive shading devices are static, i.e., held in place, but active ones are dynamic, i.e. move or rotate, using electro-/mechanical apparatuses). Shading devices are typically less effective in reducing heat gain when used inside the conditioned space, but they can still significantly reduce (glaring) daylight coming from outside. Projecting fins (typically vertical or horizontal), awnings, canopies, shutters, and blinds are common shading devices used on the external side of glazed curtain walls and windows in general [122]. The exterior curvilinear shading devices on Mesiniaga Tower have an aesthetically appealing look and at the same time ecological properties as such. In the New York Times Tower (2007, NYC, USA), linked to a dimmable lighting system, a layer of brise soleil made of ceramic rods protects the largely glazed skin. Renzo Piano, the architect of the building, calls this a "sun-coat" which reduces the transfer of heat

and light to the interior space and allows the use of clear (instead of tinted) glass (see Figure 19) [40][113].

Figure 19. The New York Times Building (NYC, completed in 2007, designed by Renzo Piano and Fox & Fowle Architects) incorporated a DSF as a passive strategy to control the daylight and solar heat gain. Source/Credit (©): photograph by Defears via Wikimedia, licensed under CC BY-SA 4.0 [107] (right: cropped).

○ **Static**

In the Doha Tower (2012, Doha, Qatar) designed by Jean Nouvel, the aluminum elements are arranged in varying proportions of perforation that respond to the solar orientation on the southern, eastern, western and northern sides of the facade in a specific pattern that is inspired by and modernizes the traditional 'mashrabiya'—the wooden elements that have been a common solution to the ecological facade to protect windows and the interior space from the hot and sunny weather in a wide geographical area from southern Iran to North Africa (see Figure 20). Another example of tall buildings incorporating passive shading devices is the Salesforce Tower (2018, San Francisco, USA) [40] (see Figure 21). This 326m tall building incorporates metal sunshades protecting its glazed skin made of Low-E glass that at the same time transmits sufficient natural light [113]. Shading devices installed parallel to the large primary structural bracings of the Public Investment Fund (PIF) Tower (2021, Riyadh, Saudi Arabia) is a prominent passive design feature of the architecture of this 385 m

Die approbierte gedruckte Originalversion dieser Dissertation ist an der TU Wien Bibliothek verfügbar.
The approved original version of this doctoral thesis is available in print at TU Wien Bibliothek.

TU Bibliothek
Your knowledge hub
WIEN

tall building [123]. Colorful passive shading devices are integrated into the outer skin of the DSF of the KfW Westarkade building (2010. Frankfurt am Main, Germany) [124].

Figure 20. The Doha Tower (aka Burj Doha), Qatar, completed in 2012, designed by Jean Nouvel. The exterior skin of the DSFs constructed of multi-layered patterns invoking traditional screens designed to shade buildings from the sun, and protect the glass from sand residue. Sources/Credits (©): photographs, from left to right, by Axel Drainville [125] (cropped), and marc.desbordes [126], respectively, both via Flicker and licensed under CC BY-NC 2.0.

Figure 21. The Salesforce Tower, San Francisco, USA, completed in 2018, designed by César Pelli. Horizontal brise soleils above each floor and vertical fins on the facades deflect sunlight and provide shade. Source/Credit (©): photograph by Dead.rabbit via Wikimedia, licensed under CC BY-SA 4.0 [127] (right: cropped).

○ **Dynamic**

Advances in meteorology, computer science, and electromechanical technologies, namely in real-time sensing, artificial intelligence, and robotics have opened new horizons for designing and implementing previously futuristic concepts of dynamic facades that respond to environmental stimuli such as wind and solar radiation [128]. The visually appealing dynamic shading devices on the facades of the twin 147 m tall Al Bahr Towers (2012, Abu Dhabi, UAE) are arguably the most iconic ones of their kind in recent decades that have been widely reported in news and journals on kinetic architecture. The triangular panels fold and unfold autonomously as umbrellas following a simple repeating origami pattern on a hexagonal structure that responds to orientation and solar radiation. In this unique DSF, the overall pattern of the dynamic exterior screen, like a huge modernized 'mashrabiya', changes parametrically with the sun's incidence angles during different days of the year to reduce glare and heat gain passing through the transparent glass skin (see Figure 22) [128][40].
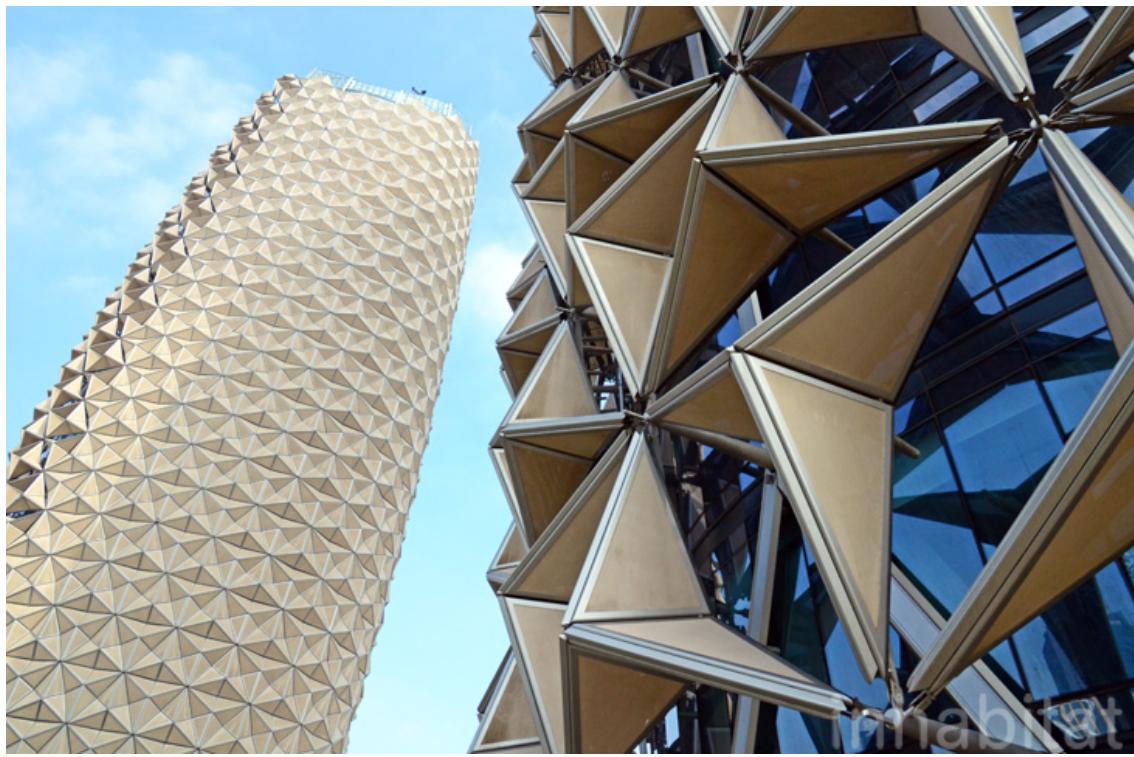
Figure 22. Al Bahr Towers (Abu Dhabi, UAE, completed in 2012, designed by AHR) feature an innovative active external shading system that comprises foldable modules that block glare and reduce heat gain and energy consumption while allowing indirect light to enter, promoting energy efficiency and user comfort. Source/Credit (©): photograph by Inhabitat via Flickr, licensed under CC BY-NC-ND 2.0 [129].

Erste Campus, the mid-rise headquarters of the Erste Group (2015, Vienna, Austria) has been awarded the German Sustainable Building Council/Deutsche Gesellschaft für Nachhaltiges Bauen (DGNB) platinum certificate based on tests conducted by the Austrian Sustainable Building Council/Österreichische Gesellschaft für Nachhaltige Immobilienwirtschaft (ÖGNI). As the result of an international architecture competition, one of the features of the building designed by Henke and Schreieck is its naturally ventilated DSF system that contains electromechanical dynamic metal shading devices in between the two glazed skins allowing for adjustment of daylight and solar heat gain with respect to varying conditions of the environment during different times of the day throughout the year (see Figure 23) [130][131][132].
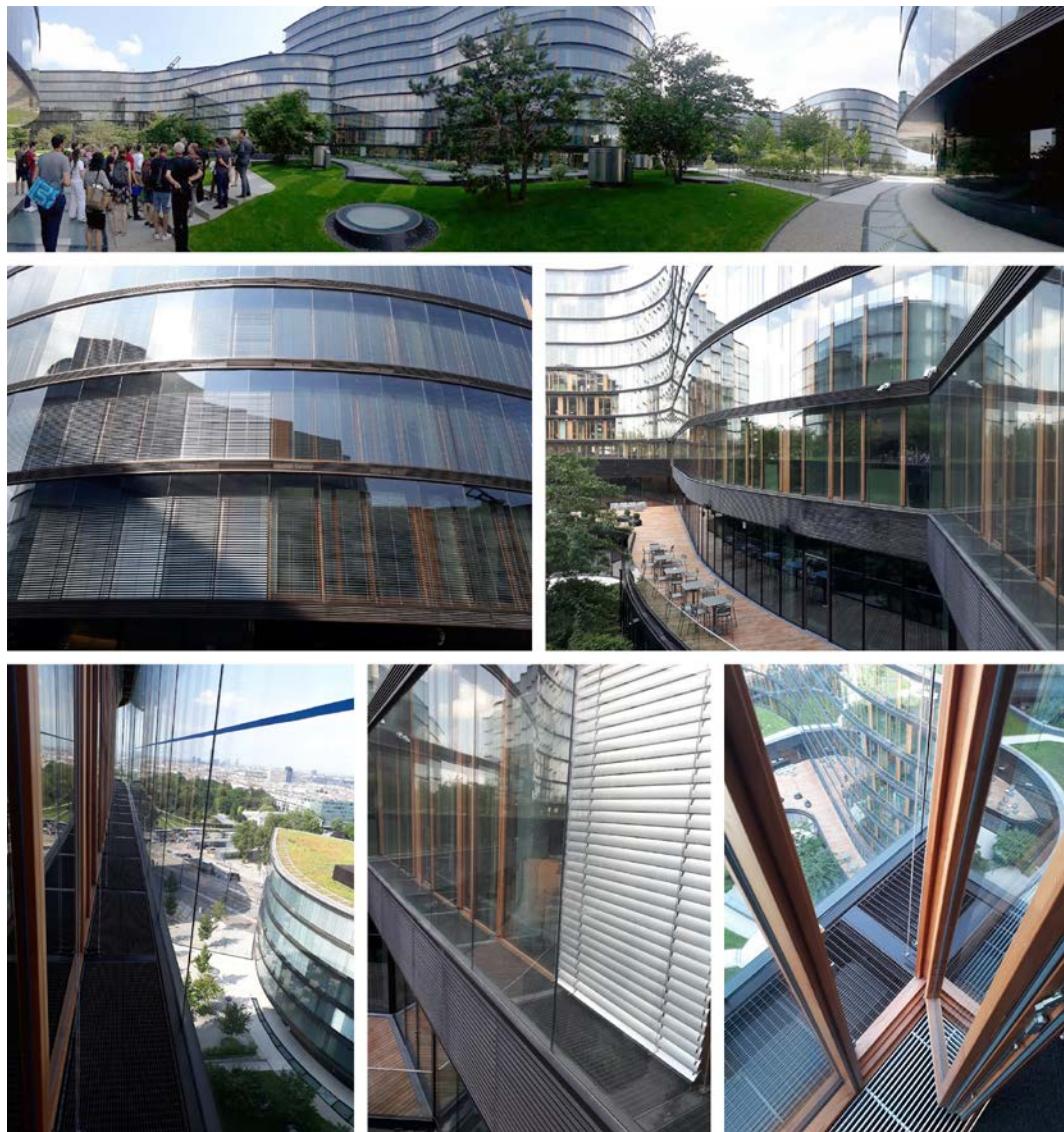
Figure 23. The DSF of the Erste Campus in Vienna incorporates passive and active strategies to provide comfort and save operational energy. Source: photographs by the researcher

The GSW Hauptverwaltung/Headquarters (1999, Berlin, Germany) is an earlier example of dynamic shading devices (sliding and vertically pivoting louvers) between DSF skins that mitigate the harsh afternoon solar radiation caused by the building's undesirable orientation (east-west), and with various colors provides a unique sense of vibrancy to the surrounding cityscape [40][133].

● **Efficient integrated structural systems**

Providing maximum structural stability with minimum possible use of (a certain given set of) structural materials has been a goal for sustainable structural and architectural design integrity because it can reduce the environmental impacts of tall buildings, as typically massive consumption of primary energy and emission of GHGs has been inevitable during the production and transportation of these materials as well as in construction stage of tall buildings. Structural systems may also significantly affect the performance of other systems in other stages of tall buildings' life cycle. In

this respect, some responsive structural configuration strategies and systems including aerodynamic and triangular overall shapes, braced tubes, diagrids, and exoskeletons (especially with respect to their effect on non-structural operational energy and GHG emissions) [40] are briefly introduced in this subsection. More information on various types of structural systems—categorized by their common height, and their placement in plan: close to the center (known as 'interior' structures), or close to the perimeter (known as 'exterior' structures)—are introduced in the next subsection.

○ Aerodynamic overall forms

Aerodynamic overall forms lead to minimized lateral loads caused by wind that are often crucial in structural design of tall buildings as the wind loads exponentially increase with the height from ground level to the top levels. When wind blows around a building, air starts swirling that forms vortex shedding pulling the structure on the sides and the back. If a lot of vortices with similar frequencies get shape, they can cause significantly larger forces especially if they meet the natural frequency of the structure [134]. Architectural/structural/wind engineers apply techniques to 'confuse' the wind in order to avoid massive forces affecting the structure and the surrounding areas; some of these techniques, known as shape strategies to reduce excitation, are: aerodynamic curvilinear geometry for overall form in plan and section; tapering the volume; using structural elements/fins with varying sections on different heights of the structure; porous volume/surfaces to allow the winds pass through; avoiding sharp corners using fillets or setbacks in cross-section design [135]. Thankfully, the results of these strategies are often aesthetically appealing as well.

For example, the aerodynamic form of 30 St Mary Axe tower (designed by Foster and Partners, completed in 2003) in London, diminished the risk of downward-washing winds that usually are reported on sidewalks around tall buildings. The circular floor plan with a central core lets in natural light and also avoids unwanted optical glare around the building thanks to its convex reflection. Some examples of buildings with aerodynamic features are: Guangzhou International Finance Center (Guangzhou, China, 2010), Burj Khalifa (Dubai, UAE, 2010), Strata SE1 Tower (London, 2010), KfW Headquarters (Frankfurt, 2010), Absolute Towers (Mississauga, Canada, 2012), Doha Tower (Doha, Qatar, 2012), Pearl River Tower (Guangzhou, China, 2013), Iris Bay (Dubai, UAE, 2015), Oasia Hotel Downtown (Singapore, 2016), and Wuhan Greenland Center (structurally topped out, planned for 2022, Wuhan, China).

○ Tripod/triangular configurations

Tripod/triangular configurations in the plan and section of structural systems when properly designed can also result in more stability of tall buildings. Frank Lloyd Wright used this strategy in his visionary proposal for Mile-High Skyscraper (Illinois, 1956). In a tripod-like triangular configuration of a structural system (e.g., Y shape in plan view) adjacent sides immediately resist loads applied to one side [40]. The Y-shape plan also disrupts the formation of massive wind vortices on the backside of the building and prevents them from matching the natural frequency of the structure which may cause destructive oscillation. In section or elevation view, the triangular overall silhouette has a smaller cross-section on top floors and a larger one on lower floors; this

causes the overall center of gravity of the building and the larger areas of facades to be relatively closer to the ground level, which in turn leads to better resistance of the structure to lateral loads. Adrian Smith has used this strategy in the design of the current world's tallest building, Burj Khalifa, in Dubai, UAE (height: 828 m) as well as the under-construction 1km high Jeddah Tower in Saudi Arabia, and the Wuhan Greenland Center (estimated completion 2023, China) [40]. This strategy has been used by many others around the world, e.g., Lake Point Tower (1968, Chicago, USA), and Tehran International Tower (2005, Tehran, Iran).

○ Exoskeletons, braced tubes and diagrids

Structural performance and geometric optimization of braced tubes and diagrids and some other common tall buildings structural systems are explained in detail in another subsection ("Geometrical Optimization Studies by K S Moon et al."; only shortly to mention: braced tubes and diagrids have the capability to save structural materials because the diagonals can carry lateral loads optimally by their axial action compared to orthogonal tubular structures where lateral loads are resisted by bending of columns). But here in the following paragraphs, the focus is on the claimed effect of these types of structural systems on other building systems namely saving space cooling energy demand due to their ability to cast a shadow on the thermal envelope of tall buildings in the cases where they are exposed to the exterior environment as exoskeletons (opposite of endoskeleton where the vertical structural elements are kept inside the thermal envelope) usually in mild and hot climates.

When it comes to contemporary tall buildings employing exoskeletons, commonly practiced types of structural systems are braced tube, and diagrid. Both systems have been esthetically appreciated by architectural designers who aim to demonstrate architectural and structural integrity in the facade of tall buildings exposed to the urban scenery. Unlike endoskeletons, exoskeletons enable interior layouts to be flexible and column-free. Diagrid system is even more common in exoskeletons that are claimed to save operational energy via casting a shadow on the thermal envelope because of its higher density of diagonal elements scattered throughout the facades compared to braced tubes. And because of the relatively larger size of RC elements than steel elements, the former has more potential to provide larger shading.

Some of the tall buildings with exoskeletons extended from the facades claimed to save operational energy via casting a shadow on the thermal envelope and reducing solar gain include:

(1) Concrete diagrid exoskeletons, e.g., O-14 Tower, Dubai, completed in 2009, designed by RUR Architecture (see Figure 1) [40][136]—"the solar protection afforded by the curvilinear outer cylinder reduced cooling expenses by about 30 percent" [137]—; COR Tower, Miami (unbuilt), by Oppenheim Architecture + Design [40][136][138]; and 170 Amsterdam, NYC, USA, 2015, by Handel Architects [136][139];
(2) Steel diagrid exoskeletons, e.g., Morpheus Hotel, Macau, 2018, by ZHA (see Figure 1) [136][140]; Brunel Building, London, UK, 2019, by Fletcher Priest Architects [141]; Shenzhen Rural Commercial Bank Headquarters,

Shenzhen, China, 2022, by SOM ("It reduces solar heat gain by an estimated 34 per cent, according to the studio" [142]) (see Figure 4);

(3) Steel braced frame exoskeleton, e.g., Hotel de las Artes, Barcelona, Spain, 1994, by SOM [136].

However, to the best of the researcher's knowledge, there is little to no scientific evidence with a clear and replicable methodology published in the available literature to support the claims about the aforementioned built tall buildings with exoskeletons (as opposed to endoskeletons) reducing the building's environmental impacts in detail. Therefore, the researcher contacted (via email) several architects and engineers who have been involved in the design and engineering of those buildings and projects. Most of the emails remained unanswered. Only two firms replied; one was Jesse Reiser (from Reiser + Umemoto/ RUR Architecture), the architect of O-14 Tower (see Figure 1), and the other response came from Zaha Hadid Architects (ZHA) press department regarding two projects: (1) Morpheus Hotel (see Figure 1), and (2) One Thousand Museum Tower, Miami, USA, 2019 (a concrete exoskeleton, a rigid tube with flowing lines of lateral bracing; see Figure 49). Jesse Reiser replied to one question in 2016 about controlling thermal bridging; the answer indicated that they had discussed it with local engineers and Arup and eventually decided not to use thermal bridging control (thermal break/insulation) for the concrete structure as they found this issue not very important in the hot climate of Dubai compared to cold climates. However, no reply was received regarding further multiple questions asked in 2017. Some examples of these questions include inquiries about their methodology to find the optimal design for the structural system, especially the exoskeleton; whether they had conducted a comparative LCA including structural, HVAC, and electric lighting systems to assess the environmental performance of the exoskeleton compared to a similar endoskeleton; and what future scenarios were considered in the assessment, among others. In 2020, ZHA responded to similar questions and requests for more information about their projects with exoskeletons. They provided interesting and extensive report documents, photos, and drawings about Morpheus Hotel, along with brief information and photos of One Thousand Museum Tower. While instructive information, especially about the parametric design process of the Morpheus Hotel, was included, none of the aforementioned questions were addressed in the documents. Therefore, the lack of available reliable scientific documentary information with replicable methodology on the life cycle environmental performance of tall building exoskeletons further motivated the researcher of this dissertation to conduct this simulation-based research and case studies and analysis, as explained in the following sections and chapters.

2.2.3   Typology of Structural Systems of Tall Buildings

This subsection briefly mentions Fazlur Rahman Khan's (also known as Fazlur Khan) contributions to the structural and architectural engineering of high-rise buildings. It then reflects on the common structural systems of tall buildings as classified by Mir M Ali and K S Moon in two widely referenced papers [41][42] in the literature (Note: in this context, "structural system" refers to the vertical components of the structural system, such as columns, bracings, and vertical frames, as opposed to the horizontal elements, namely floors and floor-beams, although both vertical and horizontal components work together). Structural systems are primarily classified into two main categories: "internal structures" and "external structures." Internal structures refer to structural systems in which lateral loads are mostly resisted by elements placed near the geometrical center in the plan view, while in external structures, these elements are located further from the center and closer to the perimeter. It is important to note that in internal structures, minor elements resistant to lateral loads can still be present around the perimeter; and in external structures, major lateral load-resisting elements are placed in the perimeter while some minor elements can be found near the central parts of the floor plans.

Fazlur Khan was a Bangladeshi-American structural and architectural engineer whose innovations during the second half of the twentieth century made significant contributions to the field of tall building design and construction. He formulated the concept of "Premium for Height," illustrated in Figure 24, based on the idea that the structural materials required to support lateral loads (predominantly wind loads, but also seismic loads) on tall building systems increase exponentially as the number of floors and aspect ratio (height-to-width ratio) grow larger. Khan aimed to minimize the hatched area in the graph by developing efficient and innovative structural systems. To achieve this goal, Khan pioneered and developed what is known as 'tube' or 'tubular' structural systems. These systems greatly reduced the amount of structural materials needed for tall buildings, increased their height limits, and minimized the number of interior columns, thus allowing for more flexible interior planning. Unlike the 'rigid frame,' the previously dominant structural system for tall buildings, which was typically conceived and analyzed as a collection of 2D orthogonal steel members in different XYZ directions, Khan conceptualized the entire structural system of a tall building in 3D space as a single tube cantilevered from the ground to withstand wind and seismic loads. This tube consisted of multiple parallel columns connected by spandrel beams, forming an integrated wall surface near the perimeter of the building while also providing space for windows and openings. This innovative idea gave rise to the 'framed tube' system. Fazlur Khan, a pioneer in Computer-Aided Design (CAD), developed various tubular systems, including the 'braced tube' used in the 100-story John Hancock Center (875 North Michigan Avenue, Chicago, USA [143]), and the 'bundled tube,' a combination of several adjacent tubes, which defined the architecture of the Willis Tower (formerly known as the Sears Tower, with a tip height of 527 m and an architectural height of 442 m; it held the title of the world's tallest building from 1973 to 1998) in Chicago, USA [144]. Khan's work included a classification of structural systems specifically designed for tall buildings, as depicted in Figure 25.
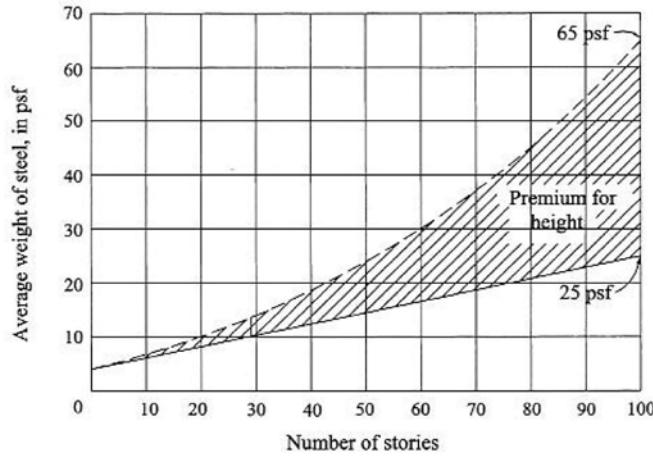
Figure 24. Premium for height; originally by Fazlur Khan. Sources/Credits (©): 'Ali, M. M., & Moon, K. S. (2018). Advances in structural systems for tall buildings: emerging developments for contemporary urban giants. Buildings, 8(8), 104' [41]. Courtesy of Mir M Ali.
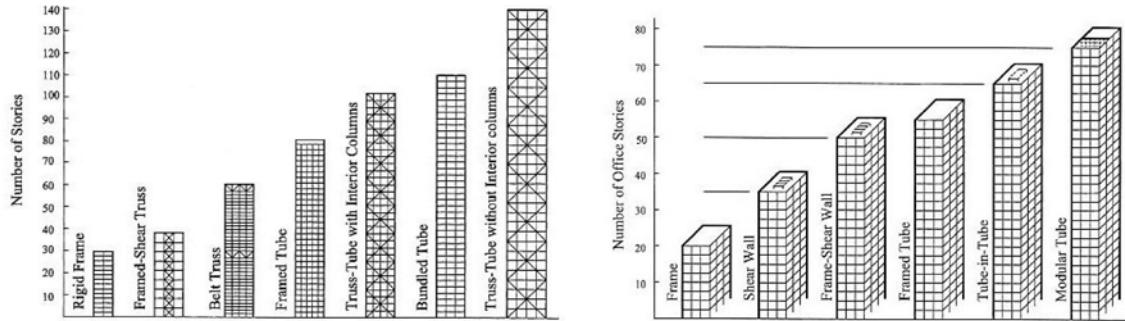

Figure 25. Fazlur Khan's classification of tall buildings' structural systems. Sources/Credits (©): 'Ali, M. M., & Moon, K. S. (2018). Advances in structural systems for tall buildings: emerging developments for contemporary urban giants. Buildings, 8(8), 104' [41]. Courtesy of Mir M Ali.

Common types of interior structures for tall buildings are illustrated in Figure 26. Figure 27 highlights the prevailing exterior structure options for tall buildings. In the description of the following categories, RC and steel (and composite structures made of RC and steel) are mentioned, as they are the most common structural materials used in tall buildings around the world (i.e., to provide perspective, according to CTBUH, among the 100 tallest buildings in the world, in 1960, 99 of them had all-steel structural systems, but by 2017, this number had gradually reduced to only 10. Out of the remaining 90 buildings, 34 had RC structures, and the rest 55 had composite or mixed materials [41]). It is worth mentioning that in the aforementioned figures and following tables (Table 3 and Table 4), the term 'concrete' refers to RC.

51
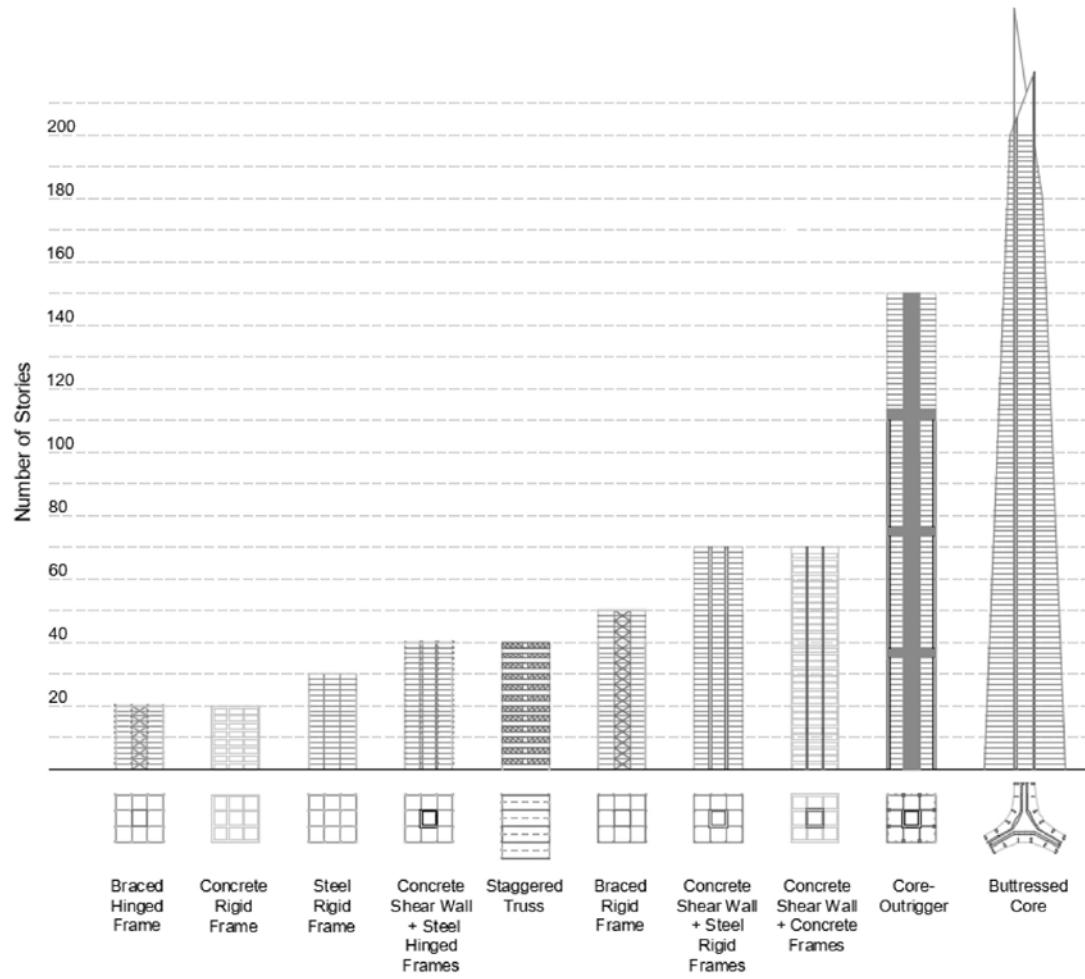
Figure 26. "Interior Structures" for tall buildings. Source/Credit (©): 'Ali, M. M., & Moon, K. S. (2018). Advances in structural systems for tall buildings: emerging developments for contemporary urban giants. Buildings, 8(8), 104' [41]. Courtesy of Mir M Ali.
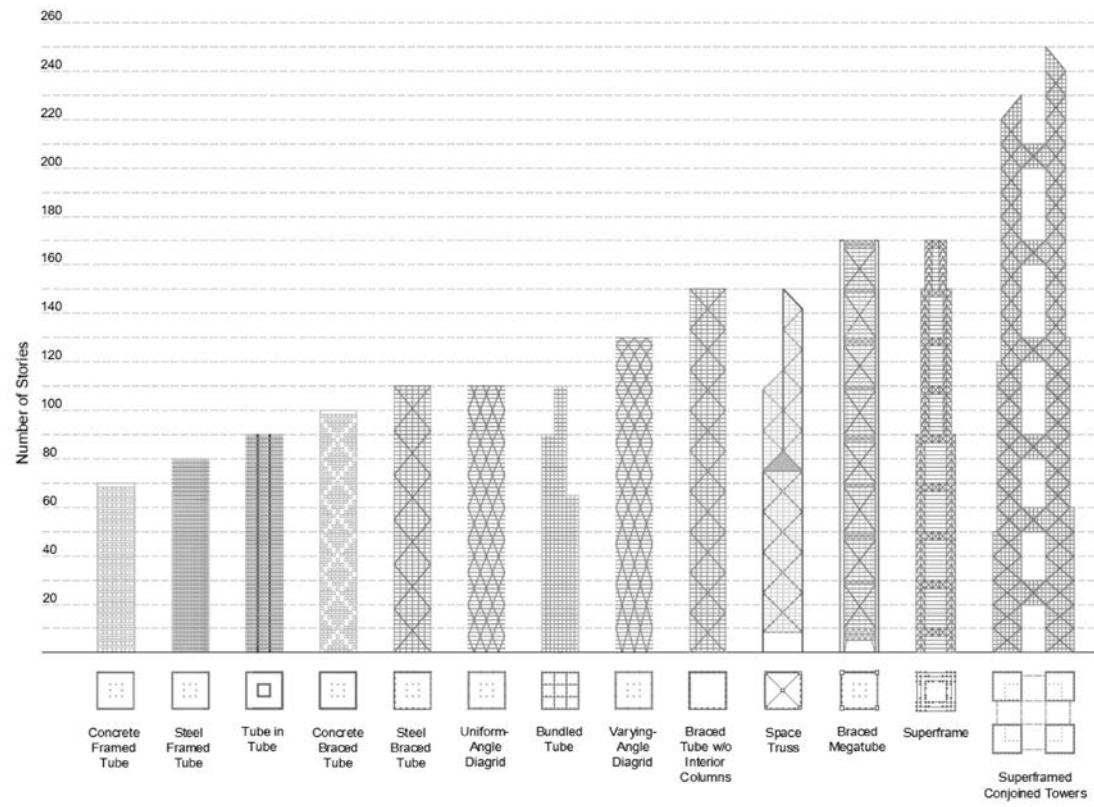
Figure 27. "Exterior Structures" for tall buildings. Source/Credit (©): 'Ali, M. M., & Moon, K. S. (2018). Advances in structural systems for tall buildings: emerging developments for contemporary urban giants. Buildings, 8(8), 104' [41]. Courtesy of Mir M Ali.

Table 3 introduces common interior structural systems, while Table 4 covers exterior structural systems. In both tables, each system is ranked by its Efficient Height Limit (EHL) (unit: stories). EHL is a rough figure representing the number of floors, indicating the maximum height each of these systems can optimally support, serving as a general rule of thumb.

Table 3. Common types of "Interior Structures" for tall buildings. Source: the researcher compiled this table as a summary of information derived from two papers by Mir M Ali and K S Moon [41][42].

Category	Subcategory	EHL	Description
Braced Hinged Frame	-	20	Consisting of steel sheer trusses and hinged frames this is a very common structural system for buildings under 20 stories. This system, compared with the rigid frames without bracings allows for shallower beams, as the shear truss members efficiently resist lateral loads by axial forces. The drawback of this system is that the connections of the bracings are costly and cause limitations in interior planning.
Rigid Frame	-	-	It allows for flexible interior planning due to its simple geometrical configuration (absence of bracings or sheer walls). Fireproofing and moment connections in the steel type are more costly while the construction of the concrete type is slower.
	Concrete	20	
	Steel	30	
Shear Wall-Hinged Frame	-	40	It is made of concrete shear walls and steel frames. Concrete shear walls efficiently resist shear forces but limit interior planning.
Staggered Truss	-	40	This steel system consists of a series of parallel floor-to-ceiling trusses arranged in a staggered pattern on adjacent column lines and spanning the full width between two rows of outer columns. The advantages of this system are fast construction, column-free ground floor, and lower minimum floor-to-ceiling height that reduces building material consumption. The system, however, is relatively weak in the long direction, and the trusses cause significant limitations in interior planning.
Shear Wall (Shear Truss)-Frame Interaction	-	-	This system has two sub-categories (listed below), both of which share a common weakness which is the limitation of the interior plan design due to the shear walls or trusses, and a common advantage which is their ability to effectively withstand lateral loads by the interaction of rigid frames with shear walls or trusses;
	Braced Rigid Frame	50	It consists of steel rigid sheer trusses and rigid frames.
	Shear-Wall/Core and Rigid Frame	70	It consists of steel rigid frames and concrete/composite sheer-walls/core.
Core-Outrigger	-	-	In this system, which has two sub-categories listed below, there is a (concrete/steel/composite) core. Outriggers connect exterior columns to the core. Virtual outriggers or offset outriggers refer to a type of outriggers that only connect exterior columns. Belt-trusses or -walls have the same height as outriggers and connect external columns or mega-columns (columns with very large cross-section areas) located on the perimeter. The drawback of this system is that the location of the outriggers is usually limited to the mechanical/refuge floors because the outrigger elements interfere a lot with the rentable space of the respective floors and greatly limit the interior planning. The advantage of this system is that the perimeter (mega) columns that are connected to the core with outriggers effectively withstand overturning moments.

	With Belt-Trusses/-Walls (and Virtual Outriggers)	80	It encompasses (virtual-) outriggers, belt trusses/walls, perimeter columns, and (central) core. The advantage of this sub-category is that it makes it possible to reduce the disturbance of the floors by using virtual outriggers (which merely connect exterior columns of the structure) instead of outriggers.
	With Mega-columns (and Belt-Trusses/-Walls)	150	It includes outriggers, (belt-trusses/-walls), perimeter mega-columns, and (central) core. Using this system provides unobstructed facades that enable architects to articulate them more freely compared to those of tubular structures.
Buttressed Core	-	200	In this system, a concrete core is supported by sheer walls extending from it. The system can be further stiffened by adding outriggers and/or fin walls. The other above-mentioned structural systems, if used in extremely tall buildings, can result in too deep interior spaces due to the large structural depth required to resist lateral loads. The buttressed core system, as an advantage, does not have that problem. The disadvantage of this system is that it greatly limits the use of space and the creation of large open spaces.

Table 4. Common types of "Exterior Structures" for tall buildings. Source: the researcher compiled this table as a summary of information derived from two papers by Mir M Ali and K S Moon [41][42].

Category	Subcategory	EHL	Description
Framed Tube	-	-	The arrangement of lateral load-bearing elements on the periphery effectively resists these forces and significantly reduces the intervention in interior planning, although narrow column spacing restricts the view.
	Concrete	70	
	Steel	80	
Braced Tube	-	-	This system has different subcategories, which are listed below. They all have in common the disadvantage that the bracings obstruct the view, and the advantages that they effectively resist the lateral loads by the axial forces in the braced tube elements, as well as reduction in shear lag (shear lag is a structural phenomenon in which parts of a cross-section are subjected to high stress whereas other parts are subjected to little or no stress).
	With Interior Columns	100-110	This widely practiced type can be made in concrete (EHL = 100) or steel (EHL = 110)
	Without Interior Columns	150	Theoretically, this is a possible type (to raise higher than the previous one—due to reduced uplift forces), and it can be made of steel or composite, but so far there is no built example of this because it requires very long-span floor systems that span the entire width of the building. In addition, in many cases, buildings require vertical elements other than columns (e.g., stairs, elevators, and MEP risers), which are usually located around the center anyway, so there is no need for a completely 'column-free' interior type of the common structural systems.
	Braced Mega-Tube	170	In this composite system, the corner mega-columns resist overturning moment more efficiently than conventional columns in conventional braced tubes [41]. Perimeter gravity columns can be designed to prevent progressive collapse (that is defined as the extension of an initial failure

			from one member to another, ultimately leading to the collapse of the entire structure or a large disproportionate part of it) [145].
Bundled Tube	-	110	In this system, which can be made of steel or concrete, the shear lag is reduced compared to framed tubes. The disadvantage of the bundled tubes are the rows of columns placed on the boundary line between the tubes, which can cause difficulties in interior planning.
Diagrid	-	-	There are two main subcategories of diagrids listed below. An advantage of both is that lateral loads are efficiently resisted by axial forces in diagonal elements. The common disadvantage is that the diagonal elements have joints with complex geometry which cause complications in the process of design and construction.
	Uniform Angle	80-100	If the angle of the diagonal elements is set optimally, they can efficiently resist both lateral and gravitational forces. This type can be made of concrete (EHL = 80), steel (EHL = 100), or composite (EHL = 100). The disadvantage of the concrete (/composite) type is the slow construction caused by the complex geometry of the joints, which requires special formwork.
	Varying Angle	130	As a system suitable for slenderer and taller buildings, it can resist lateral loads (by axial forces of diagrid members) even more efficiently than the uniform angle type. Diagrid elements of lower floors are less inclined as in lower floors there are less lateral loads compared to the gravitational load that is collected from all levels above.
Tube-in-tube	-	90-150	As the name suggests, this system consists of two inner and outer tubes, which in combination with one another can withstand lateral loads effectively. Each of these tubes can be made of concrete, steel, or composite. Depending on the type of tubes and their combination, the combined systems can have different maximum optimal heights. A minor drawback of the system is that the interior core tube may limit the interior planning.
Space truss	-	150	In this system, which can be made of steel, concrete or composite material, the axial forces in space truss elements withstand lateral loads efficiently, although these elements restrict the view and the interior planning.
Superframe	Stand-alone	100-170	This sub-category, which is usually made of concrete (EHL = 100) or steel (EHL = 170), has the advantage of effectively withstanding lateral loads by axial forces in superframe elements. However, the overall shape of the building is severely limited by the structural system.
	Conjoined towers	250+	This system offers the advantages of: (1) providing multiple emergency egress alternatives (various combinations of horizontal and vertical travel routes), (2) floor plans that are not too deep (and thus, may use natural light), while making it possible to make extremely (mega-)tall building complexes. Often proposed with composite structural materials, there is still no built example of this system. The drawback of this system is that it requires very large plots of land.

In terms of architectural expression and aesthetics, exterior systems have the potential to be integrated with facades and expose the structural logic of the building form to the exterior and the cityscape around the building. The interior systems, on the contrary, tend to conceal the structural system from the citizens and are preferred when architects seek abstract freedom to articulate non-structural patterns through facade design. Concerning dimensions related to solar-climatic aspects, building physics, energy consumption, and carbon footprint, interior systems offer better potential for incorporating more structural thermal mass within the conditioned interior space. Exterior structures, depending on the design, can be positioned inside, outside, or on the borderline between the conditioned and outdoor spaces. When not fully situated within the interior space (i.e., 'not endoskeleton' = 'exoskeleton'), they may shade the facade. The focus of the current study is to compare endoskeletons and exoskeletons of the same type of exterior structural systems. It takes into account various scenarios to provide a realistic overview of the environmental impact of this design decision over the life cycle of tall buildings through scenario planning and statistical analysis of computer simulation-based case studies.

2.2.4 Geometrical Optimization of Structural Systems in the Preliminary

Design of Tall Buildings

This subsection reviews the literature by K S Moon et al., focusing on the optimization of common and trending structural systems for tall buildings, primarily the vertical components, through geometric configurations during the preliminary design phase. The objective is to identify optimal angles and geometrical arrangements that reduce the demand for structural materials and aid in the early selection and configuration of suitable structural systems. Moon et al. conducted analyses on various structural systems, including tubular structures with braced or gravity cores, braced tubes, diagrids, and outrigger structures. These systems were studied in combination with different building heights and overall forms, ranging from prismatic (simple box form) to tilted, tapered, twisted, and freeform. The findings from their research are reviewed in this subsection of the dissertation.

Structural systems of the early tall buildings in the late 19th century employed steel frames with diagonal concentric and eccentric bracings (X-, V-, Y-, K-shape, etc.). Diagonals were utilized for their ability to resist lateral forces via their axial action, but they were not esthetically appropriated by architects, so they remained hidden and were placed in the interior core. In the late 1960s, this trend changed with the introduction of braced tubular structures, namely in the design of the John Hancock Center (100-story tall, Chicago, see Figure 1), where diagonals were integrated into all facades of the building to maximize the structural effectiveness and establish a new structural expressionist esthetic language symbolizing the integrity between architecture and structural engineering. Diagrid systems subsequently evolved: they began in the early 1960s, e.g., the IBM Building, Pittsburgh, the USA (see Figure 1), but started to become popular later, most notably with two towers designed by Norman Foster (30 St Mary Axe or Swiss Re Building, 2004, London; Hearst Tower, 2006, NYC); and one of the tallest diagrid structures built is the 103-story Guangzhou International Finance Center, 2010, designed by WilkinsonEyre. The difference between these two types of structures

lies in the fact that in conventional braced (exterior) structures the diagonals support only lateral loads and the columns support gravity loads, whereas in the diagrid system the conventional columns are usually eliminated, since the diagonal members (triangulated with spandrel beams) support both gravity and lateral loads (see Figure 28) [146].
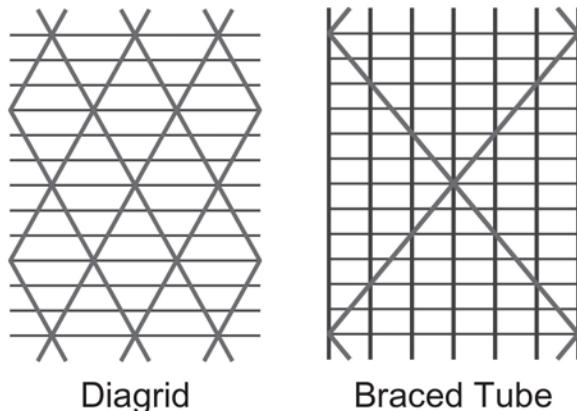

Figure 28. Diagrid vs braced tube system. Source/Credit (©): 'K. S. Moon, J. J. Connor, and J. E. Fernandez, "Diagrid structural systems for tall buildings: Characteristics and methodology for preliminary design," *Struct. Des. Tall Spec. Build.*, 2007' [146]. Courtesy of Kyoung Sun Moon.

In terms of minimizing shear deformations, diagrid structures are significantly more effective than conventional framed tubular structures, since in the latter the shear is resisted by the bending of the vertical columns, while in diagrid structures the shear is supported by the axial action of the diagonals. The optimal angle for diagrid members falls between 90° (which is the optimal angle for bending rigidity of columns) and 35° (which is approximately the optimal angle for the shear rigidity of diagonals). The optimal angle of diagrid members increases for taller buildings, as taller structures with high aspect ratios (height to width) act more like bending beams, while shorter buildings with smaller aspect ratios act similarly to shear beams. K S Moon et al. verified these assumptions through iterative simulations and structural analysis of several generic hypothetical tall building structural prototypes in Boston with different heights (a 60-story model with an aspect ratio of 7; and a 42-story model with an aspect ratio of 5; all floor heights 4m; 36mx36m square floor plan with 18 m x 18 m core) with uniform diagrids with various angles. They used the SAP2000 structural analysis program and applied wind loads with a basic wind velocity of 49 m/s according to the standard of the Structural Engineering Institute/ American Society of Civil Engineers (SEI/ASCE 7-02: Minimum Design Loads for Buildings and Other Structures, 1996 [147]) with category 3 (substantial hazard to human life in event of failure). They varied the element sizes in different scenarios to reach the h/500 (here, h meaning total height of the structure) limit for lateral displacement with the minimum possible amount of structural materials (steel) making all the optimized scenarios comparable (lateral stiffness, rather than strength, usually governs the structural design of tall buildings as opposed to low-rise buildings). The study found an optimal diagrid angle between 55° and 65° for the 42-story scenario, and between 65° and 75° for the 60-story scenario (see Figure 29) [146].
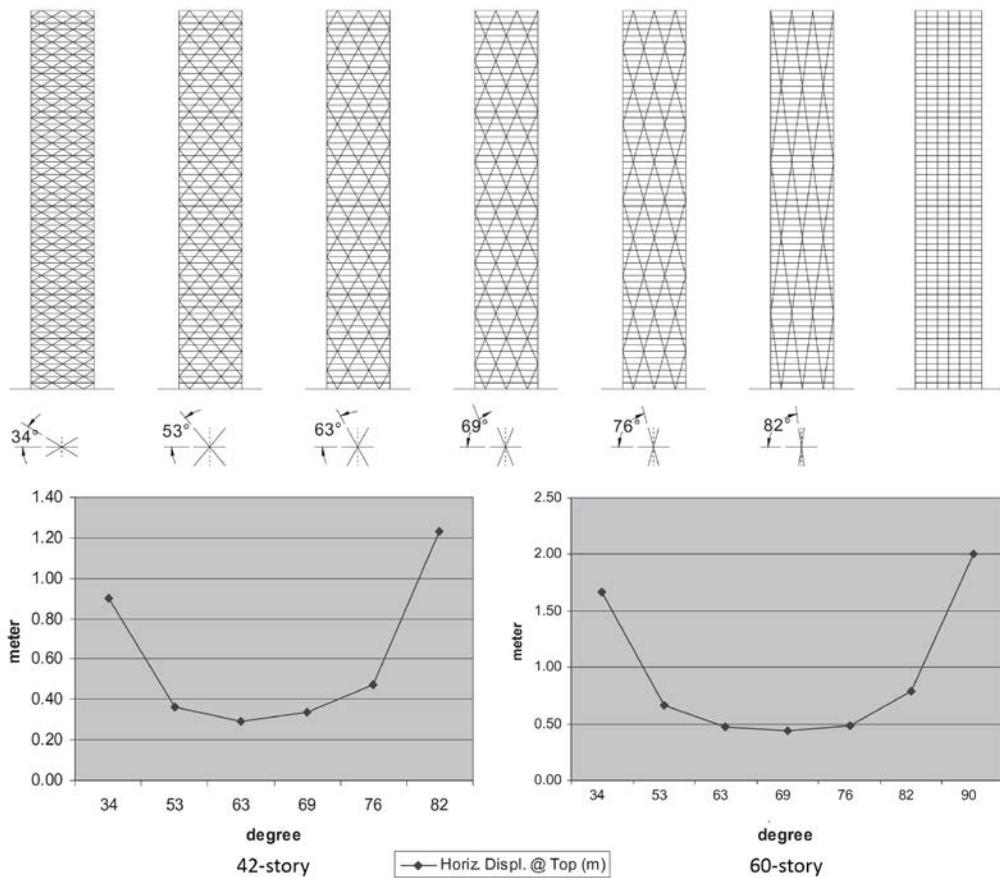
Figure 29. Top: 60-story diagrid structures with different angles; bottom, from left to right: lateral displacement at the top of the 42-story and 60-story prototypes. Source/Credit (©): 'K. S. Moon, J. J. Connor, and J. E. Fernandez, "Diagrid structural systems for tall buildings: Characteristics and methodology for preliminary design," *Struct. Des. Tall Spec. Build.*, 2007' [146]. Courtesy of Kyoung Sun Moon.

In a study in 2008, K S Moon applied a similar stiffness-based methodology to find the optimal angle for diagrid members in multiple hypothetical generic reference tall building structures of 40, 50, ... to 80 stories with aspect ratios ranging from approximately 4 to 9. This time, they included not only uniform angle diagrids, but also diagrids with varying angles from base to the top of the structures (see Figure 30). Chicago with a basic wind velocity of 40 m/s was assumed as the location. The results for uniform angle configurations were similar to those of the previous study, suggesting optimal angles around 60° to 70°, with steeper angles being suitable for taller structures with greater aspect ratios. In the cases of diagrids with variable angles, this strategy was found to be useful only for taller buildings with an aspect ratio greater than 7. As expected, the optimal solution in this case (80-story) turned out to have steeper angles near the base (73° near the base and 63° near the top); because there are relatively more lateral forces at the top of the buildings and more gravity loads around the lower levels). The optimal scenario saved about 35% of the structural material required for the diagrid members compared to the least optimal configuration with steeper angles near the top. A uniform angle of 69° proved to be the optimal scenario for 40- to 60-story buildings compared to scenarios with varying angles that saved up to about 50% of the required structural materials, which also demonstrates the importance of an optimal geometric

configuration in the early stages of design (preliminary design) of tall buildings structural systems [148][149][146].
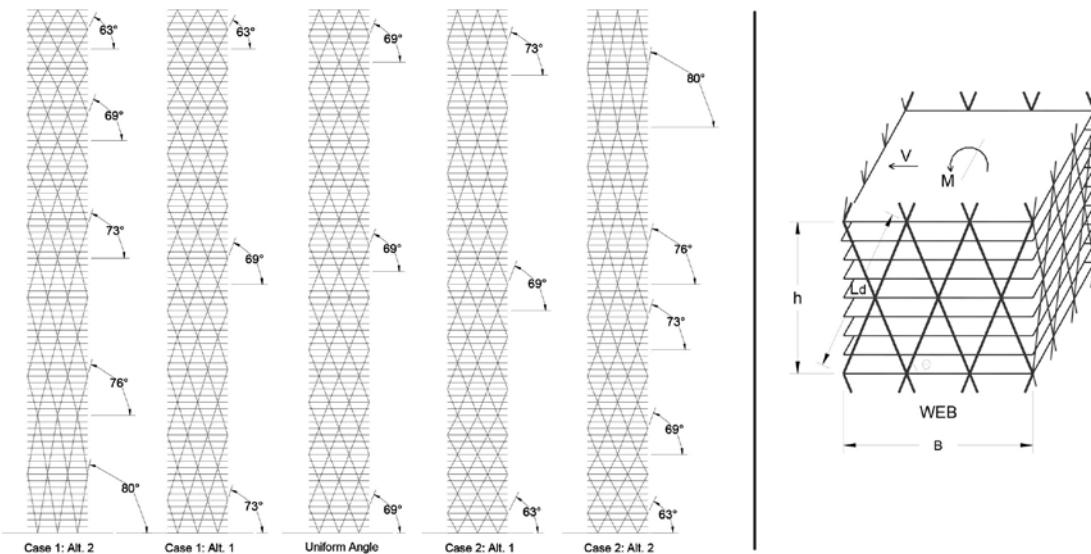
Figure 30. Left: 80-story diagrid prototypes with varying angles and an aspect ratio of 8.7; right: 3D view of a typical diagrid module. Source/Credit (©): 'K. S. Moon, "Optimal grid geometry of diagrid structures for tall buildings," *Archit. Sci. Rev.*, 2008' [148]. Courtesy of Kyoung Sun Moon.

In a study in 2010, K S Moon used a similar method and similar tall building structural prototypes, ranging from 40 to 80 stories tall (similar to the aforementioned study in 2008), with the difference that this time instead of the diagrid structures, conventional steel braced tubes with diagonal members running 8 or 10 or 12 stories were studied in different scenarios. The results showed that diagonals with angles ranging from 40° to 50° (which is also common in practice) are close to the optimum. Examples of contemporary tall buildings employing braced tubes are: John Hancock Center, Chicago, 1969, designed by Fazlur Khan and SOM (see Figure 1); Shanghai World Financial Center, 2008, by Kohn Pedersen Fox (the braced tube hidden behind the reflective curtain walls); and Broadgate Tower, 2009, London designed by SOM (facades with exposed bracings) [150][149].

In 2016, using a similar methodology, K S Moon conducted a study on the lateral performance of diagrid structures, this time with various overall form configurations ranging from prismatic form (conventional rectangular box) to nonprismatic building forms including twisted, freeform, tapered, and tilted diagrid structures of 60, 80 and 100 stories. When it comes to nonprismatic complex-shaped buildings, the diagrid structural system is one of the most suitable solutions, since its triangulated geometry can adapt to various complex shapes that have become a trend in contemporary architecture. (1) The twisted diagrid structure scenarios consisted of 1°, 2°, and 3° of twists per floor around the center of the floor plan gradually over the full height of the building. Examples of tall buildings with twisted forms are the Shanghai Tower, 2014, designed by Gensler; Infinity Tower, Dubai, estimated completion in 2024, designed by SOM; and Chicago Spire, an unfinished project by Santiago

Calatrava. (2) In the free-form scenarios, floor plans fluctuated between ± 1.5 m, ± 3 m, and ±4.5 m with respect to the typical floor plan boundaries in the prismatic scenarios. Examples of buildings with freeform diagrids are the Al Dar Headquarters building, Abu Dhabi, UAE, 2010, by MZ Architects; Capital Gate, Abu Dhabi, 2011, designed by RMJM; QIPCO/Tornado Tower, Doha, Qatar, 2008, designed by CICO and SIAT GmbH; and CCTV Headquarters, Beijing, China, 2012, designed by OMA. (3) In the tilted scenarios, angles of 0, 4, 7, 9, and 13 degrees were tested. Examples of inclined/tilted tall buildings are the Gate of Europe Towers, Madrid, 1996, designed by Philip Johnson and John Burgee; Veer Towers, Las Vegas, 2010, designed by Helmut Jahn and Francisco Gonzalez Pulido; Capital Gate (details mentioned above), and Signature Towers, Dubai, 2006 proposal by ZHA. (4) And, for tapered scenarios, the overall forms were tapered with three different angles of 1, 2, and 3 degrees in the section view. Examples of tapered tall buildings are the iconic braced tube John Hancock Center, Chicago, 1969, designed by Fazlur Khan and SOM (exposing an iconic braced tube structure); an unbuilt but remarkable tapered diagrid structure in SOM proposal for the Lotte Super Tower in Seoul; and the Guangzhou International Finance Center, 2010, designed by WilkinsonEyre [151].
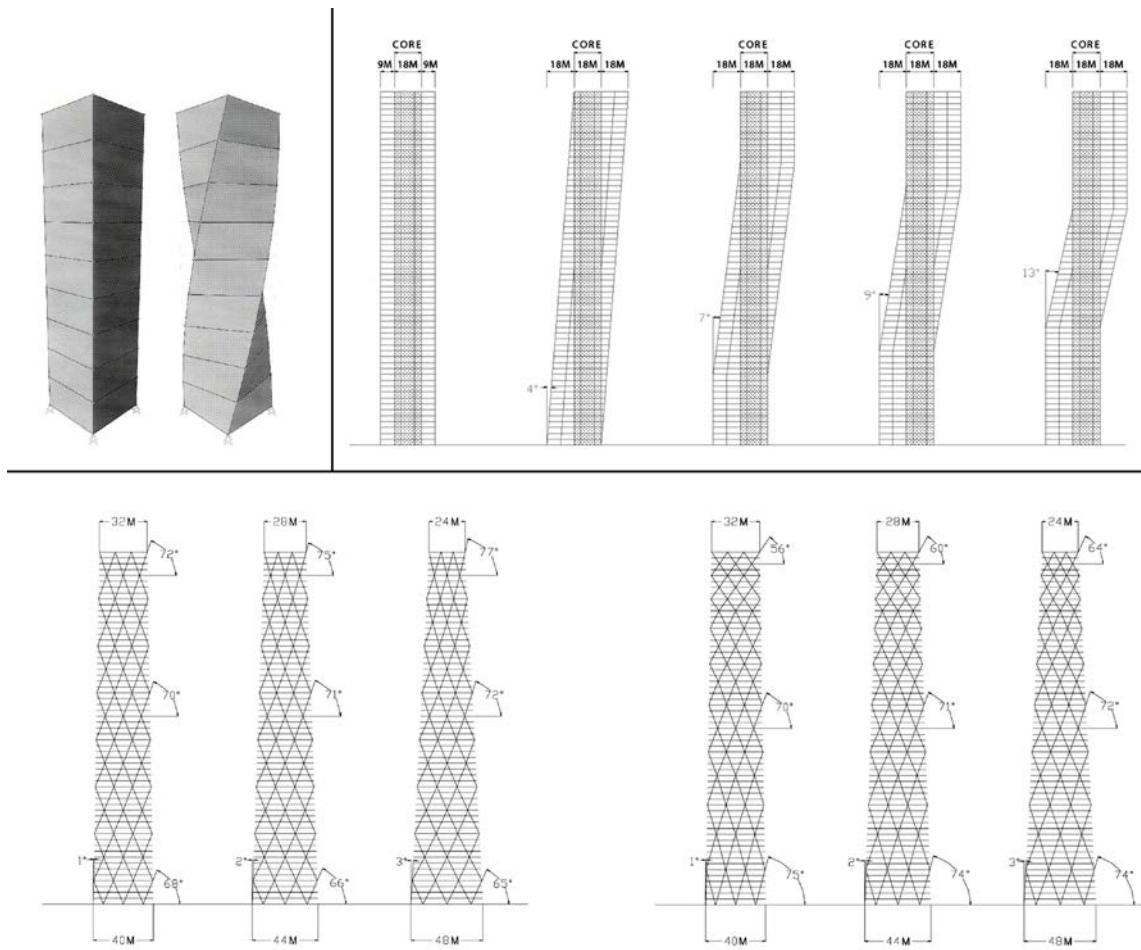
Figure 31. Some of the studied overall forms and diagrid structural layouts; top left: (prismatic vs) twisted; right: tilted with different angles; bottom: tapered diagrids with uniform and varying angles. Source/Credit (©): 'K. S. Moon, "Diagrid Systems for Structural Design of Complex-Shaped Tall Buildings," *Int. J. High-Rise Build.*, 2016' [151]. Courtesy of Kyoung Sun Moon.

The study's findings suggest that in tapered cases, increasing the taper rate enhances lateral stiffness. Similar to the previously mentioned study on diagrids with varying angles, this strategy is beneficial for very tall or slender tapered buildings with high aspect ratios. In such scenarios, the optimal angle for diagrid members increases toward the base. In tilted diagrids, the initial lateral displacement due to gravity is notable, but wind loads result in lateral stiffness comparable to prismatic configurations. In the case of free-form and twisted structures, increasing the rate of plan boundary fluctuations or twist reduces the lateral stiffness of diagrid structures. However, concerning dynamic responses in the crosswind direction, these non-prismatic forms (free-form, twisted, and tapered) outperform conventional prismatic designs because shape variations disrupt the formation of strong vortices along the building's height. This disruption mitigates wind-induced vibrations and prevents the critical phenomenon known as vortex lock-in [151].

In another similar study, also from 2016, K S Moon focused on the outrigger system for tall buildings of complex shapes, i.e., twisted, tilted, and tapered outrigger structures. Figure 32 conceptually illustrates the lateral load-carrying mechanism in an outrigger system, where the outrigger trusses connect the core to the megacolumns, resulting in a counteracting moment (Mc) that reduces the wind-induced overturning moment (Mo). It also shows a prototype structure under wind loads. Examples of outrigger structures are 125 Old Broad Street (formerly Stock Exchange Tower), Montreal, 1964, by Luigi Moretti and Pier Luigi Nervi; Jin Mao Tower, Shanghai, 1999, by Adrian Smith and SOM; Taipei 101, Taipei, 2004, by C Y Lee and C P Wang; Signature Towers, Dubai, 2006, a proposal by ZHA; International Commerce Center, Hong Kong, 2010, by Kohn Pedersen Fox Associates; and Shanghai Tower, Shanghai, 2014, by Gensler.
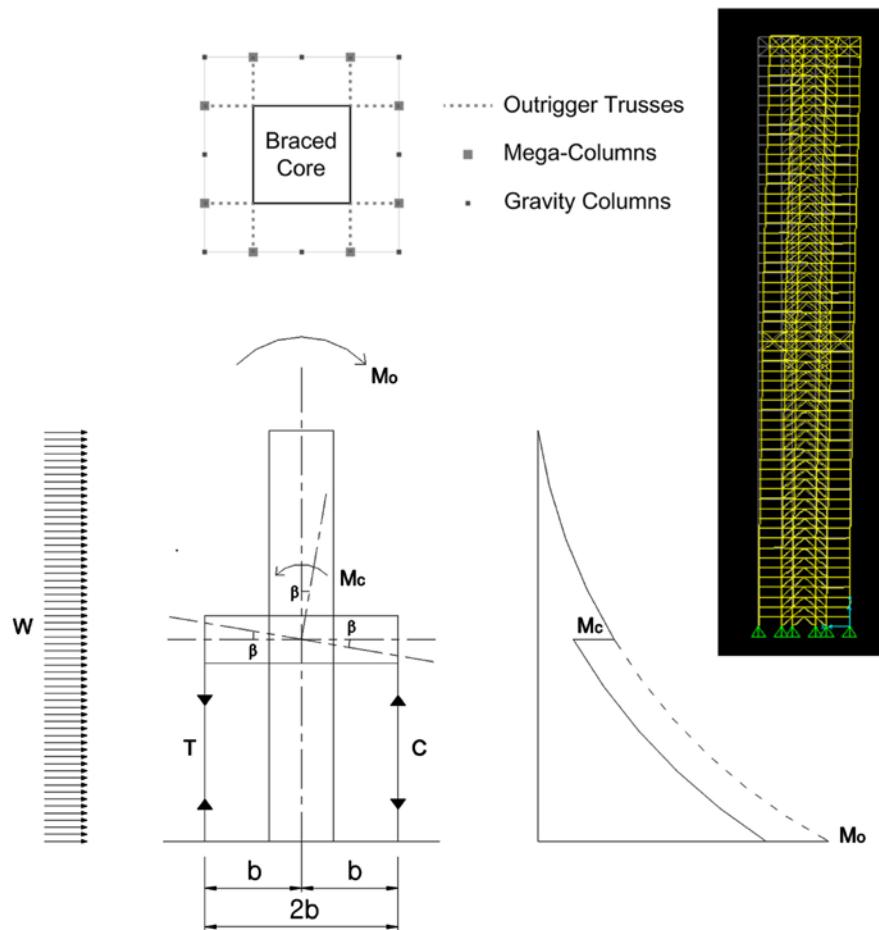
Figure 32. General layout of an outrigger structural system and its mechanism of carrying lateral loads. Source/Credit (©): 'K. S. Moon, "Outrigger Systems for Structural Design of Complex-Shaped Tall Buildings," Int. J. High-Rise Build., 2016' [152]. Courtesy of Kyoung Sun Moon.

The findings of this study on outrigger systems were similar to the aforementioned study on diagrids, with the distinction that, in tilted scenarios, the lateral stiffness of the outrigger system increases as the tilt angles increase. This enhanced lateral stiffness is attributed to the triangulation that occurs among the major components of the outrigger system, including the perimeter megacolumns, outrigger trusses, and the building's braced core [152]. This reduction in lateral displacement with increasing tilt angles is a notable advantage of the outrigger system when compared to two other structural systems commonly used in tilted tall buildings, namely braced tubes and diagrids, as previously identified in a comparative study conducted by K S Moon [153].

K S Moon also conducted two additional comparative studies on structural systems for tapered and twisted tall buildings. The results align with what has been discussed in this subsection: tapered structures exhibit superior lateral stiffness, while in twisted structures, lateral stiffness decreases with increasing twist angles. These findings are consistent across outrigger, braced tube, and diagrid structures [154][155]. It is worth noting that some of K S Moon's more recent studies [156][157] focus on the

structural systems of super tall and mega tall buildings, which fall outside the scope of this dissertation.

How is this related to the study at hand, and what is missing (the gap)?

The research papers by K S Moon et al. reviewed above are important and relevant to the current study. While they did not perform an LCA, their work provides a well-informed starting point for designing the structural systems of tall buildings. It guides the selection of suitable structural types, primarily focusing on the vertical components of these systems, in relation to desired architectural forms. Their research also seeks to find optimal geometric configurations that result in significant reductions in structural material usage during the early design stages. Saving structural materials, ceteris paribus (i.e., with other conditions remaining the same), translates to reduced costs and diminished environmental impacts throughout the life cycle of tall buildings. However, there is still a gap in these geometric configuration studies. They did not specifically address the placement of the vertical structural system in relation to the thermal envelope of buildings. This is a crucial consideration, particularly for contemporary tall buildings with exoskeletons, which often employ braced tube or diagrid systems. As mentioned earlier, buildings employing diagrid exoskeletons are frequently promoted as having diminished environmental footprints attributed to the shading effect produced by the exoskeleton on the thermal envelope. However, these prior studies primarily focused on this shading effect and did not delve into the comparative analysis of employing an exoskeleton versus an endoskeleton. Furthermore, they did not explore the potential impacts on the structural system itself or potential interactions with other building systems, such as HVAC and electric lighting, over the life cycle of tall buildings. This dissertation not only builds upon the findings of these studies but also addresses this research gap, as discussed in greater detail in the subsequent subsections of this section.

2.2.5 LCA; ISO and European Norms

LCA is a broad term addressing methodologies that aim to evaluate the consequences of human actions which are usually in the form of the production of goods. LCA can also assess the consequences of services or other types of decisions. The most common type of LCA focuses on the environmental consequences of production and has been evolving since the 1990's. In the current study, unless explicitly stated otherwise, LCA pertains to the environmental performance of buildings or structures.

A quick reminder: a building's environmental performance is just one aspect of its overall sustainability. The social and economic aspects of a building's performance, which are beyond the scope of this dissertation, are also essential components of sustainability that should be evaluated in a comprehensive sustainability assessment. These facets are outlined in the framework standard EN 15643:2021 [158]. According to EN 1990:2021-10, structures should be designed to minimize adverse impacts on non-renewable environmental resources, society, and the economy throughout their life cycle. This requirement is set by the relevant authority or, if not specified, agreed upon

Die approbierte gedruckte Originalversion dieser Dissertation ist an der TU Wien Bibliothek verfügbar.
The approved original version of this doctoral thesis is available in print at TU Wien Bibliothek.

TU Bibliothek
Your knowledge hub
WIEN

by relevant parties for a specific project. The structure's impact on the environment, society, and the economy can be reduced by selecting suitable construction processes, environmentally friendly materials, considering their production, design solutions, durability, and recyclability [159].

While LCA is widely discussed in the scientific literature and has been employed in numerous research projects to analyze the environmental characteristics of materials, elements, and buildings, there are still doubts and criticisms within the scientific community regarding the accuracy and effectiveness of LCA methods in accounting for all environmental aspects of the built environment [160][161][4].

Common LCA methodologies are input-output, process-based, and hybrid [4], as explained below:

1. Input-output LCA: This method, which has its roots in the 1940s, using aggregate industry data on economic exchanges, it converts all production inputs into economic factors. Applying a rather quick mathematical algorithm, the analysis includes and evaluates all the various upstream material and non-material inputs, which is advantageous. Its disadvantage, however, is that it cannot provide a case-specific analysis for a particular product, location or neighborhood under study, as it only uses average data from the entire industry.

2. Process-based LCA: This method divides a complex process under study into all its sub-processes, then quantifies all inputs and outputs, and repeats the analysis on all inputs until it reaches the place where the raw materials are excavated or harvested, known as the 'cradle'. Its advantage is its ability to evaluate detailed case-specific studies. Its disadvantages are: it is very complex and time-consuming; gathering reliable upstream process information is often challenging; and defining the boundaries deciding which processes are to be included in the assessment is quite arbitrary.

3. Hybrid LCA: Hybrid methods of LCA can be based on either of the aforementioned methods and aim to benefit from the advantages of both methods by combining them [161][4].

International Organization for Standardization (ISO) and European Norms (ENs) for LCA:

Two environmental management ISO reference standards for LCA are ISO 14040:2006 + Amd 1:2020 [162] and ISO 14044:2006 + Amd 1:2017 [163]. The LCA principles and framework described in ISO 14040:2006 + Amd 1:2020 encompass phases shown in the Figure 33, which are: LCA goal and scope definition (includes intended application of results of LCA or LCI), LCI, LCIA, interpretation, reporting and critical review, limitations, etc. This standard does not go through the details of LCA phases techniques and methodologies [162]. ISO 14044:2006 + Amd 1:2017 specifies requirements and provides guidelines to perform an LCA including all the aforementioned phases and the relationships between them [163].

Life Cycle Assessment Framework
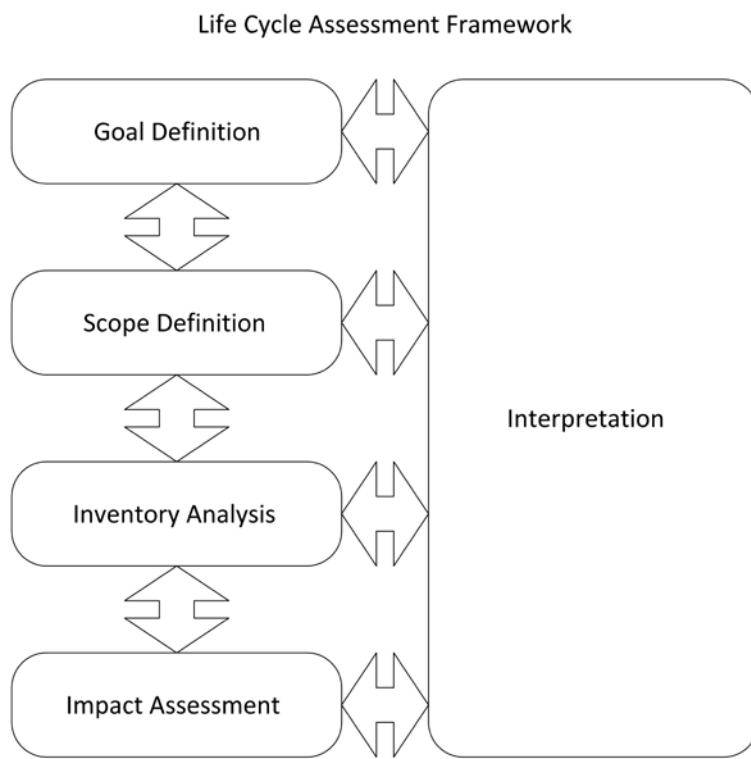
Figure 33. Framework of LCA from ISO 14040:2006 + Amd 1:2020 [162]. Redrawn by the researcher

A European standard with respect to sustainability of construction, EN 15978-1 [164], is dedicated to methodology for the assessment of environmental performance of buildings and sites be it new, old or refurbishment project. Its approach covers all stages of the building life cycle—as listed in Table 5—based on data taken from EPD and other necessary information about processes and services utilized during the life cycle. EPDs need to be made in accordance to EN 15804+A2:2019 [68] that includes core rules for the product category of construction products. While the scope of EN 15978-1 does not include the value judgments and interpretation of the assessment results, the standard explains the following: the assessment object description, the applicable system boundary, the inventory analysis procedure, the list and calculation methods of the main and optional indicators of environmental impacts as well as the relevant technical, management and local aspects, the requirements for calculation data as well as for presentation of the results in communication and reports [164]. A quick reminder: the environmental performance of a building is just one facet of its sustainability. The social and economic performance of the building, which fall beyond the scope of this dissertation, are also components of sustainability that should be evaluated in a sustainability assessment. These aspects are outlined in the framework standard, EN 15643:2021 [158]. As per EN 1990:2021-10, structures should be designed to minimize adverse impacts on non-renewable environmental resources, society, and the economy throughout their life cycle. This requirement is set by the relevant authority or, if not specified, agreed upon by relevant parties for a specific project. The structure's impact on the environment, society, and the economy can be reduced by selecting suitable construction processes, environmentally friendly materials, encompassing their production, design solutions, durability, and recyclability [159].

Table 5. Phases/stages of the building life cycle in accordance with the European Standard EN 15804+A2:2019 [68]. Redrawn by the researcher

Building Life Cycle Stages					Supplementary information beyond the building life cycle
A 1-3 Product	A 4-5 Construction	B 1-7 Use	C 1-4 End of Life		D Benefits and loads beyond the system boundary
A1 Raw material supply / A2 Transport / A3 Manufacturing	A4 Transport / A5 Construction / Installation	B1 Use / B2 Maintenance / B3 Repair / B4 Replacement / B5 Refurbishment	C1 De-construction / Demolition / C2 Transport / C3 Waste processing / C4 Disposal		Potential of reuse, recovery and recycling
		B6 Energy consumption in operation			
		B7 Water use			

Cradle-to-Gate
Cradle-to-Site
Cradle-to-Grave
Cradle-to-Cradle

2.2.6 LCA of Tall buildings Structural Systems

One of the most important literature sources relevant to the current study in terms of topic and background is about a research done by Dario Trabucco et al. (with a funding budget of $ 300,000, and with collaboration of multiple structural engineering and construction companies, contractors, etc.), and it has been published in two versions in 2015 (titled 'Life cycle assessment of tall buildings structural systems' [4]) and 2016 (titled 'A whole LCA of the sustainable aspects of structural systems in tall buildings' [5]). Their research is briefly introduced and discussed here as follows.

What did they do? And what were the variables?

They performed a 'whole' LCA of several types of conventional tall building structural systems. They examined two key environmental performance categories:

Climate Change and Resource Depletion, focusing on two corresponding indicators: GWP and EE, over the life cycle of above-grade structure (aka superstructure) of two generic (hypothetical) rectangular plan-shaped tall office buildings located in downtown Chicago, the USA. The functional unit of their work was the entire building superstructure (two height scenarios: one 246 m height scenario/60-story equivalent, and one 490 m height scenario/120-story equivalent). For each height scenario, they developed eight different configurations for the vertical structure representing some of the most common structural systems for tall buildings (i.e., concrete core with steel frame, concrete core and composite frame, all concrete structure, steel diagrid, and composite diagrid) and with some variations in the types of structural materials and beam sizes (see Figure 34). Two structural design firms worked on each scenario, resulted in 32 bills of materials [5].
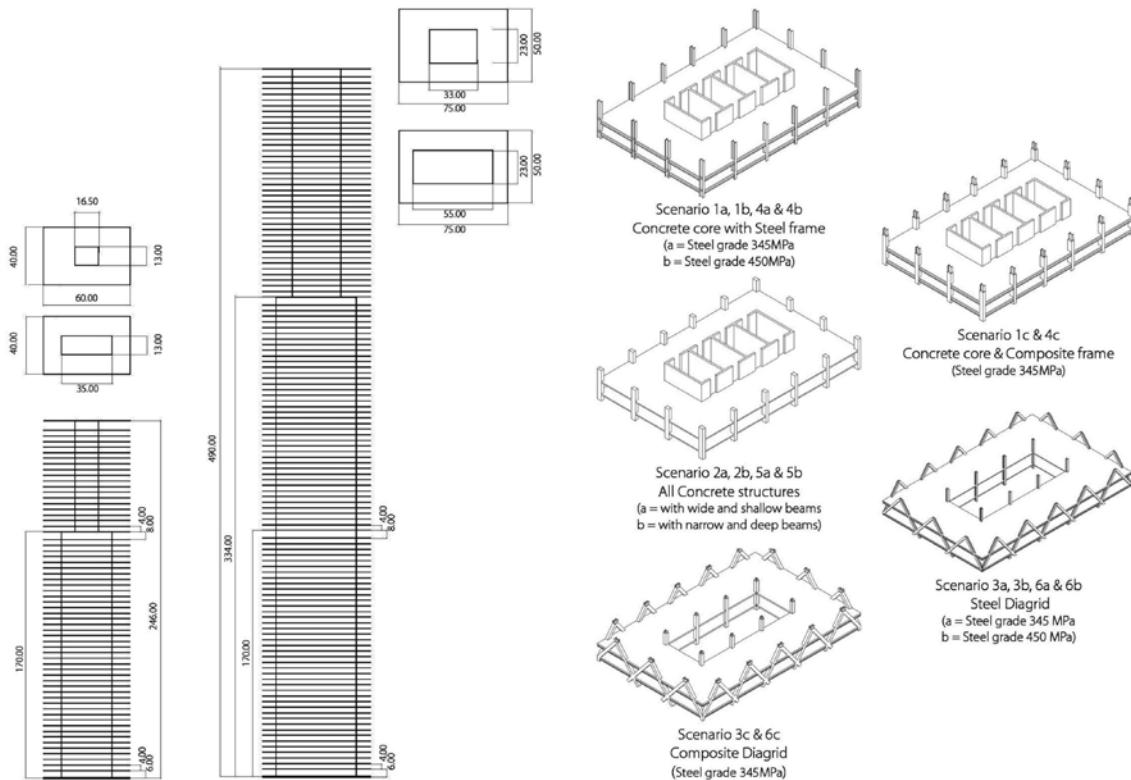
Figure 34. Description of scenarios in the study by Trabucco et al. Source/Credit (©): CTBUH in 'D. Trabucco, A. Wood, O. Vassart, and N. Popa, "A Whole LCA of the Sustainable Aspects of Structural Systems in Tall Buildings," Int. J. High-Rise Build., vol. 5, no. 2, pp. 71–86, 2016' [5]. Courtesy of Dario Trabucco.

They assessed all life cycle stages of A-D except for the stage B (the use stage) which are: product stage, construction process stage, end-of-life stage, and benefits and loads beyond the system boundary with respect to EN 15978:2011 [164] (to recall the life cycle phases, revisit Table 5). Their justification for that exceptional exclusion is that during the occupancy stage, the environmental performance of the building is more dependent on other systems (e.g., curtain walls, HVAC, etc.), and the impact of the structural system is not measurable (which is arguable and this dissertation in particular focuses on that matter in detail).

For the LCI analysis, the quantities of construction materials (i.e., different types of concrete, steel, and spray applied fireproofing) and transportation were estimated for all aforementioned scenarios. Quantities corresponding to transportation (of materials to the site), and horizontal structural elements (i.e, floor beams, slabs, etc.) was adapted from the available data of similar built projects. They also estimated the energy consumption for on-site machinery during construction stage, namely cranes and concrete pumps. For the end-of-life stage, they consulted demolition companies to estimate the energy inputs and CO_2e emission outputs of the required machinery for demolition and transporting materials to the nearby scrapyard and concrete recycling plant. They excluded the 120-story scenarios for this stage as in reality even buildings in the range of 60-story have been very rarely ever demolished (revisit Table 1).

LCIA was done by applying characterization factors (e.g., amounts of $kgCO_2e$ emission or MJ energy per kg material) to each elementary flow (materials, operations, etc) accounted in the LCI to find out the environmental impact caused by all the flows. They derived most of the characterization factors from Ecoinvent database. In case of concrete they found it very difficult to find a unique characterization factor because the mix of concrete is influenced by multiple factors depending on design decisions (e.g., strength, workability) as well as external factors (e.g., distance from mixing plant, external temperature at pouring time). In view of this, they used two sets of values for each grade of concrete: one derived from the French database of Syndicat National du Beton Pret a l'Emploi, and the other one based on processing many EPDs by concrete producers in San Francisco, the USA. They noticed that the environmental performance of concrete can also significantly be influenced by contour factors (e.g., mix of energy and modernity of plant and production infrastructure, chemical composition of raw materials, etc.) [4][5].

What were the results and findings?

Figure 35 and Figure 36 show the cumulative results (life cycle stages A1-C3) of the study by Trabucco et al. [5], comparing different types of tall building structural systems in terms of EE and GWP.

60-story equivalent scenario - GWP (A1-C3)

	1a Normal Steel + concrete core	1a Normal Steel + concrete core	1b High Strength + concrete core	1b High Strength + concrete core	1c Concrete core and composite frame	1c Concrete core and composite frame	2a All concrete wide and shallow beams	2a All concrete wide and shallow beams	2b All concrete narrow and deep beams	2b All concrete narrow and deep beams	3a All steel diagrid normal steel	3a All steel diagrid normal steel	3b All steel diagrid HS steel	3b All steel diagrid HS steel	3c Composite diagrid	3c Composite diagrid
French Ready Mix Association A1-C3 GWP [t CO2e]	22.057	19.194	21.902	18.831	21.564	18.766	21.592	27.298	18.988	23.147	23.542	21.812	21.399	21.115	22.751	19.453
US EPDs A1-C3 GWP [t CO2e]	24.657	20.800	24.501	20.437	24.323	20.441	27.294	32.116	23.816	28.528	24.679	22.949	22.536	22.252	24.160	21.295

Labels on graph: 100%, 118%, 105%, 102%

Figure 2. Graph 1: LCA results of the 60-story equivalent scenario for global warming potential. Source: CTBUH.

60-story equivalent scenario - EE (A1-C3)

	1a Normal Steel + concrete core	1a Normal Steel + concrete core	1b High Strength + concrete core	1b High Strength + concrete core	1c Concrete core and composite frame	1c Concrete core and composite frame	2a All concrete wide and shallow beams	2a All concrete wide and shallow beams	2b All concrete narrow and deep beams	2b All concrete narrow and deep beams	3a All steel diagrid normal steel	3a All steel diagrid normal steel	3b All steel diagrid HS steel	3b All steel diagrid HS steel	3c Composite diagrid	3c Composite diagrid
French Ready Mix Association A1-C3 EE [GJ]	244.424	216.702	242.404	211.972	235.764	209.916	207.121	279.177	185.091	238.914	289.123	266.519	261.258	257.472	270.043	225.903
US EPDs A1-C3 EE [GJ]	263.987	231.539	261.966	226.809	256.308	225.305	251.875	321.772	221.318	276.970	300.208	277.604	272.343	268.557	283.307	240.998

Labels on graph: 100%, 105%, 116%, 108%

Figure 3. Graph 2: LCA results of the 60-story equivalent scenario for embodied energy. Source: CTBUH.

Figure 35. GWP and EE results of the 60-story scenarios in the study by Trabucco et al. Source/Credit (©): CTBUH in 'D. Trabucco, A. Wood, O. Vassart, and N. Popa, "A Whole LCA of the Sustainable Aspects of Structural Systems in Tall Buildings," Int. J. High-Rise Build., vol. 5, no. 2, pp. 71–86, 2016' [5]. Courtesy of Dario Trabucco.

120-story equivalent scenario - GWP (A1-C3)

	4a Normal Steel + concrete core	4a Normal Steel + concrete core	4b High Strenght + concrete core	4b High Strenght + concrete core	4c Concrete core and composite frame	4c Concrete core and composite frame	5a All concrete wide and shallow beams	5a All concrete wide and shallow beams	5b All concrete narrow and deep beams	5b All concrete narrow and deep beams	6a All steel diagrid normal steel	6a All steel diagrid normal steel	6b All steel diagrid HS steel	6b All steel diagrid HS steel	6c Composite diagrid	6c Composite diagrid
French Ready Mix Association A1-C3 GWP [t CO2e]	108.010	109.405	108.010	105.912	90.417	97.642	87.190	101.714	79.525	95.435	130.250	125.222	126.519	125.222	86.208	90.375
US EPDs A1-C3 GWP [t CO2e]	119.482	125.225	119.482	121.731	103.182	116.491	107.845	125.841	97.610	116.991	133.592	144.832	129.860	144.832	95.780	101.294

Figure 4. Graph 3: LCA results of the 120-story equivalent scenario for global warming potential. The structural solution for scenarios 6a and 6b (steel diagrid) proved to be unsuitable for a 120-meter tower. Source: CTBUH.

120-story equivalent scenario - EE (A1-C3)

	4a Normal Steel + concrete core	4a Normal Steel + concrete core	4b High Strenght + concrete core	4b High Strenght + concrete core	4c Concrete core and composite frame	4c Concrete core and composite frame	5a All concrete wide and shallow beams	5a All concrete wide and shallow beams	5b All concrete narrow and deep beams	5b All concrete narrow and deep beams	6a All steel diagrid normal steel	6a All steel diagrid normal steel	6b All steel diagrid HS steel	6b All steel diagrid HS steel	6c Composite diagrid	6c Composite diagrid
French Ready Mix Association A1-C3 EE [GJ]	1.219.233	1.227.723	1.219.233	1.182.238	961.564	1.039.256	847.854	988.060	782.172	940.617	1.637.140	1.393.478	1.588.556	1.393.478	965.166	1.017.568
US EPDs A1-C3 EE [GJ]	1.296.106	1.321.045	1.296.106	1.275.560	1.046.546	1.147.458	1.001.407	1.160.026	910.662	1.087.520	1.669.722	1.505.531	1.621.137	1.505.531	1.032.224	1.089.156

Figure 5. Graph 4: LCA results of the 120-story equivalent scenario for embodied energy. The structural solution for scenarios 6a and 6b (steel diagrid) proved to be unsuitable for a 120-meter tower. Source: CTBUH.

Figure 36. GWP and EE results of the 120-story scenarios in the study by Trabucco et al. Source/Credit (©): CTBUH in 'D. Trabucco, A. Wood, O. Vassart, and N. Popa, "A Whole LCA of the Sustainable Aspects of Structural Systems in Tall Buildings," Int. J. High-Rise Build., vol. 5, no. 2, pp. 71–86, 2016' [5]. Courtesy of Dario Trabucco.

The 120-story all-steel diagrid scenario was removed from their results because it turned out to be over-designed (a concrete core is normally needed to support lateral loads in buildings of that shape and size) [4][5]. Other than that, in all other cases, the diagrid system appeared to be the optimal or near-optimal solution. In all scenarios, the most influential stages turned out to be the cradle-to-gate or material production stages (A1-A3). Each and every other stage (i.e., construction stage including transportation to site: A4-A5, end-of-life stage: C, and the benefits and loads beyond the system boundary: D) showed overall a relatively small influence compared to the "cradle-to-gate" stage. Figure 37 shows the unfolded results of one of the scenarios, as an example similar to all other scenarios in this regard: the much higher impact of the materials production stage compared to all other stages of the life cycle is evident.
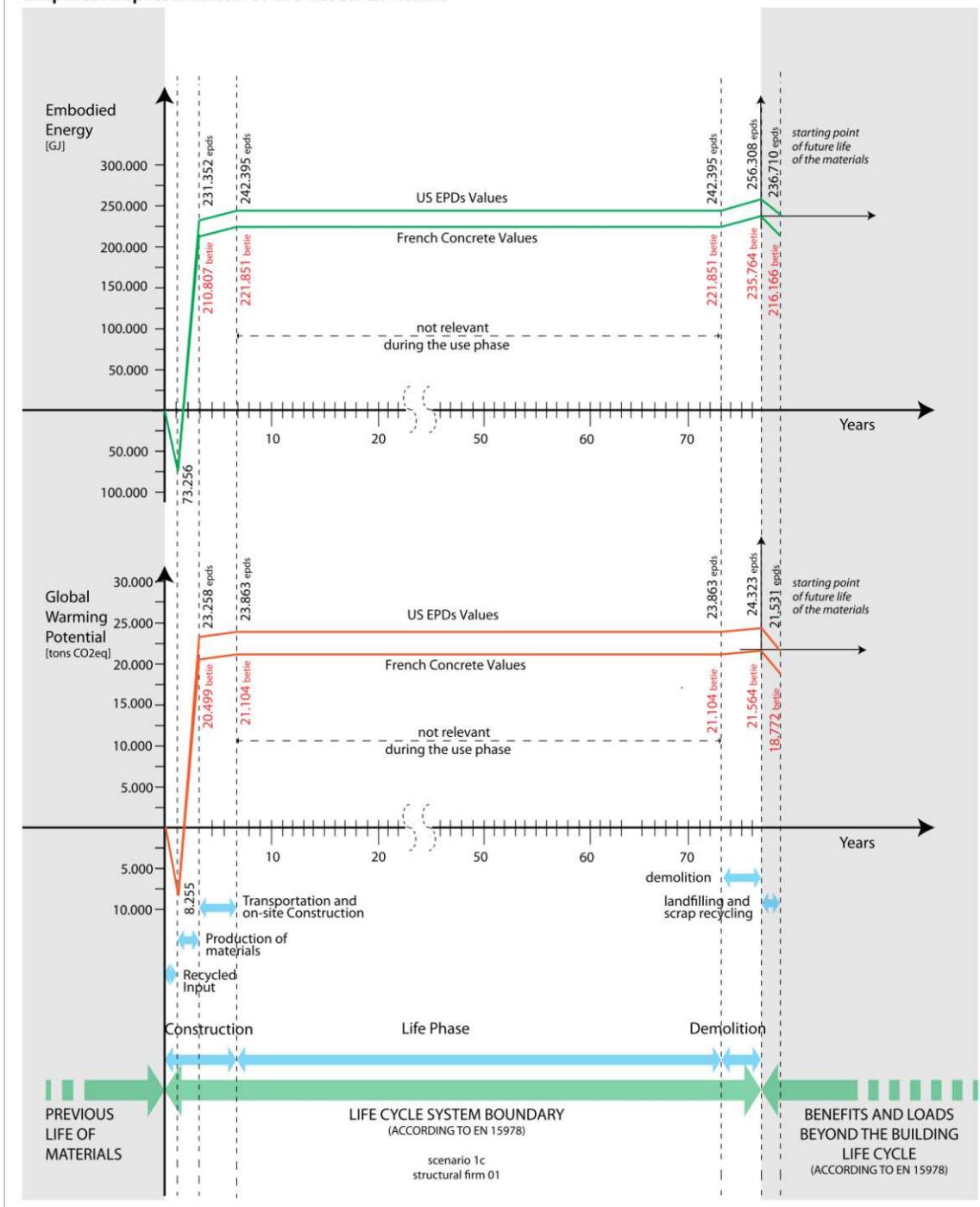
Figure 37. Production of materials proved to be by far the most impactful stage of the life cycle of the tall buildings structural systems not only in the scenario presented in this figure but also in all scenarios of the in the study by Trabucco et al. Source/Credit (©): CTBUH in 'D. Trabucco, A. Wood, O. Vassart, N. Popa, and D. Davies, Life Cycle Assessment of Tall Building Structural Systems. Chicago: Council on Tall Buildings and Urban Habitat, 2015' [4, p. 124]. Courtesy of Dario Trabucco.

The results with respect to the stage D (benefits and loads beyond the system boundary) showed greater improvements for scenarios using more steel than concrete because metals can be recycled to materials with similar properties while concrete usually recycles with downgrading. The environmental impact (EE and GWP) of transportation of construction materials and demolition typically showed a small

72

percentage of the total life cycle impact (1-3%), suggesting that it can be optimal to transport structural materials (namely recycled metals) with smallest environmental impacts in their production stage from further distances to the construction site instead of using some local materials with large amounts of those impacts.

They found out that using environmentally friendly materials (referring the materials with minimum environmental impacts found in the studied EPDs) can reduce EE and GWP up to 28% and 50%, respectively, in the whole-building structural scenarios during life cycle stages A1-C3. It is also worth mentioning that, in their results, the total weight and environmental impacts (EE and GWP) of sprayed fireproofing materials appeared negligible compared to those of concrete or steel [4][5] (for more LCA information about some spray-applied fire resistive materials, e.g., see [165]).

They also noticed that the results of such LCA studies are very case-sensitive because some small decisions or uncontrollable parameters (e.g., in design, selection of materials, form of the building, unusual shapes and slenderness, location, etc.) can largely influence the results; therefore, while the research results contribute a lot to better understanding of environmental impacts of tall buildings structural systems and improves the general knowledge of architects, engineers, clients, contractors and other stakeholders in planning, design, construction and use of tall buildings, they should not be generalized for other cases in buildings whose conditions significantly vary from those of the studied cases.

Two other conclusions in that research are: (1) Horizontal structural elements (e.g., floor slabs, beams, etc.) comprised around 50-80% and 30-60% of total weight of structural systems in the 60-story and 120-story scenarios respectively; (2) Using CR materials (e.g., fly ash, furnace slag, or silica fume) in the mix of concrete can significantly reduce the GWP and EE (and particularly in hot climates, when large amounts of concrete are poured, use of fly ash also benefits in reducing the hydration heat) [4][5][166][167].

How does it relate to the current study and what is still missing in the literature (the gap)?

The interactions of the structural system with other systems that are environmentally impactful during the use stage of tall buildings, namely HVAC and electric lighting systems, were not assessed in the research by Trabucco et al. [4][5]. In fact, the use stage of tall buildings is particularly very important because as mentioned earlier the taller the buildings are, the longer their average lifespan (as mentioned earlier, e.g., only very few of tall buildings over 150 m height have ever been demolished in the whole world [15][16], see Table 1), and exactly because of their virtually endless lifespan, it is important to find out how the structural system may influence the environmental performance of tall buildings during their use stage. Of course, since PSEs usually require very little to no maintenance or repair or replacement during the use stage in tall buildings, one might question the necessity of focusing on this stage of the life cycle of structural systems, but that argument could be only valid when the focus of the LCA is merely on the structural system (which is the case in the aforementioned research by Trabucco et al. [4][5]) and not its possible interactions with

other systems. Therefore, (emphasizing the great contribution and lessons learned from that study and others about comparing multiple types of structural systems in tall buildings), still an alternative or complementary study is needed in a way that not only focuses on structural systems but also considers the plausible interactions that the structural systems may have with other systems which are known impactful during the use stage. In this view, for instance, a comparison between using exoskeletons versus endoskeletons could be beneficial, because an exoskeleton may affect the way the interior space interacts with the outdoor environment (in terms of receiving solar radiation, shading, temperature, natural light, etc.) that may affect the energy consumption and CO_2e emissions corresponding the HVAC and electric lighting systems, in a different way compared to a case when an endoskeleton of similar structural type is utilized. Moreover, during the use stage of tall building structural systems which is usually very long, many other factors that affect the aforementioned systems may also change, for instance: the energy mix of electricity production used to feed those systems, weather temperature due to climate change, the density of buildings in the neighborhood that may cast shadow on the building, etc. These and more factors may affect the way a structural system interacts with those other systems, so, it might also affect the environmental impact in a tall building over decades if not centuries. This dissertation, therefore, aims to fill that gap in the literature, as much as it can, with regard to the impact of using exoskeletons (vs endoskeletons) on the life cycle environmental performance of tall buildings.

2.2.7 Tall Buildings Floors and Structural Systems; EE

One of the important and widely cited papers in the literature on LCA of tall building structural systems is a paper by Foraboschi et al., published in 2014 [6]. The main input variable in their study was the type of floor structure. They focused on floors because floors in total are the most massive component in tall building structural systems. Their analysis included six common floor types as follows: (a) steel–concrete floor, a composite structure made of concrete (including steel mesh) poured over corrugated sheets; (b) RC slab or conventional full-weight floor slab; And a group of four lightweight types of RC floors (consisting of certain cases of hollow core or voided slabs using lightweight products that are placed to reduce the need for the poured concrete) which are: (c) polypropylene blocks; (d) low-density polystyrene blocks combined with thin pre-cast concrete planks; (e) high-density polyethylene spheres; (f) polypropylene elements providing empty spaces in the lower parts of floors, as they are removed once the poured concrete reaches sufficient hardness [6].

They combined the aforementioned floor types into some hypothetical generic reference structures ranging from 20,30,40,..., up to 70 floors (4 m height for each floor) with RC central cores and rigid frames either made of steel or RC (with columns placed only at the building perimeter), and analyzed all the combinations and calculated the EE for each scenario. The slenderness ratio (ratio of height to width) of the building models ranged from 5 to 7. They used finite element modes for structural analysis and they included common gravity-related dead and live loads as well as wind loads and met the horizontal displacement limit of 1/400 of the height in all scenarios to make them comparable. They calculated the quantities of structural materials (inventory), and then regarding the life cycle environmental impact, only calculated the primary EE— of the whole/parts of the structural systems, or the intensity expression thereof per

corresponding NRA—with respect to the cradle-to-gate stage of the life cycle, and justified this selection on the grounds that it is the stage of the life cycle of tall building structural systems that consumes the most primary energy, while all other stages have a relatively marginal impact (e.g. transportation, construction, use stage) or occur in the very long term and also marginally (e.g., demolition, recycling, etc.). In addition, some of the omitted stages can also be very site-specific (e.g., transportation to the construction site) and therefore cannot contribute much to this type of research aimed at conventional tall buildings and not at a very unique building case [6].

What did they find and how does it relate to this doctoral research?

The findings of the study by Foraboschi et al. [6] confirmed that the floors are the most crucial parts of tall buildings' structural systems, as they include the largest portion of the entire EE. Their findings indicated that the conventional full-weight RC slabs resulted in significantly less amount of EE compared to other types of floor structures, including the lightweight ones. In other words, this study demonstrated that structures with lower weight are not necessarily more environmentally friendly (namely with respect to EE), and the researchers and practitioners should consider the life cycle environmental impact of structures in order to choose appropriate materials and combinations that serve to reduce those impacts. The case studies also showed that the structures with RC frames have significantly less EE than those of steel frames. Figure 38 shows these results [6].
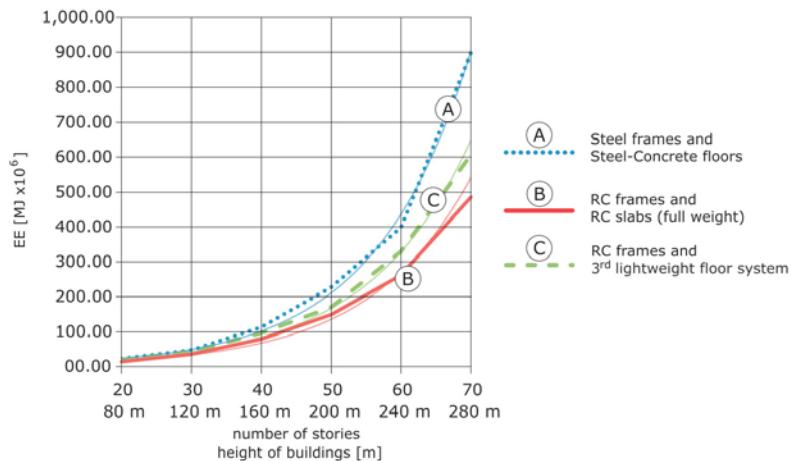
Fig. 6. Total EE consumed by the entire structure (columns, core, floors, primary beams, and secondary beams where they exist), as a function of the height of the building (or of the number of stories), for different frames and floor types. The figure also includes the continuous curves that interpolate the points (discontinuous curves) obtained from the analyses.
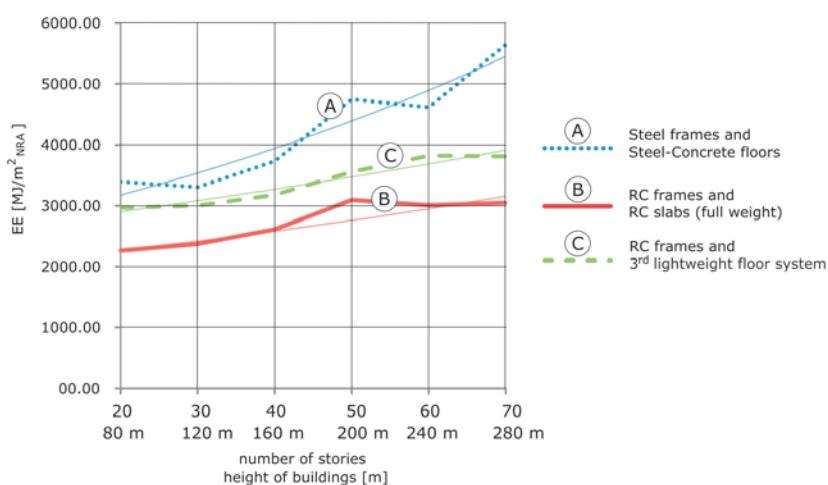
Fig. 7. EE per square meter of NRA: unitary value of the EE considered in Fig. 6. The figure also includes the continuous curves that interpolate the points (discontinuous curves) obtained from the analyses.

Figure 38. Some of the results of the study by Foraboschi et al. Source: 'P. Foraboschi, M. Mercanzin, and D. Trabucco, "Sustainable structural design of tall buildings based on embodied energy," Energy Build., vol. 68, no. PARTA, pp. 254–269, 2014' [6].

In all the cases examined in the previous research, the analysis was limited to the structural systems, with no consideration given to potential interactions between the structural system and other building systems, especially the key components during the operational phase, such as HVAC and electric lighting systems. While the findings of that study illuminated certain previously unexplored facets of the LCA of structural systems in tall buildings, particularly regarding floor systems, the aforementioned significant research gap persisted that this thesis seeks to address by exploring the implications of employing exoskeletons (vs endoskeletons) on the life cycle environmental performance of tall buildings.

2.2.8 Effect of Structural System (interacting with building services) on Life Cycle CO₂e Emissions

"Effects of structural system on the life cycle carbon footprint of buildings" [8] is the title of a study by Z. Moussavi, and A. Akbarnezhad, published in 2015. It is one of the few significant studies that has closely examined the carbon emissions of structural systems in all phases of the building life cycle and has focused on the effect of the design and thermal mass of the structural system in the operational phase, including heating, cooling, and electric lighting.

With respect to the pre-operational phase, they have compared the results of their study on a location in the USA with other studies conducted in Europe, Asia, and North America (i.e. Sweden, Greece, Japan, Singapore, and Canada). What is clear from the results is that the material extraction and processing stage is by far the most carbon-emitting phase for both steel and RC structures in all studies (ranging between 87 to 731 $kgCO_2e/m^2$ area), compared to rather a marginal share of emissions associated with the construction stage (ranging between 1.8 to 16 $kgCO_2e/m^2$ area), and the transportation stage (ranging between 0.3 to 14 $kgCO_2e/m^2$ area) [8].

In the aforementioned research, buildings with 3 (low-rise), 10 (mid-rise), and 15 (high-rise) stories were assessed in a total of 15 scenarios as the multiplication of 3 heights and 5 different structural systems and materials (see Figure 39). E.g., the high-rise prototypes were: RC with moment resisting frame, RC with shear walls, steel with moment resisting frame, steel with braced frames, and steel with moment resisting frame and braced frames. The thermal mass of all structural elements were taken into account in their models. The range of results of different stages of life cycle of tall buildings was (the unit of all the following numbers is $kgCO_2e/m^2$ area): material extraction and manufacturing (181-204), transportation (6-14), construction (8-16), operation (1206-1595), end-of-life including demolition and transportation (5-8) [8]. The lowest operational carbon footprint corresponded to the RC with shear walls, which incorporated shear walls placed at the perimeters (partially similar to an exoskeleton integrated into the facades). Although the researchers investigated all stages of buildings life cycle, the results for all alternatives showed that two stages—material extraction and manufacturing, and operation—were far more dominant than the other stages, i.e., transportation, construction, and end-of-life stage that had only marginal to negligible share from a holistic point of view.
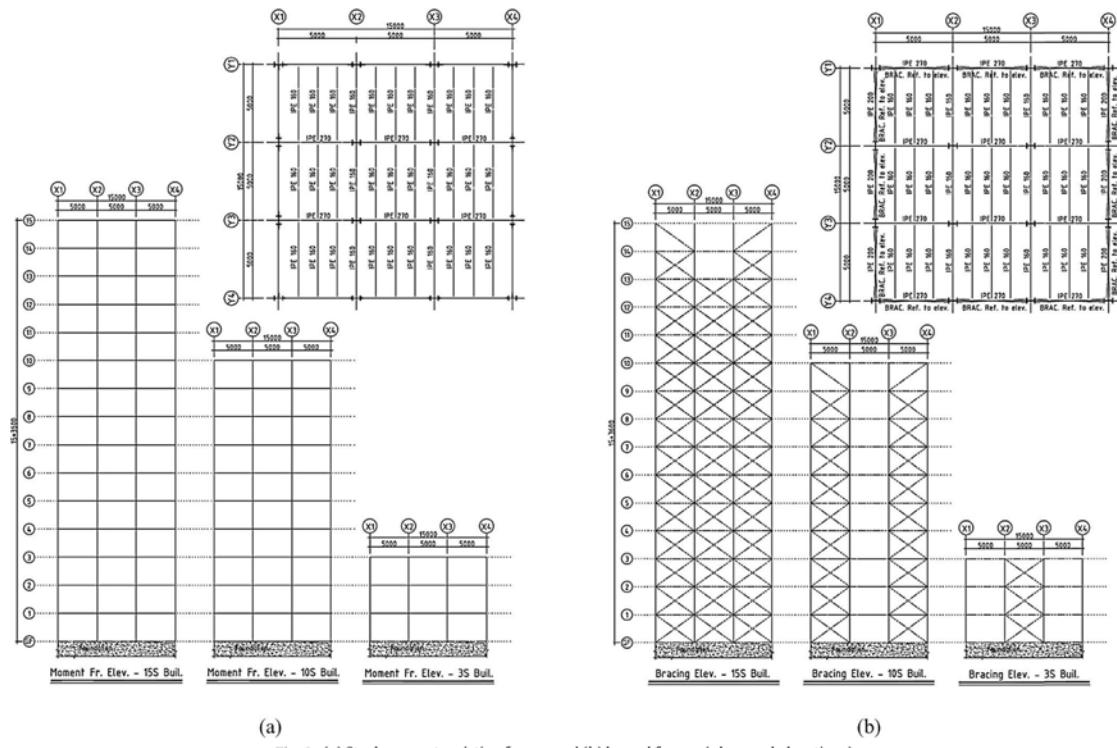
Fig. 1. (a) Steel moment resisting frames and (b) braced frames (plans and elevations).
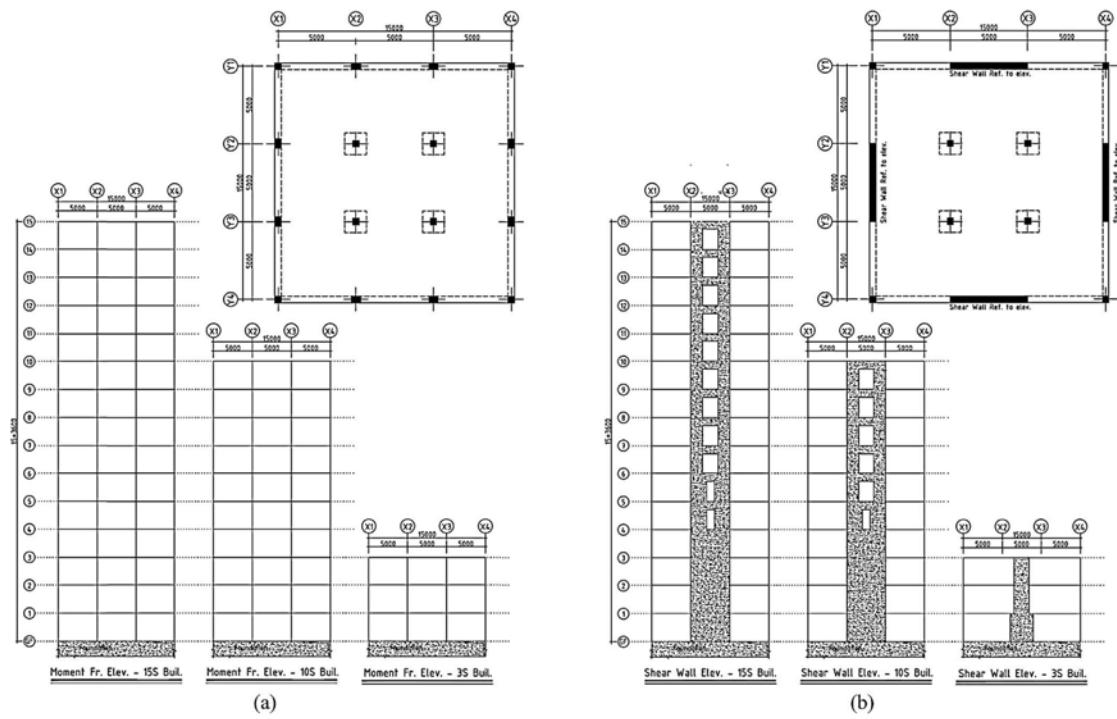
Fig. 2. (a) Concrete moment resisting frames and (b) dual moment resisting and shear wall frames (plans and elevations).

Figure 39. Alternatives of structural systems studied by Moussavi and Akbarnezhad [8]; Source/Credit (©): 'Z. S. Moussavi Nadoushani and A. Akbarnezhad, "Effects of structural system on the life cycle carbon footprint of buildings," *Energy Build.*, vol. 102, pp. 337–346, 2015'. Courtesy of Zahra S. Moussavi Nadoushani.

What is still missing? (The gap in the literature)

78

The aforementioned paper is not focused on exoskeletons, i.e., no alternative exoskeletons that can cast shadows on facades were studied. As mentioned earlier, these exoskeletons are claimed to save operational primary energy and reduce emissions under certain conditions. Furthermore, contextual scenarios and their effects were not taken into account; e.g., interactions with the urban neighborhood (as buildings can cast shadows or reflect sunlight to each other), the effect of climate change during the operational phase, the development of new technologies of HVAC and electric lighting, and possible improved electricity production leading to lower operational emissions in the long term, etc. Therefore, despite the importance of that study, it cannot answer the research questions of the current study. However, what was learned in that study was used to design this research more efficiently and effectively, specifically by focusing on the life cycle stages that have the most impact, allowing more contextual factors to be investigated rather than going into details of stages that have a marginal impact.

2.2.9 Tall building Exoskeleton Optimization; Mass and Thermal

Energy/Solar Radiation

For the purpose of introducing the scientific niche/gap in the literature, this subsection reviews and analyzes an interesting and award-winning architectural engineering research (ASCE Award Winning Journal Papers, Journal of Architectural Engineering 2019 Best Paper Award, [168]) which is one of the closest published scientific papers to the current study in terms of the subject matter; this paper by Felkner et al. (entitled "Framework for Balancing Structural Efficiency and Operational Energy in Tall Buildings") [11] specifically addresses the impact of the use of exoskeletons in tall buildings on the structural mass and operational energy consumption of these buildings.

Why is it important?

Their research is important because it is one of the very few publications to date that have demonstrated a quantitative method and tangible examples (case studies) that take into account both structural and space heating and cooling energy demands in order to find optimal integrative solutions that aim to minimize structural mass and operational (to be more precise, thermal-) energy demand at the same time. The paper shows the effect of different exoskeletons design alternatives on thermal energy demand by simulating buildings, and uses the Pareto efficiency method for optimization. Normally, these aspects (minimizing structural mass or thermal energy demand) have been addressed in separate quantitative research, i.e., each study focused on only one of them. Some other papers have addressed both aspects or even more, but only in a descriptive qualitative sense and have not presented a practical quantitative evidence-based example of a method showing how to cover those aspects and find integrative optimal solutions.

What did they do and what were the results?

They have proposed an optimization framework and applied it in a case study on multiple generic tall building design alternatives with differences in height, climate, and mainly exterior columns design as the main variable of interest. The aim of

optimization was to minimize at the same time the total weight of the structural system and the space heating and cooling energy demands. Figure 40 presents the framework and the computational tools used in the study [11].
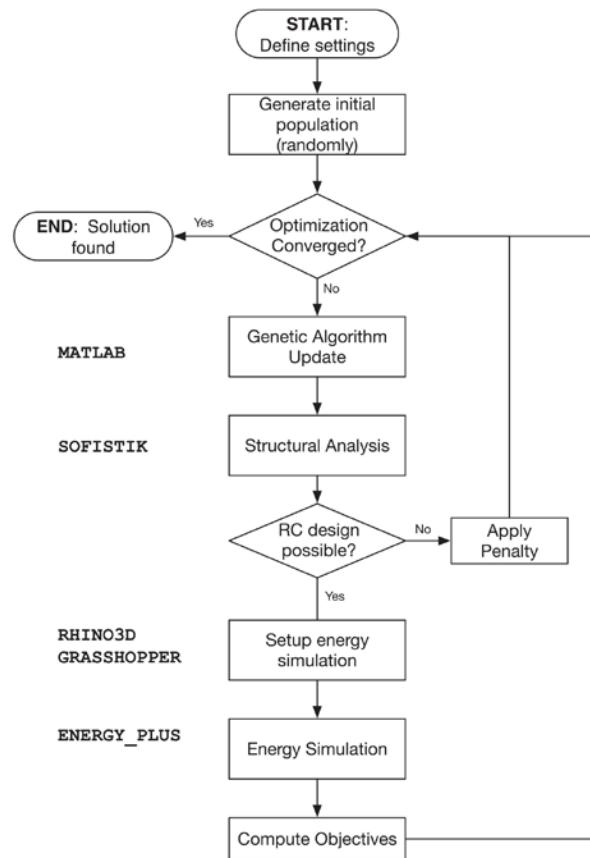
Figure 40. Multiobjective optimization framework in the study by Felkner et al. [11]. Source/Credit (©): 'J. Felkner, J. Schwartz, and E. Chatzi, "Framework for Balancing Structural Efficiency and Operational Energy in Tall Buildings," *J. Archit. Eng.*, 2019'. Courtesy of Juliana Felkner.

The optimization framework they proposed is based on two older methods: genetic algorithms and multiobjective optimization, which are briefly presented below:

Genetic algorithm:

First developed by J. H. Holland in the 1960s and 1970s [169], it is a method for solving optimization problems based on a natural selection process that mimics biological evolution through iterative procedures of crossover, recombination, and mutation procedures leading to adaptation to a particular objective (e.g., minimization, maximization), through survival of the fittest among the population that is the set of all chromosomes [170][11]. The design variables are represented by genes that constitute chromosomes (also known as candidate solutions or alternatives). At each iteration, to adapt the population of the candidate solutions to a specific objective function, offspring are bred from a certain number of fittest parents. Selection determines which parents to combine ge-netic information through a mating procedure which is called crossover. Mutation ensures diversity by introducing random variations of genes (see Figure 41) [11].
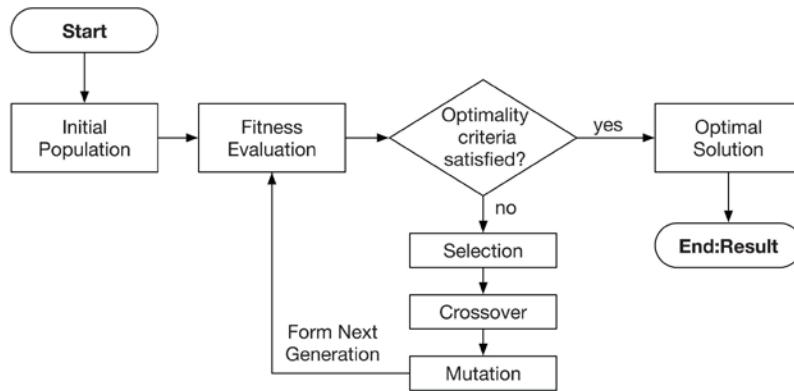
Figure 41. Overview of typical genetic algorithm. Source/Credit (©): 'J. Felkner, J. Schwartz, and E. Chatzi, "Framework for Balancing Structural Efficiency and Operational Energy in Tall Buildings," *J. Archit. Eng.*, 2019' [11]. Courtesy of Juliana Felkner.

Multiobjective optimization with Pareto front:

A multicriteria or multiobjective optimization problem can be shown as follows (see Equation 1) [171]:

Equation 1.

$$minimize \ [f1(x), f2(x), \ldots, fk(x)] \quad x \in S, k \geq 2$$

; where: *x* is the design variables; the set of general constraints for *x* is *S*, and the individual objective functions are *fi(x)*. No *x* can minimize all *fi(x)* at the same time, except in some special cases, and instead, the concept of Pareto (or non-dominated) optimality applies, which means: a design is considered Pareto-optimal if an improvement of the solution at one objective cannot occur without deterioration at another objective. Therefore, there are no unique solutions, but a set of potential non-dominant solutions, known as Pareto front (see Figure 42) [11].
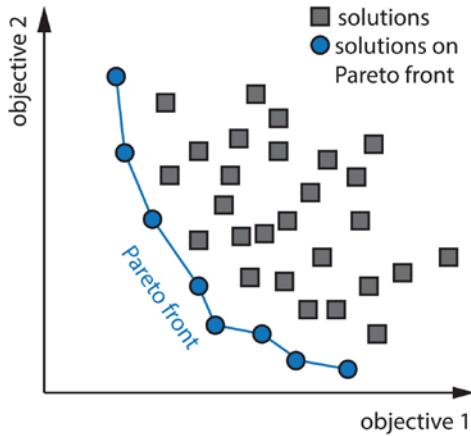
Figure 42. Pareto front example. Source/Credit (©): 'J. Felkner, J. Schwartz, and E. Chatzi, "Framework for Balancing Structural Efficiency and Operational Energy in Tall Buildings," *J. Archit. Eng.*, 2019' [11]. Courtesy of Juliana Felkner.

One way to treat a multiobjective problem is to reduce it to a scalar problem by generating a weighted average of objective functions [171]. These weighting schemes are arbitrary and require many variations to cover all possible combinations. As a more sophisticated method, evolutionary algorithms (e.g., genetic algorithms) have been suggested for solving multiobjective optimization problems, since multiple Pareto-optimal solutions can be found with a single simulation run [172][11].

Their case study application

Three generic (hypothetical) prototypes of wind-resistant exterior structures (with a height of 30, 50 and 70 stories, 3.5 m each) were modeled in order to see the effect of the design (depth and width) of the exterior columns on the structural mass and the operational energy demand for space heating and cooling (see Figure 43) [11].

Structural Analysis

The structural models included RC columns, floor slabs, and core walls. A commercial software program (SOFiSTiK) was used for structural analysis and design of columns, slabs, spandrel beams, and core walls. A maximum displacement equal to one 500th of the total height of the structure was considered to be met for the feasibility of the structures. For simplification: all floor plans were quadratic, with 9 columns on each side; and the thickness of core walls was preset according to some rules of thumb (10 cm for the top 10 floors, with an increase of 10 cm every 10 floors); a fixed amount of wind lateral loads was applied at all different sites/cities (reference wind velocity: 90 km/h = 25 m/s). The exterior tubes consisted of the peripheral columns (with variables: depth and width) connected by quadratic spandrel beams (25 cm), and floor slabs (25 cm thick) that transferred loads to the central core. The taller structures had larger cores. The materials were concrete (nominal strength of 35 MPa) and reinforcement steel (yield strength of 500 MPa). They performed two groups of simulation experiments: one with constant column width and depth on all 4 sides of the structure (2 variables); and one with 8 variables (width and depth of columns differing on 4 sides of the structure) [11].

82

Space thermal energy demand (heating and cooling)

They used EnergyPlus for space thermal energy simulation via the Diva interface in Rhinoceros/Grasshopper (GH). The facades were considered fully glazed (i.e., one case with no peripheral columns shading the facades) in their baseline thermal energy model. In the other cases, all four sides of the peripheral/exterior columns were modeled (identically to the aforementioned structural models) as fixed shading components. They run the simulations with hourly weather data files from 4 USA cities of Boston (humid continental), Houston (humid subtropical), Phoenix (desert), and San Francisco (temperate). For simplification, they modeled one floor with adiabatic surfaces on top and bottom (meaning no transfer of heat to adjacent zones). The entire floor area of a typical office building floor was considered a single zone in the model. The optimization problem they addressed, as mentioned above, was aimed to minimize the outcomes of three functions at the same time: the total mass of the structural system, space heating energy demand, and space cooling energy demand. They used a genetic algorithm tool in MATLAB R2012a called gamultiobj set with a population size of 20 and a maximum number of generations of 100 [11].

Results

They compared the tradeoffs between the normalized space thermal energy demands (expressed as percentages compared to the fully glazed facade scenario) and the mass of the structural system in different scenarios and different climates. Figure 43 shows the results with respect to the first group of experiences, where the columns were identical on all sides of buildings [11].
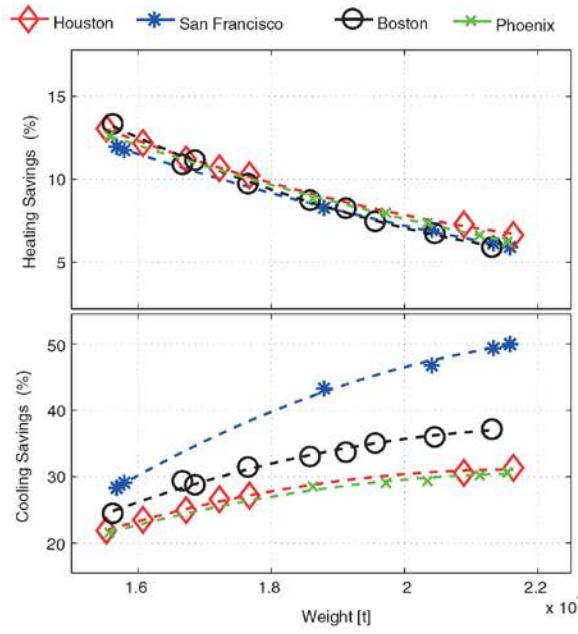
Fig. 9. Pareto sets ($N = 30$ stories) for the studied climates, showing the trade-offs between structural weight and heating and cooling savings.
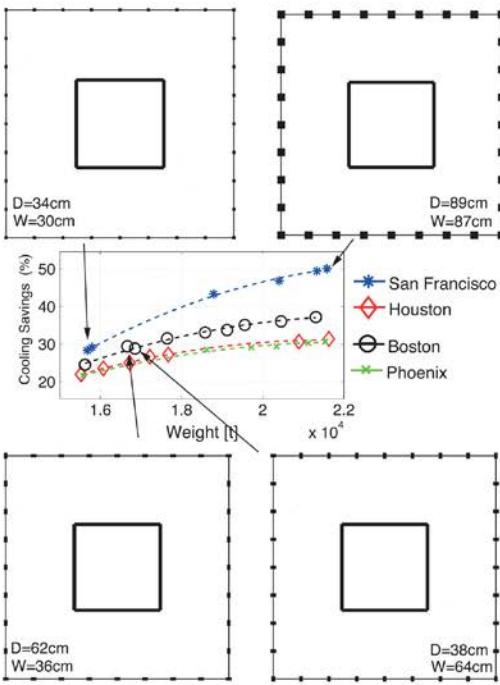
Fig. 12. Pareto set and resulting column structures for $N = 30$ stories and identical columns. The depth D and width W of the column are indicated in the individual floor plans.
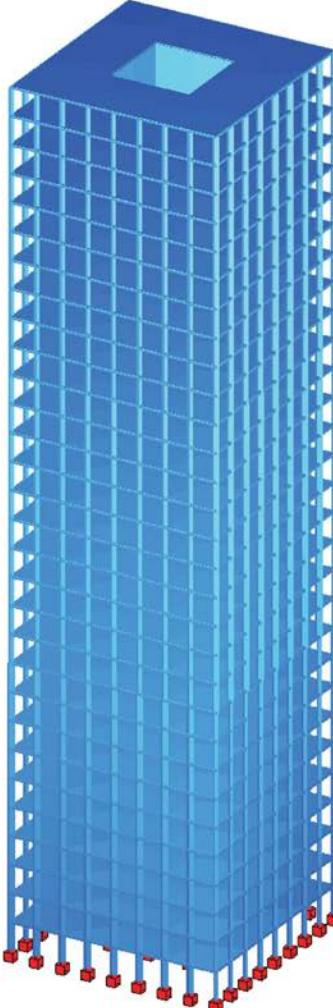
Fig. 6. SOFiSTiK structural model ($N = 30$ stories).

Figure 43. Some of the results of the study by Felkner et al. [11] (left), and one of their structural models (right). Source/Credit (©): 'J. Felkner, J. Schwartz, and E. Chatzi, "Framework for Balancing Structural Efficiency and Operational Energy in Tall Buildings," *J. Archit. Eng.*, 2019'. Courtesy of Juliana Felkner.

They found that increasing the mass and the shading provided by the exoskeleton led to a decrease in cooling energy demand and an increase in heating demand in general. In their relatively shorter tall buildings (30 stories) and in a

84

temperate climate (San Francisco), the results showed savings in both heating and cooling energy demand compared with the fully glazed facade baseline scenario. The savings in heating energy demand, in this case, was due to the reduction of the area of the fully glazed facade and the replacement of it with the thick structural columns that allow less heat transfer to the outdoor environment. In cooling-dominated climates, the cooling savings are less intense and differences between tradeoffs are not large meaning that while informing architects about trade-offs they can pick solutions freely [11].

In the second experiment, they found that in the case of heavier structures, it can be advantageous to consider different column sizes on different sides with respect to their potential in reducing cooling loads (e.g., larger in the south and lighter in the north). In the case of lighter structures, the differentiation between the sides was not so effective. The results were similar to the first experiment in the sense that the heavier structures with larger shading effects reduced cooling energy demand in general [11].

What's still missing? (The gap in the literature)

The research is valuable; however, it has notable oversimplifications and limitations, some acknowledged by its authors and others identified by the author of this dissertation. These limitations are outlined below. In designing this doctoral thesis, efforts were made to mitigate these limitations and incorporate proposed solutions.

- Life cycle primary energy consumption and carbon emissions

While the authors of the study emphasize the importance of LCA at various points in their paper (e.g., abstract, introduction, discussion, and conclusion), their methodology falls short of meeting LCA principles. Specifically: (1) the energy they calculate during the operational phase of the building pertains solely to space thermal energy demand, which cannot accurately represent or be converted into primary energy or CO_2e emissions; (2) similarly, the paper does not harmonize EE related to the structural system's mass with operational energy under a common unit (e.g., kWh, $kgCO_2e$). These issues are explained in more detail below.

- Operational Energy consumption vs demand

Heating and cooling energy demand represents the theoretical thermal energy required to be added to or removed from a space. However, the actual energy consumption to satisfy these demands depends on factors such as system type, design, and efficiency. For instance, electrical or mechanical systems like HVAC systems are responsible for the actual energy consumption, which may involve the use of fuels or electricity. The primary energy consumption associated with these systems is determined by the type of electricity production or fuel used, and it also considers the efficiency of energy transmission and distribution. In essence, heating and cooling energy demand indicate the desired thermal energy adjustments for a space, while primary energy consumption quantifies the actual amount of primary energy required to realize these adjustments in practice, considering the entire energy supply chain from production to delivery.

In their research, they aimed to minimize heating energy demand and cooling energy demand as two separate objectives. However, the actual operational energy consumption, which may not necessarily align with the sum of the heating and cooling energy demands, has been neglected (further explanation is provided below).

- Pareto front for objectives with interdependencies

The Pareto front is most effective in identifying optimal solutions when each objective parameter is distinct and independent in terms of their physical dimensions in reality. In simpler terms, it works best when these dimensions cannot be combined and expressed in a single common unit. In this case, while the three dimensions under study (structural mass, heating energy demand, and cooling energy demand) may appear separate and independent, they are interconnected since they can all be converted into primary energy consumption. The structural system could be quantified by the primary energy consumption needed to create its mass. Similarly, heating and cooling energy demand could be expressed in terms of the primary energy required to meet these demands. This aligns with the philosophy of LCA, where various factors and dimensions are transformed into a common equivalent dimension to enable comparisons. In this context, the total primary energy consumption, encompassing mass and heating and cooling energy demand, could be employed to rank design alternatives and identify the optimal solution. Converting structural mass or thermal energy demand into primary energy consumption requires additional phases of study and calculation, which are not addressed in the article. In other words, the optimal solutions found by the Pareto front with those aforementioned three parameters are not necessarily the optimal solutions in terms of total primary energy consumption or CO_2e emissions associated with them.

- Square plan with identical orientation in different climates

It is well established that optimal orientation for a given building model differs depending on location and climate with respect to solar radiation, temperature, humidity, etc. affecting the building facades [173][12][120][121]. For simplification in that study, however, the authors used quadratic floor plans with identical orientation in all building prototypes across four different climate zones (Boston in humid continental, Houston in humid subtropical, Phoenix in desert, and San Francisco in a temperate climate zone). Consequently, the prototypes were tested under unequal conditions in varying climates, and the results of their comparison may not be considered completely unbiased. For a study aiming to avoid unequal comparisons in terms of orientation, the ideal shape would be a circle, followed by regular convex polygons with a fairly large number of sides approximating a circle. These shapes would be symmetrical and identical with respect to geographic directions.

- No thermal bridging analysis

The analysis and the effect of thermal bridges caused by the incorporation of exoskeletons were not reported in that study.

- Neglect of neighboring tall buildings

Long-term scenarios should accurately represent the current state and potential changes in the urban neighborhood context. This is important because neighboring tall buildings may cast shadows on each other, impacting space heating and cooling energy demands. Additionally, there is the possibility of new buildings being constructed in the surrounding areas in the future.

- Neglecting the effect of climate change on space heating and cooling energy demands

Long-term scenarios are needed to consider probable changes in the climate due to global warming that may affect the thermal performance of tall buildings with respect to their long life expectancy.

- Identical core walls in different structural design scenarios

The various components of a building's structural system interact with each other. Both the core walls and the exterior columns close to the building facade are effective in supporting gravity and lateral loads, and changing the dimensions of one of them can affect the others as well. However, for simplification, it is assumed that the core walls are the same in the different options (different in terms of shape and dimensions of the outer columns).

This oversimplification leads to an optimization process based on biased inputs, and consequently, the results become unreliable. Fixed-dimension core walls (in layouts with identical floors with fixed thickness and without the use of beams) structurally leave no variables other than the design of the exterior columns. This means that the core walls are designed for the weakest design alternative of exterior columns, and in the other alternatives where exterior columns are larger, the core walls may be oversized and therefore not optimized. In a more appropriate research design, the thickness of the core walls would be assumed to be variable along with the design and dimensions of the external columns.

- Electric lighting system missing

Shading from the exoskeleton on the facade not only can reduce cooling energy demand and increase heating demand but also can affect the amount of daylight received inside the building. This can lead to an increase in electricity consumption to power the electric lighting, and can therefore affect operational energy consumption. So, it is important to consider daylight and electric lighting in the building simulation and operational energy consumption calculation. The simulation of electric lighting is not considered in that study, but it has been included in this dissertation and the limitation is removed.

- Identical wind loads in different locations

A certain amount of wind load (based on a reference wind velocity of 90 km/h = 25 m/s) is applied to the structures in all different cities (Boston, Houston, Phoenix, and San Francisco). This means that despite the use of different real city names, the actual wind load is not taken into account, which may lead to results that do not correspond to reality. This limitation can be overcome in one of the following ways:

The first would be to focus only on a specific city and use realistic wind loads corresponding to that city. The second way would be to apply realistic wind loads in each city and, in order to distinguish the effect of weather from that of wind loads, to use different types of combinations of levels of these two factors in the simulations and analyses. Of course, this second way would be much more complex than the first.

- No seismic loads

No seismic loading was considered in that study. It should be noted that this limitation occurred not only in that particular study but also in a wide range of published research papers in the field of high-rise buildings that use computer simulation of the overall structural systems. The common explanation for this simplification is that wind force generally plays a more decisive role for tall structures than seismic force. However, for a more comprehensive examination that yields realistic estimates, especially in regions with elevated earthquake risks such as Tokyo, Tehran, or Dubai, it would be wise to incorporate seismic loads into simulations. Structural engineering standards require seismic simulations to prevent catastrophic structural failure and damage. Moreover, recent research highlights the importance of considering seismic loads in LCA studies; a 2020 literature review by James Helal et al. unveiled that overlooking lateral loads, including static wind loads and static and dynamic seismic loads, and adopting unconventional structural analysis and design methods can significantly underestimate the embodied GHG emissions in tall building structural systems, with potential underestimations of over 20% [174]. Similarly, this limitation extends to various existing studies focused on LCA of tall building structural systems including those reviewed in this dissertation. Notably, research by Foraboschi et al. [6] and Weber et al. [13] concentrated solely on wind loads, while Moussavi Nadoushani and Akbarnezhad [8] exclusively considered seismic loads. Additionally, the study conducted by Trabucco et al. [4][5] lacks clarity regarding the methods or codes employed for structural analysis and design, particularly concerning wind and seismic loads.

2.2.10   A Study on Exoskeleton LCA (Solar Exoskeletons)

There is another remarkable and more recent paper related to the current study subject, which was done by Weber et al., published in 2022 [13]. In comparison to the aforementioned study by Felkner et al. [11], their study is briefly introduced and discussed below due to similarities in their subjects.

Weber et al. did a study on a 10-story mid-rise and 25-story high-rise rectangular office building generic models (hypothetical located in Phoenix, AZ, USA—hot dry climate) using exoskeletons of three types of: diagrid, (almost-) vertical columns (with variable angles), and mixed (combination of both); with steel and timber structural materials. They calculated the cradle-to-gate embodied CO_2e emissions of the exoskeletons (merely exoskeleton part of structural systems) as well as operational CO_2e emissions associated with electric lighting and HVAC systems. They also developed a couple of optimistic long-term scenarios considering the decarbonization of the (electricity) grid. They compared the exoskeletons with an endoskeleton as a reference. The results of the study showed a significant reduction of embodied and

operational CO_2e emissions by exoskeletons (especially when timber or diagrids were used) compared to the endoskeleton reference [13].

Therefore, the methodology of the study by Weber et al. [13] compared to the study by Felkner et al. [11] has the advantages of inclusion of HVAC and electric lighting systems that enabled to calculate of the primary operational energy consumption and thus operational CO_2e emissions, which led to having an overall view of both pre-construction and post-construction stages under the same umbrella of primary energy consumption and CO_2e emissions.

Although Weber et al's study [13] is significant, it is important to consider the limitations of its methodology, which could impact the accuracy and usefulness of its findings:

(1) first and foremost: there are confounding factors that prevent statistically distinguishing the effect of the use of exoskeletons from that of the endoskeleton; the structural type of the endoskeleton that was considered as a reference baseline for comparisons is totally different from that of the exoskeletons; they compared a common orthogonal framed type of endoskeleton with exoskeletons of other types (diagrid, etc.); therefore, the results do not allow to distinguish whether the CO_2e emissions savings were due to the use of exoskeleton (vs endoskeleton) OR due to the change in the structural type (e.g., diagrid vs orthogonal frame) OR a combination of both. Therefore, in terms of reduced environmental impact, conclusions about the superiority of exoskeletons versus endoskeletons of similar type remained questionable.

(2) Oversimplifications in structural analysis and design, leading to unreliable estimation of structural materials. Although lateral loads are crucial in the structural analysis and design of tall buildings, seismic loads were not taken into account in this study, and the wind loads are oversimplified (a constant amount of uniformly distributed surface load of 2.5 kN/m^2 was applied to all the different sides of the building envelope); i.e., the variation of wind loads (pressure and suction) on the different sides of the structures was not taken into account; moreover, no variation of wind loads was applied to the different height zones of the structural models was applied, which is an important variable in the analysis of wind loads in the structural systems of tall buildings. In addition, the software used in the study does not perform a complete check of the structural design against a given standard building code valid for construction practice (additionally, it does not have integrated dynamic analysis, and reinforcement design for RC elements). When dealing with LCA, due to the sensitivity of the difference between the mass of an endoskeleton and an exoskeleton, it is important to have reliable estimates of the amount of the structural materials (the researcher of this dissertation had also used the same software program (Karamba3D), for his initial studies published and presented at EPFL, Switzerland, in 2015 [12], however later noticed the aforementioned limitations of the program, which are adequate for some exploratory purposes of structural parametric design and rough size estimation, but not for such sensitive issues as quite realistic mass estimates needed for LCA of tall building exoskeletons, as explained above). Furthermore, in all scenarios the concrete cores have been assumed to be identical, and the presence or sizes of the slab beams (connecting the core to the exoskeletons) are also unclear, which is similar to the limitations of the Felkner et al's study, as explained above.

(3) Absence of other probable important interacting factors; only briefly listed here as these are also similar to the discussed study by Felkner et al. [11] as mentioned before: the effect of building orientation due to the rectangular layout of the plan; the thermal bridging of the exoskeletons through structural connection to the interior; the shading effect of neighboring tall buildings on each other considering the current state and probable future development of urban neighborhood; climate change and probable effect of global warming on HVAC energy consumption in long-term scenarios; and consideration of interactions between the aforementioned factors in order to distinguish, among other factors, the effect of using exoskeletons on the life cycle environmental performance.

Therefore, there remains a significant gap in understanding the impact of employing exoskeletons compared to endoskeletons on the primary energy use and carbon emissions in tall buildings, which is the central focus of this dissertation. The next section (2.3 Factorial DoE and Scenario Planning) delves into the conceptual framework and research design. It revolves around a full factorial DoE, exploring various independent variables or factors expected to interact and influence the primary focus—utilization of exoskeletons (vs endoskeletons) on the life cycle energy consumption and CO_2e emissions in tall buildings. The section will explain the rationale and choice behind each hypothesized factor and their variable levels, along with referencing additional relevant literature sources. The full factorial DoE, with permutations generating about 1440 compound scenarios, forms the groundwork for computer-simulation-based experiments in the subsequent chapter. The results of the LCI and LCIA will be further analyzed using the statistical method of GLMs for the first research question and employing mathematical decision analysis methods to address the second research question. Detailed answers to the research questions, along with discussions and conclusions, will be elaborated in the final two chapters.

2.3   Factorial DoE and Scenario Planning

As explained earlier in the previous chapter, the researcher aimed to adhere to objective, quantitative, scientific, and statistical approaches throughout the research process. To achieve this, a type of DoE called factorial DoE was chosen as the primary framework for designing the research and conducting computer simulation experiments. These experiments, as further explained in the next chapter, were followed by the use of GLMs to analyze the complex multiparametric outcomes. This analysis aimed to evaluate the magnitude and desirability of the effects of each factor and identify statistically significant interactions between every pair of factors. Each factor was assigned multiple levels representing different scenarios. Subsequently, to analyze the outcomes, three decision analysis methods, known as maximax, maximin, and minimax regret criteria, were employed. These methods helped identify optimal decisions for controllable factors while accounting for the influence of uncontrollable factors in the mathematical and statistical models.

Below, the concept of factorial DoE is explored, explaining why and how it was selected and applied in the study at hand. The subsequent subsections provide detailed introductions to various scenarios developed based on different levels of the factors. As GLMs and decision analysis methods were employed in the later stages of the research, particularly on the outcomes of the experiments, they will be introduced in the next chapter.

What is factorial DoE? Why and how was it applied in this research?

- (1) What is factorial DoE?

The purpose of DoE, also known as experimental design, is to describe variations in a response or dependent variable/s under conditions where several input factors or independent variables affect a process independently or in conjunction. These independent variables are referred to as factors, with corresponding values known as levels. Unlike the 'One Factor At A Time' (OFAT) approach, which does not explore interactions between different factors, DoE systematically covers all potential interactions among various factors. It provides a deeper and more accurate understanding of complex systems and the influence of each factor, including how they interact with one another. Both OFAT and DoE have been applied in numerous research projects across various scientific and technological disciplines, including various engineering fields. In both OFAT and DoE approaches, each factor has a baseline level, serving as a reference point. In OFAT, each experiment involves adjusting only one factor away from its baseline level. In contrast, in a full factorial DoE, which represents the most comprehensive form of DoE, multiple experimental runs are needed for each level of a factor to account for all possible permutations of levels of other factors as well. Another variant is fractional design, which omits certain combinations, often due to practical challenges in conducting experiments or collecting data [175]. In factorial designs each factor has a base level that can act as a control group. In factorial designs, each factor has a baseline level that serves as a control group. Factors in experimental design can be categorized as controllable or uncontrollable in real-world scenarios.

However, in some cases, even uncontrollable factors can be managed during research experiments, whether conducted in a laboratory or through computer simulations.

- (2) Why and how was factorial DoE applied in this research?

In the present investigation, full factorial DoE was employed (for brevity, the term 'full' is omitted in other parts of the text). The choice of factorial DoE was based on its alignment with the research questions, objectives, and the nature of the study. The primary independent variable of interest was the 'employment of exoskeletons (vs. endoskeletons),' while 'primary energy consumption' and 'CO_2e emissions' served as the main response variables. In the language of applied statistics for DoE, the first research question could be framed as follows: 'What is the magnitude and desirability (positive or negative) of the effect of the primary variable of interest, considering its interactions with other factors, including those that are controllable and uncontrollable in reality?' The researcher established various scenarios by defining the levels of these other factors to simulate real-world situations computationally. This approach facilitated a comprehensive understanding of how the primary variable of interest influences the main response variables across diverse scenarios.

For the statistical analysis of the experiment outcomes following the factorial DoE, the researcher utilized the GLM in the R programming language (further explained in the next chapter). This resulted in addressing the first research question.

The second research question followed the first one, focusing on optimal decision-making regarding the choice of alternatives (i.e., controllable factors levels) in the presence of uncontrollable factors (i.e., context factors). Again, the full results of the experiments based on factorial DoE were employed to encompass all possible scenario interactions. The researcher utilized three objective approaches in decision analysis, covering three different viewpoints: optimistic, conservative/robust, and cautious criteria (further elaborated in the next chapter, 3.5.2 Decision Analysis).

Table 6 presents the full factorial DoE for this research, including all factors and their levels, along with their assumed controllability (from the perspective of architectural engineers involved in the early design stage of tall buildings, i.e., controllable/uncontrollable), as well as the time span in the building life cycle when they actively impact primary energy consumption and CO_2e emissions. The rationale for the selection of each factor and its levels is explained separately in the following subsections. This table is very important, and readers may need to recall or refer to it while reading the upcoming chapters.

Table 6. Factorial DoE in this study; factors, levels, type of factors and active appliance phase. Source: the researcher

Factor	Levels	Type of factor | Direct Impact Phase
PTC: Placement of outer Tube with respect to Curtain Wall (PTC) **Highlight: PTC is the main variable/factor of interest in this research** *(subsection 2.3.1)*	A. IN B. MID C. OUT	Controllable | Pre-operational and operational phases
TBC: Thermal Bridge Control (TBC) *(subsection 2.3.2)*	A. NA (not available) B. WO (without) C. W (with)	Controllable | Pre-operational and operational phases
CR: Cement Replacement (CR) *(subsection 2.3.3)*	A. FA15 (15% fly ash) B. FA30 (30% fly ash) C. GGBFS25 (25% GGBFS) D. GGBFS50 (50% GGBFS)	Controllable | Pre-operational phase
PDWPRC: Percentage of Desalinated Water in Production of Reinforced Concrete (PDWPRC) *(subsection 2.3.4)*	A. 0 B. 50 C. 100	Uncontrollable | Pre-operational phase
PTSAU: Percentage of Transported Sand from Australia (PTSAU) *(subsection 2.3.5)*	A. 0 B. 50 C. 100	Uncontrollable | Pre-operational phase
TYP: (green-) Technology Year Pattern (TYP) *(subsection 2.3.6)*	A. 20_20_20 (2020-2020-2020) B. 20_50_80 (2020-2050-2080)	Uncontrollable | Operational phase
WDYP: Weather Data Year Pattern (WDYP) *(subsection 2.3.7)*	A. 20_20_20 (2020-2020-2020) B. 20_50_80 (2020-2050-2080)	Uncontrollable | Operational phase
UD: Urban Density (UD) *(subsection 2.3.8)*	A. L (low) B. H (high)	Uncontrollable | Operational phase

A simplified version of the conceptual framework of this study was presented in the previous chapter. Figure 44 presents a more comprehensive version that lists moderating variables and highlights the major mediating variables in relation to LCI and LCIA.
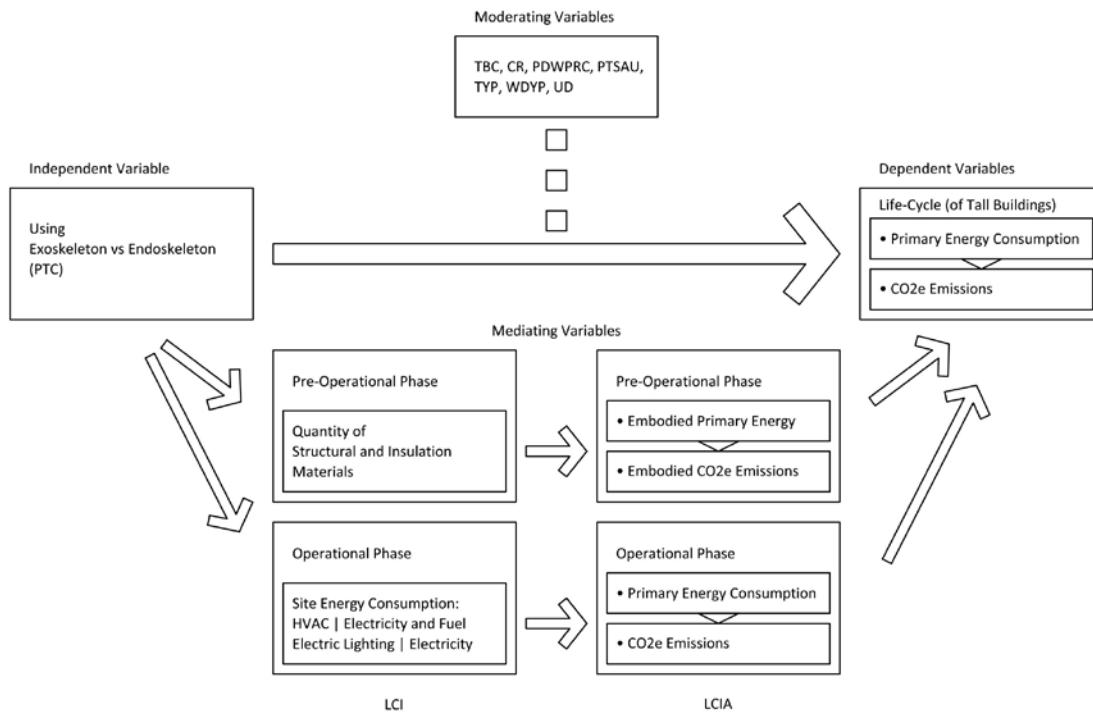
Figure 44. Conceptual Framework with the list of moderating variables as well as major mediating variables including LCI and LCIA. Source: the researcher

To uncover more details about the conceptual framework, Figure 45 shows all the factors (independent variable as well as moderating variable) involved in the DoE. It also illustrates on which phase of the life cycle of tall buildings each of them may have an impact. Showing the levels of each factor and all the scenarios made of all possible combinations of the levels of different factors would make the diagram too complicated to comprehend, therefore a separate figure will merely illustrate those scenarios. However, all possible scenarios got modeled and analyzed during the computer simulation-based case studies and statistical analysis that are explained in the next chapter.
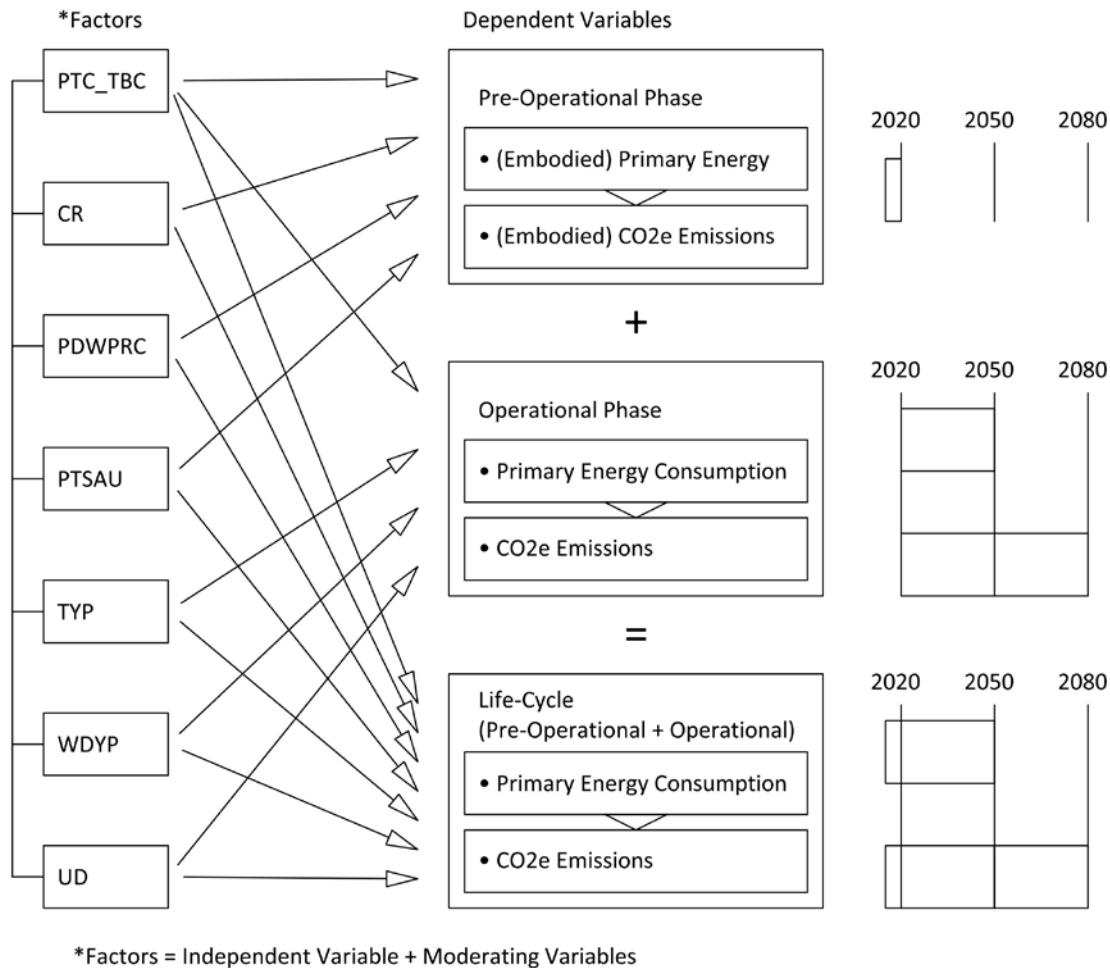
Figure 45. An unfolded version of the Conceptual Framework illustrating the potential main impact of different factors during the phases of the life cycle of the tall buildings under study. Scenarios (i.e., combinations of all levels of different factors) are not included in the diagram to simplify it. Source: the researcher

Figure 46. shows all possible scenarios of the full factorial DoE of the study at hand, which includes all factors and levels for the pre-operational phase (180 scenarios), the operational phase (40 scenarios), and the entire life cycle (1440 scenarios), which is the combination of the pre-operational and operational phases. These scenarios have been the basis for the computer experiments and statistical analysis that are explained in detail in the next chapters.
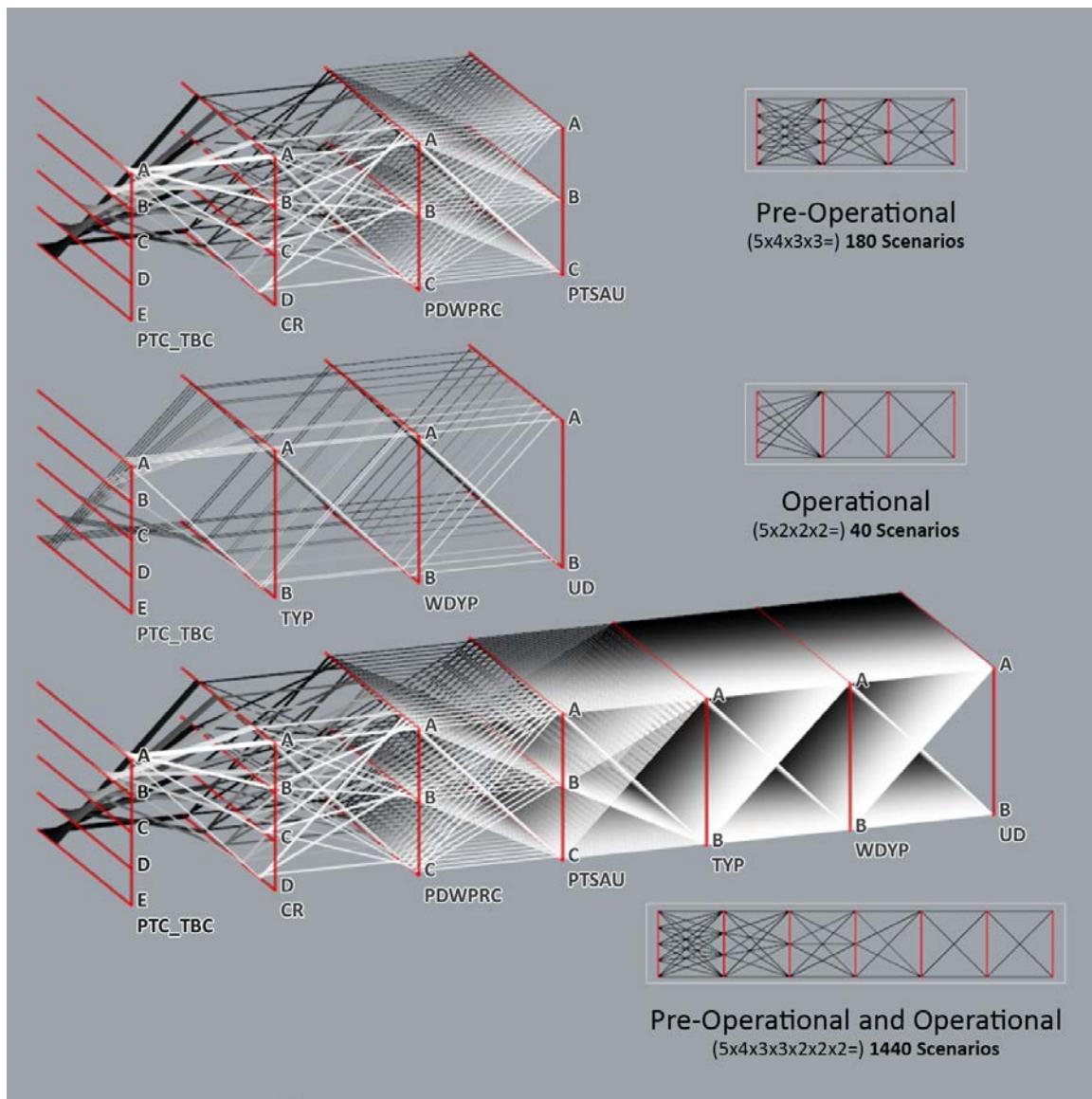
Figure 46. All possible scenarios of the full factorial DoE are illustrated. In the 3D diagrams, each thin simple polygonal chain (connecting all factors) represents one unique scenario for the computer experiments and analysis. Each vertical line represents a factor at different levels (refer to Table 6 and Table 9 for more information on factors and levels). Source: the researcher

2.3.1 PTC

The PTC factor is the main input variable of interest in this research, as it determines whether the skeleton is an exoskeleton or an endoskeleton. Since the background and literature review sections explained in detail why this factor is important and highlighted the gap in the literature regarding the environmental impacts of using exoskeletons in tall buildings, only the levels of the factor are introduced here. In fact, all other factors included in the present investigation, which are presented in the following subsections, were essentially selected to investigate their possible

interactions with PTC, in order to shed light on the impact of PTC (exoskeletons vs endoskeletons) in a variety of complex multivariate conditions/scenarios.

The PTC factor is classified into three levels as follows (Figure 47 illustrates the three PTC levels in a simplified diagram; another related illustration can be found in Figure 66):

(1) IN: stands for endoskeleton, the baseline level, in which the skeleton is kept inside the thermal envelope of the building; it is the most common mode in the design of tall building structures worldwide; Figure 48 shows the 30 St Mary Axe (London, completed in 2003, designed by Foster and Partners) as an example of this type;

(2) MID: a type of exoskeleton that is partially located inside the thermal envelope; this type is also referred to as exoskeleton although it is actually something between an exoskeleton and an endoskeleton, or a combination of both; One Thousand Museum (Miami, USA, 2019, by ZHA) is an example of this type, shown in Figure 49; John Hancock Center (see Figure 1) also incorporates this type of exoskeleton;

(3) OUT: represents the most common type of exoskeletons for tall buildings in which the outer layer of the skeleton frame/tube is kept completely outside the thermal envelope; beams and/or slabs connect the exoskeleton to the interior horizontal or vertical structural members (e.g., slabs, beams, central core walls or columns); an example of this type of exoskeleton is ZHA's Morpheus Hotel, shown in Figure 50; other examples of this type are the O-14 tower, the United Steelworkers Building (see Figure 1), and the Shenzhen Rural Commercial Bank Headquarters (see Figure 4). Table 7 includes a summarized description of the PTC factor and the list of its levels.
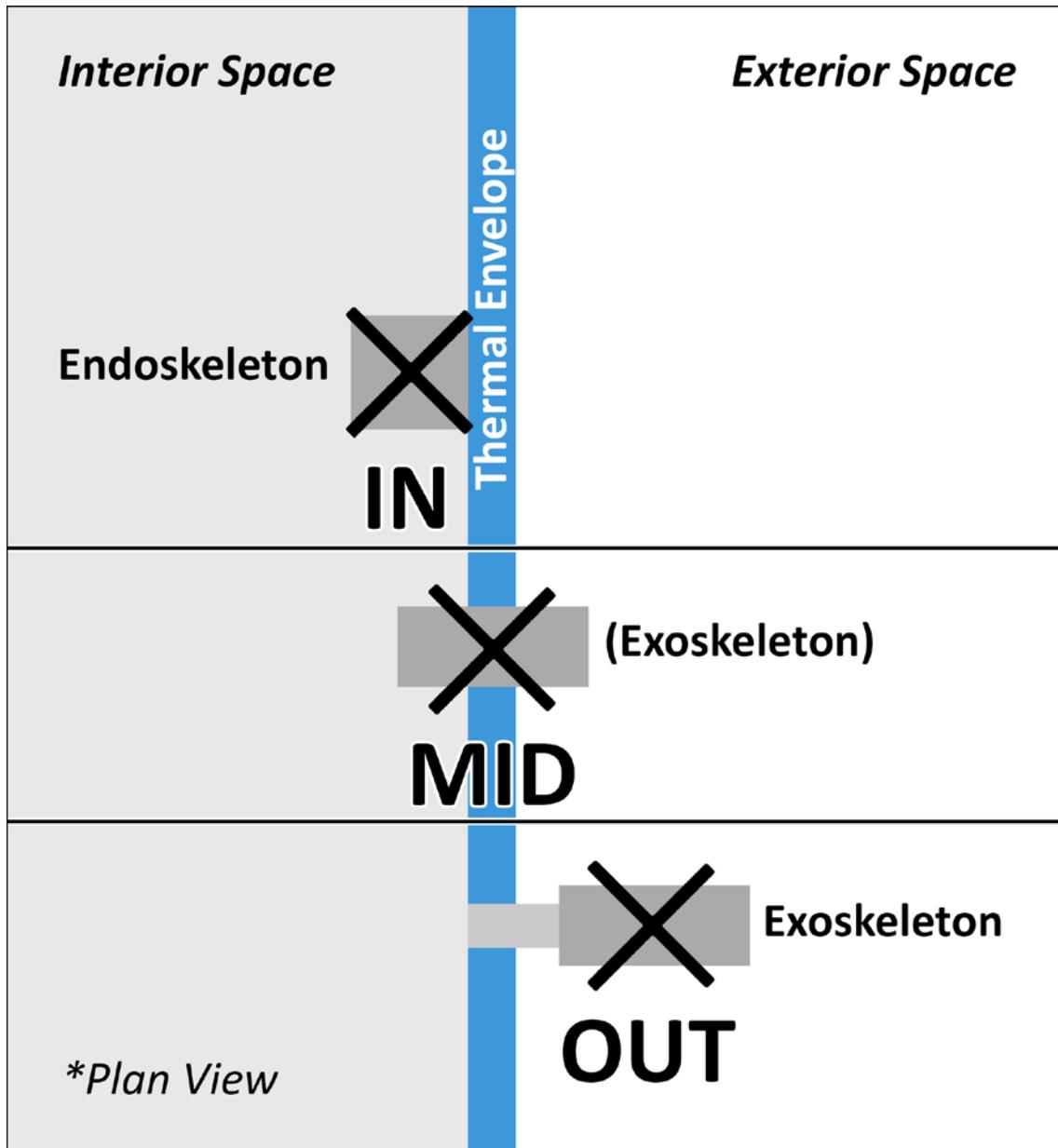
Figure 47. Diagram of types of skeleton; endoskeleton vs exoskeleton; PTC factor levels (IN, MID, and OUT). Source: the researcher

Figure 48. Example of the level IN of PTC factor; 30 St Mary Axe (formerly known as Swiss Re Building and commonly referred to as Gherkin), designed by Norman Foster, incorporates a diagrid frame as an endoskeleton. Although the skeleton is visible from the outside through the transparent portions of the facades, it remains almost entirely within the thermal envelope (see photos left and top right). There is only a relatively small part of the skeleton at the entrances that is directly exposed to the outside environment. Only these small parts can be considered exoskeletons (see bottom right photo). Sources/Credits (©): photographs by (left) BotMultichill and Elekhh via Wikimedia, licensed under Public Domain [176], cropped; (top right) Fastily via Wikimedia, licensed under CC BY-SA 3.0 [177]; (bottom right) Mark Hillary via Flickr, licensed under CC BY 2.0 [178].
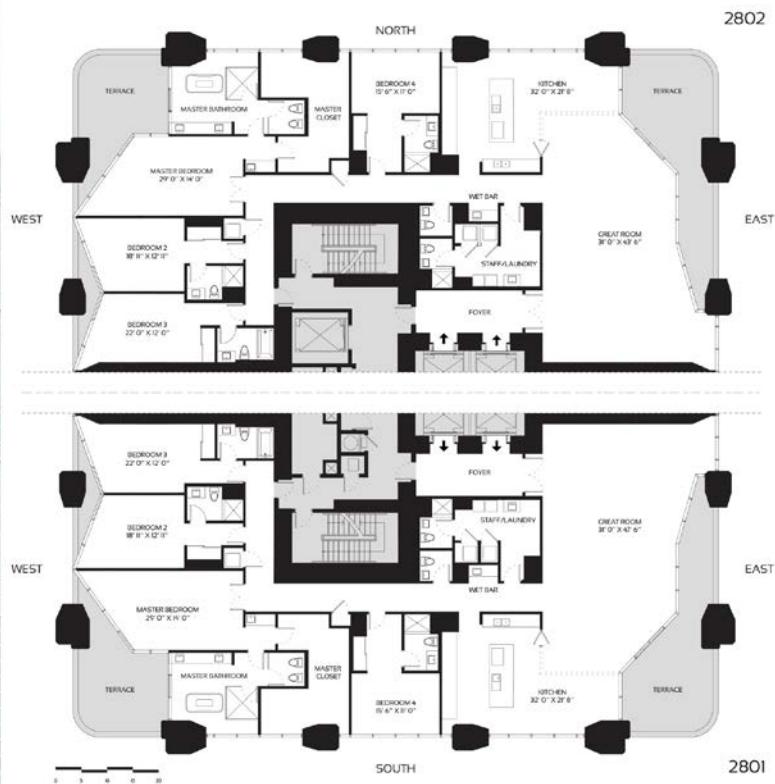
Figure 49. Example of the MID level of the PTC factor; One Thousand Museum, a high-rise residential building designed by ZHA, incorporates an exoskeleton in parts of which the (inclined) columns are centered with respect to the thermal envelope. For example, in the 28th floor plan shown here, the columns on the top and bottom sides are partially in the interior space and partially exposed to the exterior environment. Sources/Credits (©): photograph by Godsfriendchuck via Wikimedia, licensed under CC BY-SA 4.0 [179], cropped; Floor plan, courtesy of ZHA.

Figure 50. Example of the OUT level of the PTC factor; Morpheus Hotel by ZHA incorporates an exoskeleton diagrid frame that is fully placed in the exterior environment. Beams connect the exoskeleton to the rest of the structural system in the interior space. Sources/Credits (©): photograph by Störfix via Wikimedia, licensed under CC BY-SA 3.0 DE [18], cropped; drawing (25th floor plan) courtesy of ZHA.

Table 7. Description of the factor PTC and the list of its levels. Source: the researcher

Factor	Levels	Type of factor) | Direct Impact Phase
PTC: Placement of outer Tube with respect to Curtain Wall **(the main variable/factor of interest in this research)**	A- IN B- MID C- OUT	Controllable | Pre-operational phase

2.3.2 TBC

Local green building standards indicate that structural thermal bridges should be avoided. However, if they are included in the design, they should be mitigated by applying insulation materials [180][181].

The assumed levels are with (W) or without (WO) applying additional insulation materials to control the thermal bridges caused by exoskeletons. Table 8 includes a summarized description of the TBC factor and the list of its levels. There is specific note about the baseline level of this particular variable. As mentioned earlier the baseline level (control group) for PTC is IN. However, in IN alternatives there is no thermal bridges because all PSEs are kept inside the thermal envelope (curtain wall). So, controlling thermal bridges for the IN group is meaningless, therefore the TBC level of NA was defined; i.e., these combinations should be omitted: IN_WO, IN_W. Moreover, the combination of NA with exoskeletons (PTC levels: MID and OUT) would also be logically meaningless, so these combinations should also be omitted: MID_NA and OUT_NA. Therefore, TBC factor is integrated with the PTC factor to make a compound factor of PTC_TBC, with levels of: IN_NA, MID_W, MID_WO, OUT_W, and OUT_WO, as it is presented in Table 9 and Figure 51. By collapsing the two factors into this one-way layout which includes all the possible combinations of their levels, it will be possible to fit statistical models to estimate the difference between WO and W for particular categories, or across the board without running into rank-deficiency problems or throwing away cases with "missing" data [182].

Table 8. Desciption of the factor TBC and the list of its levels. Source: the researcher

Factor	Levels	Type of factor | Direct Impact Phase
TBC: Thermal Bridge Control	**A- NA** **B- W** **C- WO**	Controllable | Pre-operational phase

Table 9. The PTC_TBC compound factor and its levels as a substitute for the factors PTC and TBC. Source: the researcher

Compound Factor	Levels	Type of factor | Direct Impact Phase
PTC_TBC	**A- IN_NA** **B- MID_WO** **C- OUT_WO** **D- MID_W** **E- OUT_W**	Controllable | Pre-operational and operational phases
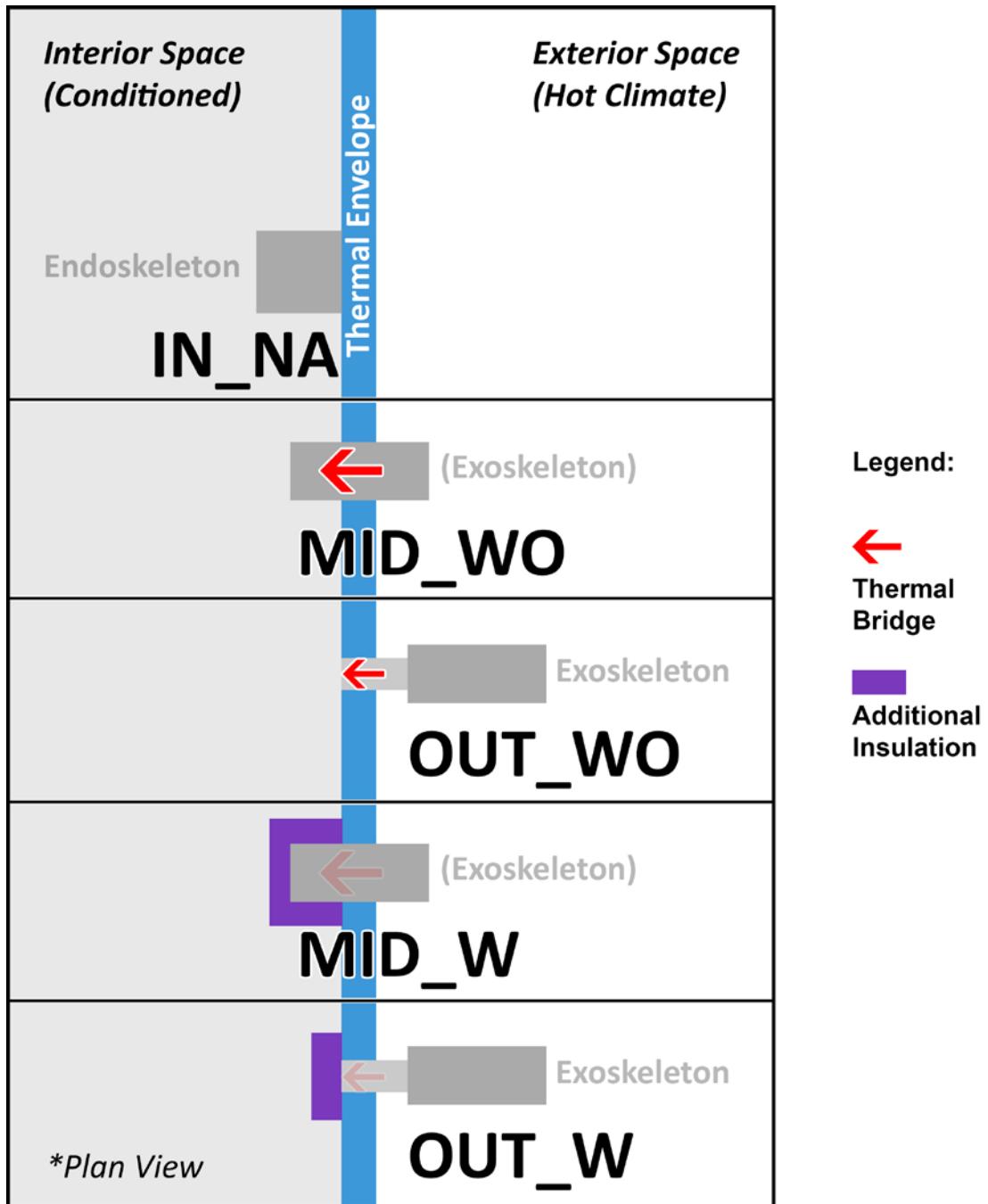
Figure 51. Levels of the compound factor PTC_TBC. Source: the researcher

2.3.3 CR

In this subsection, the researcher first explains the energy- and especially CO_2e-intensity in production of (Portland-) cement and its significant contribution to the total amount of GHGs emissions caused by humans, and then introduces Fly Ash (FA) and Granulated Blast-Furnace Slag (GGBFS) as two common alternatives of CR materials—also known as Supplementary Cementitious Materials (SCMs) [183][184]—that was considered in computer experiments of the study at hand, and

points out why this factor (the CR factor) and its levels has been considered beside and in connection to the main factor of interest in this study.

The most common type of cement used in the current construction industry is the pure (100%) Ordinary Portland Cement (CEM I) [185][186][187]. After (1) oxidation of fossil fuels, and (2) deforestation and other land-use changes, (3) the rapidly evolving cement production industry that contributes as much as 8 % of global CO_2 emissions is the third major source of anthropogenic emissions of carbon dioxide in the world [183]. Global cement production in the year 2018 emitted about 1.5 Gt CO_2. Total cumulative emissions from 1928 to 2018 was around 40 Gt CO_2, and more than 70 % of this amount have occurred since 1990. Growth of cement production over the past two decades has been much faster than global fossil fuel production; it has almost quadrupled since 1990, and increased more than 30-fold since 1950. Current average per capita per year amount of cement production in the world is more than 500 kg. Cement production leads to carbon dioxide emissions in two ways: (1) the chemical reaction of $CaCO_3 \rightarrow CaO + CO_2$ [188]: during the production of clinker which is the main component of cement, when heat is applied, carbonates (mainly $CaCO_3$, contained in limestone) are decomposed into oxides (mainly lime, CaO) and CO_2 (clinker itself is made through a chemical reaction of CaO, and SiO_2 aka Silica contained in clay); (2) combustion of fossil fuels in order to heat the raw materials to well over 1000 ° C which is a primary-energy-intensive procedure [189].

The possibility of reducing GHG emissions from cement production through increased use of materials like FA and other supplementary cementing materials has been studied by researchers for decades [190][184]. Studies demonstrate that the addition of FA and GGBS can enhance workability and compressive strength, ultimately improving the mechanical properties of concrete [191]. E.g., results of an experimental study show that the compressive strength of concrete increases by approximately 10% at 28 days and by 30% at 180 days when using a mixture of 60% cement, 10% FA, and 30% GGBFS [192]. FA and GGBFS are the most well-known and widely used supplements for Portland clinker, while other CR materials include natural pozzolans and limestone filler, among others [193]. While the utilization rate of FA in cement and concrete compositions is about 30%, GGBFS exceeds 90% [194]. However, high quantities of CR do not always result in lower GHG emissions per unit of strength. The outcome depends on factors such as the type of CR and considerations related to allocation or transportation changes [183]. The optimal consumption ratios for supplementary materials depend greatly on the type of alternative material and are typically below the highest replacement level [193]. Variability in quality and differences resulting from various coal combustion methods contribute to the limited utilization of FA for disposal purposes [194].

FA is one of the residues left over from burning coal to generate electricity and heat. It is collected by electrostatic precipitators or bag filters before the flue gases are released. Recent research has also explored ash from the combustion of fuels other than coal, particularly renewable biomass [194]. GBFS is a by-product of pig iron production in a blast furnace operating at temperatures between 1300 and 1500°C. The formation process involves melting iron ore waste, flux, primarily limestone and dolomite, and inorganic components from fuel combustion, typically coke. Slag, a less dense substance, flows on the surface of molten iron in the blast furnace and is periodically discharged [194]. GBSF exits the blast furnace at approximately 1400 to

1450°C and is gradually cooled, either by air or rapidly through a water jet granulation process. This process leads to the creation of blast furnace slag, which is used in the production of cement and concrete [194].

The reason why the researcher included this factor (CR) could be summarized as follows: (1) since many researchers have studied CR for years, and the use of FA and GGBFS in construction projects is common, experienced architectural engineers are relatively well aware of its effectiveness in reducing GHG emissions. Therefore, it may help as a scale to better understand the intensity of the impact of the primary variable of interest in this research compared to it; (2) as a secondary goal; since the present investigation evaluates the energy and carbon footprint of HVAC and electric lighting systems at the operational/long-term use stage, it also puts the environmental effect of CR in a new perspective, because CR has typically been evaluated only at the pre-operational or end-of-life stages of structural systems, but here it will be evaluated with its likely interactions with two main building systems at the operational/use stage (i.e., HVAC and electric lighting).

In this research, this factor is assumed to be controllable from the perspective of architectural engineers involved in the early stage of the design of tall buildings.

Four levels were considered: CR with FA (15% and 30%) and with GGBFS (25% and 50%). The reasons for choosing these levels, in addition to what has been mentioned before about the prevalence of these two CR alternatives and their range of effective percentages, are as follows: (1) 15% FA was selected as the baseline. A question may arise here: why not 0% FA/GGBFS, or in other words, why not set 100% CEM I as the baseline? This was because of the new local building code that makes it mandatory to use CR materials [195, p. F 18]; (2) the other three levels were included in the Inventory of Carbon and Energy (ICE) database v.2.0 and v.3.0 [47][48]. Using them makes it easy for the audience to control the calculations and relate to the results (more details in the next chapter). Table 10 includes a summarized description of the CR factor and the list of its levels.

Table 10. Description of the factor CR and the list of its levels. Source: the researcher

Factor	Levels	Type of factor | Direct Impact Phase
CR: Cement Replacement	A- **FA15 (15% fly ash)** B- **FA30 (30% fly ash)** C- **GGBFS25 (25% GGBFS)** D- **GGBFS50 (50% GGBFS)**	Controllable | Pre-operational phase

2.3.4   PDWPRC

PDWPRC was assumed as an uncontrollable factor from the perspective of architectural engineers in the early stage of the design of tall buildings. Levels: 0, 50, and 100 percent (this is a continuous linear variable; different percentages linearly lead to linear responses, so two extreme levels would be sufficient; however, for verification purposes, three levels were included in the models).

In recent decades, freshwater resources, including rivers, lakes, and groundwater, have been overused, especially in hot desert climates, and have sometimes created unstable and life-threatening conditions [196]. Although the use of desalination can help preserve natural freshwater resources, the process of desalination results in extra consumption of energy and emitting GHGs, depending on the technology used [197]. It is also a costly process, and the brine (aka concentrate or reject), which is a by-product of the process should be disposed carefully as it can poison marine organisms [198].

Naturally, under the same conditions, and if all or part of the water required in the process of producing RC is supplied using desalination, the more desalinated water used, the more energy and carbon will be consumed and emitted. Table 11 includes a summarized description of the PDWPRC factor and the list of its levels.

Table 11. Description of the factor PDWPRC and the list of its levels. Source: the researcher

Factor	Levels	Type of factor | Direct Impact Phase
PDWPRC: Percentage of Desalinated Water in Production of Reinforced Concrete	**A- 0** **B- 50** **C- 100**	Uncontrollable | Pre-operational phase

2.3.5 PTSAU

PTSAU was assumed uncontrollable. Levels: 0, 50, and 100 percent (this is a continuous linear variable; different percentages linearly lead to linear responses, so two extreme levels would be sufficient; however, for verification purposes, three levels were included in the models).

The UAE is among the manufacturers and exporters of cement. Most structures in this country, are made of RC. In recent years, the resources of marine sand have been scarce, while formerly, significant amounts of this natural resource, were spent on the construction of artificial islands. The required sand for concrete production is imported in the UAE e.g., to build the Burj Khalifa (the tallest structure in the world). Most of the imports are shipped from Australia [199], which is about ten thousand kilometers away from the Emirates. Although, for similar distances, GHG emissions and energy consumption of maritime transport (approx. 0.1 MJ/tkm [200][201][202][203]) is generally less than land transportation (approx. 0.3 - 1 MJ/tkm [200][201][202][203]) and aviation (approx. 1.5 - 50 MJ/tkm [200][201][202][203]), due to the relatively very low cradle-to-gate EE of sand (approx. 0.01 MJ/kg [204]), its cradle-to-site energy (approx. 1.01 MJ/kg) reaches about one hundred times of that—merely because of 10,000 km maritime transportation. The commonly negligible share of sand in the EE of concrete increases so that cradle-to-site energy of concrete in the UAE might reach up to about 30% greater than the similar cases in the UK—e.g., the cradle-to-gate EE of concrete C40/50 MPa using CEM I = 1.17 MJ/Kg [47][48]. Nonrenewable resources (fossil fuel for maritime transportation [205]) are spent to transport another

nonrenewable resource (sand) and additional GHGs also emit to the atmosphere (approx. 0.02 kg CO_2e per kg concrete).

This issue is not limited to the UAE, e.g., Singapore has imported larger amounts of sand—mainly from Indonesia, Malaysia, Cambodia, and Thailand—for extension of land in the sea [199] Aggregates suitable for construction purposes are typically collected from river beds and marine areas. These resources are not renewable. Rapid population growth and demand for construction in many parts of the world especially in Southeast Asia, India, and North Africa has even led to the involvement of mafia groups in smuggling and trading these resources, and to political conflicts among countries in some cases [199][206]. Table 12 includes a summarized description of the PTSAU factor and the list of its levels.

Table 12. Description of the factor PTSAU and the list of its levels. Source: the researcher

Factor	Levels	Type of factor | Direct Impact Phase
PTSAU: Percentage of Transported Sand from Australia(AU)	**A- 0** **B- 50** **C- 100**	Uncontrollable | Pre-operational phase

2.3.6 TYP

Technological advancements in construction over the past few centuries, especially in recent decades, have brought about significant improvements. These advancements have led to faster, more cost-effective, and larger-scale construction projects, as well as enhanced human comfort within built environments. In light of the depletion of non-renewable energy and material resources, as well as growing concerns and predictions related to climate change, there has been a global shift toward the development of environmentally friendly technologies. Many technologies that are now considered conventional or even mandatory, even in developing countries, were rare or nonexistent just a few decades ago. For instance, today's construction practices include the use of airtight double-pane or triple-pane windows with thermal insulation, replacing old, low-performance single-pane windows. Similarly, contemporary lighting systems, such as fluorescent lamps, high-intensity discharge lamps, and Light-Emitting Diode (LED) lamps, are highly energy-efficient, in contrast to older, less efficient luminous (Tungsten) incandescent bulbs.

Therefore, it is plausible that many technologies supporting or surrounding an (exo-)skeleton in a tall building may gradually transition to more environmentally friendly options in the coming decades, as an optimistic scenario. These potential advancements, which may unfold in the distant future, are beyond the control of architectural engineers involved in the early stages of tall building design at present. However, it is possible to formulate scenarios and use simulations to assess how the incorporation of exoskeletons might interact with these potential technological developments.

In the study at hand, the factor of green technology development encompasses a range of sub-factors listed below. The significance of each factor and why it's considered are explained. More detailed technical information regarding calculations and simulation experiments can be found in the following chapter and is not included here. The decision to package multiple factors as a single compound factor aims to prevent excessive complexity in the results, which could hinder comprehension for the audience. Alternatively, these factors could have been included separately in computer simulations and statistical analyses. As mentioned earlier, these factors are similar in that they all relate to the future improvement of technologies, particularly from an optimistic perspective, and are beyond control in the early stages of tall building design. For each factor, two levels are assigned: an optimistic scenario where technologies continually improve during the operational phase of tall buildings, and a pessimistic scenario representing a steady-state or 'business as usual' situation with no green technological advancement during the operational phase.

▪ COP of HVAC systems

The COP of HVAC systems has gradually improved in previous decades and continues to do so. Scientists and industry experts project future improvements in COPs [207, p. 51], which are moving closer to their theoretical limits due to the second law of thermodynamic [208]. A higher COP results in a smaller energy and carbon footprint for a building. Therefore, any potential positive or negative impact of incorporating exoskeletons on HVAC energy usage and carbon footprint may be influenced by variations in COP.

▪ Efficacy of (LED-) electric lighting systems

Similar to the COP of HVAC, there are theoretical limits to the efficacy of lighting systems. High-performance LEDs are significantly more efficient than older, common technologies. However, they are still far from reaching their theoretical limits, leaving room for future improvements, as predicted by scientists [209, p. 61]. Exoskeletons may cast shadows or reflect light, potentially affecting daylighting and glare inside buildings, given their location between the exterior environment and interior spaces. Consequently, their impact on electricity demand might interact with the efficacy of electric lighting systems.

▪ Controlling structural thermal bridging

Decades ago, the mitigation of thermal bridges was not common practice. PSEs, typically made of steel or RC, were in direct contact with both the interior and exterior spaces without any form of thermal break or insulation materials in between. In contrast, modern exterior walls and windows usually have much lower U-values than PSEs. This substantial contrast in thermal transmittance between the facade and structural materials can result in more noticeable thermal bridging. In response to this issue, various new products have emerged from manufacturers (e.g., Schöck [210][211], and Farrat [212]), to serve as structural thermal breaks. Some of these products can be integrated into new structures, while others can be retrofitted to existing

ones. In principle, these elements, made from materials with low thermal transmittance and high structural performance, can be integrated with RC, steel, or other load-bearing components to create a thermal break between the interior and exterior zones. They find typical applications in external-to-internal structural connections, facade system connections, concrete frame to steel connections, balustrades and roof penetrations, steel and masonry connections, structural columns, and exoskeleton structures. However, their current application is limited in size to handling structural loads (of RC columns) that are not overly large. Consequently, they are not yet capable of effectively controlling thermal bridging in RC columns of tall buildings, such as diagrid elements forming an exoskeleton that functions as the primary structure of a tall building (in this context, the researcher consulted technologists from Schöck twice during this research).

Nevertheless, as an optimistic scenario, it seems plausible that such technologies may develop in the future.

Thermal bridging caused by exoskeletons could potentially impact the performance of HVAC systems, subsequently affecting primary energy consumption and CO_2e emissions.

▪ Energy mix in electricity production

The carbon footprint of electricity production in different countries and cities depends on their energy mix, which can change over time. Many countries are striving to reduce their dependence on coal, oil, and other non-renewable fossil fuels with significant carbon footprints. Instead, they aim to transition to cleaner and more sustainable technologies, primarily supported by renewable energy sources (e.g., solar, and wind power).

A pessimistic scenario could entail a steady-state scenario with no advancements in the energy mix of electricity production during the operational period.

As the incorporation of exoskeletons may impact electricity demand (through their potential influence on the performance of HVAC and electric lighting systems), their effects on primary energy consumption and CO_2e emissions could interact with advancements in green electricity production.

In summary, the present investigation defines the factor of advancement/development of green technologies (briefly referred to as TYP: Technology Year Pattern). It comprises four (sub-)factors, each considered uncontrollable from the perspective of architectural engineers involved in the early design stages of tall buildings:

- COP of HVAC systems
- Efficacy of (LED-) electric lighting systems
- Controlling structural thermal bridging
- Energy mix in electricity production

The rationale for selecting each sub-factor has been explained earlier. Two levels are assumed for each sub-factor, representing two scenarios: an optimistic scenario (TYP_20_50_80) in which technologies progressively become more environmentally friendly over 60 years of the operational phase (from 2020 to 2050 to 2080); and a pessimistic scenario (TYP_20_20_20) in which technologies remain unchanged throughout the 60-year period. Additional details on these levels can be found in the next chapter. As a side note, in the terminology used in the following chapter, a specific year (as opposed to a pattern of years) is referred to as a Technology Year (TY). Table 13 includes a summarized description of the TYP factor and the list of its levels.

Table 13. Description of the factor TYP and the list of its levels. Source: the researcher

Factor	Levels	Type of factor) | Direct Impact Phase
TYP: (green-) Technology Year Pattern	**A- 20_20_20 (2020-2020-2020)** **B- 20_50_80 (2020-2050-2080)**	Uncontrollable | Operational phase

2.3.7 WDYP

There is a strong consensus among scientists worldwide that global warming is occurring and will have serious implications for the performance of the built environment, which must be considered at present [213]. In other words, buildings constructed today may experience significantly different weather conditions in the coming decades due to the effects of climate change. The need for primary energy (and consequently the associated GHG emissions) to operate HVAC and electric lighting systems during a building's use stage depends on the climate of the location. Therefore, if significant climate change occurs in the future, estimations based on current weather data may become inaccurate and diverge from reality. Likewise, the magnitude and desirability of the effects of employing exoskeletons may also change if the climate changes in the future. Climate change could also interact with other factors in this study; for example, advancements in green technologies, especially the increased use of renewable low-carbon energies (e.g., solar), may interact with the global warming factor and reduce its negative impacts on primary energy consumption and CO_2e emissions. These hypotheses require thorough experimentation to determine their validity. Unlike most literature sources dealing with examples of LCA of tall building structural systems, which have not focused on the potential effects of the structural system on HVAC and electric lighting systems (e.g., [4][5], and [6]), even those that considered one or both of these systems in their models (i.e., three studies [8], [11], and [13]), did not account for any climate change during the use stage of the tall building prototypes, which is, of course, an optimistic scenario.

In this research, this factor is assumed uncontrollable from the perspective of architectural engineers involved in the early stage of tall building design.

Two levels were considered to represent two future scenarios: one optimistic and the other pessimistic. In the optimistic scenario, a weather data file identical to the year 2020 will repeat with no change until 2050 and again with no change until 2080.

In the pessimistic scenario, the weather data file for 2050 and 2080 includes data associated with a global warming scenario developed and introduced by the Intergovernmental Panel on Climate Change (IPCC) (more details in the next chapter). As a side note regarding the terminology used in the next chapter, it should be noted that whenever a specific year (rather than a pattern of years) was addressed, it was referred to as the Weather Data Year (WDY). Table 14 includes a summarized description of the WDYP factor and the list of its levels.

Table 14. Description of the factor WDYP and the list of its levels. Source: the researcher

Factor	Levels	Type of factor | Direct Impact Phase
WDYP: Weather Data Year Pattern	A- **20_20_20 (2020-2020-2020)** B- **20_50_80 (2020-2050-2080)**	Uncontrollable | Operational phase

2.3.8 UD

This subsection emphasizes the significance of UD and the need to consider scenarios involving the presence or absence of neighboring buildings when assessing the operational performance of the building prototypes under study in simulations. In the study at hand, UD, quantifying the density of (similar) tall buildings in an urban area, typically expressed using the FAR. This specific aspect of UD is essential for understanding the interactions and impacts of tall buildings in urban environments.

Depending on the orientations and distances between tall buildings built relatively close to each other, they may cast shadows, reflect daylight (which can lead to glare in extreme conditions), all of which can impact the performance of their HVAC and electric lighting systems. When a tall building with an exoskeleton casts shadows or reflects sunlight onto its own facades and is situated in an area without other significantly tall buildings nearby, the effect of the exoskeleton on HVAC and electric lighting systems may differ from its impact when the building is surrounded by other tall buildings that may also cast shadows or reflect sunlight onto each other. Hence, an interaction may exist between the two factors of UD and the incorporation of exoskeletons.

A literature review paper focusing on energy efficiency and carbon emissions in high-rise buildings (2005-2020) revealed a recurring issue: the absence of urban context in simulations conducted in contemporary studies on tall buildings. This omission can lead to inaccuracies in reported results, particularly concerning HVAC and electric lighting systems [214]. Furthermore, within the specific context of the literature sources examined in the previous section of this dissertation, quantitative studies addressing the influence of structural systems on the operational performance of other building systems (e.g., HVAC and electric lighting) consistently omitted the inclusion of neighboring buildings in their simulations (see [13][8][11]). Indeed, the omission of neighboring buildings in those studies represents an oversimplification or limitation that this research aims to address. As a solution, the simulations in this study encompass scenarios involving neighboring buildings and consider critical aspects of

urban density, such as solar radiation, shading, and glare. These considerations are particularly relevant in the context of employing exoskeletons.

Given the research's holistic approach, which aims to maintain a balance between avoiding oversimplification and preventing excessive complexity, a comprehensive analysis of the UHI phenomenon is not within the scope of this study. This decision is rooted in the complexity of Computational Fluid Dynamics (CFD) modeling and simulation, the unavailability of microclimatic meteorological data, and the intricate, multivariate, and highly site-/case-sensitive nature typically associated with such analyses. Previous studies have demonstrated that multiple factors can influence UHI, including Sky View Factor (SVF), albedo, emissivity, and the morphology of urban texture [215][216][217], as well as the presence of vegetation, which is often found on rooftops and at ground level in the spaces between or surrounding buildings [218][219]. Furthermore, the effects of UHI can vary dramatically depending on the specific urban design and setup. Nevertheless, based on an expert interview conducted by the researcher [220], it is anticipated that the lack of the CFD and microclimate wind effects is likely to have only a minimal impact on the heating and cooling energy performance of high-rise buildings, particularly those equipped with typical HVAC systems, especially in hot climates; these effects are more significant for outdoor (pedestrian) thermal comfort and natural ventilation purposes. Additionally, based on the experiences and findings of another building simulation expert [221], it has been observed that the impact of UHI on urban air temperature is relatively minor when compared to certain other factors, such as variations in radiant temperature across an urban area, or the long-term effects of global warming. Anyway, for more site-/case-specific future research, software programs such as Dragonfly [222] and Urban Weather Generator (UWG) [223] can be used to integrate the detailed effect of UHI into the extendable parametric workflow framework of the current study.

Below, additional historical and contemporary examples are presented to emphasize the importance of considering the presence or absence of neighboring buildings when conducting scenario planning for tall buildings.

Shibam Hadramawt, also known as the 'Manhattan of the desert' or 'the oldest skyscraper city in the world' [224][225], is an ancient city located in the hot desert climate of Yemen. Its origins trace back to 300 AD, with most of its existing structures dating back to 1532. This city serves as an historical example of the accumulation of numerous relatively 'high-rise' buildings, ranging from five to eleven stories in height, densely packed and casting shadows on one another. These structures, considered high-rise relative to other similarly aged urban areas, create a distinctive urban landscape. Notably, within this UNESCO-protected World Heritage site since 1982, the tall buildings, constructed primarily from mud brick, cast desired shadows, especially on lower levels and streets between them [226][224] (see Figure 52 for a photo of Shibam Hadramawt).

Figure 52. Old walled city of Shibam Hadramawt in Yemen. Source/Credit (©): photograph by Dan via Flickr, licensed under CC BY-SA 2.0 [227].

In the context of designing a new building within today's centers of tall building development, it becomes essential to consider the potential impact of existing surrounding structures on the project, and vice versa. However, historical and contemporary examples abound, ranging from relatively small neighborhoods to entire cities, where the emergence of tall buildings has occurred unpredictably. In some cases, tall buildings that were planned either never materialized or faced significant delays in their construction. For example, consider Vienna and Austria's current tallest building, known as DC Tower I, boasting a height of 250 meters to the tip and an architectural height of 220 meters. This building earned the prestigious CTBUH Best Tall Building Europe 2014 Award of Excellence. The initial project plan envisioned a pair of twin towers, with the first tower successfully completed in 2013. However, despite approximately a decade passing since then, the construction of the second tower, DC Tower II, with a height of about 175 meters, has seen progress in its substructure but awaits the erection of its superstructure as of 2023 [228][229][230] (see Figure 53). It is evident that the completion of the second tower, situated on the southeastern side in close proximity to the first one, would inevitably impact the solar-climatic performance of the initial tower, along with its influence on the surrounding area and adjacent buildings over the years. Conversely, and on a larger scale, Shenzhen (in China) [231][232] and Dubai (in the UAE, see Figure 54) [232][233][234] serve as prominent examples of cities that experienced a rapid emergence of numerous tall buildings within just a few decades, surprising and unpredicted to most.

Figure 53. Left: the substructure of DC Tower II in 2023; Right: DC Tower I (completed in 2013) in Vienna, Austria. Source: photograph by the researcher

Figure 54. Urban transformation and proliferation of tall buildings in Dubai (1990 vs 2015); the top photo, taken in 1990, shows Sheikh Zayed Road, a prominent highway in Dubai, with a limited number of tall buildings. In contrast, the bottom photo, from 2015, shows Dubai's evolution into a global center of tall building agglomeration. Sources/Credits (©): photographs by (top) Prasanaik via Wikipedia, licensed under CC BY 3.0 [235] (cropped); and (bottom) Tim Reckmann via Wikimedia, licensed under CC BY 2.0 [236] (cropped).

In Tehran (a growing and the most populous city in Iran and West Asia, which in recent decades has also become notorious for the destruction of ancient gardens and trees and for the uncontrolled and dense construction of tall buildings in some of its areas [237]) there is a residential neighborhood called Shahrak-e-Omid consisting of several tall buildings with relatively long distances between them, all of them covered with green areas which, interestingly, even after several decades, have not been subject to new high-rise construction and the footprint of the buildings remains relatively small (see Figure 55).

Figure 55. Shahrak-e-Omid, a residential neighborhood in Tehran, Iran, is noted for its relatively smaller built-up area and larger green spaces, which is a rarity compared to typical neighborhoods in Tehran. Source: photographs by the researcher

All these examples highlight the uncertainty regarding the future of urban context from the standpoint of architects/architectural engineers. This underscores the significance and necessity of scenario planning, which takes into account a range of potential effects arising from low to high UD during the research, design, and urban neighborhood planning phases related to tall buildings. In this research, the UD factor is considered uncontrollable from the perspective of architectural engineers involved in the early stages of tall building design. Two extreme levels have been considered: one characterized by a low-density urban context with no tall buildings in proximity to the prototype under study, and the other marked by a high-density context where towers are closely situated (further details are provided in the following chapter). Table 15 provides a summarized description of the UD factor, including a list of its levels.

Table 15. Description of the factor UD and the list of its levels. Source: the researcher

Factor	Levels	Type of factor | Direct Impact Phase
UD: Urban Density	A- **L (low)** B- **H (high)**	Uncontrollable | Operational phase

2.3.9   Response Variables and Scope

The main response variables in the present investigation address two impact categories: Resource Depletion and Climate Change (Global Warming Potential), represented by the indicators primary energy consumption and CO_2e emissions, respectively. The selection of specific impact categories and their corresponding indicators in this dissertation results from comprehensive consideration of the research's primary objectives and the overarching focus on assessing the environmental and resource-related implications of tall building exoskeletons compared to endoskeletons. While there are many other impact categories and associated indicators within the realm of LCA, including acidification potential, eutrophication potential, ozone depletion potential, and human toxicity potential, the chosen categories have been prioritized due to their direct relevance to the built environment and tall building systems. Resource Depletion encompasses primary energy consumption, addressing the critical issue of energy resource utilization. Climate Change is represented by CO_2e emissions, a fundamental measure of greenhouse gas emissions and their contribution to global warming. While other impact categories are undoubtedly important in the broader context of sustainability and LCA, these chosen categories best serve the specific objectives of this research.

The scope of the estimation of primary energy consumption in the study at hand covers two items: (1) the terms "embodied" and "pre-operational" interchangeably address the first item that is the primary energy embodied in structural materials (and in insulation materials used for controlling the structural thermal bridging—where applicable/in some scenarios); i.e., cradle-to-gate / product stage: A1, A2, A3; in addition, since long distance transportation of sand in the location of the study had often been reported, this factor as a segment of the sub-stage A4 from the construction stage is also assessed as an exception (to recall the life cycle phases, revisit Table 5); (2) the term "operational" addresses the primary energy required to operate the electric lighting and HVAC systems, i.e., sub-stage B6; this item itself has two parts; one is the primary energy required to produce and provide electricity to operate the electric lighting and the HVAC systems in various scenarios except for the space heating in some scenarios (i.e., the near future scenarios and pessimistic future scenarios); the other one is the primary energy (natural gas) as the fuel for space heating in the aforementioned scenarios. A combination of quantitative results from multiple state-of-the-art studies, conducted separately on the life cycle primary energy and CO_2e emissions of high-rise structural systems [4][5][8][13], HVAC [238][239][240][8], and electric lighting systems [241, pp. 49–52][242], supports and confirms the fact that the aforementioned items or sub-stages are by far the most impactful key players throughout the life cycle of those systems. Thus, this scope is sufficient to provide a holistic and fairly reliable picture without involving other sub-stages of each system (that are either irrelevant to the subject matter or can affect the results only marginally but overcomplicate the

assessment, and lead the researcher to omit other variables or scenarios in the study to keep it feasible for the researcher and understandable for the audience). I.e., the crucial sub-/stages are A1-A2-A3 for the high-rise structures (and part of A4 as an exception for this particular study with respect to the PTSAU factor), and B6 for the HVAC and electric lighting systems (that are in interaction with the structural system, as hypothesized in this research).

Primary energy, in the present investigation, in the pre-operational phase includes only the non-renewable energies, but in the operational phase, it includes the total of both renewables and non-renewables. Primary energy, in general, can be referred to as non-renewable primary energies, renewable primary energies, or the total of both at the same time. Some LCI databases for EE and emissions often do not take renewables into account (so was the main database that was used in this research, ICE [47][48]).

It should be noted that the share of renewable energy in the production of structural materials, especially concrete/cement and steel at the time of conducting this research was small especially because large amounts of heating energy are needed in the production process (except for electric arc in steel production that requires electricity). This justifies the use of fossil fuels in these specific cases because from the point of view of managing large-scale energy resources in countries and cities, the use of renewable energy, which is usually available as electricity, is better used in cases where electricity is a necessity. Because, in general, electricity is a far more ordered and expensive form of energy than heating energy, it can be counterproductive to replace fossil fuels for heating purposes. By such logic, for instance, CTBUH experts have not separated the declared embodied renewable and non-renewable primary energies in their research report on LCA of high-rise structural systems [4][5]. Partly similarly, here, the reason why the researcher reported the total primary energy (renewables + non-renewables) for both the pre-operational and the operational phase was that (1) at present, as already mentioned, renewable energies have a marginal share, especially in the local industry; and in particular regarding the electricity production in Dubai, the renewables have had insignificant share in the mix of energy of power generation, therefore, in the study at hand, the embodied (primary energy/carbon in structural materials) nearly equals the embodied non-renewables anyway; (2) the former trend is supposed to change drastically in the long term future, as the government has aimed optimistic scenarios to make Dubai the world's least carbon footprint city by 2050 with 75% share of renewables in the electricity production. Projections in 2080 show even more dominance of renewables [243].

If the renewables are not taken into account in the Primary Energy Factors (PEFs) in the mixes of energy for the production of electricity, those factors become very small decimal numbers close to zero (with respect to future scenarios, i.e., 2050 and 2080). The crucial point here is that even if in the future electricity production becomes independent of non-renewables, the actual capacity for the production of electricity in cities and in the world will not be unlimited. Therefore, it is needed to avoid overconsumption/waste of electricity under any circumstances. Multiplication of near zero numbers (e.g., instead of near one numbers) can hide the undesirability of such overconsumption of electricity in the future and thus it can mislead the decision makers at the present, i.e., they may not take the high electricity consumption of design alternatives seriously and may vote for them in the hope that electricity will be supplied

from renewable sources in the future, while such an optimistic picture for the future may only come true in years, but decades, and there is no guarantee that they will become a reality.

The other response variable in this research is CO_2e emissions which represents the environmental impact of GWP. In terms of the calculation process steps, it comes together but one step after the calculations of primary energy consumption. In other words, as a prerequisite, it is necessary to estimate the primary energy consumption first, and based on the type of energy, a coefficient (derived from relevant databases) multiples the amounts of the primary energy to result in the amounts of GHGs associated with that. Similar to primary energy consumption, CO_2e emissions in this research are reported as the total amounts associated with renewable and non-renewable energies. Obviously, renewable energies result in significantly lower amounts of GHGs (sometimes close to zero). Therefore, there would be no surprise to see small figures for CO_2e emissions linked with optimistic long-term future scenarios (i.e., 2050 and especially 2080).

3   Chapter No. 3

Computer Experiments and Analysis

3.1   Introduction and Workflow Diagram

This chapter provides comprehensive details on the research methods and materials, including computer simulations, calculations and estimations, as well as the statistical and mathematical analyses employed to eventually address the research questions. Throughout this process, many technical files and algorithms were developed and utilized, with the key ones digitally attached to this dissertation. An appendix listing these files, referenced throughout this chapter, is included at the end of the dissertation for the audience's convenience. Table 16 briefly lists the main software programs and programming languages applied in the different parts of this research. The following sections of this chapter explain in more detail why they were selected and how they were applied.

Table 16. Software programs and programming languages applied in the study at hand. Source: the researcher

Software Program or Programming Language	Main Usage in This Research
Rhinoceros® [244] 5.0	2D and 3D Geometrical modeling, and hosting GH
Grasshopper® [245] (GH) 0.9.0076	Visual programming language in Rhinoceros, hosting LB+HB, and Python for various purposes.
ETABS® [246] 9.7.4	Structural analysis and code-compliant design, with respect to a wide range of static and dynamic loads (dead and live gravity loads, wind and seismic loads) and their combinations.
Galapagos [247] in GH 0.9.0076	Evolutionary solver (genetic algorithm) used in conjunction with the Building Geometrical Model Generator algorithm to adapt the diagrid layouts to fit the structurally optimal angle.
Ladybug [248] (LB) VER 0.0.63-0.0.64 + Honeybee [249] (HB) VER 0.0.66	Used in conjunction with Rhinoceros + GH to create models and connect them to the programs in the next row with respect to HVAC and electric lighting systems simulation
EnergyPlus™ [250] V8-1-0, OpenStudio® [251] 2.4.0, CCWorldWeatherGen [252] V1.9, THERM [253] 7.5, Radiance [254] 5.0.a.12, DAYSIM [255] 4.0	Used in conjunction with LB+HB for energy modeling, simulation and analysis; generating weather data regarding climate change, heat transfer and thermal bridging, daylighting and electric lighting.
Python™ [256] 3.7.4	Programming/scripting in GH to develop additional integrated tools for different purposes—e.g., parametric geometry generator, structural building codes, LCI an LCIA tools, etc.
Microsoft Excel [257] (Excel)	Data storage, visualization, calculation, statistical (decision-) analysis, and visualization
R [258] 3.6.1	Statistical programming language, used to analyze the results of the factorial DoE using GLMs.

A side note here about the software tools developed by the author in GH/Python: For many parts of the computer experiments, simulations or calculations, where the existing tools were unavailable, costly or problematic, the researcher developed his own tools mostly as GH/Python components. The tools are created so that the audience who are even a little familiar with Python or GH can see the codes and check the calculation procedures. For this reason, each complex component is equipped with a textual output that reports the steps taken in the algorithm in human language (English). Moreover, inside the codes, again, there are hints written in human language to help that group of audience to easily walk through the codes. All these tools are available as digital files attached to the dissertation (the researcher may make them available online as well). But here, in this present report, the codes of the tools are not presented because of two reasons: (1) to avoid writing a too long chapter or very long appendices which could become very time-consuming and impractical to read; (2) more importantly, not necessarily all the target audience of this research are assumed familiar with GH/Python. So, this dissertation is written so that could communicate with most architectural engineers involved in early design stage of tall buildings whether they know computer programming or not. Similarly, writing complex formulas of mathematics, physics or statistics are also avoided; instead, steps and logics of main algorithms are explained in conventional textual sentences and paragraphs.

The hardware and operating system used in all parts of the study at hand are presented in Table 17.

Table 17. Specification of the hardware and operating system used in this research. Source: the researcher

Hardware, and Operating System Items	Specifications
Processor	Intel® Core™ i7-4720HQ
CPU	2.60GHz,
Video Cards	Intel(R) HD Graphics 4600, NVIDIA GeForce GTX 960M
HDD	1TB
RAM	16GB
Operating System	Windows 64-bit (V. 8.1)

Figure 56 illustrates the Workflow Diagram of this research. The workflow has been simplified to fit on one page. All parts of the diagram are explained in detail in this chapter except the following: The Factorial DoE and Scenario Planning were described in detail in the previous chapter (however, the methods of inclusion of scenarios, factors and levels in the computer simulation-based case studies are explained in this chapter); The Results of the GLMs Analysis and Decision Analysis compose the next chapter; and the Interpretation of Results of Analysis, including the answers to the research questions, comes in the last chapter of the dissertation.
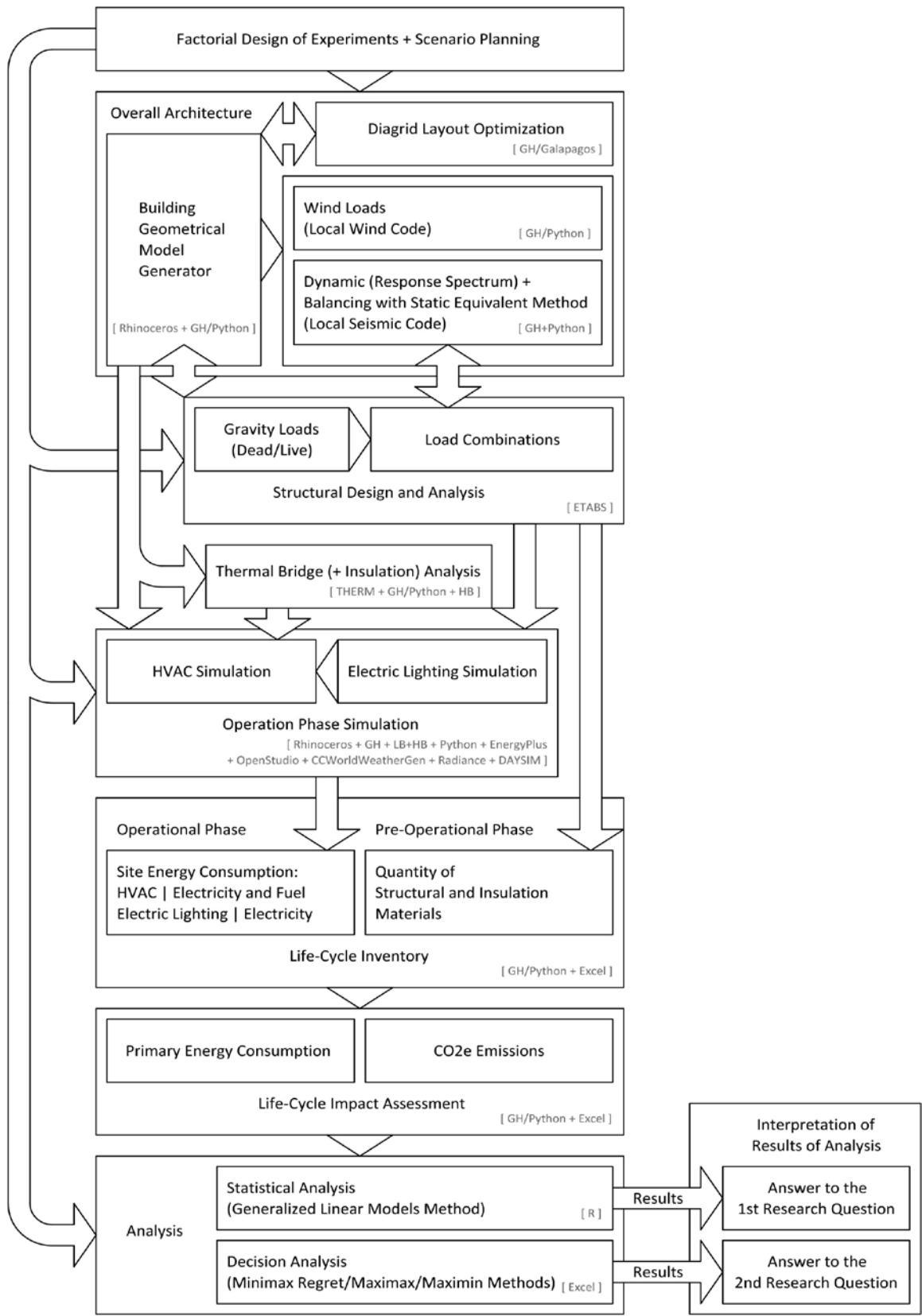
Figure 56. Workflow Diagram of the present investigation (names/abbreviations of software tools are mentioned between square brackets in gray). Source: the researcher

121

3.2 Overall Architecture, and Geometrical Model Generation

3.2.1 Overall Architecture

In order to make the results of this study useful for a large audience dealing with different building design projects (so that they can relate to it), it was necessary to try to keep the overall architecture and other engineering properties of prototypes close to conventional tall buildings. Therefore, the properties of the prototypes were set either in accordance with existing buildings and databases or in some particular cases meeting optimum item/systems where the existing literature has repeatedly recommended a specific item/system.

The overall function was considered as an office building. The prototypes consisted of 40 architectural occupied stories—an average tall building in Dubai has approximately 40 stories, each typical story with a height of 4.08 m (see Figure 59), based on the data available at the CTBUH Skyscraper Center database [259]—equivalent to 46 structural stories on the ground floor/base; Architectural ground-floor was considered double-height as well as the 20th and the 40th floors where mechanical floors were placed were considered double-height (this was done in compliance with CTBUH Tall Building Height Calculator [260]). The (outer) tube was extended in the size of two typical floors on top the roof—similar to Shenzhen Rural Commercial Bank Headquarters (Figure 4), O-14 (Figure 1), and some other towers with exoskeletons. A sky lobby was located at the 20th floor. A shuffle elevator connected the ground-floor to the sky-lobby which divides the building into two zones for local elevators. The capacity, speed and the number of the elevators as well as the size of associated voids in the floors plans were estimated using the online tool of KONE Quick Traffic (Elevator Traffic Calculation) [261]. About 80% of typical floor plans was dedicated to open office area, and the remaining 20% incorporated the core area including elevators, pantry, lavatories, floor electrical room, etc. (see Figure 57, Figure 58, and Figure 59).

Regarding the functional unit, all alternatives shared an identical radius of the core shear walls' axis (9.5 m), an identical radius of floors (21 m) (Figure 57), and identical total height and arrangement of all floors (Figure 59). The total Gross Floor Area (GFA) of the entire floors of the building prototypes was taken into account to calculate the intensity of primary energy consumption and CO_2e emissions, which are reported in detail in the following sections of this chapter. For comparison of tall buildings' structural systems in the early design stage, it is a common practice to keep the GFA constant rather than the Net Floor Area (NFA) (e.g., see [4][5][6][11][13], as well as other literature sources reviewed in the subsection 2.2.4). This is done to avoid overcomplexity in the methodology workflow and to facilitate result comparisons. Even small changes in the dimensions of cross-sections of columns or core shear walls during the structural design would affect the NFA. Maintaining the NFA constant would require altering the dimensions of the entire building's perimeter and core areas, necessitating numerous geometric changes in the main beams, floors, thermal envelope, etc. for each aforementioned potential small variation in cross-section design of columns or core shear walls. This would be an impractical and confusing procedure.

However, as a side note, it is worth mentioning that when the GFA is constant, the endoskeleton and exoskeleton elements occupy slightly more interior or exterior

space, respectively, which would give an advantage to each depending on the specific conditions of the real-life projects, where there are certain limitations with respect to the available exterior or interior space (revisit Figure 58).
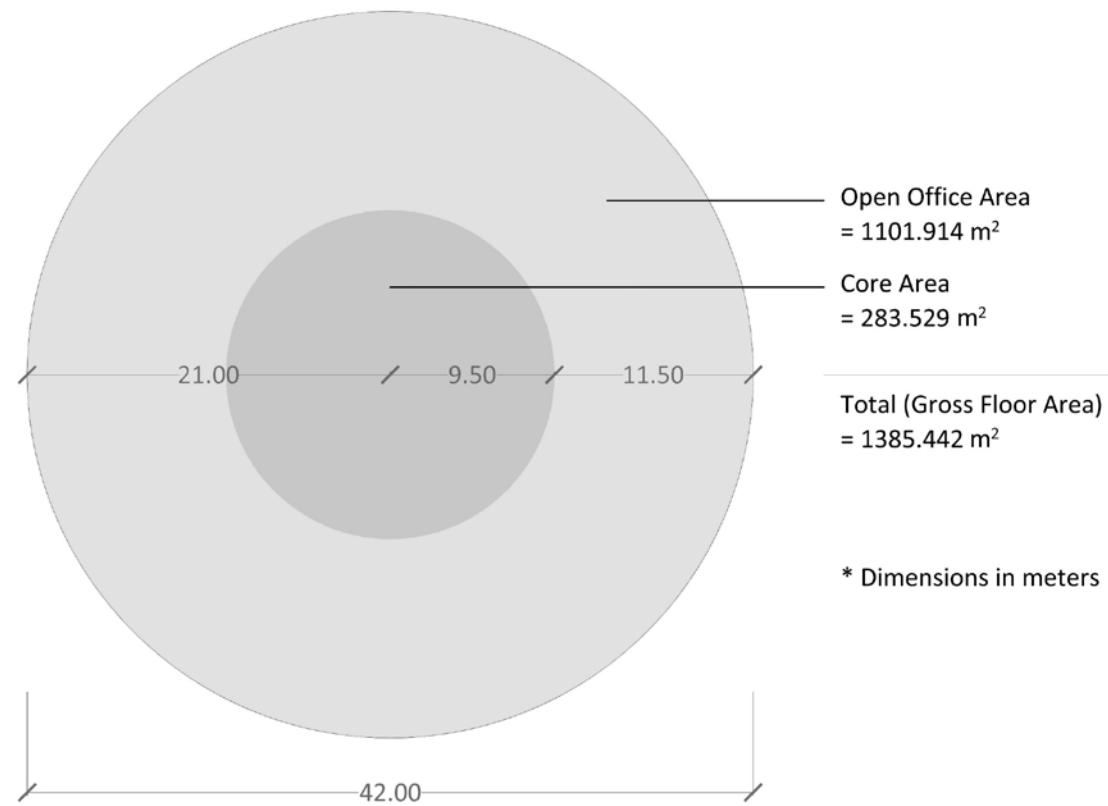
Figure 57. Typical floor plan areas. Open Office Area, in light gray = approximately 80% of the Gross Floor Area (GFA). Core Area, in dark gray = approximately 20% of the GFA. Source: the researcher
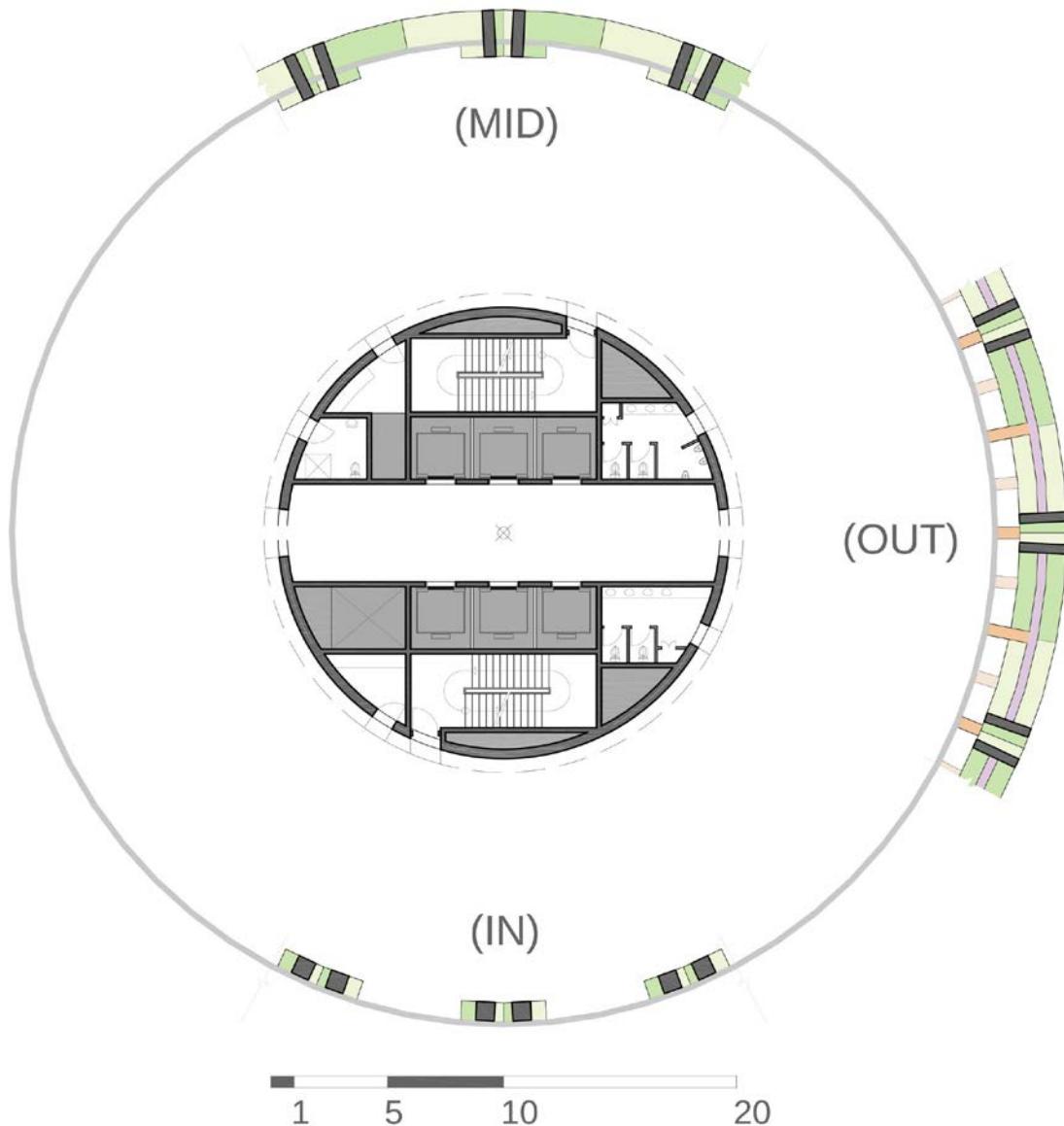
Figure 58. Typical floor plans. For the sake of brevity, this one image represents three images, each one partly shown: typical floor plans of the two prototypes incorporating exoskeletons (MID and OUT) as well as the endoskeleton control group prototype (IN).
Green: diagrid elements
Orange: radial beams
Pink: spandrel/ring beams
(Dimensions in meters)
Source: the researcher

124

Total height: +187.68 m	STORY 46	
	STORY 45	
	STORY 44	
	STORY 43	ZONE 6
40	STORY 42	
39	STORY 41	
38	STORY 40	
37	STORY 39	
36	STORY 38	
35	STORY 37	
34	STORY 36	ZONE 5
33	STORY 35	
32	STORY 34	
31	STORY 33	
30	STORY 32	
29	STORY 31	
28	STORY 30	
27	STORY 29	
26	STORY 28	ZONE 4
25	STORY 27	
24	STORY 26	
23	STORY 25	
22	STORY 24	
21	STORY 23	
	STORY 22	
20	STORY 21	
19	STORY 20	ZONE 3
18	STORY 19	
17	STORY 18	
16	STORY 17	
15	STORY 16	
14	STORY 15	
13	STORY 14	
12	STORY 13	
11	STORY 12	ZONE 2
10	STORY 11	
09	STORY 10	
08	STORY 9	
07	STORY 8	
06	STORY 7	
05	STORY 6	
04	STORY 5	
03	STORY 4	ZONE 1
02	STORY 3	
01	STORY 2	
	STORY 1	
GF ±0.00	BASE	

1 5   10   20

Figure 59. Left: Typical section of prototypes (vertical ribbons are elevator shafts). Double height floors: ground floor, 20th floor (mechanical floor + sky lobby), and 40th floor (mechanical floor). **Typical floor to floor height: 4.08 m. Total (architectural) height: 187.68 m**. Right: Zone numbers (for diagrid columns and core walls), and story numbers refer to structural models in ETABS. Source: the researcher

For the endoskeleton/control group (IN), a conventional cross-section of a square with variable dimension was assumed to be calculated in the structural analysis and design process. Similar to highlighted buildings in the literature whose exoskeletons are in the form of shading devices with relatively vast surfaces (e.g., IBM in Pittsburg, O-14 in Dubai, etc.; revisit Figure 1), a fixed width of 2 m was assumed for the cross-section of exoskeleton PSEs (in both MID and OUT groups), and the depth remained variable also to be calculated in structural analysis and design process that is explained in the subsection 3.3.1 Structural Simulation.

3.2.2 Diagrid Tall Building Geometrical Model Generator

Designing or simulating tall buildings involves a challenging and time-consuming initial phase of geometric modeling before structural analysis. These structural models serve as the foundation for architectural, mechanical, electrical, and other models, encompassing elements like beams, columns, core walls, and floor boundaries. Errors or inaccuracies in these models can lead to issues in subsequent stages. For high-rise structures, especially those with complex geometries like diagrids and non-orthogonal forms, manually creating a single preliminary geometric model can take hours to days.

The researcher developed a sophisticated, intelligent, multi-parametric algorithm as a BIM solution capable of rapidly generating the basic geometric model of an entire tall building with a regular convex polygonal plan shape, diagrid exterior structure, and interior core within a matter of seconds. These interactive models encompass the geometry, including 2D and 3D polylines and meshes, of all PSEs, such as the axes of columns/diagrid elements, beams (including girders, spandrel beams, radial beams, and secondary beams), floor slabs, and core walls. These generated models not only serve as the foundation for structural analysis but also for various architectural, mechanical/HVAC, and electrical lighting models, whether individually or as integrated systems.

This algorithm (which was presented during the Vienna young Scientists Symposium, VSS2019, at TU Wien [32]), was developed in Python/GH within the environment of the software program Rhinoceros. The reasons for this selection were: (1) the high-accuracy and advanced geometric functionality of Rhinoceros; (2) the inclusive parametric platform of GH which makes it possible to connect models to several other parametric engineering platforms at the same time or for further studies; (3) simplicity, robustness and the open-source nature of Python and its growing libraries.

The algorithm consists of two main parts: One takes multiple potentially independent variables as input parameters (e.g., number of segments of the base polygon, geometric density of the diagrid pattern, number of floors, floor-to-floor height, radius of the inner and outer tubes, minimum and maximum spans of the main and secondary beams, etc.) and produces geometric models of different elements, each collected in separate groups, as outputs (e.g., slabs, various beams, diagrid elements, core walls, etc.). Using the Galapagos genetic algorithm [247], the second part is an optimizer that is an evolutionary solver loop connecting the outputs and inputs

126

mentioned above. The numerical values of the optimal angles for the diagrid elements—the findings of the research by K S Moon et al. [146]—are merged as the fitness criteria in this phase, which was an angle of 63 degrees for the case studies of this research, since they were similar to some building models tested in the aforementioned literature source (in terms of type of structure, number of floors and height, slenderness and lateral loads); another study in the literature (see [262]) has also confirmed that the 63-degree angle is optimal for tall diagrid structures explicitly with cylindrical form and with specifications similar to the cases used in the study at hand. It is worth mentioning that the algorithm is intelligent enough to avoid logical errors and not generate useless models (e.g., diagrid nodes misaligned with the rhythm of floor levels, overlapping geometries or empty set outputs that may cause errors when running other potentially interconnected BIM applications, etc.). It took only 7 seconds (using the hardware specifications presented in the previous section) for the algorithm to generate the entire building's geometrical model for this research and adapt the diagrid layout to align with the optimal 63-degree angle. Figure 60 displays a selection of models generated during a test run. The test run details are as follows: (1) Building specifications (given parameters): 44 floors (40 floors, 3 of which are double-height), floor-to-floor height of 4.08m, core radius of 9.5m, envelope radius of 21m, etc.; (2) Task question: What is the optimal number of segments of the polygon (plan shape) that would fit the 63-degree angle for the diagrid layout?; (3) Result: 64 segments (a 64-gon), found in approximately 7 seconds, with 47 models generated and tested.
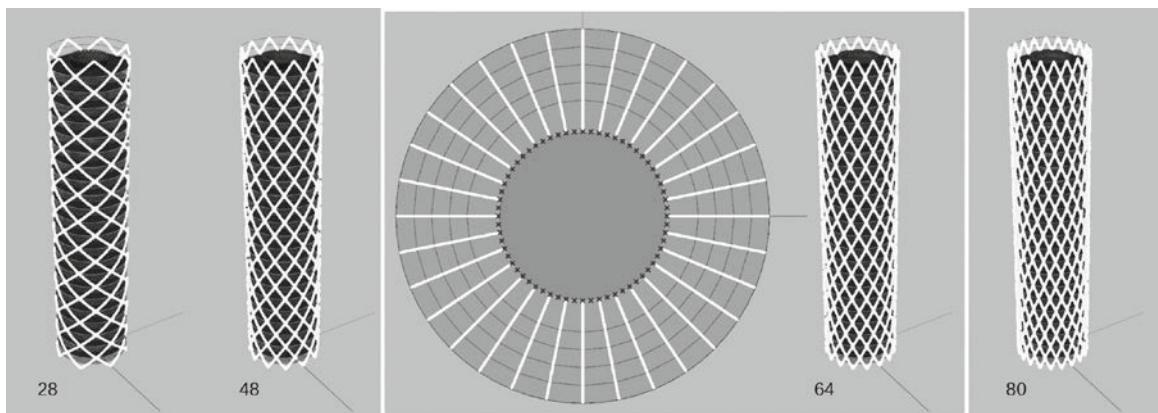
Figure 60. Four of the 47 generated models, generated in approximately 7 seconds. From left to right, the regular polygons have 28, 48, 64, and 80 segments. The middle of the figure shows a plan view of the modeled slab, core wall, and beams elements of the result, with an optimal diagrid layout, on a plan with 64 segments (64-gon). Source: the researcher

The goal of the development of this complex parametric tool was not only to support the present investigation but also to serve other similar research in the future by the researcher or others. It is beyond the scope of this research to go through the algorithm, however, for those in the audience who might be interested in it, the whole parametric algorithm is available as an attachment (in the file Diagrid_Tall_Building_Geometry_Generator.gh). The presented BIM solution significantly accelerates the process of accurate geometric model generation and structural optimization. Regarding the former, as the geometry of cylindrical diagrid systems is relatively more complex than those of most other typical structural systems in tall buildings (e.g., orthogonal rigid frame, framed tube or truss-tube with rectangular plan shapes), the outputs of this solution could also serve as blueprints to generate the

other types. Alternatively, parts of the algorithm could be deactivated or modified for further customized setups.

3.3 Pre-operational (Embodied) Stage

3.3.1 Structural Simulation

3.3.1.1 Introduction, Gravity Loads, and Load Combinations

The researcher used the ETABS software program for the analysis and design of the three primary structure prototypes (IN, MID, and OUT). ETABS is a valid common computer program for the analysis and design of structural systems, and scholars have widely used it in studies on diagrid structures (e.g., see [263][264][265][266][267][268]). Many countries have adopted to ACI Standards; they are located in North, Central, and South America, Asia, and the Middle East (including the UAE, Iran, Kuwait, etc.) [269]. Due to the adaptivity of the local building standards, two standards were used in ETABS for design code checking: International Building Code (IBC) [270][271], and ACI 318-19 [272] by the American Concrete Institute (ACI).

All required load cases and combinations, including the gravity loads (loads in gravity direction), were applied in accordance with the standards of the ASCE as outlined in ASCE/SEI 7-16 [273], as well as in compliance with the IBC [270, p. 365], other relevant literature [6], and through consultation with local professional structural engineers. These standards are also the main references for the local building code [195]. Table 18 presents the gravity loads. Table 19 presents the load combinations that were used during the structural analysis process in this research. The wind and seismic analysis is further explained in the following parts.

Table 18. Gravity loads. Source: the researcher

Shell/area load on floor slabs | Dead	250 Kgf/m^2
Shell/area load on floor slabs | Live	300 Kgf/m^2
Frame/line load of facade curtain walls on perimeter ring beams | Dead	400 Kgf/m

Table 19. Load combinations applied in structural analysis in accordance with ASCE/SEI 7-16 [273], and IBC [270]. *EQ refers to the equivalent static method in seismic analysis; **SPEC refers to the dynamic sismic analysis method of muli-mode response spectrum. Source: the researcher

Load Combination	Dead Scale Factor	Live Scale Factor	Wind Scale Factor	EQ* Scale Factor	SPEC** Scale Factor
LC 1	1.4	-	-	-	-
LC 2	1.2	1.6	-	-	-
LC 3	1.2	1	1.6	-	-
LC 4	1.2	1	-1.6	-	
LC 5	1.2	-	0.8	-	-
LC 6	1.2	-	-0.8	-	-
LC 7	0.9	-	1.6	-	-
LC 8	0.9	-	-1.6	-	-
LC 9	1.2	1	-	1	-
LC 10	1.2	1	-	-1	-
LC 11	1.2	-	-	1	-
LC 12	1.2	-	-	-1	-
LC 13	0.9	-	-	1	-
LC 14	0.9	-	-	-1	-
LC 15	1.2	1	-	-	1
LC 16	0.9	-	-		1

3.3.1.2   Wind

Wind loads were calculated based on the local wind code [274]. For this purpose, the researcher translated the relevant parts of the code into Python and created a GH/Python component called the "Wind Code", which is explained in detail later in the following paragraphs. The local wind code was incomplete in the parts dealing with cylindrical building forms. Therefore, for those parts, the researcher used Eurocode 1: Actions on structures - Part 1-4: General actions - Wind actions, BS EN 1991-1-4:2005+A1:2010 [275], which was also a main reference in the local code (the researcher also considered newer versions: ÖNORM B 1991-1-4:2019 [276], and ÖNORM B 1991-1-4:2023 [277], but no changes in the code with respect to the particular methods and parameters used in this study were observed). The diagrams in Figure 61 illustrates the intensity, direction, and distribution of wind loads throughout the plan and height of a cylindrical tall building. Figure 62 presents the calculated wind loads corresponding to different sides and height zones of each prototype in this study. Please refer to Figure 61 as a visual guide for better understanding the placement of F1, F2,..., F5, and H0, H1,..., H4 in Figure 62.
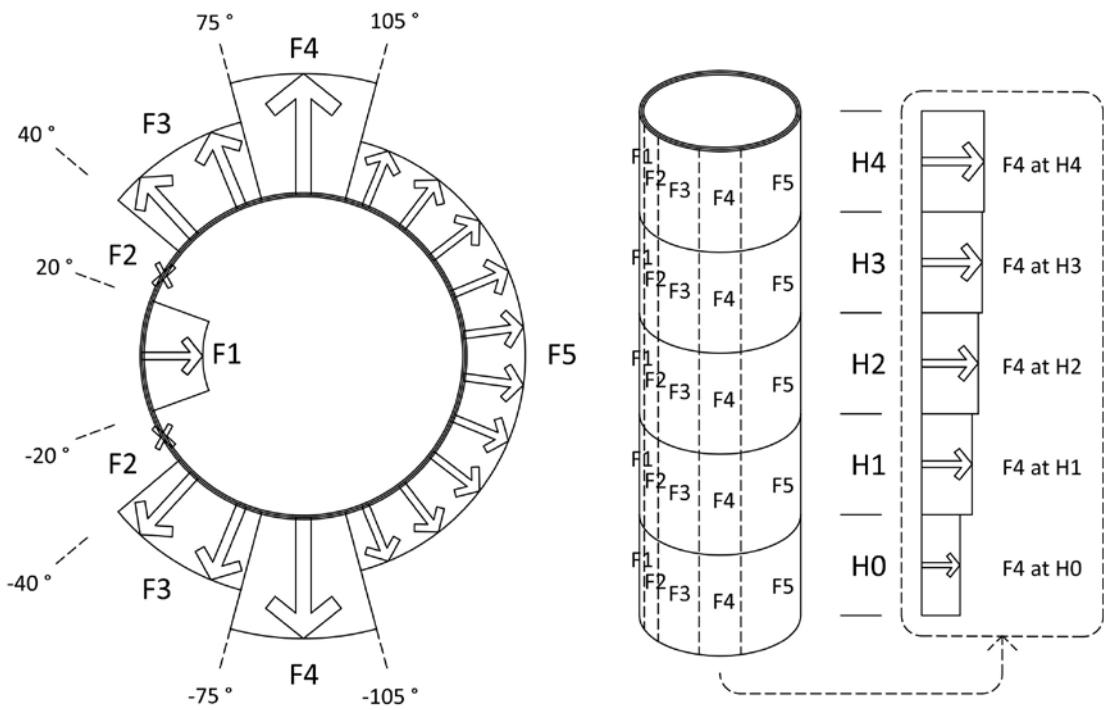
Figure 61. Intensity and distribution of wind loads on a cylindrical tall building. Left: Different zones and directions of loads in plan view. Middle: Different height zones. Right: An example demonstrating the increase of wind loads with height. Source: the researcher
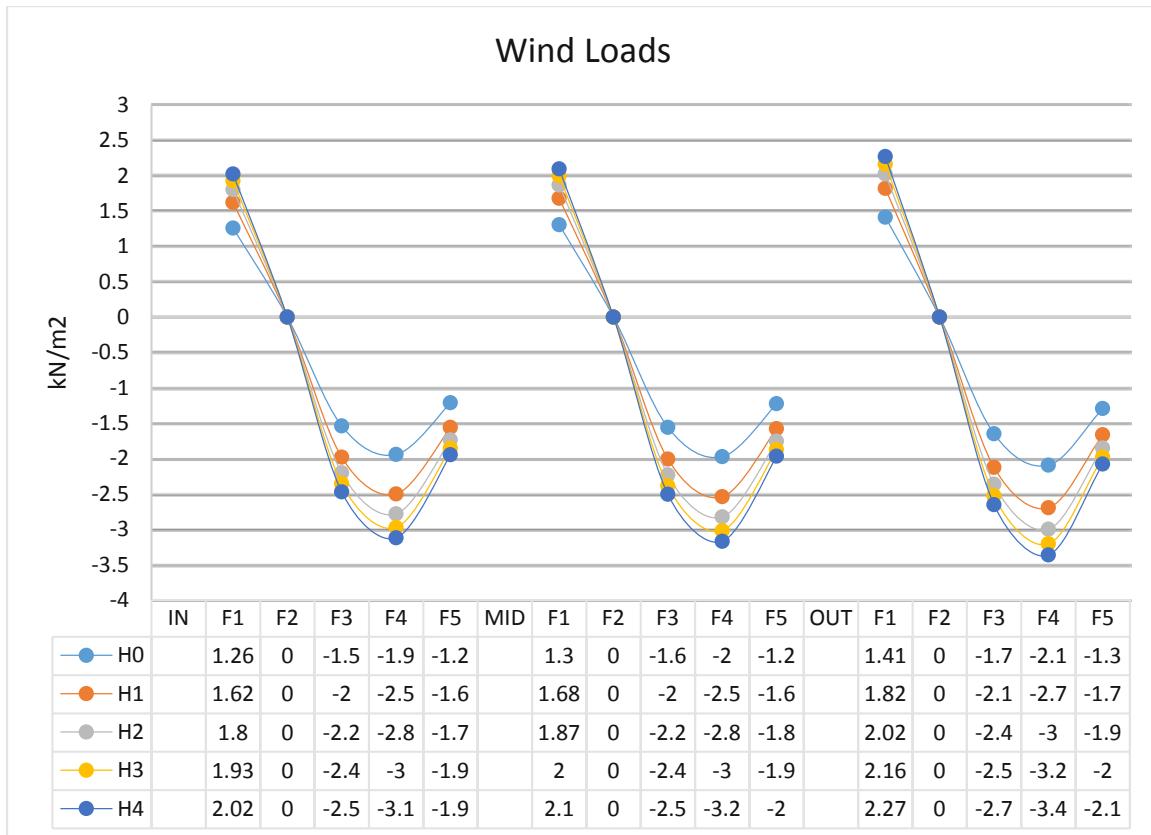
Figure 62. Wind Loads on different heights and different sides around the three structure prototypes (IN, MID, OUT).

	IN	F1	F2	F3	F4	F5	MID	F1	F2	F3	F4	F5	OUT	F1	F2	F3	F4	F5
H0		1.26	0	-1.5	-1.9	-1.2		1.3	0	-1.6	-2	-1.2		1.41	0	-1.7	-2.1	-1.3
H1		1.62	0	-2	-2.5	-1.6		1.68	0	-2	-2.5	-1.6		1.82	0	-2.1	-2.7	-1.7
H2		1.8	0	-2.2	-2.8	-1.7		1.87	0	-2.2	-2.8	-1.8		2.02	0	-2.4	-3	-1.9
H3		1.93	0	-2.4	-3	-1.9		2	0	-2.4	-3	-1.9		2.16	0	-2.5	-3.2	-2
H4		2.02	0	-2.5	-3.1	-1.9		2.1	0	-2.5	-3.2	-2		2.27	0	-2.7	-3.4	-2.1

Note: H0 to H4 represent different height zones of the structures (H0: lowest, H5: highest)

F1 to F5 represent forces applied on unit area of building envelope surfaces around floor plans in different directions as listed below:
F1: -20 to 20 degree # + parallel to wind direction
F2: 20 to 40 degree # 0 neutral area
F3: 40 to 75 degree # - perpendicular to face
F4: 75 to 105 degree # - perpendicular to face
F5: 105 to -105 degree # - perpendicular to face
Source: the researcher

Here, the algorithm of the GH/Python component of the "Wind Code" is explained step by step. Some of the numerical values shared between the three superstructure prototypes (IN, MID, and OUT) are also mention. However, more details and all calculated numerical values are available in the corresponding attached technical file. The component also generates a report in English, which makes it user-friendly and easy to double-check or replicate. The input variables of the component were: (1) height of the structure ($h = 187.68$ m); (2) Wind Envelope Radius ($WER = 21$ m); (3) Terrain Number ($TN = 2$); (4) the height of the location in meters from the sea level ($d = 25$ m); and (5) Friction Coefficient (Cfr). The component was used three times to estimate the wind loads on the three prototypes. For each of them, the following process was done:

First, it calculated the slenderness ($l = 4.46$) of the structures, which is equal to $h/(2 * WER)$; Then, depending on the value of l, and in accordance with the Eurocode [275, p. 83], it found the indicative value of the end-effect factor ($psl = 0.987$) as a function of solidly ratio (ph) versus l ($ph = 1$ was assumed for overall wind envelope area). Parameters of pressure distribution around circular cylinders, in compliance with the local wind code [274, p. 20], and Eurocode [275, p. 71], were: the position of the minimum pressure in degree ($amin = 75$); the position of the flow separation in degree ($aA = 105$); the value of the minimum pressure coefficient ($Cp0min = -1.5$); and the base pressure coefficient ($Cp0A = -0.8$). The values of pressure coefficient without end-effect ($Cp0$) which varied around the circular plan, according to the local wind code [274, p. 14], and Eurocode [275, p. 70], were: for -20 to 20 degrees ($Cp01 = 0.8$); for 20 to 40 degrees ($Cp02 = 0$); for 40 degrees to $amin$ ($Cp03 = -1$). The structures were divided into 5 zones in height; it is assumed that the wind loads are constant along the height of each zone; the number of zones were set to 5 (larger than the l), because according to the local code, each zone's height had to be smaller than the diameter of the structure [274, p. 16]. These zones in height, as well as the zones of distribution of varying loads around the cylindrical structures with respect to the aforementioned angles are illustrated in Figure 61.

Based on the Eurocode [275, p. 69], external pressure coefficient (Cpe) of circular cylinders was determined by Equation 2.

Equation 2.

$$Cpe = Cp0 \cdot pslA$$

; where $pslA$ (the end-factor) was calculated by Equation 3.

Equation 3.

$$pslA = 1 \qquad \text{for} \quad 0° \leq a \leq amin$$
$$pslA = psl + (1 - psl) \cdot \cos\left(\frac{\pi}{2} \cdot \left(\frac{a - amin}{aA - amin}\right)\right) \qquad \text{for} \quad amin < a < aA$$
$$pslA = psl \qquad \text{for} \quad aA \leq a \leq 180°$$

; where aA is the position of the flow separation as shown in Figure 61.

In accordance with the local code [274, p. 8], TN 2 ("areas with low vegetation and isolated obstacles where the average obstacle separation is more than 20 times the average obstacle height") was selected (the component can also handle other types of terrain). For this type of terrain, the surface friction length ($z0$) was 0.05 m, and the minimum friction height ($zmin$) was 2 m. Height-dependent surface friction coefficients $Ce(z)$ were calculated for different heights using Equation 4 [274, p. 7].

Equation 4.

$$\text{For } z \geq zmin: Ce(z) = kr \ln\left(\frac{z}{z0}\right)$$
$$\text{For } z < zmin: Ce(z) = Ce\,(zmin)$$

; where the terrain factor (kr) depending on $z0$ was estimated by Equation 5.

$$kr = 0.23 \cdot (z0)^{0.07}$$

The topography coefficient ($CT = 1.025$) was determined using Equation 6 [274, p. 8].

$$CT = 1 + 0.001 \cdot d$$

The turbulence intensity, $IW(z)$, depending on height was defined by Equation 7 [274, p. 10].

$$\text{For } zmin \leq z \leq 200m: IW(z) = \frac{1}{Ct \ln(z/z0)}$$
$$\text{For } z \leq zmin: I_w(z) = IW(zmin)$$
$$\text{For } z \geq 200m: I_w(z) = IW(200)$$

The peak pressure at external height ze, called $qp(ze)$, was calculated by Equation 8 [274, p. 12].

$$qp(ze) = \left[Ce^2 \cdot CT^2 \cdot [1 + 7IW(z)]\right].\left[\frac{1}{2}ro.Vb^2\right]$$

; where the density of the air (ro) and the basic wind velocity (Vb) were assumed to be 1.25 kg/m^3 [274, p. 12], and 30 m/s [274, p. 6], respectively.

Since the openings on the facades were insignificant, the forces on internal surfaces (Fin) were negligible and were not assessed [274, p. 15]. Therefore, the total wind loads (F) for each unit of surface area (1 m^2) at different heights were calculated using Equation 9.

$$F = Fex + Ffr$$
$$with$$
$$Fex = Cs . Cd . qp(ze). Cpe$$
$$Ffr = qp(ze). Cfr$$

; where Fex is the forces on external surfaces; Ffr is friction forces; according to the local code, due to the relatively high roughness caused by the exoskeletons compared

with the smooth surfaces of curtain walls, the values of *Cfr* for alternatives IN, MID, and OUT were estimated to be 0.01, 0.02, and 0.03, respectively [274, p. 16]; *Cs* is load correlation coefficient, and *Cd* is dynamic amplification factor [274, p. 15]; In compliance with the Eurocode (Annex D, "*Cs×Cd* for multistorey concrete buildings"),and with respect to the size of the structures in diameter and height, the value of *Cs×Cd* estimated to be approximately 1 [275, p. 112]. The total wind loads were estimated for the zones around the cylindrical structures at the middle of the height of each zone in height, and the results were collected and presented in Figure 62. Figure 63, as an example, illustrates the deformation of the superstructure alternative OUT subjected to wind loads.
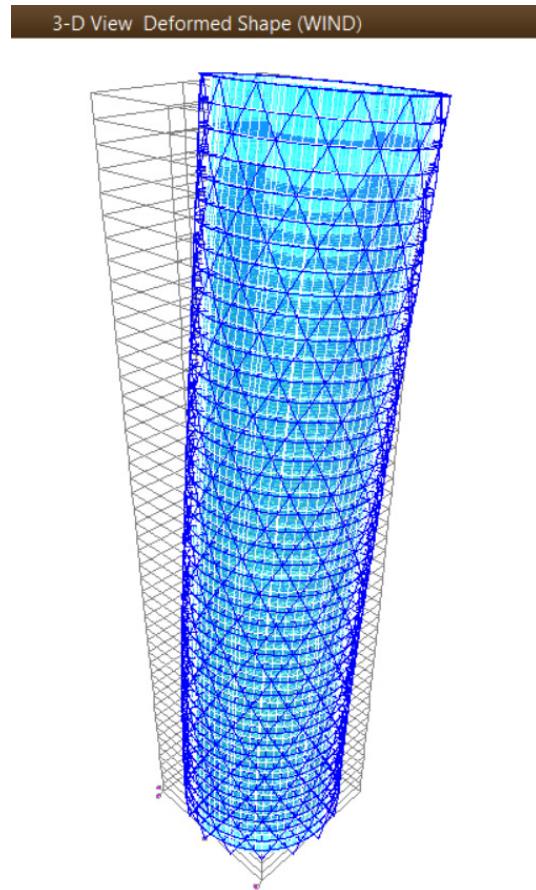
Figure 63. The superstructure alternative OUT analyzed under the static wind load case. Screenshot of wireframe preview of the model. Deformed shape scale factor for visualization: 250. Source: the researcher

3.3.1.3 Earthquake

Seismic loads were analyzed using both the dynamic method of multi-mode response spectrum (an advanced linear dynamic analysis method recommended for tall buildings) and equivalent static method, in compliance with the local seismic design code [278, p. 20]. To facilitate this analysis, the researcher translated relevant sections of the local code into Python and created a GH/Python component called "Seismic Design Code". This component calculated the parameters necessary to determine the elastic response spectrum, which was then applied in ETABS. Figure 64 displays the

134

resulting elastic response spectrum. In the final stage of analysis and design, the base shears of the two methods were balanced according to the local seismic code [278, p. 24]. The process and algorithms are described in the following paragraphs.
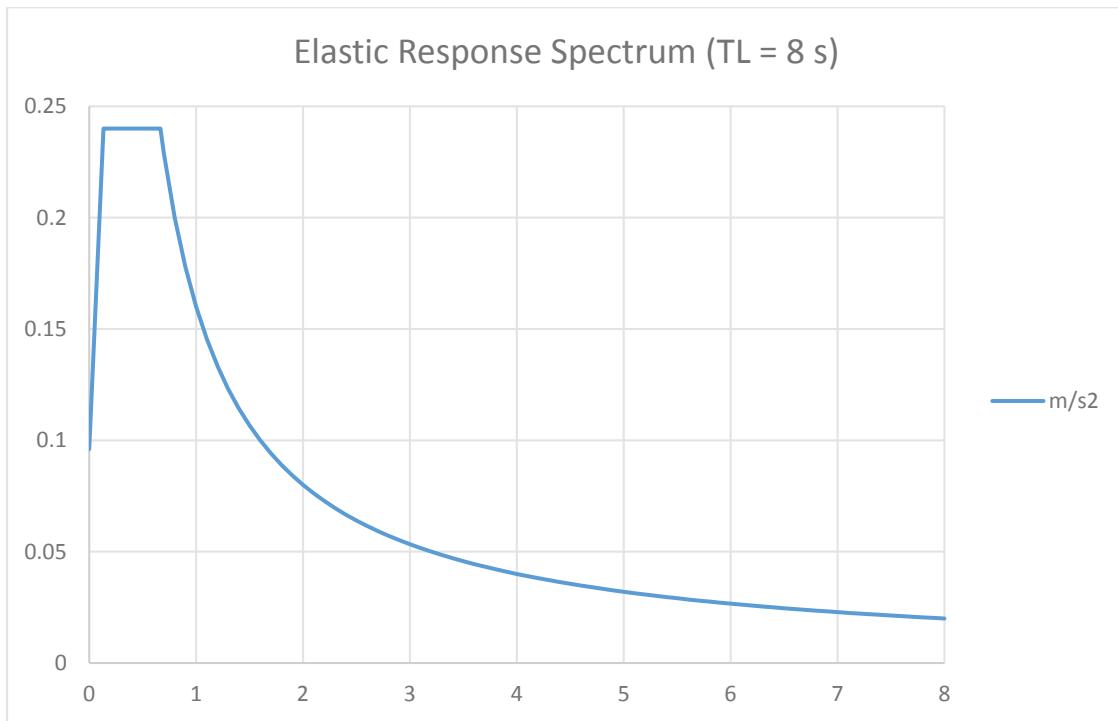
Figure 64. Elastic Response Spectrum in this study. Spectral accelations are in unit of *g* (gravity) in m/s^2. Transition period of response spectrum to long-period range (TL) = 8 second. Calculations based on the local Seismic Design Code [278]. Source: the researcher

Here, the algorithm of the Python component "Seismic Design Code" is explained. More details are available in the corresponding attached technical file. The component is open-source, and it also generates a textual report in English that makes it easier for the audience to double-check or replicate the process. The input variables of the component were: (1) total height of structure (*HN* = 187.68); and (2) soil class (*SC* = D) (the component is able to assess other classes of soil and structures with different heights as well). The acceleration of gravity (*g*) was assumed to be 9.81 m/s^2. The empirical factor for the calculation of predominant period in the earthquake direction (*Ct*) was assumed to be 0.050, and the natural period of predominant mode (first mode), *T1*, was estimated to be 2.54 s using the Equation 10 [278, p. 23].

Equation 10.

$$T1 = Ct \cdot HN^{3/4}$$

With respect to the minimum performance objectives for tall buildings, the normal building occupancy class (i.e., residence, hotel, office building, etc.), under the medium earthquake level (*E2*) was considered, which targets life safety and controlled damage [278, p. 12].

Stiff soil (*SC* = D) was selected from a list in Annex A [278, p. 98] (other listed *SC*s were: A- hard rock, B- rock, C- very dense soil and soft rock, E – soft clay soil,

and F- soils requiring site response analysis). Based on the local code [278, p. 8], for the selected *SC* and aforementioned earthquake level, the values of the short period (0.2 second) elastic spectral acceleration (*SSD*), and the 1.0 second elastic spectral acceleration (*SID*) were 0.24 and 0.16 (in the units of *g*, in m/s²), respectively. The response spectrum long corner period (*TS* = 0.67 s) and the response spectrum short corner period (*To* = 0.13 s) were calculated following the Equation 11 [278, p. 7].

Equation 11.

$$TS = \frac{S1D}{SSD} \quad ; \quad To = 0.2TS$$

As the structures under study had a dual system primarily consisting of the exterior diagrid frame connected to the core walls via beams and floor slabs, the behavior factor (*q*) was estimated to be 3.0 [278, p. 35]. The building importance factor (*I* = 1.0) for office buildings was assumed. Taking to account that *T1* (2.54 s) was greater than *TS* (0.67 s), the seismic load reduction factor (*qR_T* = 3.0) was calculated in compliance with Equation 12 [278, p. 18].

Equation 12.

$$qR\_T = 1 + \frac{\left(\frac{q}{I} - 1\right)T1}{TS} \qquad (0 \le T1 \le TS)$$

$$qR\_T = \frac{q}{I} \qquad\qquad (TS < T1)$$

The transition period of response spectrum to long-period range (*TL*) for Dubai was assumed to be 8 s. Having in mind that *T1* (2.54 s) fell between *TS* (0.76 s) and *TL* (8 s), the elastic spectral acceleration (*SAE_T* = 0.063 in *g* units in m/s²) representing the horizontal component of earthquake ground motion, was calculated using Equation 13 [278, p. 7].

Equation 13.

$$SAE\_T = 0.4\ SSD + 0.6\frac{SSD}{To}T1 \quad (To \le T1)$$

$$SAE\_T = SSD \qquad\qquad (To \le T1 \le TS)$$

$$SAE\_T = \frac{S1D}{T1} \qquad\qquad (TS \le T1 \le TL)$$

$$SAE\_T = \frac{S1D\ .\ TL}{T1^2} \qquad\qquad (TL \le T1)$$

The design spectral acceleration (*SAR_T* = 0.021 in *g* units in m/s²) was calculated using Equation 14 [278, p. 19].

Equation 14.

$$SAR\_T = \frac{SAE\_T}{qR\_T}$$

136

The base shear coefficient (C), for the equivalent static method applied in ETABS was calculated to be 0.026 (in g units in m/s^2), which is the larger of *SAR T* and a minimum of *0.11×SSD×I* [278, p. 22] (= 0.026 in g units in m/s^2), as required by the local code.

Next, the process of balancing the base shear forces in dynamic analysis with those in the equivalent static analysis was carried out separately for each superstructure alternative. The maximum value of each response quantity due to two horizontal components of the earthquake (base shear forces in the x and y directions) was estimated by taking the square root of the sum of the squared values of the response quantities calculated for each horizontal component [278, pp. 24, 27]. The directional combination of base shear loads in the equivalent static analysis method was larger than in the dynamic multi-mode response spectrum analysis method by a certain ratio, which was calculated and then multiplied by the existing scale factor (initially C) to find an updated scale factor. This updated scale factor was then applied in the response spectrum case data in ETABS for the next run of analysis. The design of the structural elements was checked, and the sizes of cross-sections and rebars were adjusted/increased wherever needed. This process was repeated as a loop until it reached an equilibrium where the directional combination of base shear loads in both methods balanced, and further repetition had no effect on the scale factor. The final response spectrum analysis scale factors calculated for the superstructures IN, MID, and OUT were 4.16, 3.50, and 3.66, respectively.

In the multi-mode response spectrum analysis method, a sufficient number of vibration modes (*NS*) is required, which is determined based on the criterion that the minimum sum of effective participating masses in each lateral direction of earthquake must be equal to 90% of the total mass of the building [278, pp. 25, 26]. Based on the analysis results in ETABS, the *NS* in the final design of the alternatives IN, MID, and OUT were 18, 7, and 10, respectively. However, to be on the safe side, 21 modes were included during the entire analysis and design processes. As an example, Figure 65 illustrates the deformation of the superstructure alternative OUT under several vibration modes.
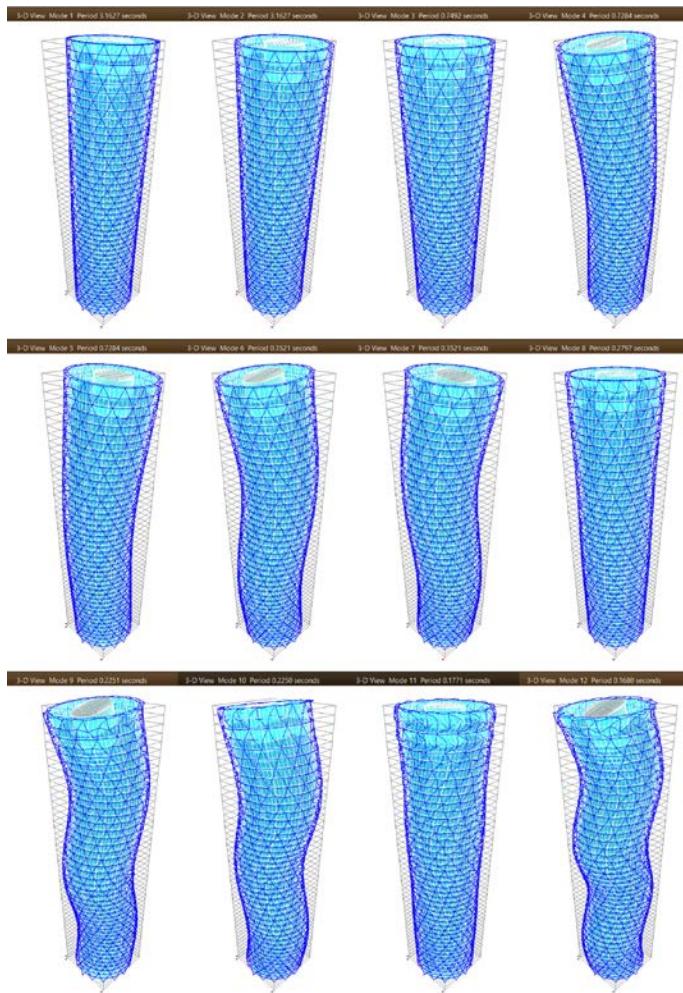
Figure 65. The top left to bottom right shows vibration modes 1 to 12 deforming the superstructure alternative OUT under earthquake loads using the multi-mode response spectrum analysis method. The screenshots are taken from wireframe previews of the model (with a shape mode scale factor of 10000 for visualization). Source: the researcher

3.3.1.4 Modeling, Analysis, and Design Process

The modeling, analysis, and design process of all three superstructure prototypes (IN, MID, and OUT) involved the following general steps:

1. Basic geometric modeling was performed in Rhinoceros using a GH algorithm, including Python scripting components developed by the researcher, as explained in subsection 3.2.2.
2. The geometric models of the prototypes generated in the previous step were exported as DXF files to the ETABS program for structural analysis and design.
3. Typical RC floor slabs with a depth of 200 mm were assigned to all floors. The level of the top of the beams was assumed to be equal to the level of the top of floor slabs.

138

4. The thickness of the concrete cover was set to 51 mm for the diagrid columns and shear walls, and 40 mm for the beams and slabs.

5. All structural loads, encompassing gravity (dead and live) loads, wind loads, seismic loads, and their respective load combinations, were defined and applied in accordance with the detailed explanations provided in the preceding subsections of this section.

6. The superstructure models were divided into zones, each consisting of eight typical floors/structural levels, except for the highest zone with six remaining levels (as shown in Figure 59). The PSEs in each level of each zone were considered identical to similar ones in other levels of that zone.

7. To ensure structural stability, the researcher initially overestimated the size of cross-sections of diagrid elements. Gradually, the size of cross-sections was reduced while meeting standard requirements, which were automatically checked by ETABS.

8. In each step, the maximum amount of rebars (6% volumetric, according to ASCE 7-05 [273], with a minimum of 1% and a maximum of 6% of rebars allowed in columns) was initially placed in a cross-section and then reduced to the minimum possible amount to avoid failure.

9. If a cross-section failed, a larger one was initiated, always in increments of 50 mm.

10. The aforementioned process was repeated until an equilibrium state was reached, where further reduction in cross-section size was not possible.

11. The number of full building model trials and errors for each prototype until reaching the final designs were as follows: 15 for INs, 20 for MIDs, and 13 for OUTs. Each full structure analysis process in ETABS took approximately 35, 50, and 60 minutes, respectively.

12. In a similar fashion, and in parallel with the diagrid elements, the core walls were designed. The radial and spandrel/ring beams were initially designed based on common rules of thumb. Several size possibilities were then checked in a trial-and-error fashion until the smallest feasible design was reached for each case.

Fire Resistance Ratings:

In accordance with the local fire and life safety code of practice, buildings taller than 128 m (similar to prototypes in this research) are required to have a fire resistance rating of (two to) four hours (for more details, see [279, pp. 62, 68]). For this purpose, all final designs of PSEs in this study, including RC columns, core walls, beams, and floor slabs (presented in the next subsection, 3.3.2), underwent a thorough evaluation against the 2018 IBC (Sixth Version: Nov 2021) [280, Ch. 7], confirming their compliance with a four-hour fire resistance rating.

For example, concerning columns, all the columns in the study at hand had a concrete cover with a thickness of 51 mm, complying with the IBC code [280, Ch. 7, 722.2.4.1.1]. The minimum dimensions of diagrid columns with a square cross-section in this research were 400 mm (at the top zone in the case of endoskeletons; see Table 23), exceeding the required minimum dimension of 14 inches = 356 mm (see [280, Ch. 7, Table 722.2.4]). The minimum dimensions of diagrid columns with a rectangular cross-section in the present investigation were 300 × 2000 mm (at the top zone in the

cases of exoskeletons; see Table 24 and Table 25), surpassing the required minimum dimension of 10×36 inches = 254×914 mm (see [280, Ch. 7, Table 722.2.4]). Similarly, all other PSEs in this research, including shear walls, beams, and floor slabs, were double-checked and met the IBC [280, Ch. 7] requirements.

The final superstructure alternatives of the study at hand, including the one with an endoskeleton (IN), and the ones with an exoskeleton (MID and OUT), are shown in Figure 66. Further specification of the PSEs for each is provided in the next subsection, 3.3.2.
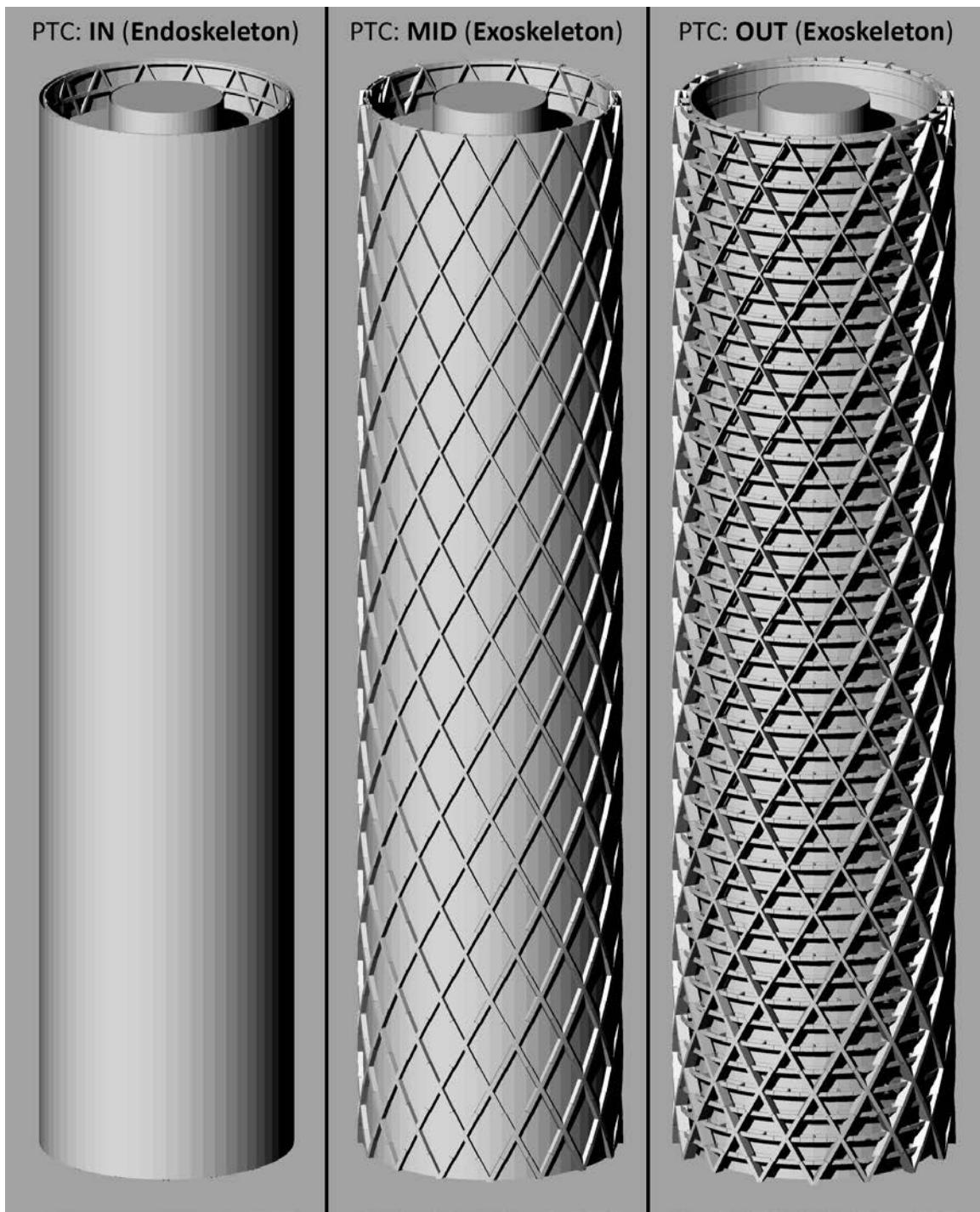
Figure 66. The superstructure prototypes finalized (after structural analysis and design), images from left to right: IN, MID, OUT. Source: the researcher

3.3.2 Pre-Operational (Embodied) Inventory and Impact Assessment

The final structural designs in ETABS for the three alternative superstructures (IN, MID, and OUT), which were optimized and checked for compliance with analysis and code requirements, were the basis for preparing the LCI and LCIA with respect to the pre-operational phase, as they include the exact sizes of all RC structural elements as well as the design of the required reinforcement (steel rebars).

Subsequently, the whole calculations and quantity estimation process and impact assessment were done, including bills of materials for all structural elements, insulation materials for controlling thermal bridges, as well as corresponding characterization factors for impact assessment, etc. This was carried out in a Rhinoceros/GH file named "Pre_Operational_Inventory_and_Impact.gh". This file included multiple components that the researcher developed in Python, which are open source and self-explanatory. The algorithm of each component includes notes about the applied scientific references, standards, and formulations, and generates a textual report in English that makes them user-friendly for the intended audience, allowing them to check or replicate the process with all the details. Due to the vast amount of details covered by the file (e.g., the rebar design for beams on each floor of each superstructure alternative was different from other floors), it was not possible to include all of them in the dissertation in printed form. However, the following parts of this subsection explain all of the important steps of the LCI and LCIA processes with respect to the pre-operational (embodied) stage. The description of statistical and mathematical analysis methods applied to the LCIA are later explained in the last section of this chapter. The next chapter includes the results of the analysis.

3.3.2.1 Floor Slabs

The floors slabs (outside and inside the core area) were assumed identical for the three superstructure alternatives (IN, MID, and OUT). For the quantity estimation of the floor slabs located between the core and the outer perimeter of floors the researcher developed a GH/Python component called "Slabs QE". The input variables of the component were: (1) the gross area of 1101 m^2 for each typical floor (as shown in Figure 57); (2) rebar diameter of Φ14 mm; (3) with spacing of 200 mm; (4) in 2 layers of mesh; (5) within slabs with the depth of 200 mm were assumed; (6) number of slabs above the ground were 41 (as it was shown in Figure 59); and (7) an additional 5% of reinforcement material was assumed to cover other items (e.g., overlaps, waste, etc.). This additional 5% was also assumed for other RC elements (i.e., slabs inside the core areas, core shear walls, diagrid columns, and beams that are explained in the next parts), but is only mentioned once here to avoid redundancy. The density of concrete and reinforcement steel for the quantity estimations of all types of RC elements were assumed to be 2400 kg/m^3 and 7850 kg/m^3, respectively.

Based on the input data, the component calculated the total volume of rebars and the slabs, and consequently calculated the total mass of concrete and rebars. Similar process was also done for quantity estimation of the slabs inside core areas using a similar GH/Python component called "Inside Core EQUIV QE". The difference with the previous component was that for the latter the area of 283 m^2 (as shown in Figure 57) and number of slabs of 46 were assumed. The increase in number of inside core

slabs was because this area is included two times within double-height floors (ground floor, mechanical floors, as well as the core spaces above the roof—as it can be seen in Figure 59). The resulting values for mass of concrete and steel reinforcement for the floor slabs (both outside and inside the core area) are included in Figure 69, Figure 70, Figure 71, and Figure 72.

3.3.2.2   Core Shear Walls

For quantity estimation of structural materials with respect to the core shear walls, the researcher developed a GH/Python component named "Core Shear Walls QE". The inputs of the component were: (1) a core radius of 9.5 m (as shown in Figure 57); (2) a typical story height of 4.08 m; and (3) zones data. The zones data, which differed for each superstructure alternative (IN, MID, and OUT), refer to 6 zones in height (5 zones each including 8 stories height, and the highest zone including 6 stories height). The design of the shear walls was constant along the height of each zone. The data of each zone represents the final design in ETABS, including wall thickness and reinforcement design specifications—i.e., longitudinal rebar size and spacing (in mm) and the cross-sectional area of the shear rebars per meter length in the core walls—as presented in Table 20, Table 21, and Table 22, for the superstructure alternatives IN, MID, and OUT respectively. Based on these data, for each superstructure, the aforementioned Python component first calculated the volumes of rebars (all longitudinal, shear, and ties) and walls in each zone, and then estimated the total mass of concrete and rebars of the core shear walls, which are included in Figure 69, Figure 70, Figure 71, and Figure 72. The component also calculated the average core wall thickness for each superstructure, which were later used in HVAC modeling (IN: 378 mm, MID: 352 mm, OUT: 387 mm).

Table 20. Superstructure IN; Core Shear Walls Design Data. Source: the researcher

Zones Data	Zone 1	Zone 2	Zone 3	Zone 4	Zone 5	Zone 6
Story UP	8	16	24	32	40	46
Story DN	1	9	17	25	33	41
Wall Thickness (mm)	550	450	350	300	300	300
Long. Bar Size (mm)	16	16	14	14	14	14
Long. Bar Spacing (mm)	100	200	200	200	200	200
Shear Bar (cm^2/m)	21.65	17.71	13.78	11.81	11.81	11.81

Table 21. Superstructure MID; Core Shear Walls Design Data. Source: the researcher

Zones Data	Zone 1	Zone 2	Zone 3	Zone 4	Zone 5	Zone 6
Story UP	8	16	24	32	40	46
Story DN	1	9	17	25	33	41
Wall Thickness (mm)	500	400	300	300	300	300
Long. Bar Size (mm)	20	16	14	14	14	14
Long. Bar Spacing (mm)	100	200	200	200	200	200
Shear Bar (cm^2/m)	17.61	14.09	10.56	10.56	10.56	10.56

Table 22. Superstructure OUT; Core Shear Walls Design Data. Source: the researcher

Zones Data	Zone 1	Zone 2	Zone 3	Zone 4	Zone 5	Zone 6
Story UP	8	16	24	32	40	46
Story DN	1	9	17	25	33	41
Wall Thickness (mm)	600	450	350	300	300	300
Long. Bar Size (mm)	25	25	14	14	14	14
Long. Bar Spacing (mm)	200	200	200	200	200	200
Shear Bar (cm²/m)	23.62	17.71	13.78	11.81	11.81	11.81

3.3.2.3 Diagrid Columns

Similarly, for quantity estimation of structural materials with respect to the core diagrid columns, the researcher developed a GH/Python component named "Diagrid QE". The inputs of the component were: (1) the number of diagrid elements per story that was 32; (2) the length of each diagrid element that was 4571 mm in accordance to the geometrical models; and (3) zones data. The zones data, which differed for each superstructure alternative (IN, MID, and OUT), refer to 6 zones in height identical to the core walls as mentioned earlier. The data of each zone represents the final design, including the depth (t3) and width (t2) of diagrid columns, the number of rebars distributed in parallel with depth ("2-dir") and width ("3-dir"), and the diameter size of the rebars (Φ) as presented in Table 23, Table 24, and Table 25, for the superstructure alternatives IN, MID, and OUT, respectively. Based on these data, for each superstructure, the aforementioned Python component first calculated the volumes of rebars (including longitudinal rebars, and ties) and diagrid elements in each zone, and then estimated the total mass of concrete and rebars of the diagrid elements, which are included in Figure 69, Figure 70, Figure 71, and Figure 72. The component also calculated the average diagrid element size for each superstructure, which were later used in HVAC modeling (IN: 730 x 730 mm, MID: 587 x 200 mm, OUT: 457 x 200 mm).

Table 23. Superstructure IN; Diagrid Columns Design Data. Source: the researcher

Zones Data	Zone 1	Zone 2	Zone 3	Zone 4	Zone 5	Zone 6
Story UP	8	16	24	32	40	46
Story DN	1	9	17	25	33	41
Depth (t3) (mm)	1050	950	800	600	500	400
Width (t2) (mm)	1050	950	800	600	500	400
Num of Bars in 2-dir	9	9	8	6	5	4
Num of Bars in 3-dir	9	9	8	6	5	4
Long. Bar Size (mm)	40	32	32	32	28	25

Table 24. Superstructure MID; Diagrid Columns Design Data. Source: the researcher

Zones Data	Zone 1	Zone 2	Zone 3	Zone 4	Zone 5	Zone 6
Story UP	8	16	24	32	40	46
Story DN	1	9	17	25	33	41
Depth (t3) (mm)	800	700	650	550	450	300
Width (t2) (mm)	2000	2000	2000	2000	2000	2000
Num of Bars in 2-dir	8	7	6	5	4	3
Num of Bars in 3-dir	20	20	20	20	20	20
Long. Bar Size (mm)	40	32	20	20	16	14

Table 25. Superstructure OUT; Diagrid Columns Design Data. Source: the researcher

Zones Data	Zone 1	Zone 2	Zone 3	Zone 4	Zone 5	Zone 6
Story UP	8	16	24	32	40	46
Story DN	1	9	17	25	33	41
Depth (t3) (mm)	700	550	450	400	300	300
Width (t2) (mm)	2000	2000	2000	2000	2000	2000
Num of Bars in 2-dir	8	6	5	4	3	3
Num of Bars in 3-dir	24	24	20	20	20	20
Long. Bar Size (mm)	32	32	32	20	20	14

3.3.2.4   Beams

For the quantity estimation of structural materials (concrete and reinforcement steel) the researcher developed a GH/Python component called "Beams QE". which was adapted for each superstructure alternative (IN, MID, and OUT). The input data gathered from ETABS (especially with respect to the reinforcement design), was very large in size. Due to the integration of this input data, the Python code for the component became very large, with over a thousand lines of code. Therefore, it was not possible to include all the details here in the dissertation text. However, all the details are available in the attachment file "Pre_Operational_Inventory_and_Impact.gh" for those who are interested in checking or replicating the method. All the important inputs and the process of quantity estimation are explained below.

The zones with respect to the beams were defined at different height levels: (1) because some types of beams (i.e., radial beams and slab beams) were absent at the double-height stories and at the crown of the superstructures, each of these stories had its own separate zone (i.e., stories 1, 22, 43, 45, and 46); (2) Odd-stories below the middle of the superstructures (i.e., stories 3, 5, 7,..., 21); (3) Even-stories below the middle of the superstructures (i.e., stories 2, 4, 6,..., 20); (4) Odd-stories above the middle of the superstructures (i.e., stories 23, 25, 27,..., 41); (5) Even-stories above the middle of the superstructures (i.e., stories 24, 26, 28,..., 44).

In each zone, beams were classified into different types (i.e., radial beams connecting the core walls to the diagrid elements, spandrel beams, secondary beams to support slabs, etc.) which are visualized in Figure 67, and Figure 68. The main difference between beams at even versus odd-stories was that at even-story levels, half of the radial beams end at diagrid nodes, while at the odd-stories, all of the radial beams

end at diagrid elements, but none of them end at the diagrid nodes. The radial beams that ended at the diagrid nodes carried larger loads, resulting in larger cross-sections. The sizes of each type of beam, which are listed in Table 26, remained constant throughout the height of the structures. It is worth noting that the aforementioned classification of height levels (i.e., below versus above the middle of height) was based on differences in the values related to the reinforcement steel design, as explained below.
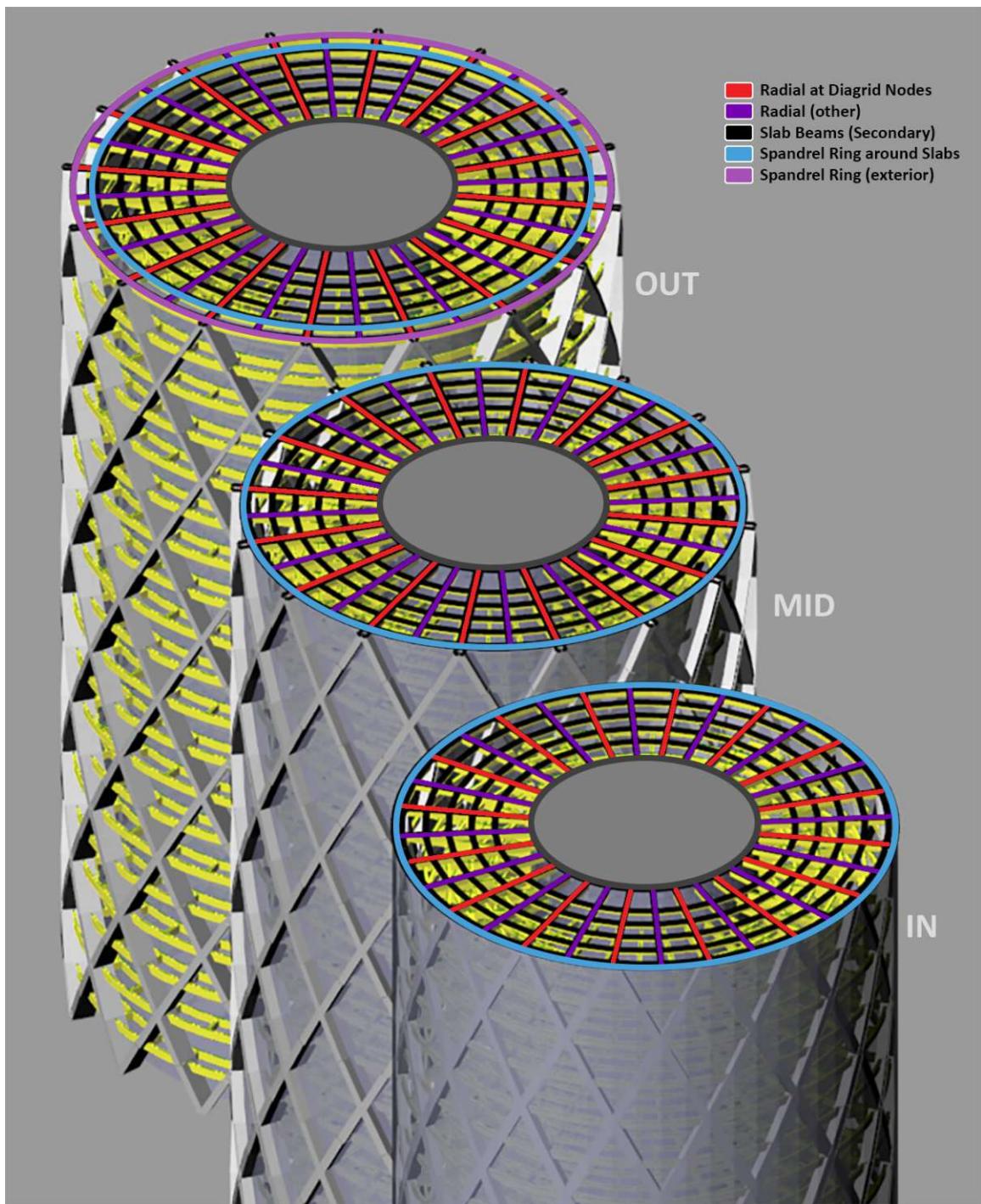
Figure 67. Types of beams at typical even-story levels, where half of the radial beams end at diagrid nodes. The image shows the structural story 20, located at the height of 81.60 m above the base level. Stories above this level have been hidden for better visualization. Source: the researcher
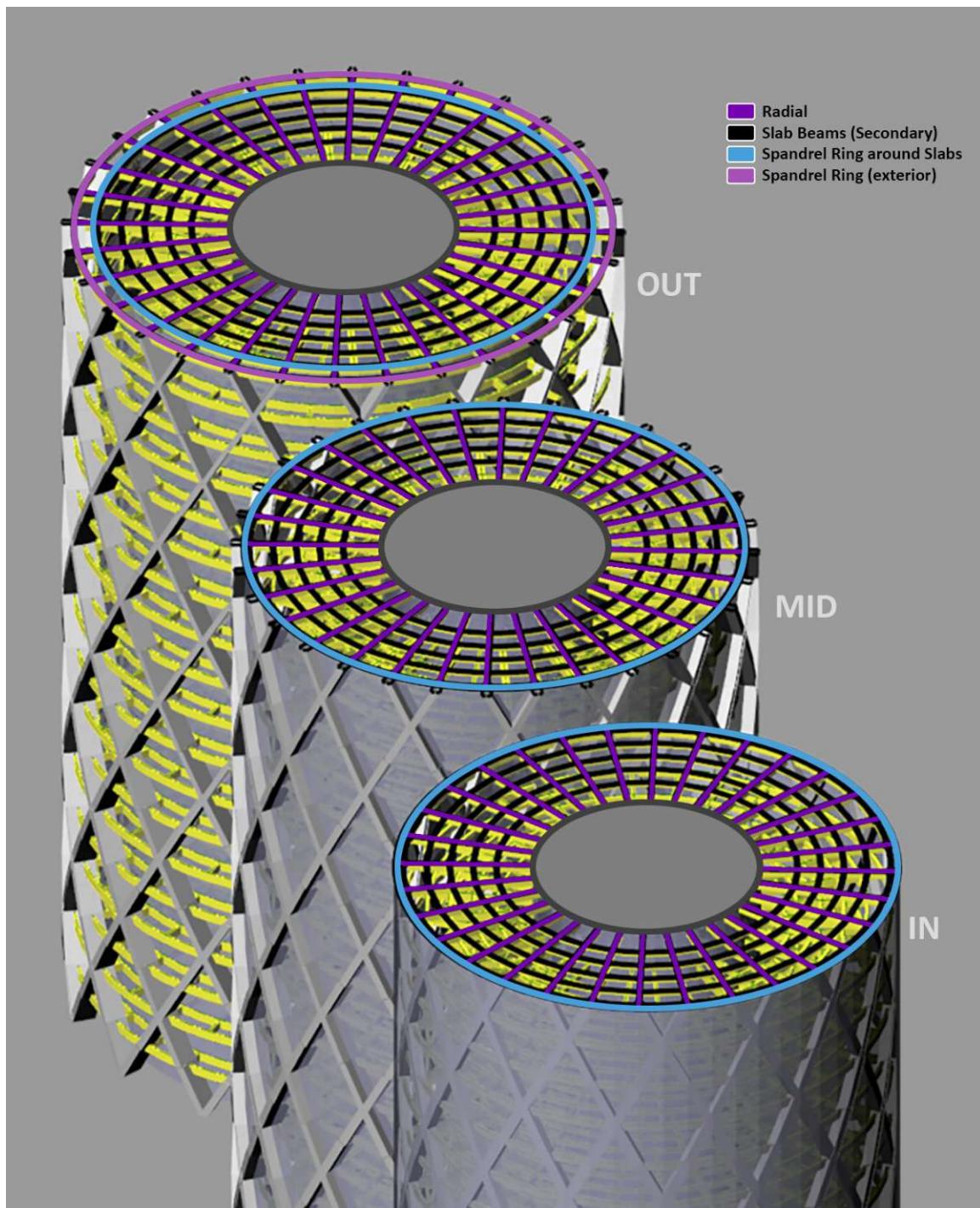
Figure 68. Types of beams at typical odd-story levels, where all of the radial beams end at diagrid elements, but none of them end at the diagrid nodes. The image shows the structural story 19, located at the height of 77.52 m above the base level. Stories above this level have been hidden for better visualization. Source: the researcher

Table 26. Beams' cross-section sizes (Width × Height, in mm). Source: the researcher

Beam Type \ Alternative	IN	MID	OUT
Radials (even-stories, at diagrid nodes)	300 × 700	600 × 700	600 × 800
Radials (others)	300 × 700	300 × 700	300 × 800
Spandrel Rings	300 × 700	300 × 700	300 × 800
Secondary Slab Beams	300 × 400	300 × 400	300 × 400

The data for reinforcement design obtained from ETABS were very large in size, as they varied not only per each story and type of beam but also for different beams of the same type in one story, due to the applied lateral loads (seismic and wind). For each beam in each superstructure, ETABS resulted cross-sectional area values for longitudinal rebars as well as shear rebars in three domains of the beam, i.e., beginning, middle and end domain. Since the plans were circular and symmetrical in various directions, the maximum reinforcement values for each domain of each type of beam in each zone were selected, and those values were assigned to all beams of the same type and zone.

The Python component, double-checked the amount of reinforcements for each beam and corrected them whenever they were less than the minimum requirements in accordance with the minimum set by the ACI 318-19 code [272]. At any section of beams where there was a need for tension reinforcement, i.e., longitudinal rebars, a minimum area of reinforcement (called *A s,min*) was required. *A s,min* had to be the larger of *crtn1* and *crtn2* in Equation 15 ,and Equation 16 [272, pp. 135, 136].

Equation 15.

$$crtn1 = \frac{0.25\sqrt{f_c'}}{f_y} b_w d$$

Equation 16.

$$crtn2 = \frac{1.4}{f_y} b_w d$$

; where, f_c' is the specified compressive strength of concrete which was assumed to be 40 MPa; f_y is specified yield strength of nonprestressed reinforcement steel which was assumed to be 400 MPa; b_w is the width of the beam in mm; and d is the effective depth of the beam in mm, which is the distance from the extreme compression fiber to the centroid of the tension reinforcement.

Similarly, for beams' shear rebars, a minimum area of reinforcement of *A v,min* was required. *A v,min* had to be the larger of *crtn1* and *crtn2* in Equation 17, and Equation 18 [272, p. 138].

Equation 17.

$$crtn1 = 0.062\sqrt{f_c'}\frac{b_w}{f_{yt}}$$

149

Equation 18.

$$crtn2 = 0.35 \frac{b_w}{f_{yt}}$$

; where f_{yt} is the yield strength of the shear reinforcement steel, which was assumed to be 300 MPa.

Other inputs of the Python component, in addition to the size of cross-sections of beams and other parameters mentioned in the aforementioned equations, included detailed geometrical data about the number and length of all different types of beams, gathered from the geometrical models identical to those utilized in ETABS for structural modeling, and the concrete cover depth of 40 mm. The component corrected the amounts of longitudinal and shear rebars wherever needed, calculated the volume of all beams and rebars, and estimated the total mass of concrete and reinforcement steel for each of the three superstructure alternatives (IN, MID, and OUT), which are included in Figure 69, Figure 70, Figure 71, and Figure 72.

3.3.2.5   Total Mass of Superstructures, and Breakdown by Element Type

As mentioned in each of the previous parts of this subsection, Figure 69, Figure 70, Figure 71, and Figure 72 represent the data and graphs with respect to the estimated total mass of the superstructure alternatives (IN, MID, and OUT) and the breakdown by structural element types for each alternative.

Figure 69. Superstructure IN; Mass Breakdown by Element Type. Source: the researcher

Figure 70. Superstructure MID; Mass Breakdown by Element Type. Source: the researcher

Figure 71. Superstructure OUT; Mass Breakdown by Element Type. Source: the researcher
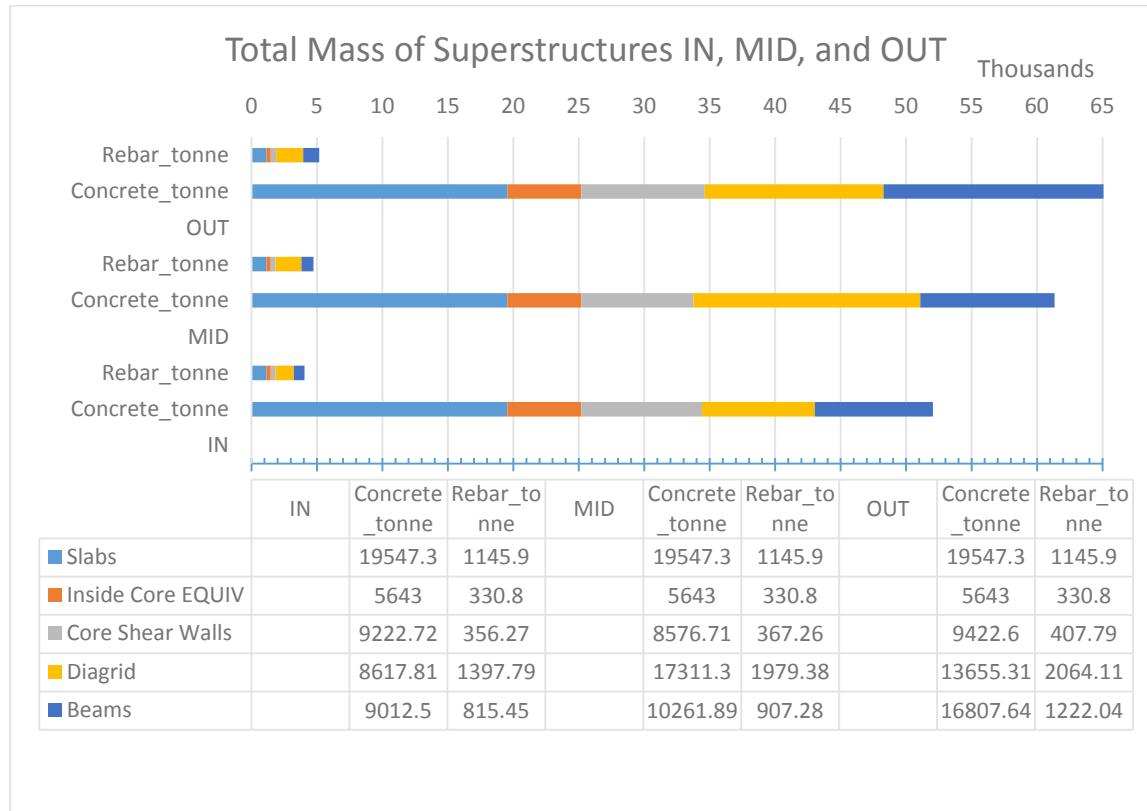
Figure 72. Total Mass of Superstructures IN, MID, and OUT. Source: the researcher

152

3.3.2.6   Embodied Primary Energy and Carbon of Superstructures, and CR Effect

Due to the lack of local country-specific LCI databases in the UAE, the characterization factors from the ICE database v.2.0 [47] and v.3.0 [48] (published in 2011 and 2019 respectively) were considered to estimate the primary energy consumption and CO_2e emissions embodied in the primary structures (explained in this part) and in the insulation materials for controlling thermal bridges (explained in the next part). Table 27 includes the cradle-to-gate (life cycle stages A1-A3) impact characterization factors of these materials. In countries (especially developing countries) where country-specific LCI databases do not exist, it is common for the scientific community to use databases from other countries and to rely on experts views and experiences in research and industry, individual EPDs, etc. to cope with this currently inevitable limitation of the data available in those countries (e.g., see [281][282][283][284][285][286][287][288][289][290][291][292]). The researcher chose the ICE database after consulting with a CTBUH specialist in embodied and life cycle carbon performance of tall buildings [293], and with a local professor (Head of the programs for MSc in Sustainable Design of the Built Environment, and PhD in Architecture and Sustainable Built Environment, at the British University in Dubai) [294][288]. The simulated buildings in this research were assumed to begin their operational phase in 2020. Based on the interrelated reasons and considerations outlined below, the researcher opted to use the ICE database and found it more pragmatic and reasonable to employ data from the older version (v.2.0) of the database, as opposed to the newer version (v.3.0):

1. The ICE database was originally created for the UK but has also been employed in scientific LCA studies around the world (e.g., from Indonesia [289] to Turkey [290] and Chile [291]), including the Middle East region, namely the UAE [286], Iran [287], and Saudi Arabia [292], primarily due to the absence of country-specific LCI databases in such developing countries and the ICE database's comprehensiveness and reliability. Created by academic professors, it adheres to a clear methodology based on standards EN 15804 [68] and EN 15978 [164], and is freely available for researchers worldwide.

2. One of the reasons why the ICE version 2.0 (2011) data was considered more appropriate and reasonable than version 3.0 (2019) data for the UAE around 2019-2020 stems from the energy mix in electricity production. In 2020, the UAE's energy mix was more similar to that of the UK in 2011, with both having less than 5% renewables. This contrasts with the UK's energy mix in 2019, which had more than 30% renewables [295][296]. The fuel mix and carbon ratios associated with electricity generation in a country or region are crucial in determining the amounts of primary energy and GHG emissions in the LCI databases [297]. Often, industries and infrastructure in developing countries are more similar to relatively older industries and infrastructure in developed countries; therefore, older LCI databases from developed countries have been used in developing countries where such country-specific databases do not exist [281][292][291][289][283].

3. Similarly, as another example of a developed country, in Germany in 2019, the energy mix of electricity production included more than 47% share of renewable sources [298]. Furthermore, according to an official German database, dated 2018 [299], the embodied (non-renewable primary) energy (life cycle stages A1-A3: production) in one kilogram of concrete C45/55 (which has even slightly higher compressive strength than the C40/50 MPa used in this research), was 0.625 MJ/kg, i.e., 37.5% less than that of the concrete C40/50 MPa in the ICE database version 2.0 (note that, under similar conditions, concretes with higher compressive strength have more EE and GHG emissions) [47][48]. Therefore, using the newer LCI databases of Germany or UK (dated around 2019-2020) for the UAE at the same dates would be too optimistic.

4. The results of several EPDs dated 2017, conducted in accordance with ISO 14025:2006 [67] and certified by the (USA) National Ready Mixed Concrete Association (NRMCA) on production stage (A1-A3) of different types of ready-mix concrete in Dubai [300] also supports the assumption that the ICE database version 2.0 of 2011 [47] could be reasonably in agreement with the actual situation in Dubai approximately in 2020, as the amount of (renewable) primary energy and GWP in one kilogram of concrete type C40/50 MPa were reported close to and slightly higher than those in the 2011 UK database, i.e., 1.2 MJ and 0.14 kgCO$_2$e, compared to the averages approximately 1 MJ and 0.14 kgCO$_2$e respectively. It is also worth mentioning that the proportion of amount of the embodied renewable energies to non-renewables in the aforementioned EPD in Dubai was marginal, i.e., approximately one percent.

5. Similar results of a whole life cycle EPD on reinforcement carbon steel products, dated 2015, conducted in accordance with EN 15804:2012+A1:2013 [301] and certified by the (UK's-) Building Research Establishment (BRE) [302], was slightly higher but still close to the ICE database version 2.0 [47]; in one kilogram of the material in the stage A1-A3, the embodied (non-renewable) primary energy was approximately 14 MJ and the GWP was 1 kgCO$_2$e, compared to 17.4 MJ and 1.4 kgCO$_2$e. The proportion of renewable to non-renewable primary energies was only about 9%, while in the 2017 database of Germany it was reported as high as 43%. In the ICE database only the non-renewable fuels were reported.

6. As a final point to mention here, one might ask why the researcher did not use conventional LCA software programs (e.g., GaBi, openLCA, SimaPro, One Click LCA, Umberto®, etc.)? This was due to the following reasons: (1) First, the major challenges of the study at hand, which were relatively time-consuming, were the geometric, structural, HVAC and daylighting modeling and simulations running various scenarios that could not be performed using an LCA software program anyway. The researcher performed them in Rhinoceros/GH or collected the data from other programs (e.g., ETABS), but finally gathered and integrated them into the Rhinoceros/GH environment. Only the final statistical/mathematical analysis was performed in R and Excel. (2) Second, in line with one of the objectives of this research, the researcher first searched the relevant

literature for the most crucial life cycle stages for the different aspects; i.e., stages A1-A3 for structural systems, and operational phase for HVAC and electric lighting systems. This significantly reduced the inventory and impact calculations. Taking this and the previous point into account, the researcher preferred to perform the inventory and impact calculations in GH (using the ICE database), which was found user-friendly and transparent, and therefore recommendable to future researchers and practitioners in the field. (3) Third, even the most well-known LCA software programs were not completely reliable at least by the time the present investigation was in progress; e.g., there is a study in the literature that revealed significant differences in results of some of those programs for the same project in a developing country due to the absence of an integrated global network of LCI databases [303]. (4) Last but not least, as discussed by the researcher et al. (in a theoretical book chapter regarding performing LCA in developing countries, published in 2020 [288]): 'An online conversation with one of the managers of an internationally well-known LCA software and service provider companies, showed that they were not aware of the import of sand from Australia to the UAE and therefore they had neglected that contribution to EC and EE of concrete. And only after the questioner mentioned the fact, they replied: "We have average transport distances, and you can also adjust them if you know those values"! In other words, if the design team of a project in Dubai does not know that the sand is being supplied from far away resources, the software will not help them either! Given that many projects in Dubai are designed by non-native specialists and through international competitions, such a miscalculation is likely to occur' [288] (the aforementioned paper [288], which included the above discussions on LCI data in the UAE, was referred to in a scientific LCA paper in 2021 by a researcher and two professors of civil engineering and environmental engineering at the United Arab Emirates University [284]).

Nevertheless, an attempt was made by the researcher to mitigate the aforementioned limitation, by including the two local factors of PDWPRC and PTSAU (to recall, see 2.3.4 and 2.3.5) in the assessment that will be further explained in the following part of this subsection (see part 3.3.2.8).

To estimate the pre-operational (embodied) primary energy and CO_2e emissions of the three superstructure alternatives (IN, MID, and OUT) and the effect of CR, the researcher developed a GH/Python component called "RC Embodied Energy & Carbon." The input variables of the component for each superstructure were: (1) total concrete mass; (2) total reinforcement steel mass; and (3) total GFA of prototypes. The estimation process/algorithm was as follows. As mentioned in the previous chapter, four levels of CR were considered: a baseline level of 15% FA and three other levels of 30% FA, 25% GGBFS, and 50% GGBFS. For completeness, the researcher also temporarily included an additional level of 0% (i.e., 100% CEM I) in this part (it is worth reminding that the most common type of cement used in the current construction industry is the CEM I [185][186][187]). Based on the cradle-to-gate impact characterization factors of the structural materials listed in Table 27, the Python component estimated the total embodied primary energy and total amount of CO_2e

emissions. It then divided these values by the total GFA of each superstructure (58191.26 m^2) to calculate the intensities of primary energy and CO$_2$e emissions in MJ/m^2 and kg CO$_2$e/m^2, respectively. To match the units with the operational phase, the values in MJ were converted to kWh. The results are presented in Figure 73, and Figure 74.

Table 27. Impact characterization factors for structural and insulation materials.

Material \ Characterization Factor			Embodied Primary Energy	Embodied CO$_2$e Emissions	Reference
Concrete C40/50 MPa	CR	0% (using 100% CEM I)	1.17 MJ/kg	0.188 kgCO$_2$e/kg	[47][48]
		15% FA	1.10 MJ/kg	0.174 kgCO$_2$e/kg	
		30% FA	0.99 MJ/kg	0.155 kgCO$_2$e/kg	
		25% GGBFS	1.03 MJ/kg	0.153 kgCO$_2$e/kg	
		50% GGBFS	0.87 MJ/kg	0.115 kgCO$_2$e/kg	
Steel Rebars			1.04 MJ (for 100 kg rebar per m^3 of concrete)	0.077 kgCO$_2$e (for 100 kg rebar per m^3 of concrete)	
Closed-Cell Polyurethane Foam			101.5 MJ/kg	4.26 kgCO$_2$e/kg	
Gypsum Board			4.76 MJ/kg	0.39 kgCO$_2$e/kg	

RC Embodied Primary Energy Intensity (kWh/m^2)

	IN	MID	OUT
0%(CEM I)	779.44	913.61	988.61
15% FLY ASH	760.56	891.67	965.28
30% FLY ASH	731.11	856.94	928.33
25% GGBFS	741.94	869.72	941.67
50% GGBFS	699.17	819.17	888.06
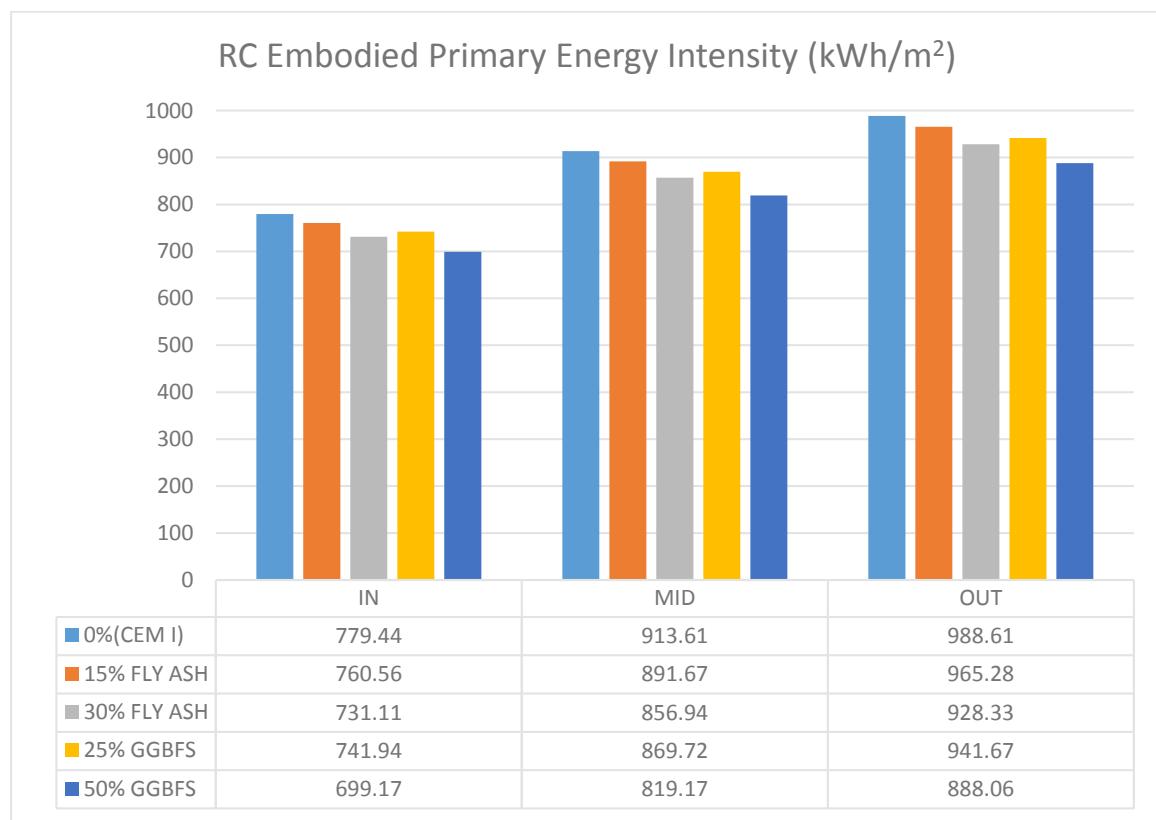
Figure 73. Embodied primary energy intensity in the RC superstructures (IN, MID, and OUT) with and without different CRs. Source: the researcher

RC Embodied Carbon Intensity (kgCO$_2$e/m^2)

	IN	MID	OUT
0%(CEM I)	305.45	358.65	385.89
15% FLY ASH	291.95	342.76	368.99
30% FLY ASH	273.64	321.18	346.05
25% GGBFS	271.71	318.91	343.64
50% GGBFS	235.09	275.77	297.77
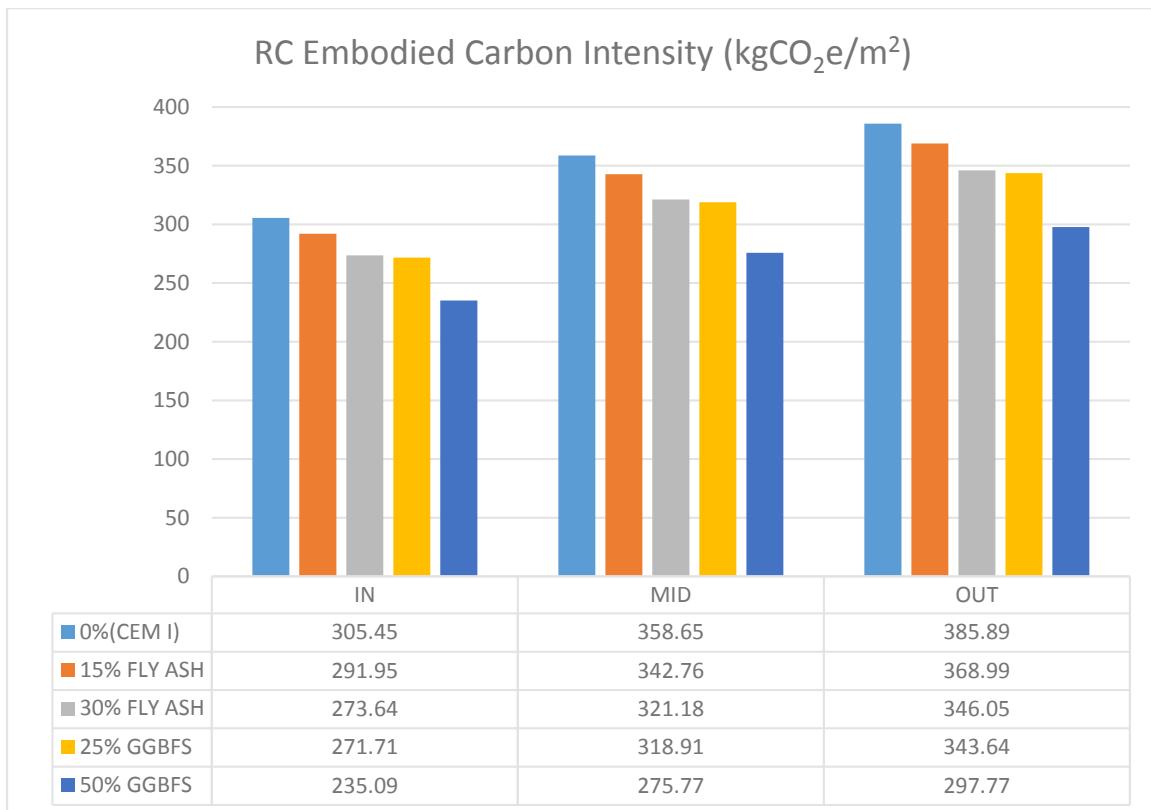
Figure 74. EC intensity in the RC superstructures (IN, MID, and OUT) with and without different CRs. Source: the researcher

3.3.2.7   Insulation Materials

Similarly, to estimate the quantities of insulation materials and their embodied primary energy and CO₂e impacts, the researcher developed a GH/Python component called "Insulation QE, EE & EC." As explained in the previous chapter, there were no thermal bridges in the superstructure with endoskeleton (IN), so the estimation was carried out for superstructures with exoskeletons (MID and OUT) for their scenarios with thermal bridge control via insulation (Factor: TBC, Level: W).

The input variables of the component for each superstructure were: (1) the density of the insulation polyurethane foam (32 kg/m^3), and gypsum board (800 kg/m^3); (2) impact characterization factors as listed in Table 27; (3) total GFA (58191.26 m^2); (4) detailed sizes of insulated areas based on the geometrical models; (5) and the number/location of the insulated areas. The component calculated the volume of insulated material, then calculated the mass, and consequently estimated the total embodied primary energy and total amount of CO₂e emissions. It then divided these values by the total GFA to estimate the intensities in MJ/m^2 and kgCO₂e/m^2, respectively. Finally, the values in MJ were converted to kWh. The results are presented in Table 28.

157

Table 28. Embodied impact intensity of insulation material to control thermal bridges (Factor: TBC, Level: W) in superstructures with exoskeleton (MID, and OUT). Source: the researcher

Impact \ Superstructure Alternative	MID	OUT
Embodied Primary Energy Intensity (kWh/m^2)	18.61	9.17
Embodied CO$_2$e Emissions Intensity (kgCO$_2$e/m^2)	2.79	1.40

3.3.2.8   PDWPRC and PTSAU (Local Factors)

As mentioned in the previous chapter, in order to include local factors and increase the reliability of the assessment, the researcher adjusted the generic inventory data of the ICE database [47] in accordance with two local factors: Percentage of Desalinated Water used in Production of Reinforced Concrete (PDWPRC) and Percentage of Transported Sand from Australia (PTSAU). Detailed calculations are available in GH/Python component called "RC (Local)" developed by the researcher. The estimation algorithm/process is presented below.

The input variables for the Python component for each superstructure alternative (IN, MID, and OUT) were: (1) total concrete mass; (2) total reinforcement steel mass; (3) total GFA; (4) percentage of sand from Australia; (5) percentage of desalinated water; (6) test year (which was set to 2020); (7) test year's PEF for electricity; and (8) test year's GHG emissions for electricity in kgCO$_2$e/kWh. The last two input variables were obtained from the outputs of another GH/Python component called "PE & GHGE (Local)" which is explained later in the next section.

The researcher inquired with the Dubai Electricity and Water Authority (DEWA) and the Dubai Municipality in 2019 and 2023 about local data on the environmental impact of structural materials, desalinated water, and the impact characterization factors of local electricity. No data was provided in response from DEWA or the municipality. Therefore, the researcher made the following estimations. The amount of water required for the production of RC was calculated with respect to the production of rebars, cement, and in mix of concrete C40/50 MPa. The data used in the calculations and the references are available in Table 29. Water production for the year 2020 was estimated in a linear way between 2017 and 2030. According to local data, Multi-Stage Flash (MSF) and Reverse Osmosis (RO) are two common technologies of water desalination; the former is more energy intensive than the latter.

Table 29. Local water desalination and concrete (C40/50 MPa) data. Source: the researcher

Data Items	Values	References
Cement content	400 kg/m^3	[47]
Mass ratio of sand to total sand and aggregates	0.48	[304]
Blue water footprint of Portland cement	2.2 l/kg	[305]
Blue water footprint of unalloyed steel	11.8 l/kg	[305]
Water to cement ratio	0.42	[306]
Water production (MIGD), year 2017	445 MSF, 25 RO	[307]
Water production (MIGD), year 2030	445 MSF, 305 RO	[307]
MSF: Total Equivalent Electrical Energy	23.75 kWh/m^3	[307]
Seawater RO: Total Equivalent Electrical Energy	4.25 kWh/m^3	[307]

Impact characterization factors for maritime transportation of sand was estimated as an average value of data found in different scientific references and presented in Table 30.

Table 30. Impact characterization factors for long distance maritime transportation. Source: the researcher

Primary energy	CO_2e emissions	Reference
0.085 MJ/tkm	0.0058 kg CO_2e/tkm	[202][201][200][203]

To provide a step-by-step overview of what the component "RC (local)" did for each superstructure based on the aforementioned input data, the following steps are listed here (more details are available in the corresponding attached technical file):

- Regarding desalinated water:

  o It first calculated the amounts of total cement, sand and aggregate contents; then calculated the total blue water with respect to cement and reinforcement steel.

  o Based on the water-to-cement ratio, it calculated the total amount of water content of concrete.

  o Then, it calculated the portion of RO in the test year; then estimated the total equivalent electrical energy for water desalination in the test year (in kWh/m^3).

  o Next, it calculated primary energy consumption and CO_2e emissions (in total as well as intensity per m^2 of GFA) of desalinated water with respect to: (1) total water content of concrete; (2) total blue water footprint for cement; and (3) total blue water footprint for reinforcement steel. Then, these three groups of values were summed up, and the results are available in Table 31. Results for the PDWPRC level 0% are not included in the table since they had a value of zero. It is worth mentioning that due to a lack of local data on the amounts of embodied water, including desalinated water, used in the production of CR materials (i.e., FA and GGBFS), the potential interaction effect of RC with PDWPRC was not taken into account.

- Regarding transportation of sand from Australia:

  o It calculated the total mass of sand content.

  o Then, it estimated the primary energy consumption and CO_2e emissions for transporting the mass of sand over 10,000 km from Australia and finally calculated the impacts' intensities (per m^2 of total GFA). The results are presented in Table 32. Results for the PTSAU level 0% are not included in the table since they had a value of zero.

Table 31. Intensity of impact of PDWPRC in each superstructure (IN, MID, and OUT). Source: the researcher

PDWPRC	Impact Type\ Superstructure Alternative	IN	MID	OUT
50%	Primary Energy Intensity (kWh/m^2)	36.70	43.02	46.57
	CO$_2$e Emissions Intensity (kgCO$_2$e/m^2)	4.55	5.33	5.77
100%	Primary Energy Intensity (kWh/m^2)	73.40	86.04	93.13
	CO$_2$e Emissions Intensity (kgCO$_2$e/m^2)	9.09	10.66	11.53

Table 32. Intensity of impact of PTSAU in each superstructure (IN, MID, and OUT). Source: the researcher

PTSAU	Impact Type\ Superstructure Alternative	IN	MID	OUT
50%	Primary Energy Intensity (kWh/m^2)	41.65	49.09	52.08
	CO$_2$e Emissions Intensity (kgCO$_2$e/m^2)	3.06	12.06	12.79
100%	Primary Energy Intensity (kWh/m^2)	83.31	98.19	104.17
	CO$_2$e Emissions Intensity (kgCO$_2$e/m^2)	20.46	24.12	25.59

3.4   Operational Stage

3.4.1   HVAC Simulation

3.4.1.1   Introduction

The researcher used a combination of software programs and programming languages in an integrated parametric setup to simulate HVAC and electric lighting systems, which allowed for the calculation of site energy consumption (electricity or fuel used to operate the HVAC and electric lighting systems). The simulation process will be explained in detail in the following parts of this subsection and in the following subsection. The software programs and programming languages included Rhinoceros, GH, LB+HB, EnergyPlus, OpenStudio, CCWorldWeatherGen, THERM, Radiance, DAYSIM, and Python (to recall the brief introduction to the applied software programs and programming languages, revisit Table 16). This was a reasonable selection of programs and programming languages for the purpose of this study, as they were all well-established and have been validated through extensive research and use. This validation allows them to accurately simulate the models in conjunction with the unique sets of parameters (i.e., factors and levels) for each experimental scenario that were planned in the full factorial DoE.

Rhinoceros is 3D modeling software used to create accurate geometrical models of zones, exoskeletons, urban neighborhoods, etc. It also serves as a host for the visual programming platform GH as a plugin. GH itself, as a parametric environment, hosts LB+HB, as well as Python. LB and HB are open-source plugins in GH used for simulating and analyzing building and environmental performance. LB+HB connect

the models in GH to the standard validated engines of EnergyPlus (via OpenStudio), THERM, Radiance, and DAYSIM (these programs are commonly used in research, e.g., see [308][309][310][311]). CCWorldWeatherGen was used to integrate future scenarios of weather data related to climate change into the simulation models. THERM, a heat transfer analysis program, was used in combination with researcher-defined algorithms in Python and GH to simulate thermal bridges and insulation materials to calculate the U-values of the building envelopes. Two open-source software programs, Radiance and DAYSIM, were used to analyze the daylighting and electric lighting performance of the building prototypes, which will be explained in detail separately in the next subsection of this chapter. Specifically, for simulating the HVAC system and calculating its site energy consumption, EnergyPlus and OpenStudio were used. Both are open-source software programs for whole-building simulation; OpenStudio is used to create, edit, and analyze building simulation models with EnergyPlus as the simulation engine for physics-based calculations related to building systems (e.g., HVAC and electric lighting). Python was employed to add and integrate researcher-defined algorithms to control parameters, automate procedures, and provide other additional functions which were not available as ready-made tools.

This subsection explains the entire HVAC simulation process, including key steps such as geometric modeling of building zones, defining program and zone boundaries, selecting and specifying materials and constructions, modeling thermal bridges and heat transfer, defining shading objects and thermostats, importing weather data files, modeling the urban neighborhood, configuring the HVAC system, running the simulation models, and collecting site energy consumption data for each experiment. In multiple cases, the researcher adjusted parameters based on the factors and levels defined in the DoE process or by consulting the local green building code. When necessary information was lacking, other building codes, international standards, or peer-reviewed research reports were used. In some instances, parameters were adjusted to the default values built into the HB components, which are not mentioned in this report to avoid redundancy. However, readers interested in the references underlying these defaults can find the information in the simulation files, as the HB components include descriptive text for additional details. These references are derived from valid building codes or standards such as the American Society of Heating, Refrigerating and Air-Conditioning Engineers (ASHRAE) Standard 90.1, the International Energy Conservation Code (IECC), and Leadership in Energy and Environmental Design (LEED), as well as peer-reviewed scientific research papers and best practices applied by HB developers. As a side note, it is worth mentioning that in the context of building energy performance modeling, the term "construction" carries a slightly different meaning compared to its common usage. In energy modeling, "construction" refers to the layering of various materials that make up different building elements (e.g., walls, facades, roofs, floors, etc.) and their technical properties in terms of heat transfer, optics, and other physical aspects.

3.4.1.2   Controlling Parameters of Scenarios

Given the multitude of variable and interdependent parameters across different scenarios, in order to prevent human errors in simulation settings, the researcher developed a component in GH/Python named "Scenario Par". This component served as a centralized controller in a user-friendly manner. Its outputs were connected as

inputs to various components, as detailed in subsequent parts of this subsection and the following subsection on electric lighting simulation. The input variables were defined as dropdown menus to select possible levels for factors PTC, TBC, UD (including the height location of the tested typical floor in cases of high UD), TY, and WDY.

The controller automatically detected any logical errors in the settings and generated a textual report of the inputs and outputs, facilitating quick verification by the user. The outputs included parameters determined based on the inputs, such as the type of curtain wall construction (including the effect of thermal bridges on U-value in exoskeleton cases), structural core walls, floor/ceiling construction (including the volume of structural beams as thermal mass), structural shading elements (in exoskeleton cases), and the urban neighborhood buildings (in cases of high UD).

3.4.1.3   Geometrical Model, Zones, Programs and Adjacencies

Architectural and structural models were the basis for the HVAC and electric lighting models. To reduce simulation run times and avoid errors in EnergyPlus with complex shapes, the typical office floor plan model was simplified to an equivalent octagonal shape, where all open office zones and other zones (corridors, elevator shafts, electrical room, break room, lavatories, staircases, etc.) have identical areas to the architectural and structural models. The geometrical simplification method was carried out in Rhinoceros and it was in line with validated research literature on simulating tall buildings using EnergyPlus [312]. It was also recommended by the developers of the energy modeling software HB [313][314].

The octagonal plan still had the desirable neutrality in terms of orientation as it was symmetrical with respect to the main geographical directions. The open office was divided into eight smaller zones (facing North, Northeast, East, Southeast, South, Southwest, West, and Northwest) separated by 'airwalls', which allowed treating the open office zones as a single entity while preventing errors in EnergyPlus caused by concave and complex shapes and also accelerating simulation run time. The programs, EnergyPlus constructions, and adjacencies of the zones were set using the HB components "Mass2Zone", "setEPZoneCnstr", and "solveAdjc" respectively. Figure 75 illustrates all zones of a typical floor and their programs.
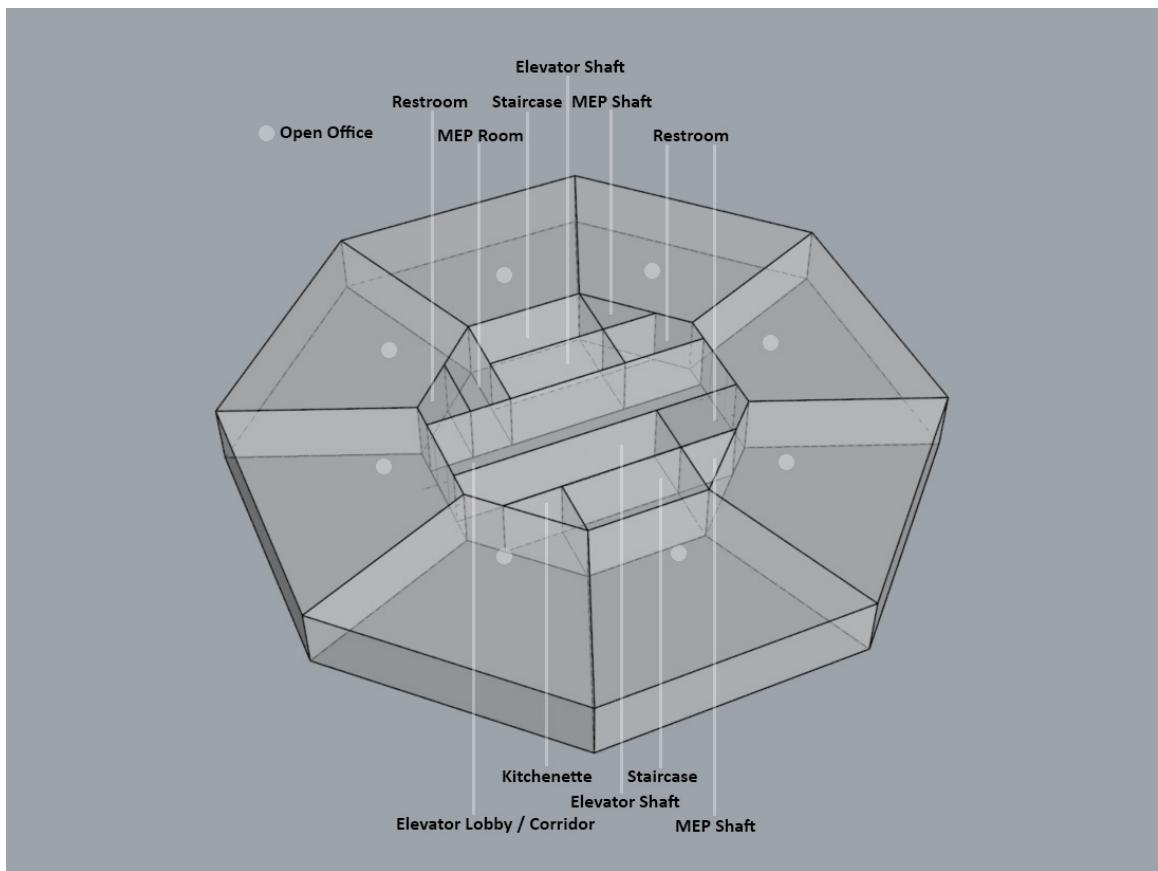
Figure 75. Model of a typical office floor, including all zones and their corresponding programs.
Source: the researcher

Materials and constructions are explained in the following part. As the office floors were typical and similar, the adjacencies between floors (ceilings) were defined as 'adiabatic' using the HB component "makeAdiabaticByType". For the alternatives with exoskeletons (MID and OUT), equivalent geometrical models were made in Rhinoceros as well and were assigned to the corresponding models via the controller, and interacted with the environment to cast shadow or reflect solar radiation and daylight. Similarly, the urban neighborhood towers for scenarios with high UD were included in the corresponding models. These processes are further described in the following parts of this subsection.

3.4.1.4   Materials and Constructions

This part explains the materials and constructions that were defined and used in the simulations.

- Core walls: The average thickness of the core walls for the IN, MID, and OUT alternatives, which were derived from the final structural simulation files, was 378mm, 353mm, and 386mm, respectively. Corresponding EnergyPlus materials and constructions were defined and added to the library using HB components (EPOpaqueMat, EPConstruction, and addToEPLibrary). In accordance with the EnergyPlus construction library, the following properties were assigned to the aforementioned concrete materials/constructions:

163

roughness = MediumRough, conductivity = 1.95 W/m-K, density = 2400 kg/m^3, specific heat capacity = 900 J/kg-K, thermal absorptance = 0.9, solar radiation absorptance = 0.7, visible light absorptance = 0.7 (the last three properties are common for non-metallic materials and were used for other materials unless stated otherwise).

- Opaque parts of curtain walls/facades: Similarly, EnergyPlus materials and constructions for the opaque parts of the facades for the IN, MID_WO/W, and OUT_WO/W alternatives were defined and added to the library. The roughness was defined as smooth. The calculation of the U-values, including the thermal bridge/control effects of all alternatives, is explained thoroughly in the next section (see Thermal Bridge Simulation).

- 'Windows' or non-opaque parts of curtain walls/facades: Fenestrations with a glazing ratio of 2/3 were assumed for all alternatives. In accordance with the local green building code [88, p. 47], the following properties were used to define the EnergyPlus material/construction using HB component "EPWindowMat": light transmittance = 0.2, shading coefficient 0.25 (equivalent solar heat gain coefficient = 0.22 [315, p. 30.39]). For all alternatives, the window height and sill height were set to 1.1 m and 0.4 m, respectively, using the HB component "glazingCreator".

- Interior ceilings/floors: The following six layers were defined as EnergyPlus construction for ceilings from top to bottom layer (and identically in opposite order for floors): (1) carpet, (2) low-weight concrete for raised floor, (3) F05 ceiling air space (from EnergyPlus library), (4) high-weight concrete, (5) F05 ceiling air space, (6) F16 acoustic tile (from EnergyPlus library). The ceiling height was set to 2.70 m using the HB component "setZoneProp". The properties of the materials were as follows:

    o   Carpet: roughness = MediumRough, thickness = 0.0127 m, conductivity = 0.06 W/m-K, density = 288 kg/m^3, specific heat capacity = 1380 J/kg-K.

    o   Low-weight concrete for raised floor: roughness = MediumRough, thickness = 0.03 m, conductivity = 0.53 W/m-K, density = 1280 kg/m^3, specific heat capacity = 840 J/kg-K.

    o   High-weight concrete: roughness = MediumRough; thickness = 0.272 m, 0.284 m, and 0.297 m for IN, MID, and OUT alternatives, respectively (0.2 m were the structural slabs, and the rest was added as an equivalent volume of structural beams to include the thermal mass of beams. It is important to mention that this method was applied, because for the EnergyPlus simulation of interior thermal mass, the placement or shape of the mass is not important; what matters is the volume and material, which were included in the model). Other properties were assumed to be the same as those of the concrete material previously explained in the description of the core walls.

164

- Interior shades: To ensure a comfortable interior space, avoid exceeding the Discomfort Glare Index (DGI), and minimize the need for electric lighting, the fenestrations were equipped with EnergyPlus windows interior shades, which are commonly used in practice. The HB component "EPWindowShades" was utilized, and the setting parameters were set according to the software help suggestions, as follows:

  o Shade material: The modeled shades had a default material with the following properties: solar reflectance = 0.65, transmittance (ability to transmit light) = 0, emittance (ability to emit thermal radiation) = 0.9, conductivity (ability to conduct heat) = 221 W/mK, and thickness = 0.25 mm.

  o Shade control type, schedule, and set-point: The shading system is set to operate when the DGI exceeds the EnergyPlus-recommended upper limit (set-point) of 22 for offices.

  o Other properties: The shades were set 0.20 meters away from the glass with an assumed air permeability of 0.5.

3.4.1.5   Thermal Bridge Simulation

Due to the non-orthogonal 3D geometry of diagrid members (revisit Figure 66) as well as their intersections and joints with each other and with other structural elements (ring beams, radial, beams, and slabs), and considering the presence of the thermal envelope and insulation materials (revisit Figure 51), a conventional 2D section model could not adequately represent the entire construction of the thermal envelope.

In such situations, there are two common approaches to simulate the thermal envelope with structural thermal bridges, and to calculate the overall U-value: (1) Utilizing non-orthogonal 3D thermal bridging simulation software programs (e.g., SOLIDO by physibel), which involve complex meshing and modeling techniques, and are typically expensive; (2) Employing two method simultaneously, namely the **parallel-path method** and **isothermal-planes method**, to transform the 3D problem into a series of 2D ones [316][317][318][319][320]. For this purpose, a 2D program such as THERM (a free-of-charge and reliable software program) is suitable for this compound method. The actual overall U-value falls between the U-values obtained from these two methods.

The researcher selected and implemented the second option, which is explained as follows:

- **Parallel-path method**: A 2D planar section model is created for each alteration in the conductivity of materials within a module representing the facade construction scenario (this was done in Rhinoceros). All parallel sections should be parallel to each other and parallel to the horizontal plane. For each section, a U-value is calculated using the software program THERM. The overall U-value is determined by the area-weighted average of U-values from all the aforementioned models (for this task the researcher developed a GH/Python component called

165

"PARL Paths U-value"). This method may slightly underestimate the impact of thermal bridges in the z-axis of the sections.

- **Isothermal-planes method**: In this method, only one 2D model represents the entire construction (i.e., superimposition of all models from the parallel-path method). For each part of the model, a hypothetical material is assigned with a conductivity equivalent to the area-weighted average of the materials superimposed in that part of the model–this equivalent conductivity is referred to as "Keff" (for this task, the researcher developed a GH/Python component called "PARL Paths U-value"). The overall U-value is equal to the U-value of this single compound model. This method may slightly overestimate the effect of thermal bridges in the z-axis of the sections.

THERM7.5 [253][317] was utilized in this research for conducting 2D analysis of sections. It incorporates the ISO 15099 [321] standards along with additional algorithms. Based on the finite-element method, its two-dimensional conduction heat-transfer analysis can simulate complex geometries of building components and products (e.g., windows, walls, roofs, foundations, doors, and other items) where thermal bridges are a concern. It allows users to assess local temperature patterns associated with issues like condensation, moisture damage, and energy efficiency. THERM is a valid state-of-the-art computer program developed at Lawrence Berkeley National Laboratory (LBNL), and endorsed by the USA Department of Energy (DOE) [253][317].

To control/mitigate thermal bridges in the exoskeleton prototypes of this study (revisit Figure 51), a layer of open-cell polyurethane foam (10 cm thick) was applied on and around the vulnerable areas (on the interior side of thermal bridges). Additionally, two layers of fire-rated gypsum board were incorporated for assembly protection. These choices were driven by several reasons: (1) The open-cell polyurethane foam's widespread use as insulation, with an expected service life well in excess of 50 years (similar to gypsum board [322]), known for its effectiveness in hot climates [323][324] (also common in cold climates, e.g., as seen in the Canadian building envelope thermal bridging guide [325, p. A2.24]); (2) Due to its porous texture, air/vapor can pass through it (it is vapor permeable). This is particularly favorable in hot climates where it is cooling dominated [326][316], meaning that vapor coming with heat from outside, if passed through exterior walls (here, RC diagrid columns, beams, etc.) can enter the air in interior (air-conditioned) space; otherwise it may get trapped between walls and insulation layer (e.g., closed-cell polyurethane) and thus make mold and other moisture related problems in interior space; (3) Vapor easily transmits through gypsum board. Similarly, paint color finishing on gypsum boards in such condition should also be vapor permeable [327]; (4) Gypsum board has another function as well, that is it protects the thermal insulation and other materials in case of fire [279, pp. 28, 126][328][329][330]. Installing two layers of fire-rated gypsum board (each with thickness of 5/8 inch = 15.9 mm) provides 1 hour fire rating protection for the assembly [331][330][280, Ch. 7, Table 722.2.1.4][332]. The local fire and life safety code mandated that all buildings taller than 90 m (similar to prototypes in the present investigation) must be equipped with sprinklers in all areas [279, p. 67], and the required fire rating for facades (curtain walls / window walls) in tall office buildings with sprinklers was 1 hour [279, pp. 55, 59].

In compliance with the local green building standards [180][181][333] the U-value of (opaque) external walls should be smaller than 0.57 W/m²K—it was assumed to be 0.55 W/m²K in this research. The conductivity of RC elements was assumed to be 2.3 W/m-K [334]. The conductivity of polyurethane foam insulation and gypsum board were assumed to be 0.024 W/m-K and 0.159 W/m-K, respectively, as provided in the THERM7.5 library (Material-Arch.lib). The Emissivity of all these materials was set to 0.9.

Applying the aforementioned methods and materials, the overall U-value of the facade was calculated for 4 alternatives of exoskeletons (MID and OUT) with or without controlling thermal bridges: MID_W, MID_WO, OUT_W, and OUT_WO. All final results are listed in Table 33 (a GH file named "U_values_calculation.gh" includes all calculations; 2D and 3D geometrical models are available in a Rhinoceros file named "Thermal_bridges_geometry.3dm").

Table 33. Overall U-value of all facade alternatives; including alternatives incorporating exoskeletons (MID and OUT) with or without insulation material applied upon the thermal bridging areas, and the control group alternative IN that has no thermal bridges. Source: the researcher

Alternative	IN	MID_W	MID_WO	OUT_W	OUT_WO
U-value (W/m²-K)	0.55	0.69	1.01	0.67	0.70

3.4.1.6   TYP Sub-Factor: Controlling Structural Thermal Bridging
In the optimistic scenarios, concerning the development of green technologies (TYP_20_50_80) (for more information, see the introduction of the TYP factor in the previous chapter; 2.3.6 TYP), it was assumed that the structural thermal bridging will be controlled to match the U-value of the curtain walls in 2050 and 2080. In the pessimistic scenarios, it was assumed that between 2050 and 2080 there is a renewal of insulation materials for thermal bridging mitigation, so the recurrence of corresponding embodied primary energy and CO2e emissions were taken into account.

3.4.1.7   UD

To avoid subjectivity in modeling UD while making a model that is easy to remember as an example for the audience of the research, the researcher modeled a homogeneous state where the effect of one building on its neighbors equals the effect of its neighbors on it. In doing so, a hypothetical infinite hexagonal grid was assumed, and identical prototypes were copied onto this modular grid. In this way, one prototype building can represent the whole urban tissue made of identical buildings homogeneously distributed. To represent an urban neighborhood with high density (Factor: UD, Level: H), the distance between neighboring buildings was set equal to the diameter of one building, resulting in dense urban tissue as illustrated in Figure 76. The FAR, in this case, was calculated to be 9.07, which is comparable to the high-density areas in Manhattan, NYC (with a FAR of 10 [335]) and some high-density parts of Dubai where tall buildings are agglomerated. FAR is defined as the ratio of GFA to plot area [195]. For the low-density scenario (Factor: UD, Level: L) where the surrounding structures are not significant in comparison with the prototype under study,

only one prototype was modeled. There is a scientific literature source—published by the (USA) National Renewable Energy Laboratory (NREL)—about detailed simulations during the design of the One World Trade Center Tower (formerly known as Freedom Tower) in which most of the surrounding tall buildings are relatively not very close or not as tall as the building under study. The results of that study showed that one floor in the middle of the tower can represent the whole tower with good precision (i.e., less than one percent error) [312].
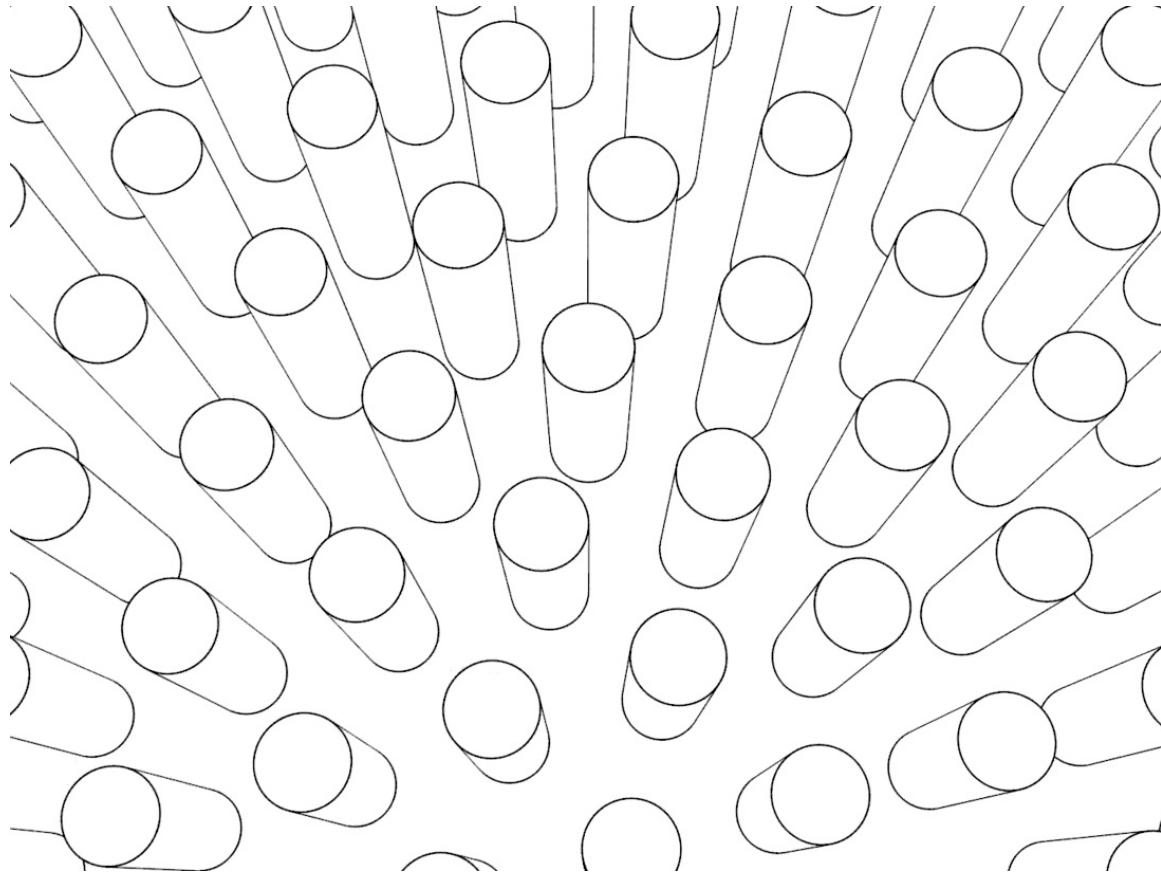
Figure 76. Homogeneous high-density urban neighborhood context (Factor: UD, Level: H, with a FAR of 9.06) modeled in this study. Source: the researcher.

To reduce the computational runtime of simulations without sacrificing accuracy, the researcher removed parts of surrounding buildings that were visually masked by other parts, as well as entire buildings that were entirely masked by others. Similar to the study mentioned in NREL's publication [312], in simulations of prototypes in low-density urban areas, one floor in the middle of the building height was modeled (with adiabatic floors and ceilings to function as typical floors in EnergyPlus). This floor included all objects from other floors that could potentially affect its performance through shading or reflecting solar radiation.

In simulations of prototypes located in high-density urban areas, however, for added accuracy, three test floors were examined. These test floors were evenly spaced within the building height, specifically at the 1/6, 3/6, and 5/6 positions of the building height. The results from these three test floors were averaged. This increased the total number of simulation runs for both HVAC and electrical lighting systems but was

necessary to ensure accurate estimates, given the varying shadow conditions in different parts of the prototypes under study.

The process of modeling the mesh surfaces and adding opaque materials/constructions of the urban neighborhood and the exoskeleton objects was very similar. Therefore, to avoid verbosity, both are explained in the next part, under "exoskeletons".

The glazing parts of the surrounding buildings were assigned a glazing Radiance material which was defined using a free online research tool called "jaloxa.eu" [336] which functioned based on an EN (i.e., British Standard 8206-2:2008 Lighting for buildings – Part 2: Code of practice for daylighting [337]), and Radiance software reference book [338]. The researcher applied the following settings:

- Glazing properties: LG10: Double glazing low E glass + low E glass + argon. This resulted in a glazing transmittance of 0.65.

- Maintenance properties: the applied settings were urban surroundings, office atmosphere, normal vertical glazing, and normal exposure for location. This resulted in a maintenance factor of 90%.

- Framing: a metal frame with a large pane was selected, which resulted in a framing factor of 0.80.

- The aforementioned properties resulted in a total corrected transmittance of 0.468.

Figure 77 shows a prototype tall building in the high-density urban neighborhood context.
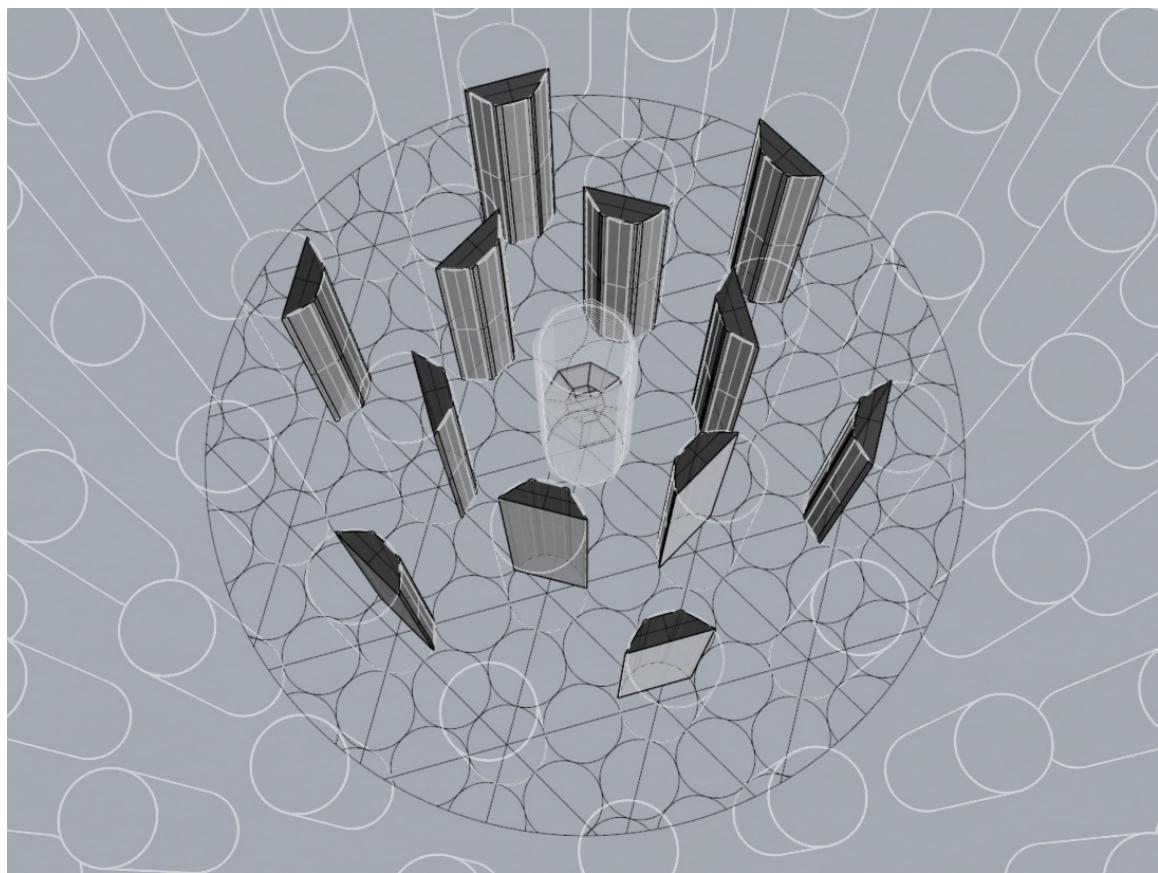
Figure 77. Prototype tall building model in a high-density urban neighborhood context (Factor: UD, Level: H). Only the effective sides of neighboring buildings were modeled, as shown in the figure. Source: the researcher

3.4.1.8   Exoskeletons

The geometries for the exoskeletons, as well as the urban neighborhood towers, were integrated into the HVAC and electric lighting simulations using the HB components "HB_EPContextSrf" and "createHBSrfs" respectively. A minimum number of one quad in the initial grid per face was assumed for mesh settings using the HB component "Custom Mesh Settings". The exoskeletons and opaque parts of the urban neighborhood towers were assigned an exterior white painted concrete material from the Radiance library. The geometries of the exoskeletons around a typical office floor for the MID and OUT alternatives are shown in Figure 78 and Figure 79 respectively.
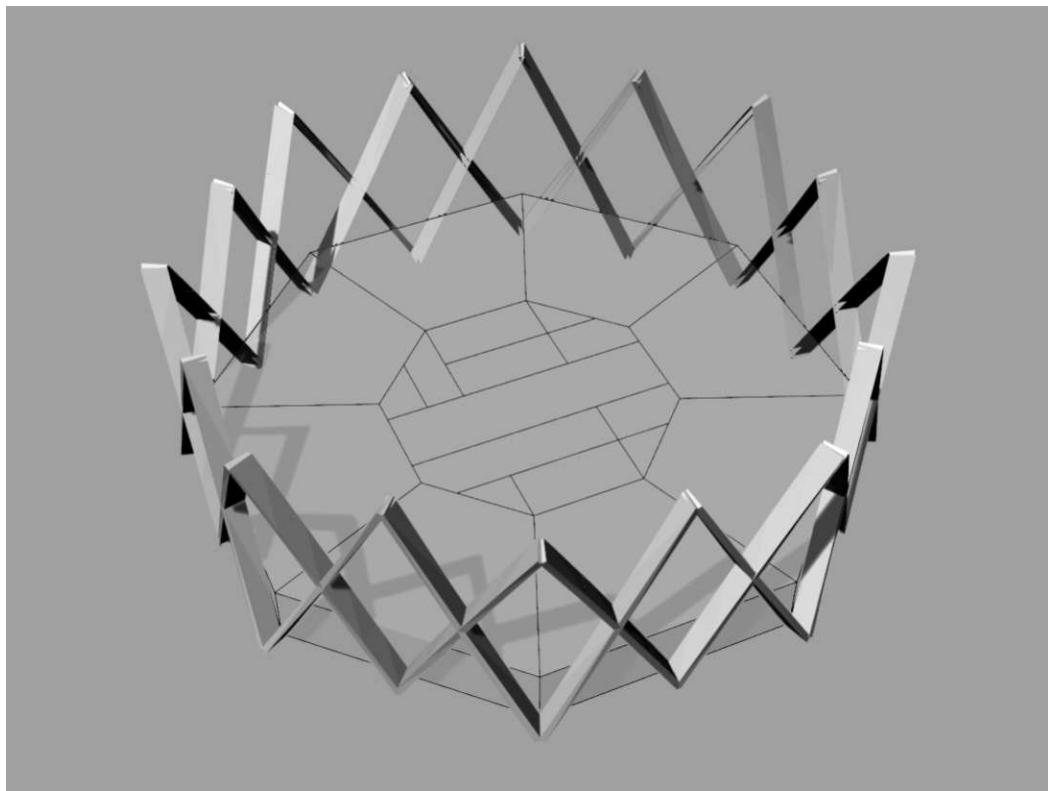
Figure 78. Geometrical model of exoskeleton MID (Factor: PTC, Level: MID) around a typical office floor. Source: the researcher
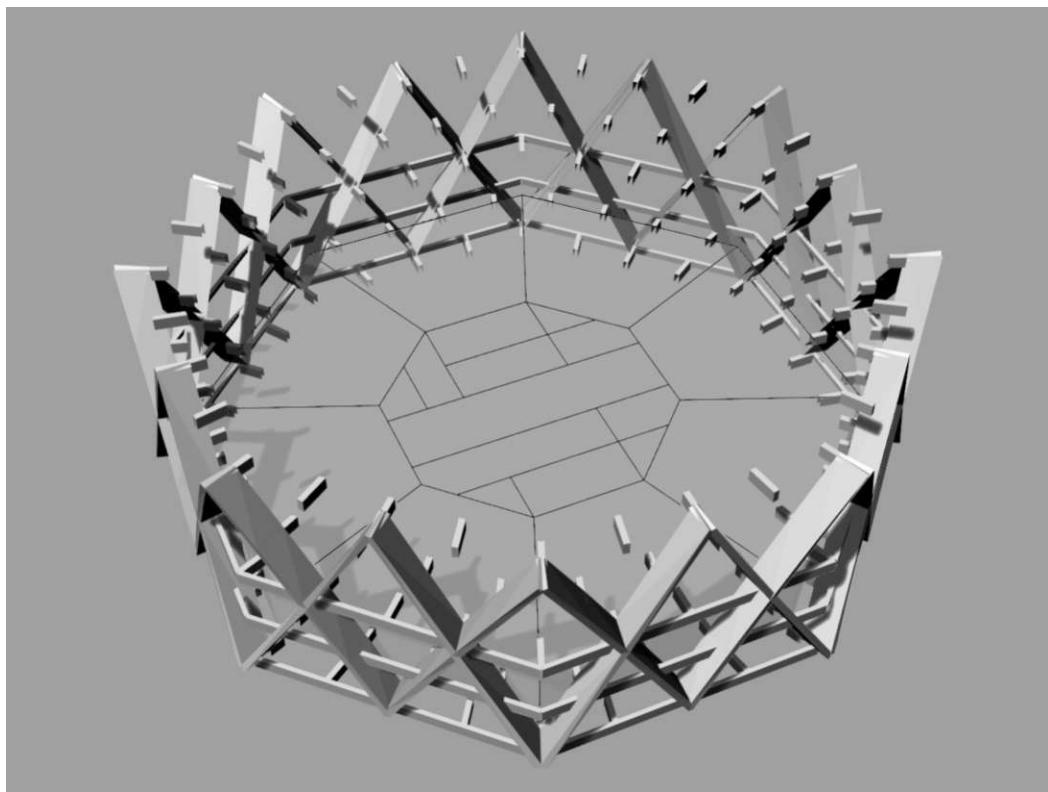
Figure 79. Geometrical model of exoskeleton OUT (Factor: PTC, Level: OUT) around a typical office floor. Source: the researcher

Simulation runtimes for HVAC and electric lighting systems were significantly increased by the inclusion of exoskeletons (PTC: MID and OUT) and a high-density urban neighborhood (UD: H), despite using optimized geometrical models that removed ineffective vertices and surfaces. The HVAC simulation runtimes ranged from 6 minutes (PTC: IN, UD: L) to 45 minutes (PTC: OUT, UD: H). Similarly, the electric lighting simulation runtimes ranged from 4 minutes (PTC: IN, UD: L) to 24 minutes (PTC: OUT, UD: H).

3.4.1.9 HVAC System

Using the HB component "HVACSystem", an HVAC system of FCU + DOAS was assigned to the models of all alternatives. The air, cooling, and heating details explained below this paragraph were other inputs to this component. Among the several types of HVAC systems available in OpenStudio, EnergyPlus, and HB, the researcher (after consulting two experts, an NREL research engineer [339], and an HB lead developer [340]) selected FCU + DOAS with a central plant and an air-cooled chiller (instead of a water-cooled chiller). The main reasons for this selection were: (1) ease of modeling and the avoidance of multiple errors in OpenStudio and EnergyPlus [339]; (2) water scarcity in the region; and (3) FCU + DOAS is a relatively efficient and common HVAC system for tall buildings in hot climates. For example, the researcher initially tested a Variable Air Volume (VAV) HVAC system (which is also a common system for modern office buildings [238][341][240]), but it resulted in significantly higher energy consumption. This was primarily because FCU systems have a separation between the heating/cooling needs of the ventilation air and the heating/cooling needs of the zones, which saves energy over VAV systems. VAV systems attempt to satisfy both the need for ventilation and the need to heat and cool the space entirely with supply air, which can lead to wasteful practices. FCUs use water that is pumped into the FCU through pipes, which requires less energy than blowing air through ductwork. The default FCU template in HB has a heat recovery system that comes by default, giving it an advantage over the VAV [340]. Details of air, heating and cooling settings for the selected HVAC system (FCU + DOAS) were set as follows, using HB components "AirDetails", "HeatingDetails", and "CoolingDetails":

- Air details: Draw-through fans were set with the following HB suggested default values: a total efficiency of 0.7, a motor efficiency of 0.9, and a pressure rise of 500 Pa. Heating and cooling supply air temperatures were set to 35°C and 12°C, respectively. The air-side economizer was set to "Differential Dry Bulb," which means that the HVAC system increases outdoor airflow if there is a cooling load and the return/exhaust air is warmer than the outdoor air. Heat recovery was set to "Sensible," which means that the exhaust air first passes through a sensible heat exchanger with the outdoor fresh air to recover heat that would otherwise be lost. The recovery effectiveness was set to 0.7, which is also in line with the local standard [88, p. 54].

- Heating details: The heating efficiency was set to 0.9, which is a common value for systems with boilers and is calculated by dividing usable converted heat energy by the contained energy in the fuel. For the optimistic future scenarios (TY_2050 and TY_2080), an electricity-driven heat pump system with heating COP similar to the corresponding cooling COP was assumed. This is further

172

explained in the next part of this subsection (see "TYP Sub-Factor: COP of HVAC Systems").

- Cooling details: A central plant with an air-cooled chiller heat rejection type was assumed. The supply temperature was set to 6.67°C. The cooling COP is also explained in the next part (see "TYP Sub-Factor: COP of HVAC Systems").

As a side note, it is worth mentioning that although Dubai is in a cooling-dominated climate, the need for heating is not necessarily zero. This is primarily because of the following: (1) Heating devices are used during periods of low winter temperatures [342]; (2) Sometimes, when the air temperature is comfortable but humidity is too high, it is necessary to cool the air significantly to remove excess humidity (which happens below the dew point), and then reheat it before distributing it to interior spaces. This is done to maintain indoor comfort conditions and prevent the space temperature from falling below a comfortable level [340].

3.4.1.10   TYP Sub-Factor: COP of HVAC systems

In the optimistic scenarios, concerning the development of green technologies (TYP_20_50_80) (to recall the introduction of the TYP factor, refer to subsection 2.3.6), it was assumed that the COP of the HVAC systems will improve in 2050 and 2080 in comparison with the beginning of the operational phase (2020). In accordance with a scientific report published by the DOE, the estimated values of the COP for the years 2020, 2050, and 2080 were assumed to be 3.75, 5.02, and 6.30, respectively [207, p. 51]. These values also met the acceptable range with reference to the local green building code [88, p. 50].

3.4.1.11   WDYP

The EnergyPlus software processes EnergyPlus Weather files (EPW) that contain hourly values of key weather variables for a typical year to integrate the meteorological data associated with the geographical context of a building in its process of performance modeling and simulation. EPW files of hundreds of cities around the world are available for free on the EnergyPlus website [343], but the EPW file for Dubai was not available. The 'Present-day' weather data file used in the present investigation was courtesy of the Meteonorm [344] global climate database. To convert the present-day weather file to the weather files for the years 2050 and 2080 in pessimistic scenarios, the researcher used the software program CCWorldWeatherGen (Version 1.9), which uses the 'morphing' method to generate future weather files. The morphing method combines the results of climate models with present-day weather data and, by doing so, provides weather time series that preserve the average weather conditions of future climate scenarios while maintaining realistic weather sequences [213]. This climate change world weather file generator, created by the Sustainable Energy Research Group at the University of Southampton, applies Intergovernmental Panel on Climate Change Third Assessment Report (IPCC TAR) model summary data of the UK's Hadley Centre Coupled Model, version 3 (HadCM3) A2 experiment ensemble [345][252][346]. The A2 scenario is rather pessimistic (2.0 – 5.4 °C), reflecting global

warming in a more heterogeneous world (Regionalization) than a homogeneous one (Globalization), with rather an economic focus than an environmental one. Other popular tools to obtain climate change weather data such as Meteonorm or WeatherShift™ (which is a collaborative project of Arup North America Ltd and Argos Analytics LLC) [347], were also available, but the former was costly, and the latter did not include the weather file for the required location in this research [348].

3.4.1.12   Other Settings, Running HVAC/Energy Simulations, and Results

The following zone threshold set-points were set according to ASHRAE [349, p. F09, 9.12] and local standards, and a scientific research paper [350]: cooling set-point of 23.88°C (= 75°F), cooling setback of 29.44°C (= 85°F), heating set-point of 21.11°C (= 70°F), heating setback of 15.55°C (= 60°F), maximum humidity of 60%, and minimum humidity of 30% [88, p. 48]. Using the HB component "setEPNatVent", a "Window Natural Ventilation" setting was assumed for the open office zones operating on a 15% fraction of areas of the facade fenestrations. The setting included the following: minimum and maximum indoor temperatures were set to 0.75°C higher than the aforementioned heating set-point (21.86°C) and 0.75°C lower than the cooling set-point (23.13°C). The minimum outdoor temperature was set to 12°C, and the maximum outdoor temperature was set to equal the cooling set-point (23.88°C).

The shadow parameters (HB component "shadowPar") were: frequency of 30 days, meaning a shadow calculation was performed every 30 days and this average value was assumed for all days during the 30-day period in energy simulations. A maximum figure of 10000 points was assumed to be calculated in the shadow simulation. This was set significantly higher than the HB default value of 200 points in order to ensure accuracy to include the effects of exoskeletons and the urban neighborhood towers in the corresponding scenarios.

With respect to energy simulation parameters (Using the HB component "EnergySimPar"), the timestep was set to 6, which means that the energy balance calculation is run every 10 minutes (one hour divided by 10). Solar distribution was set to "Full Exterior," which includes direct sun and whether surrounding objects block it. In the interior space, it is assumed that all beam solar radiations fall on the floor. A window view factor calculation distributes diffuse solar energy on the interior surfaces.

The following EnergyPlus simulation outputs were selected (using HB component "EPOutput"): zones' energy use (e.g., heating, cooling, electricity for lights and plug loads), gains and losses (e.g., solar gains, people gains, and infiltration losses/gains), comfort metrics and map variables (e.g., operative temperature, mean air/radiant temperature, relative humidity, air flow, and air heat gain), as well as HVAC parameters (latent and sensible fractions of heating/cooling loads, flow rate and temperature of supply air). The timestep was set to "hourly".

For each of the 120 operational phase scenarios models, in order to export HB zones into an OpenStudio file for running annual hourly energy simulations through EnergyPlus, the following inputs were specified in the HB component "exportToOpenStudio": the EPW weather files, energy simulation parameters, HB zones, as well as exoskeletons and urban neighborhood context as discussed in detail

earlier in this subsection. The EnergyPlus simulation result file was used as the input for the HB component "readEPResult" to read it. For each run, the following results were collected: cooling energy (electricity needed to power chiller/cooling coil), heating energy (fuel energy or electric energy to run boiler/heating element), ventilation fan electric energy, and water pump electric energy. Each one of these values was normalized by dividing it by the GFA of 1385.44 m^2 to find the annual Energy Use Intensity (EUI) values in kWh/m^2. To cross-verify and save all the main inputs and outputs of the simulations easily, the researcher created a GH/Python component called "Output Par" that summarizes and stores all the aforementioned EUI values, annual electric lighting EUI (which is explained in detail in the next subsection), as well as a list of the main input scenario factors/levels parameters (explained at the beginning of this subsection; see "Controlling Parameters of Scenarios"). To archive the simulation settings and results of each scenario, a separate GH file was saved named with the abbreviations of the factors/levels involved.

As mentioned earlier, the HVAC simulation runtimes ranged from a minimum of 6 minutes (PTC: IN, UD: L) to a maximum of 45 minutes (PTC: OUT, UD: H).

3.4.2 Electric Lighting Simulation

3.4.2.1 Introduction

Similar to the HVAC modeling and simulation process, the software programs used for the electric lighting simulation were Rhinoceros, HB + LB in GH. The geometric model, materials, and standards were also similar to the aforementioned models, except for some supplementary properties, sensors, tools and parameters that were needed to be added for the purpose of the electric lighting simulation and are introduced in this subsection. The associated Rhinoceros and GH files (which include the HVAC and electric lighting models) are available in the appendix; both are named "HVAC_ElectricLighting" with ".3dm" and ".gh" extensions respectively. EPW files associated with the years 2020, 2050, and 2080 were generated using the CCWorldWeatherGen program (see [252] for more information on this program). Whenever default values suggested by HB components have been used, they are not mentioned to avoid verbosity.

For the electric lighting simulation, HB served as a parametric interface to connect the models in Rhinoceros with the Radiance-based DAYSIM software engine, which has been widely utilized in practice and research projects worldwide (e.g., see [351][254][352][353]). DAYSIM, using Radiance as its core engine, encompasses validated daylighting analysis methods for calculating annual availability and needs of lighting in building design based on backward ray tracing, color, luminance/radiance, illuminance/irradiance and glare effects as well as realistic sky, neighborhood and other environmental conditions.

3.4.2.2 Set Radiance Materials

Three materials were required to be added in order to support the model with the lighting aspects of the finishing layers inside the zones for the purpose of electric lighting simulation (HB "setRADMaterials" component); "White_painted_room_walls" for walls, "White_ceiling_panels" for ceilings, and "carpet_ary01"/"CARPET001" for raised floors. The first two materials already existed in the Radiance library of materials (therefore, found and used via the HB "callFromLibrary" component). However, the carpet material had to be defined by the researcher. During the process, the researcher noticed a minor issue with the HB components "radTransMaterial" and "radTransMaterialByColor". There was a false error message: "Sum of Diffuse Transmission, Specular Transmission, Specular Reflection and Diffuse Reflection cannot be more than 1." While it is true that the sum of those coefficients cannot exceed 1, none of them actually represents the "colour". It appears that the components mistakenly assumed that "colour" equated to "diffuse reflectance". In accordance with a Radiance reference book [338, pp. 23, 37]:

Equation 19.

$$diffuse\ reflectance\ =\ (1-specular\ reflectance)\times colour\times(1-specular\ reflection\ modifier)$$

; where the weighted average reflectance (known as the "colour" value) is calculated using Equation 20.

Equation 20.

$$colour\ =\ (0.265\times red)+(0.67\times green)+(0.065\times blue)$$

The researcher resolved the issue by developing a new GH/Python component named "radTransMatTrans" which adheres to the principles outlined in the Radiance reference book. Figure 80 illustrates the formulas and behavior of light when interacting with translucent materials [338].
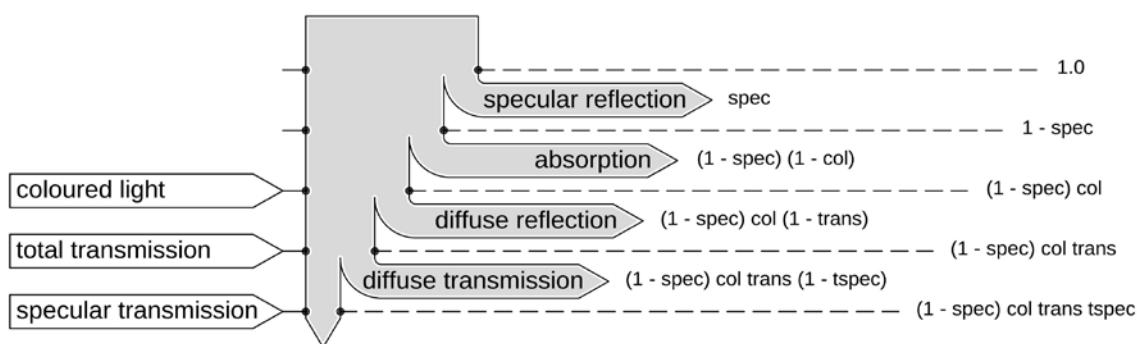
Figure 80. Behavior and formulations of light passing through a (translucent) material. Image revision drawing by the researcher based on the original from the source (/credit ©): Radiance reference book [338]: Jacobs, A. "Radiance Cookbook, version 10 October 2014." (2014), page 23.

The new component takes inputs for red, green, and blue values of 'colour'; specular reflectance; roughness modifier; specular reflection modifier; and transmissive specularity modifier". More information about the definitions are available online

[354]. This component is open-source and accessible online (see [355]) and generates an automatic report that is self-explanatory. The specular reflectance value (0.0011) for a gray carpet material was obtained from an academic database of architectural materials available online [356]. Other parameters to define the Radiance material were either generated by the aforementioned new component or set to the relevant values suggested by the HB component help.

3.4.2.3   Annual Daylighting/Energy Simulation

To perform daylight analysis (which involves exporting GH/HB geometries to Radiance files and running annual daylighting/energy simulations using the HB component "runDaylightAnalysis"), an analysis recipe was required in addition to all the HB objects mentioned earlier. The analysis recipe (HB component "annualDaylightSimulation") comprises parameters set as follows:

- EPW files: These were selected according to present-day and future climate change scenarios, as explained in the previous subsection.

- Test points/vectors/mesh: HB automatically placed a test point/sensor in the center of each zone with a mesh size of 10 m. The researcher initially experimented with smaller mesh sizes to include more test points, but the overall results showed only marginal variations, along with a significant increase in computation time. A few extra points were generated in random positions in the zones, but these were filtered out by a GH/Python script (component "findMid") developed by the researcher. The height of the sensors from the floor was adjusted to match that of a standard office desk/working plane, which is 30 inches = 0.762 m.

- DAYSIM parameters (HB component "DSParameters"): A conceptual shading recipe (HB component "conceptualDynamicSHDRecipe") was applied as a dynamic shading group. A threshold of 50 W/m^2 triggers the sensors activating the lowering of the louvers to block all direct solar radiation while transmitting 25% of the diffuse daylight.

3.4.2.4   Lighting Control

The settings applied to create an electric lighting control recipe for DAYSIM (HB component "lightingControl") are listed below:

- Lighting control type: Set to "manual on/off with auto dimming", which is common in contemporary modern office buildings [357][353].

- Sensor points (test points): As defined earlier.

- Lighting Set Point (LSP), and Lighting Power (LP):

     o   The local green building code recommended an illuminance of 400 lux for office zones (i.e., open office, corridors, electric rooms) [88, p. 53]. A European standard for lighting in office buildings suggests an average illuminance of 200 lux for the other zones (i.e., shafts, voids toilets, dining rooms, etc.) [89]. Therefore, LSPs of 400 and 200 lumens were applied in the model accordingly.

     o   To calculate LP, it was necessary to have the efficacy/lumens per watt (LPW) value of the electric light sources (LP = LSP / LPW). LPW values of warm white phosphor-converted LED light sources for the present time and future scenarios were derived from a technical report book published by DOE [209, p. 61], as explained in the next part. This type of LED light source was selected because it is common in modern buildings and is energy-efficient with a long service life.

- Standby power: Set to 0.15 watts in accordance with a technical report by the International Energy Agency [358, pp. 23, 29, 33].

3.4.2.5   TYP Sub-Factor: Efficacy of (LED-) Electric Light Sources

In the optimistic scenarios, concerning the development of green technologies (TYP_20_50_80) (to recall the introduction of the factor TYP, revisit subsection 2.3.6, in the previous chapter), it was assumed that the efficacy of the LED light sources would improve during the operational phase (in 2050 and 2080) compared to the beginning of the phase (2020). The efficacy values for the years 2020 (for all scenarios), and 2050 and 2080 (for optimistic future scenarios), which were derived from a technical report by DOE [209, p. 61], are 210, 330, and 340 LPW, respectively. Since an LSP of 400 lumens was assumed, the corresponding calculated LP values became 1.90, 1.21, and 1.17 watts.

3.4.2.6   Other Settings, Running Electric Lighting/Energy Simulations, and Results

Annual simulations were performed for all scenarios and standard DAYSIM results were read into HB using the "readAnnualResults" component. The inputs of this component were:

- The results of the annual daylighting/energy simulations using Radiance as described earlier.
- Occupancy files: lighting schedules for all the zones were made by HB component "getHBZoneEPSchedules".
- Lighting control: as described earlier.

The above process resulted in an HTML file for each scenario, which includes the annual electric lighting electricity EUI for each zone in kWh/m^2. All results for each scenario were read (using the Honeybee component "DSElectricalLightingUse"), integrated, and saved in a separate GH file, identical to that of the HVAC simulations.

178

As mentioned earlier, the electric lighting simulation runtimes ranged from a minimum of 4 minutes (PTC: IN, UD: L) to a maximum of 24 minutes (PTC: OUT, UD: H).

3.4.3 Operational Inventory and Impact Assessment

All the results of the operational phase simulations, including HVAC and electric lighting systems, were collected and combined into an Excel file called "Operational_Inventory_and_Impact_Key_Years.xlsx". The content of this file corresponds to both LCI and LCIA concerning the key years of operational phase (2020, 2050, and 2080). Due to the file's large size, as it included data collected from over two hundred simulation runs, it was not practical to present it as a table in this dissertation. Instead, it is attached separately. However, the file's structure and methodology are explained in detail here.

3.4.3.1 <u>Inventory</u>

As mentioned earlier, the operational phase simulations included many scenarios for HVAC and electric lighting systems. For each simulation scenario in high-density urban neighborhoods (UD: H), three runs were performed for a typical floor on different heights (i.e., at 1/6, 3/6, and 5/6 of the building's height). The average values of each three of those results were calculated to represent one corresponding simulation scenario. The collected results for each simulation scenario included the following: annual EUIs for (1) cooling, (2) heating, (3) electric fans, (4) electric pumps, and (5) electric lighting (all in kWh/m^2). The delivered energy used for all these items was electricity, except for some cases of heating which required natural gas as fuel. These cases included the heating systems in all scenarios in 2020, as well as future heating systems concerning pessimistic technological scenarios in 2050 and 2080 (TYP: 20_20_20). In optimistic future technological scenarios of 2050 and 2080 (TYP: 20_50_80), a heat pump heating system using electricity was assumed, as explained earlier.

Consequently, as part of the LCI concerning the operational phase, the following items (both in kWh/m^2) were calculated and added to the spreadsheet depending on the scenarios: (1) the total amount of annual delivered EUI of electricity for all scenarios, and (2) the total amount of annual delivered EUI of natural gas (for 2020, and future scenarios with respect to TYP: 20_20_20).

Regarding the LCIA with respect to the key years of the operational phase, after calculating the characterization factors (which are explained in the next part), the following items were calculated and added to the aforementioned spreadsheet depending on each scenario: (1) the total annual operational primary energy consumption (in kWh/m^2); and (2) the total operational GHG emissions (in kgCO$_2$e/m^2).

3.4.3.2 <u>Characterization Factors</u>

This part presents the estimation method and results with respect to the characterization factors required for the LCIA. These characterization factors include the local PEF and GHG emissions for natural gas heating in 2020, as well as the local PEF and GHG emissions for electricity production in key years, namely 2020, 2050, and 2080.

To facilitate this process, the researcher developed a GH/Python component called "PE & GHGE (Local)", which is included as a separate attachment file named "Characterization_Factors.gh". This component was also used for the pre-operational LCIA and is included in the corresponding attachment GH file named "Pre_Operational_Inventory_and_Impact.gh". It is worth mentioning that the algorithm in the technical files is self-explanatory since it generates a real-time textual report. However, the most important parts of the algorithm of the component is explained below.

The PEF for natural gas heating in 2020 was estimated to be 1.09. The amount of GHG emissions associated with natural gas heating in 2020 was estimated to be 0.3 $kgCO_2e/kWh$. These estimations were derived from a 2018 report on source energy factors for fuel delivered to buildings by NREL [359, p. Table 5], due to the absence of actual local data.

According to scientific literature sources [360][361], the mix of energy used for local electricity generation in 2012 was 96% natural gas, followed by 3% gas oil (diesel), and 1% fuel oil (heavy oil). The same percentages were assumed to be constant until 2015, as the Dubai Clean Energy Strategies project was initiated at that time. In the optimistic scenarios concerning the development of green technologies (TYP_20_50_80), which are introduced in the previous chapter, it was assumed that the energy mix used in electricity production will improve during the operational phase (in 2050 and 2080) compared to the beginning of the time period. The Dubai Clean Energy Strategies project's official predictions were used to estimate the future energy mix, as that project is focused on creating an environmentally friendly energy mix. Based on the project's predictions, the energy mix for electricity production in 2030 will be 25% solar energy, 7% nuclear, 7% coal, and 61% natural gas. The project's goal is to make Dubai the least carbon footprint city in the world by 2050, with clean energy sources making up 75% of the energy mix [362]. Accordingly, the energy mix prediction for electricity production in 2050 is estimated to be 58.59% solar, 16.41% nuclear, 2.57% coal, and 22.43% natural gas.

Due to the lack of actual local data, the national data from the NREL report mentioned earlier was used to estimate the PEF for electricity. The data concerning source energy factors by fuel type for electricity generation and source energy factor components per delivered kWh of electricity were gathered from two tables in the report and combined in Table 34.

Table 34. Source energy factors for electricity generation by fuel type (kWh of source energy per kWh of generated energy), and source energy factor components per delivered kWh of electricity. Source: Table B-1 and Table B-2 of [359]: M. Deru and P. Torcellini, "Source Energy and Emission Factors for Energy Use in Buildings (Revised; No. NREL/TP-550-38617)," Golden, CO (United States), 2018.

Energy group	Source energy factors for electricity generation (kWh of source energy per kWh of generated energy)	Source energy factor components per delivered kWh of electricity
Coal	3.09	0.67
Natural Gas	2.63	0.53
Petroleum Fuels	3.12	0.97
Nuclear	3.08	0.67
Solar	1.00	0.00

To calculate the local PEFs for electricity in 2015, 2030, and 2050, the corresponding share fraction of each energy group was multiplied by the sum of its factors listed in Table 34, and then summed together to cover the entire local electricity energy mix. However, as these results only included one of the key years of the study (2050), a regression line ($y = -0.0312x + 65.963$, $R^2 = 0.99$) was fitted to the PEF results of 2015, 2030, and 2050 to predict PEFs for the other key years (2020 and 2080). The estimated PEFs for the key years are provided in Table 36.

The process for estimating GHG emissions was similar to the PEF calculation. The average life cycle GHG emissions for electricity generation for different energy groups were obtained from an international report by IPCC available online via the World Nuclear Association [363] as listed in Table 35. A regression line ($y = -0.0093x + 19.15$ in $kgCO_2e/kWh$, $R^2 = 0.99$) was fitted to the results to facilitate predictions for other key years. The estimated predictions are provided in Table 36.

Table 35. Average life-cycle carbon dioxide-equivalent emissions for different electricity generators. Source: [363] IPCC, "Average life-cycle carbon dioxide-equivalent emissions for different electricity generators," 2018. [Online]. Available: https://www.world-nuclear.org/nuclear-essentials/how-can-nuclear-combat-climate-change.aspx. [Accessed: 31-Mar-2023].

Energy group	Average life cycle GHG emissions for Electricity Generation in $kgCO_2e/kWh$
Coal	0.82
Natural Gas	0.49
Petroleum Fuels	0.73
Nuclear	0.01
Solar	0.05

Table 36. Estimated local PEFs and GHG emissions associated with electricity. The values for the years 2050 and 2080 correspond to optimistic future scenarios (i.e., Factor: TYP, Sub-Factor: Energy Mix in Electricity Production). Source: the researcher

Key Test Year	PEF	GHG Emissions ($kgCO_2/kWh$)
2020	2.94	0.36
2050	2.00	0.09
2080	1.07	0.00

The resulting characterization factors, which include estimated local PEFs and GHG emissions associated with electricity in 2020, 2050, and 2080, as well as the PEF and GHG emissions related to natural gas heating in 2020, were integrated into the Excel file named "Operational_Inventory_and_Impact_Key_Years.xlsx" to convert the inventory data into impact assessment data. As previously mentioned, this file contains both LCI and LCIA results for the key years of the operational phase (2020, 2050, and 2080). Therefore, another file in long format, called "results02_Operational_ary025.csv," was created for statistical analysis in R. The difference between the contents of these two files is that the former includes annual data for the key years (2020, 2050, and 2080), while the latter includes cumulative data for the operational phase periods (2020 to 2050 and 2020 to 2080). The average of the annual data values for 2020 and 2050 was multiplied by 30 to estimate the value of the period between 2020 and 2050. Similarly, the average of the annual data values for 2050 and 2080 was multiplied by 30 to estimate the value of the period between 2050 and 2080.

A total LCIA datasheet, containing impact assessment data for both embodied and operational phases, was created as a file named "results03_EmbodiedAndOperational_ary031_ALL.csv". This file was utilized for statistical analysis in R, as explained in the next section. The reason why this important datasheet is not presented here in table form and is only available as a file attachment is due to its large size, which includes 1441 rows and 27 columns.

3.5   Analysis

3.5.1   GLM Analysis

What is Generalized Linear Model (GLM)? Why and how was it applied in this research?

- What's GLM?

GLM, initially developed by Nelder and Wedderburn in 1972 [364], is an extended and generalized version of typical linear model (experimental design is also basically a regression model) that includes a broad class of statistical models, e.g., linear regression, Poisson regression, log-linear models, Analysis of Variance (ANOVA) etc. Unlike the typical linear regression approach of data transformation followed by standard least squares analysis which requires normally distributed response data, GLM works for a variety of normal and non-normal distributions using a link function (a link function determines the relationship between the response mean and the linear predictor), i.e., GLM response variable data accepts any distribution that is a member of the rich and flexible collection of distributions known as the 'exponential family' (normal, Poisson, binomial, exponential, and gamma distributions); this makes GLM very useful in dealing with reality where various distributions may happen in the results of experiments. To write the aforementioned text briefly as equations, a standard normal-theory linear regression model that could also be considered as a special case of GLM can be written as Equation 21:

Equation 21.

$$y = \beta 0 + \beta 1 x 1 + \beta 2 x 2 + \cdots + \beta k x k + \epsilon$$

where β's are unknown parameters, including $\beta 0$ that is the intercept; x's are (experimental-design-) factors, and ϵ is a normally distributed random variable—(in statistical terms) known as error with the mean of zero. The mean of y is μ in the Equation 22 that is equal to the linear predictor $x'\beta$.

Equation 22.

$$E(y) = \mu = \beta 0 + \beta 1 x 1 + \beta 2 x 2 + \cdots + \beta k x k = x'\beta$$

Nowadays there are many software programs to fit GLM, e.g., 'SAS Proc Genmod' and 'R function glm()' [175][365].

- Why was GLM applied in the study at hand?

The researcher selected GLM as a tool to analyze the experiments because of the following: (1) first and foremost, GLM exactly matches with the concept of DoE and thus it could end up in replying to the first research question by detecting and measuring the statistically significant main effect of the main independent variable of interest (i.e., employment of exoskeletons) on the response variables (i.e., primary energy, and CO_2e emissions in different life cycle stages) while taking into account the possible interactions of the main independent variable of interest with other independent variables (be it controllable or uncontrollable) that represent various plausible scenarios. (2) as stated earlier, GLM is able to handle non-normal distribution of response data which was the case in this research; the main reason for this was the great variety of scenarios that, while enriching the quality of life cycle analysis, led to the fragmentation of the output data and distinguished it from a normal distribution, which of course was not surprising. (3) GLM allowed for using categorical independent variables; this was especially crucial to cover a few states/levels of the main variable of interest (IN, MID, and OUT) which were not possible to address in the form of a continuous variable/number.

- How was GLM applied in the study at hand?

The researcher used the 'R' function of 'glm()' to fit GLM to the experimental data. The free open-source software environment and programming language of R is dedicated to statistical computation, and backed by contributions of a large number of statisticians from around the world, it has become a quick and reliable platform for various purposes including analysis of complex multiparametric data of GLMs. The researcher prepared a long format dataset made of the whole data of the full factorial experiments including all possible combinations of various levels of all factors and the corresponding responses in different time-spans both cross-sectionally and longitudinally (i.e., life cycle stages separately and cumulatively); and then ran the GLM function with 'backward elimination' to optimally fit the GLM (meaning including the important main and interaction effects and omit the ones that weakens the model in fitting the experimental data); in other words, to fit the most accurate models with involving the least number of parameters. More details about the procedure can be found in the appendix as well as in the beginning of the next chapter.

3.5.2   Decision Analysis

To reply to the second research question, the researcher employed three methods of decision analysis known as maximax, maximin, and minimax regret criteria. This subsection briefly explains these methods and why and how they were applied in this research.

The decision-making methods of maximax, maximin, and minimax regret fall under the broader categories of game theory and decision theory, which are originally branches of mathematics and economics focused on strategic decision-making. They are used to find the optimal course of action by analyzing various scenarios and

potential outcomes. The usage of these decision analysis methods is not limited to economics. They represent three types of decision-maker strategies/approaches (optimistic, conservative, or cautious, respectively) as simple mathematical algorithms used for decades in various industries, engineering, and design disciplines. All these three decision analysis methods are suitable for complex, multi-faceted problems and conditions with deep uncertainty, where the probabilities/likelihoods of occurrence of context scenarios (i.e., 'states of nature') are unknown [366][367]. This was the primary reason for selecting and applying them in this research because all factors—except for the controllable factors, i.e., employment of exoskeletons (PTC_TBC), and CR, whose different combinations of levels define the design/decision alternatives—were uncontrollable from the perspective of architectural engineers involved in the early stage of tall building design, and the probabilities of occurrence of the possible present and future scenarios created by these uncontrollable factors were unknown.

The three methods are:

Maximax Criterion associates with an **optimistic/aggressive** point of view by seeking to maximize the maximum gain/payoff. It ranks the decision alternatives (corresponding to controllable factors) based on their most desirable outcomes (i.e., maximum payoffs) in all context scenarios (corresponding to uncontrollable factors).

The mathematical formulation is as follows (Equation 23):

Equation 23.

$$Maximax\ Decision = \arg\max(\max(Payoff_1), \max(Payoff_2), \dots, \max(Payoff_n))$$

; where $Payoff_i$ represents the potential payoffs associated with each decision alternative i, and $max(Payoff_i)$ calculates the maximum payoff for each alternative. The decision-maker selects the optimal alternative/argument, which is the alternative with the highest maximum payoff.

Maximin Criterion, seeking to minimize the maximum loss, represents a **conservative/robust** attitude where the worst outcome of alternatives in various projected states of nature (i.e., scenarios made up of combinations of uncontrollable parameters) is found first, and then the alternatives are ranked by their best outcomes in the aforementioned worst conditions.

The mathematical formulation is as follows (Equation 24):

Equation 24.

$$Maximin\ Decision = \arg\max(\min(Payoff_1), \min(Payoff_2), \dots, \min(Payoff_n))$$

; where, similar to the maximax criterion, $Payoff_i$ represents the potential payoffs associated with each decision alternative i. The decision-maker selects the optimal alternative, which is the one with the highest minimum payoff.

Minimax Regret Criterion is a more balanced approach, equivalent to a **cautious** standpoint in decision making. Alternatives are first analyzed under each state of nature, and the distance of their outcomes from the outcome of the best-functioning alternative in that particular state of nature is listed. This distance is called regret (the best-functioning alternative obviously causes no/zero regret as it has zero distance to itself). Alternatives are ranked by their maximum corresponding regret with respect to all states of nature. The one with the minimum of maximum regret is selected as the optimal option respecting this criterion. In other words, the minimax regret method aims to minimize the maximum regret that might be resulted from choosing a specific alternative.

So, the mathematical formulation involves comparing the regret associated with each alternative and selecting the one with the smallest maximum regret. Suppose *Regret$_i$* represents the regret associated with decision alternative *i* when considering a specific state of nature. The formulation is as follows (Equation 25):

Equation 25.

$$Minimax\ Regret\ Decision$$
$$= \arg min\left(\max(Regret_1),\max(Regret_2),\dots,\max(Regret_n)\right)$$

; in this formulation, the decision-maker first finds the maximum regret for each alternative and then selects the optimal alternative, which is the one that minimizes this maximum regret.

The researcher applied the three aforementioned algorithms in Microsoft Excel spreadsheets containing all the decision alternatives and their payoffs in accordance with various combinations of levels of uncontrollable factors (i.e., states of nature) taken from the experimental data. Details about the results of the analysis are presented in the next chapter.

4   Chapter No. 4

Results of Analysis

This chapter is divided into two sections. The first section provides comprehensive results of the GLM analysis, directly addressing the first research question. The second section presents the detailed results from the decision analysis, directly addressing the second research question. To facilitate audience recall, the research questions are restated below:

- Research Question 1 (answered by the results of GLM analysis): What is the impact of exoskeletons (vs endoskeletons) on the life cycle primary energy consumption and CO_2e emissions of tall buildings? I.e., how effective and desirable is it compared to and in interaction with some other controllable and uncontrollable factors from the perspective of architectural engineers in the early stage of design? This question was followed by:

- Research Question 2 (answered by the results of decision analysis): What would be the optimal decision or decisions about the controllable factors, made objectively (based on quantitative data), by architectural engineers considering such uncontrollable circumstances?

To quickly review the factors and their corresponding levels, as well as the conceptual framework, the audience is advised to revisit the following tables and figures in the second chapter: Table 6 (and Table 9), Figure 44, Figure 45, Figure 46, and Figure 66.

4.1   Results of GLM Analysis

In the following, unless otherwise stated:
The data in the tables are rather comprehensive (including list of estimates of coefficients of influential factors/levels, and corresponding ranking of absolute value, standard error, t-value, and p-value) but maybe not so optimal for the audience to grasp. Therefore, each table is followed by two visualization bar-charts—both are common ways of data visualization in the field of DoE; the first one is sorted by the desirability of the main effect and interactions of factors/levels (smallest to largest; the most desirable on top), and the second one sorted by their magnitude regardless of direction (sorted by absolute value) relative to the size of the intercept (the most influential on

top). Intercepts correspond to the baseline levels of all factors, denoted as level 'A' for each factor; to recall, please refer to Table 6 (and Table 9).

All numbers demonstrating the estimates of GLM coefficients or their percentage relative to the baselines (intercepts) are rounded and reported with **no decimal places** in the text as well as in bar charts. This is to make them easier to communicate with the audience; it is assumed that tiny differences are not of interest due to the nature of the subject matter, diversity of factors and time spans. Yet, for the sake of completeness, those numbers are indexed in the tables with 2 decimal places.

1. Similarly, to avoid over-complexity, factors/levels with absolute value of coefficients estimated less than 0.5% of their corresponding intercept (they round to 0 as integer) are omitted in all the following tables, figure, and textual report. In some cases, it remarkably reduced the size of datasets without losing important information.

2. The t-value equals the quotient of the estimate divided by the standard error, indicating the t-test, providing information about the magnitude and direction of the effect of the listed parameter (factor, level, or interaction). $Pr(>|t|)$ is the p-value of the t-test; it determines the level of significance associated with the parameter, indicating whether the effect is statistically significant or not [368]. For simplification, the corresponding columns are omitted in tables where standard errors were very small (i.e., 0.0000, which refers to standard errors smaller than 0.0001) and thus the t-values were very large.

3. Complete tables of results of GLM together with all the numerical values, tests, and steps taken in R software are available in detail in the appendix.

4. The fit of the models was evaluated using various fit statistics, including the chi-square test, pseudo-R^2 values (McFadden and Cragg-Uhler), and the Akaike Information Criterion (AIC) and Bayesian Information Criterion (BIC). Detailed numerical values and results of these fit statistics can be found in the aforementioned attached R report file. The models demonstrated a good overall fit to the data, as the pseudo-R^2 values were high, and AIC and BIC values were favorably low (a good balance between fit and complexity). In addition, multiple simulation results were randomly checked, which confirmed the predictions of the statistical models.

5. **All the factors and levels reported** below in the tables, figures, and the texts are those which were **statistically significant—with p-value smaller than 0.05**—i.e. their influence on the response variables were not accidental. To save the time of the readers, the report has been shortened by avoiding multiple repetition of the phrase "statistically significant" as much as possible. In other words, each and every item listed in the tables or figures below is a part of the (long-) answer to the **first research question**.

6. As a small reminder: the words "**desirable, good, better, etc.**" are used to describe **decrease** in use of primary energy or emitting GHGs. Therefore, it relates with **negative/small** numbers. With the same logic, "**undesirable,**

bad, worse, etc." comes with the **increase** in use of primary energy or emitting GHGs. Therefore, it relates with **positive/large** numbers.

7. Percentages are all with respect to the baselines. Factors and their levels (including the base levels) involved in each phase are listed in the Table 6.

8. Results of each phase is reported in 2 (paired) parts: one for Primary Energy, followed by another one for CO_2e Emissions. In most cases the list of factors/levels and their order of magnitude were alike and only numbers were different. Identical textual compositions and statements are used in both parts of each pair of reports wherever possible in order to make it convenient for the readers if they would like to detect these similarities and differences in the pattern of the texts too.

As previously mentioned, intercepts represent baseline levels for all factors studied. Before delving into detailed analyses of all factors, levels, and interactions for each life cycle phase or time span, it is helpful to provide an overview and comparison of the intercepts to establish a sense of scale for the audience.

For this purpose, Figure 81 and Figure 82 present this overview and comparison for primary energy consumption and CO_2e emissions. These figures reveal two key observations:

1. Patterns of relative magnitudes, while not identical, are fairly similar for primary energy and CO_2e emissions;
2. Operational impacts, even in the medium-term (30 years: 2020-2050), are by far (approximately 7-8 times) larger than the pre-operational/embodied (-2020) ones. This ratio doubles (to approximately 15-16 times) with respect to the long-term (60 years: 2020-2080) operational impacts. The doubling of the ratio was, of course, because the baseline scenarios remained the same for both 30 and 60 years of operation.

Furthermore, Figure 83 and Figure 84 serve as visual aids to grasp the ranges of coefficients affecting primary energy consumption and CO_2e emissions across different phases or time spans, relative to each corresponding intercept. While not necessarily tied to a particular factor, these figures present a general overview of the sizes of the most influential coefficients. Coefficients correspond to effects of different factors, levels, or their interactions.

Detailed data for the effects of all factors and their interactions in all periods will be presented in the subsequent subsections of this section. The audience may refer back to these figures as points of reference while reading the following subsections to recall the relative magnitudes of all intercepts (Figure 81 and Figure 82), and the range of coefficients in each period relative to their corresponding intercepts (Figure 83 and Figure 84).
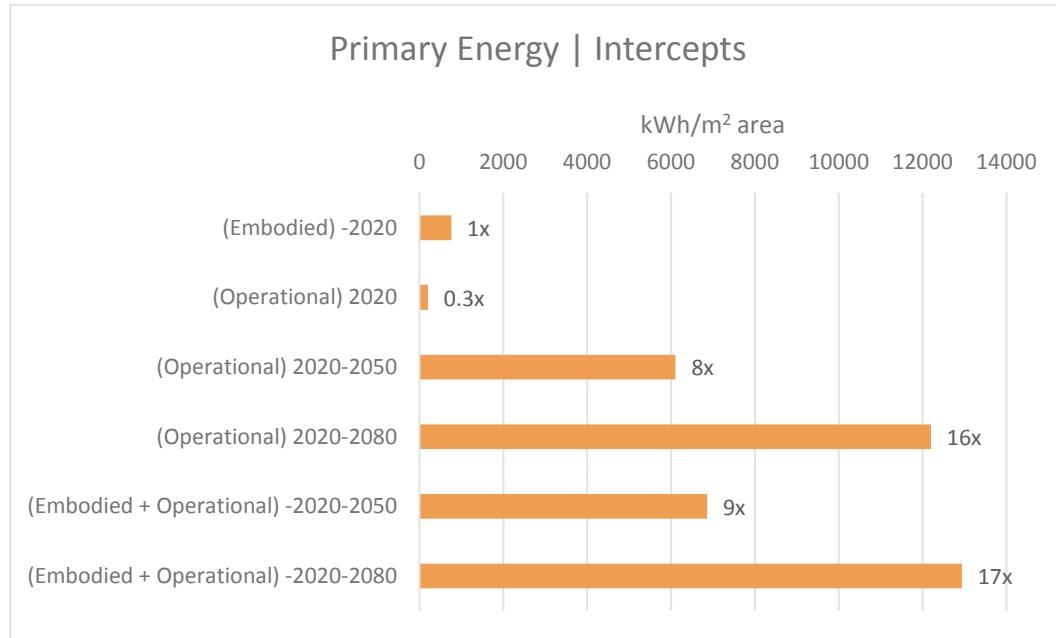
Figure 81. Overview and comparison of intercepts for primary energy consumption intensity in various life cycle phases/time spans. The magnitudes on the right side of each bar are relative to the pre-operational (embodied) phase (-2020) set as 1x. Source: the researcher
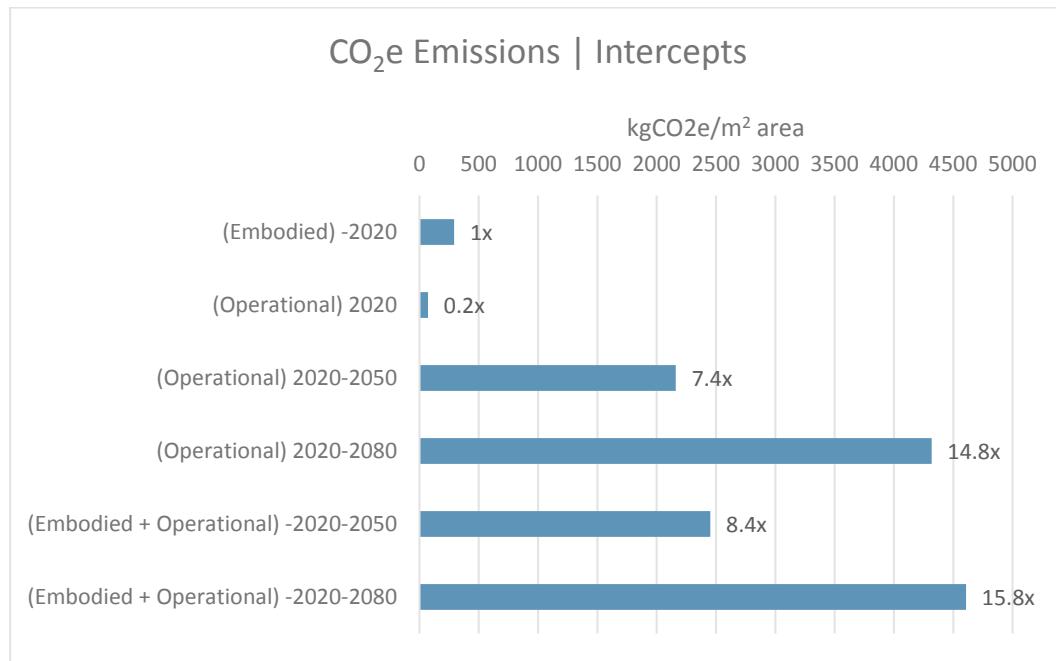
Figure 82. Overview and comparison of intercepts for CO2e emissions intensity in various life cycle phases/time spans. The magnitudes on the right side of each bar are relative to the pre-operational (embodied) phase (-2020) set as 1x. Source: the researcher
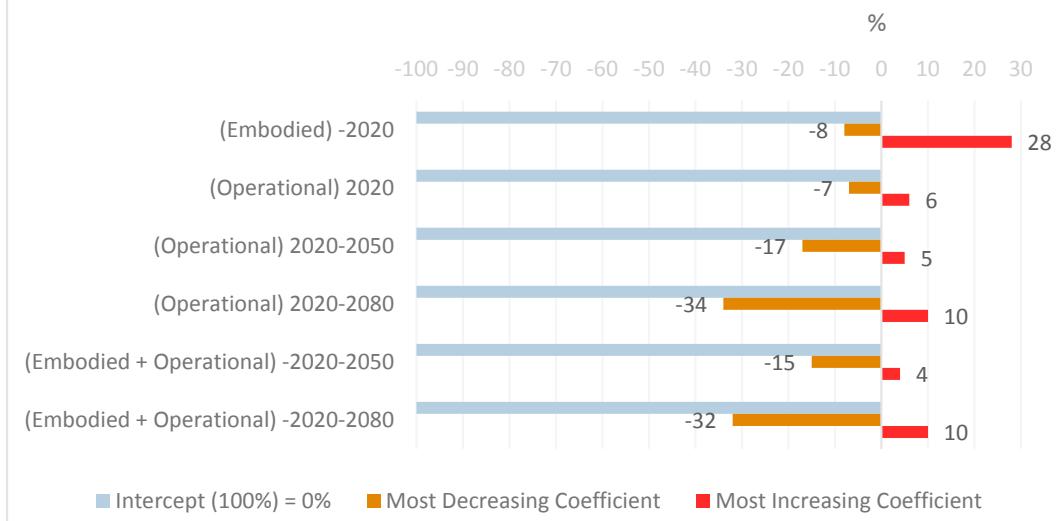
Figure 83. Ranges of coefficients for primary energy consumption in different phases/time spans relative to each corresponding intercept. Source: the researcher
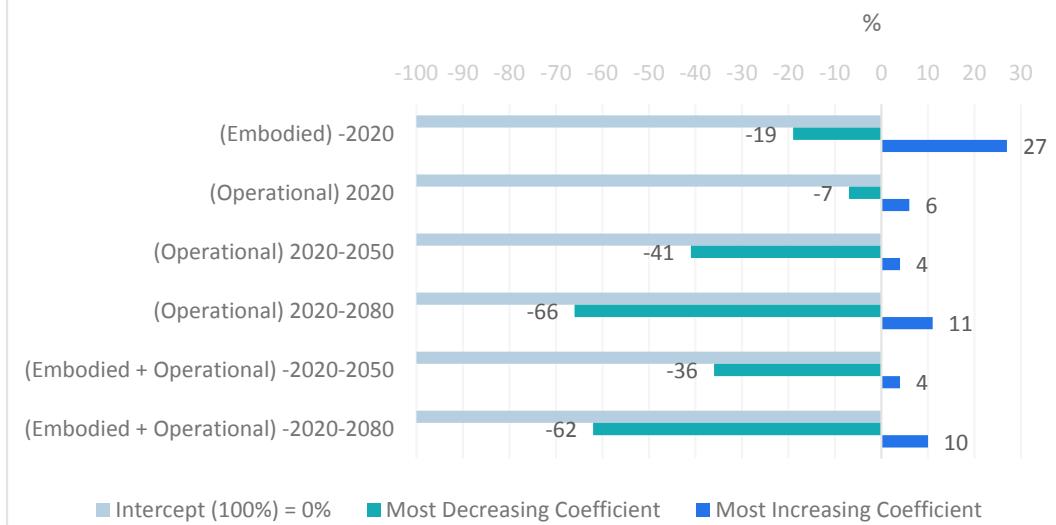
Figure 84. Ranges of coefficients for CO_2e emissions in different phases/time spans relative to each corresponding intercept. Source: the researcher

191

4.1.1 Primary Energy (Embodied) -2020

      The incorporation of exoskeletons increased the amount of EE. Among them, skeletons partly exposed to the environment (MIDs) showed relatively better results (17% & 20%) compared with the ones fully exposed (OUTs) (27% & 28%). The larger numbers belonging to the thermal bridge controll indicate an undesirable effect of the insulation materials in this particular phase. This is only 1% in the case of OUTs but more evident in the case of MIDs (3%). CR (GGBFS50) was the only factor showing a desirable main effect (-8%). It also showed desirable interaction with exoskeletons. Its interaction with OUTs (-2%) was larger than MIDs (-1%). Long distance transportation of sand and using desalinated water had 11% and 10% main effects respectively. Both showed 3% interaction with OUTs and 2% with MIDs. The baseline indicated 761 kWh/m^2 area (Table 37, Figure 85, and Figure 86).

Table 37. GLM Simplified Summary | Response Variable: Primary Energy (Embodied) in kWh/m^2 area. Source: the researcher

| Coefficients:	Estimate	|Est.| Rank	Std. Error	Pr (>|t|)
(Intercept)	760.56	NA	0.00	0.0000
CR_D_GGBFS50	-61.39	7	0.00	0.0000
PTC_TBC_C_OUT_WO:CR_D_GGBFS50	-15.83	12	0.00	0.0000
PTC_TBC_E_OUT_W:CR_D_GGBFS50	-15.83	12	0.00	0.0000
PTC_TBC_B_MID_WO:CR_D_GGBFS50	-11.11	18	0.00	0.0000
PTC_TBC_D_MID_W:CR_D_GGBFS50	-11.11	18	0.00	0.0000
PTC_TBC_B_MID_WO:PDWPRC	12.64	16	0.00	0.0000
PTC_TBC_D_MID_W:PDWPRC	12.64	16	0.00	0.0000
PTC_TBC_B_MID_WO:PTSAU	14.88	15	0.00	0.0000
PTC_TBC_D_MID_W:PTSAU	14.88	14	0.00	0.0000
PTC_TBC_C_OUT_WO:PDWPRC	19.74	10	0.00	0.0000
PTC_TBC_E_OUT_W:PDWPRC	19.74	10	0.00	0.0000
PTC_TBC_C_OUT_WO:PTSAU	20.86	8	0.00	0.0000
PTC_TBC_E_OUT_W:PTSAU	20.86	8	0.00	0.0000
PDWPRC	73.40	6	0.00	0.0000
PTSAU	83.31	5	0.00	0.0000
PTC_TBC_B_MID_WO	131.11	4	0.00	0.0000
PTC_TBC_D_MID_W	149.72	3	0.00	0.0000
PTC_TBC_C_OUT_WO	204.72	2	0.00	0.0000
PTC_TBC_E_OUT_W	213.89	1	0.00	0.0000
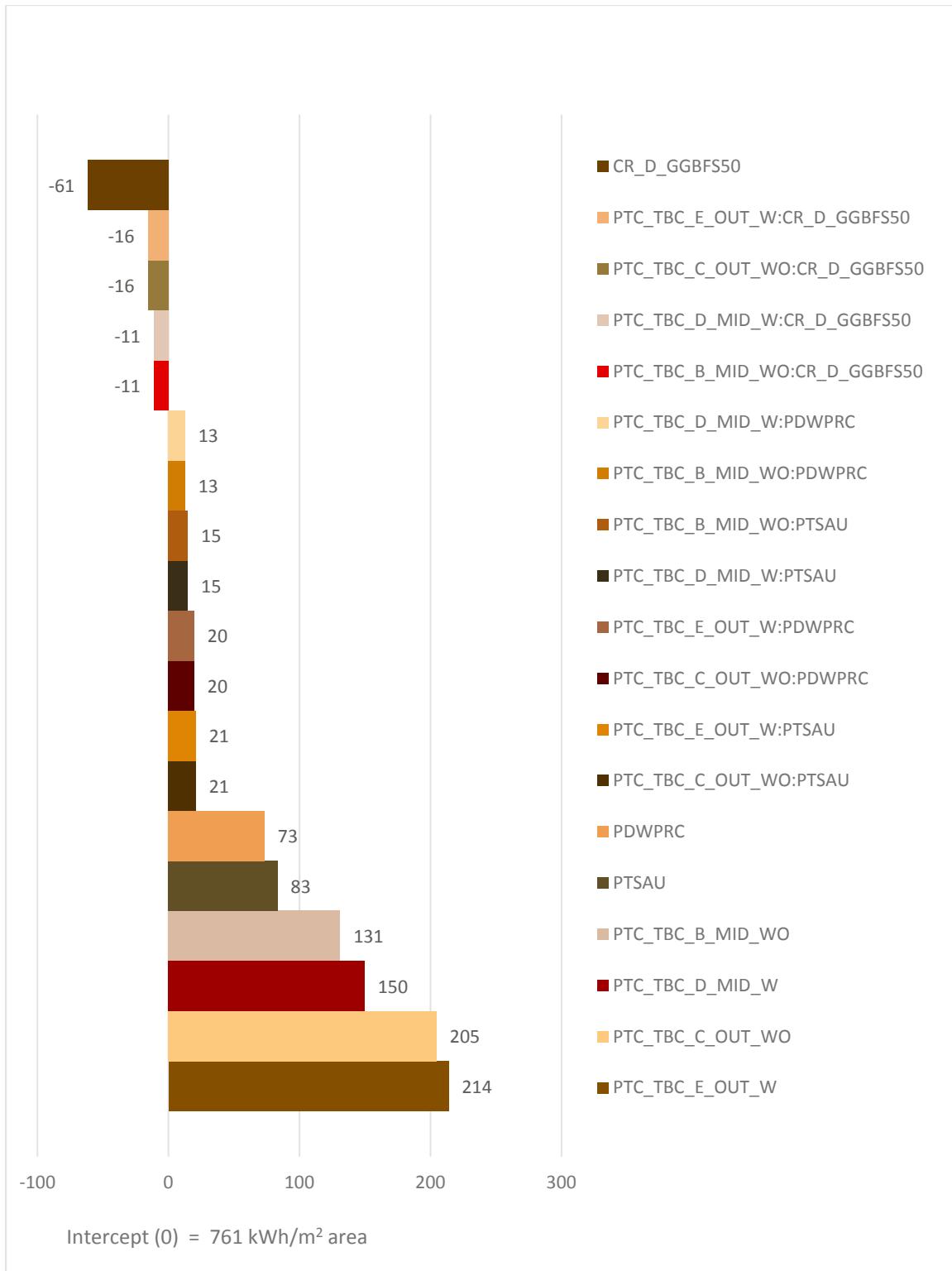
Figure 85. GLM Estimates | Primary Energy (Embodied). Source: the researcher
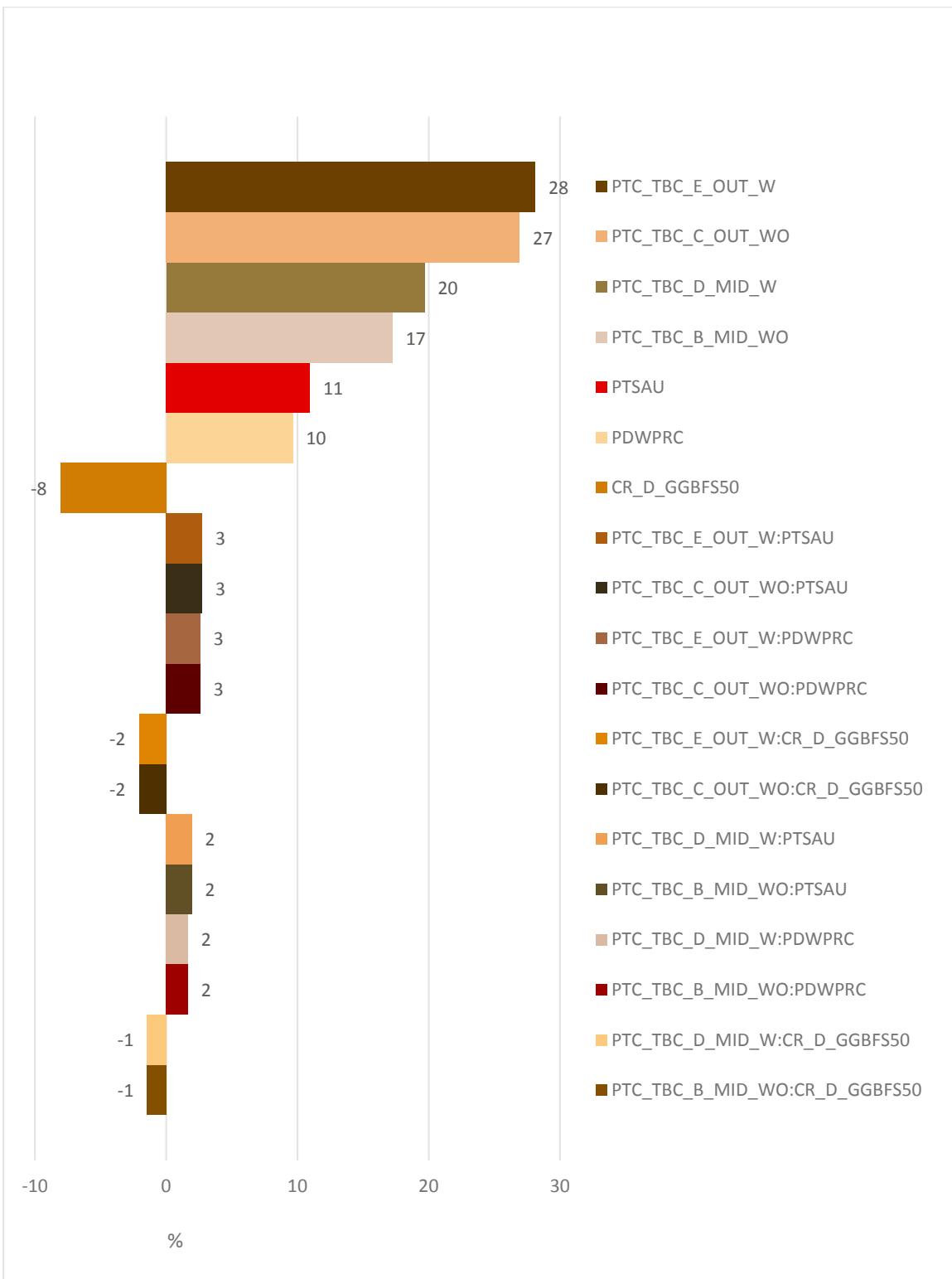
Figure 86. GLM Estimates (sorted by absolute value), in percentage compared with the intercept | Primary Energy (Embodied). Source: the researcher

4.1.2 CO_2e Emissions (Embodied) -2020

The utilization of exoskeletons led to an elevation in embodied CO_2e emissions. Among them, skeletons partly exposed to the environment (MIDs) showed better results (17% & 18%) compared with the ones fully exposed (OUTs) (26% & 27%). The larger numbers belonging to the thermal bridge control indicate an undesirable effect of the insulation materials in this particular phase. This is only 1% in both cases of OUTs and MIDs. CR (GGBFS50) was the only factor showing a desirable main effect (-19%). It also showed desirable interaction with exoskeletons. Its interaction with OUTs (-5%) was larger than MIDs (-3%). Long distance transportation of sand and using desalinated water had 7% and 3% main effects respectively. The former showed 2% interaction with OUTs and 1% with MIDs, and the latter showed 1% interaction for both. The baseline indicated 292 $kgCO_2e/m^2$ area (Table 38, Figure 87, Figure 88).

Table 38. GLM Simplified Summary | Response Variable: CO_2e Emissions (Embodied) in $kgCO_2e/m^2$ area. Source: the researcher

| Coefficients:	Estimate	|Est.| Rank	Std. Error	Pr (>|t|)
(Intercept)	291.95	NA	0.00	0.0000
CR_D_GGBFS50	-56.87	3	0.00	0.0000
PTC_TBC_C_OUT_WO:CR_D_GGBFS50	-14.35	7	0.00	0.0000
PTC_TBC_E_OUT_W:CR_D_GGBFS50	-14.35	7	0.00	0.0000
PTC_TBC_B_MID_WO:CR_D_GGBFS50	-10.12	9	0.00	0.0000
PTC_TBC_D_MID_W:CR_D_GGBFS50	-10.12	9	0.00	0.0000
PTC_TBC_B_MID_WO:PDWPRC	1.57	19	0.00	0.0000
PTC_TBC_D_MID_W:PDWPRC	1.57	18	0.00	0.0000
PTC_TBC_C_OUT_WO:PDWPRC	2.44	17	0.00	0.0000
PTC_TBC_E_OUT_W:PDWPRC	2.44	16	0.00	0.0000
PTC_TBC_B_MID_WO:PTSAU	3.66	14	0.00	0.0000
PTC_TBC_D_MID_W:PTSAU	3.66	14	0.00	0.0000
PTC_TBC_C_OUT_WO:PTSAU	5.12	12	0.00	0.0000
PTC_TBC_E_OUT_W:PTSAU	5.12	12	0.00	0.0000
PDWPRC	9.09	11	0.00	0.0000
PTSAU	20.46	6	0.00	0.0000
PTC_TBC_B_MID_WO	50.80	5	0.00	0.0000
PTC_TBC_D_MID_W	53.60	4	0.00	0.0000
PTC_TBC_C_OUT_WO	77.03	2	0.00	0.0000
PTC_TBC_E_OUT_W	78.43	1	0.00	0.0000
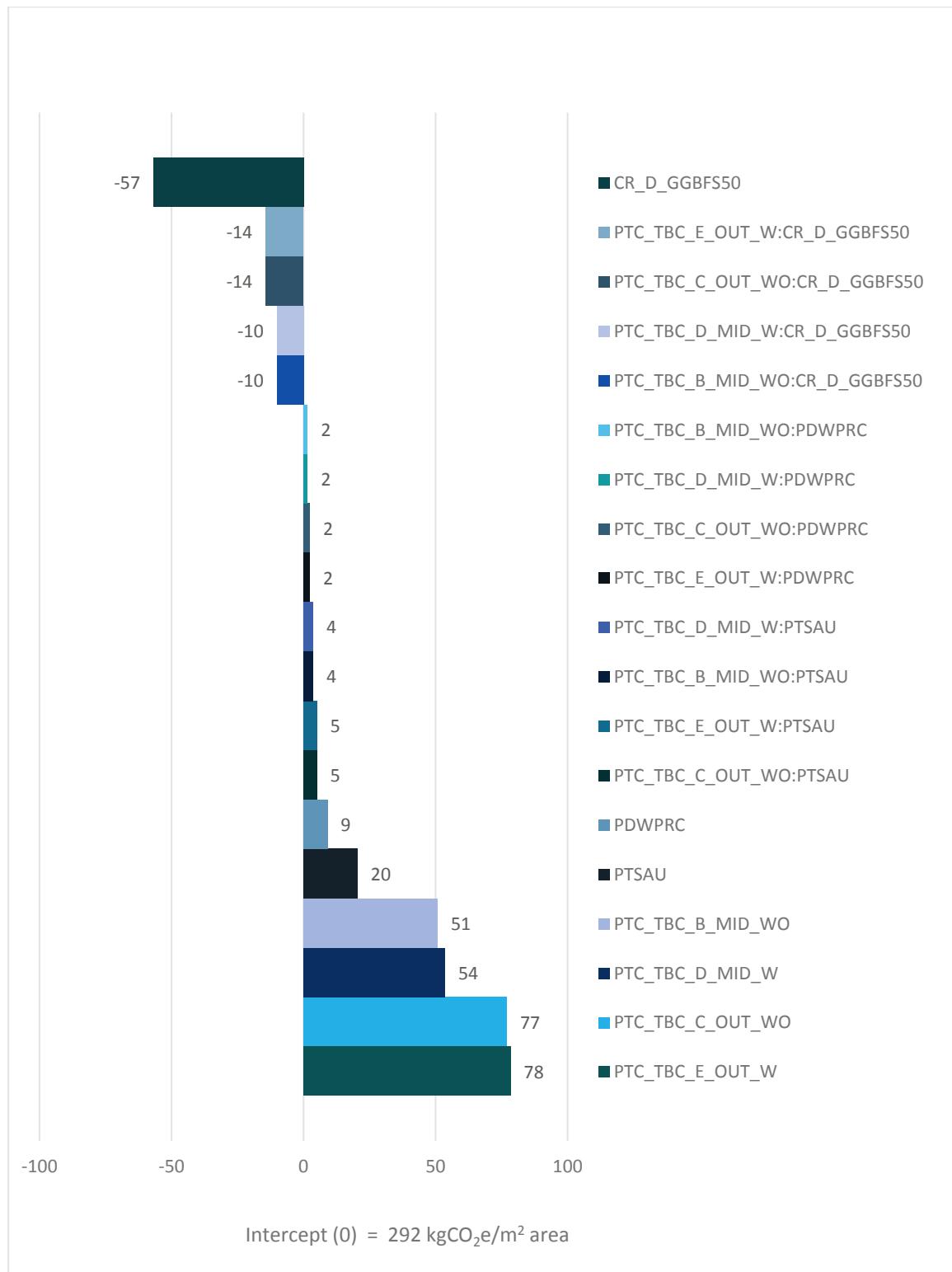
Figure 87. GLM Estimates | CO$_2$e Emissions (Embodied). Source: the researcher
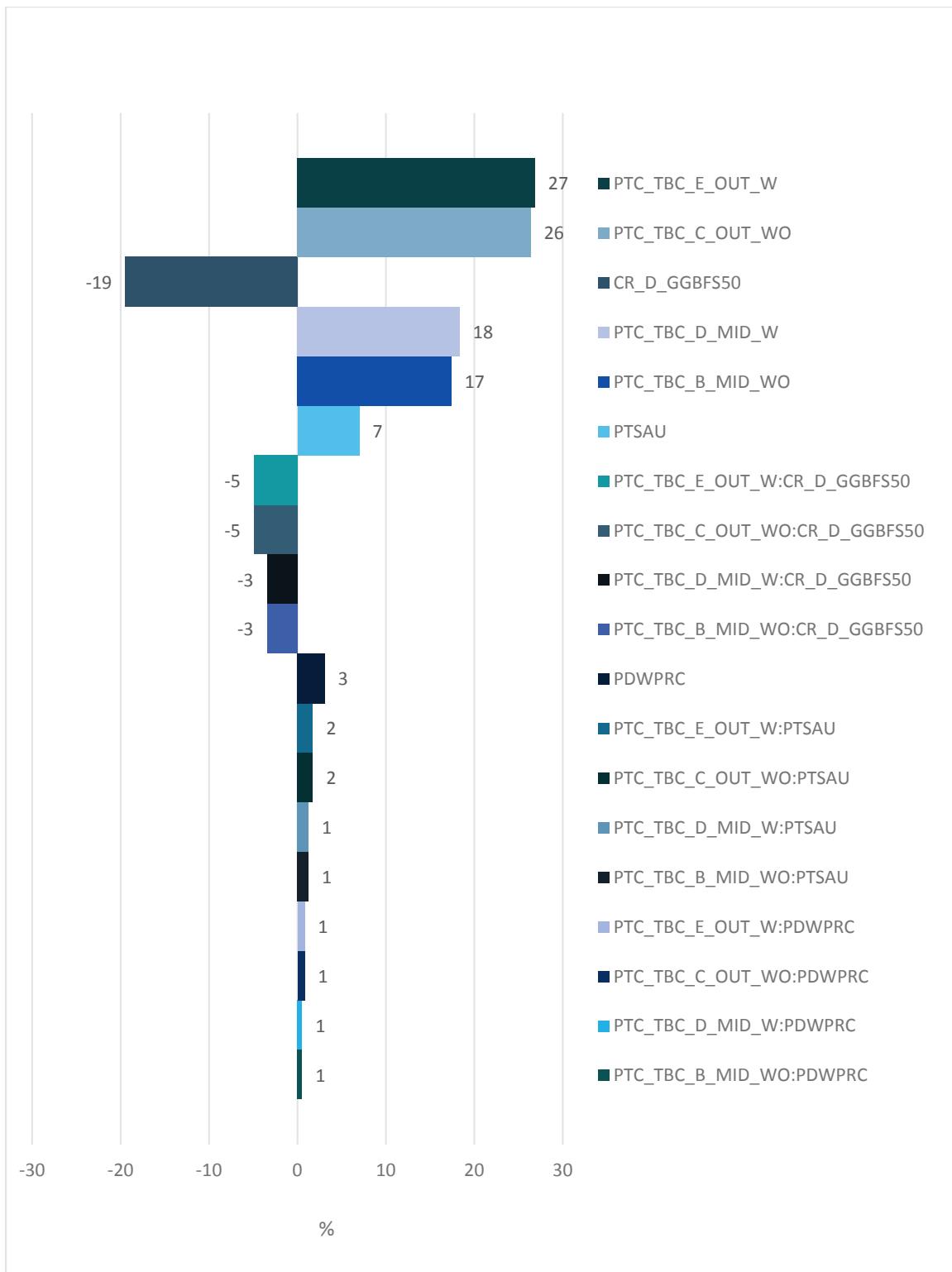
Figure 88. GLM Estimates (sorted by absolute value), in percentage compared with the intercept | CO_2e Emissions (Embodied). Source: the researcher

4.1.3   Primary Energy (Operational) 2020

The operational primary energy in the year 2020 was influenced by 9 main effects and interactions. The largest main effects—which were equal and desirable (-14%)—belonged to three factors/levels: using the exoskeletons fully exposed to the environment (OUTs whether with or without controlling the thermal bridging), and high density of the urban tissue. Incorporation of exoskeletons partly exposed to the environment (MIDs) also showed desirable but smaller effects; -8% with, and -6% without controlling the thermal bridges. Four interactions resulted, and all were undesirable; using exoskeletons in high density urban tissue. This interaction was equal (11%) in the case of OUTs whether with or without controlling the thermal bridges. Controlling the thermal bridges reduced the effect of interaction in the case of MIDs from 7% to 6%. The baseline indicated 204 kgCO$_2$e/m^2 area (Table 39, Figure 89, and Figure 90).

Table 39. GLM Simplified Summary | Response Variable: Primary Energy (Operational) 2020 in kWh/m^2 area. Source: the researcher

| Coefficients:	Estimate	|Est.| Rank	Std. Error	Pr (>|t|)
(Intercept)	203.94	NA	0.00	0.0000
UD_B_H	-14.10	1	0.00	0.0000
PTC_TBC_E_OUT_W	-14.09	2	0.00	0.0000
PTC_TBC_C_OUT_WO	-13.95	3	0.00	0.0000
PTC_TBC_D_MID_W	-8.35	6	0.00	0.0000
PTC_TBC_B_MID_WO	-6.35	8	0.00	0.0000
PTC_TBC_B_MID_WO:UD_B_H	6.20	9	0.00	0.0000
PTC_TBC_D_MID_W:UD_B_H	6.53	7	0.00	0.0000
PTC_TBC_E_OUT_W:UD_B_H	11.35	5	0.00	0.0000
PTC_TBC_C_OUT_WO:UD_B_H	11.36	4	0.00	0.0000
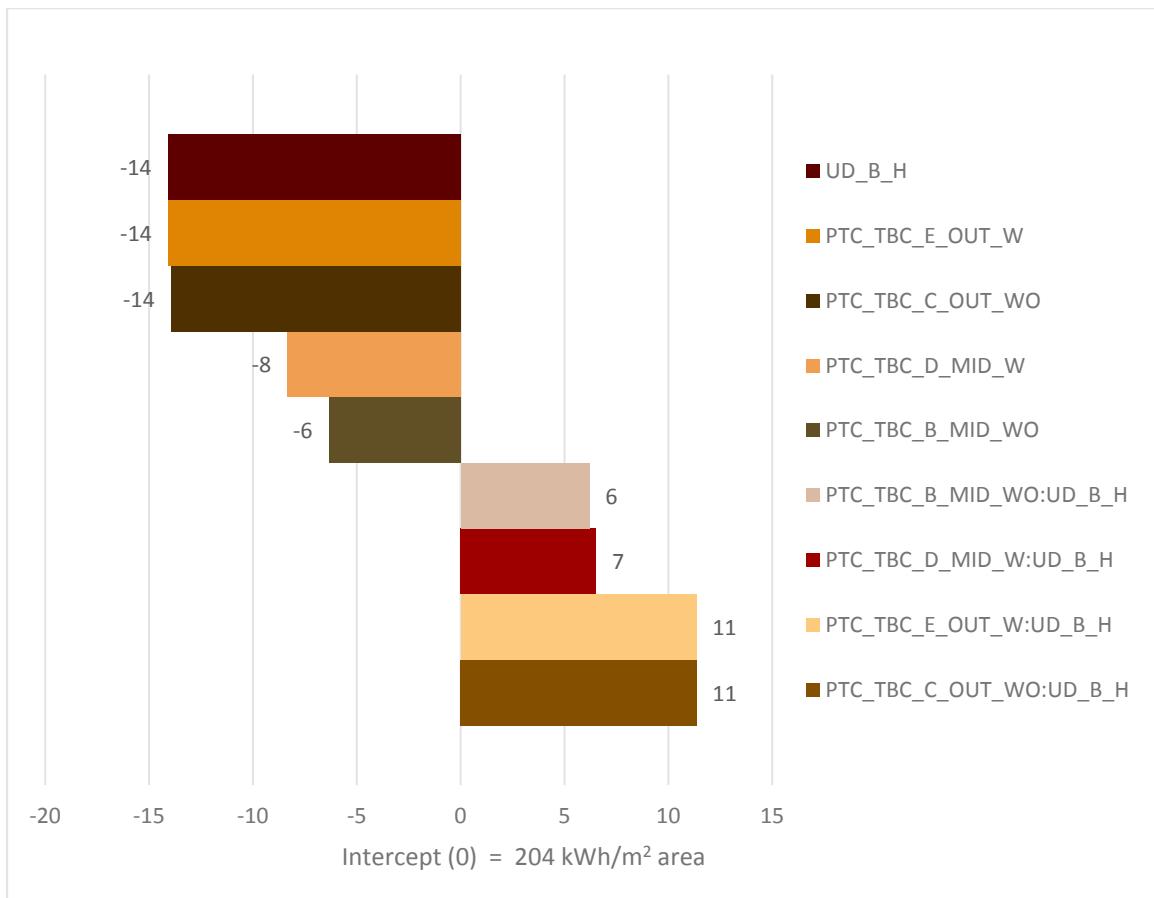
Figure 89. GLM Estimates | Primary Energy (Operational) 2020. Source: the researcher
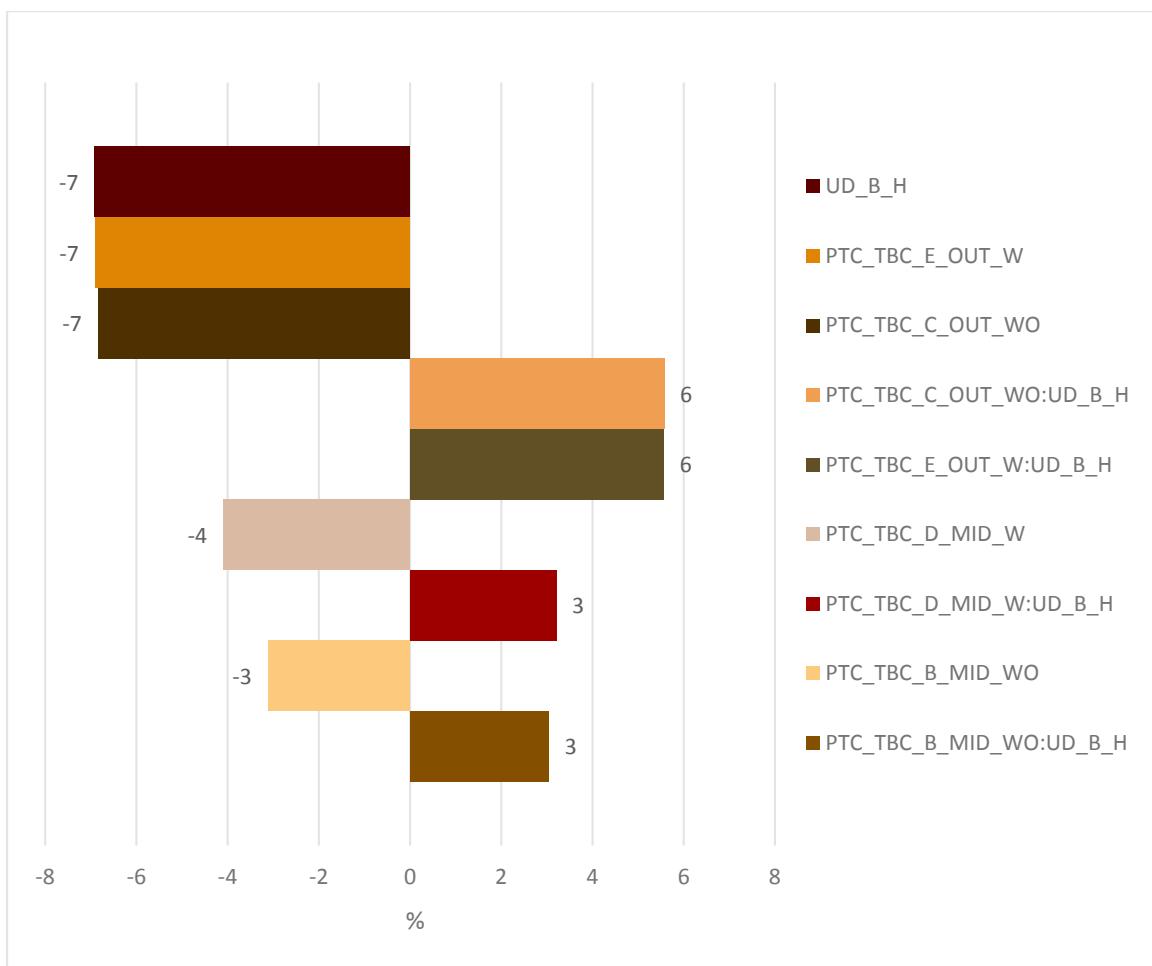
Figure 90. GLM Estimates (sorted by absolute value), in percentage compared with the intercept| Primary Energy (Operational) 2020. Source: the researcher

4.1.4 CO₂e Emissions (Operational) 2020

The operational CO_2e emissions in the year 2020 was influenced by 9 main effects and interactions. The largest main effects—which were equal and desirable (-5%)—belonged to three factors/levels: using the exoskeletons fully exposed to the environment (OUTs whether with or without controlling the thermal bridging), and high density of the urban tissue. Incorporation of exoskeletons partly exposed to the environment (MIDs) also showed desirable but smaller effects; -3% with, and -2% without controlling the thermal bridges. Four interactions resulted, and all were undesirable; using exoskeletons in high density urban tissue. This interaction was equal (4%) in the case of OUTs whether with or without controlling the thermal bridges. Controlling the thermal bridges reduced the effect of interaction in the case of MIDs from 7% to 6%. The baseline indicated 72 $kgCO_2e/m^2$ area (Table 40, Figure 91, and Figure 92).

Table 40. GLM Simplified Summary | Response Variable: CO₂e Emissions (Operational) 2020 in kgCO₂e/m² area. Source: the researcher

| Coefficients:	Estimate	|Est.| Rank	Std. Error	Pr (>|t|)
(Intercept)	72.28	NA	0.00	0.0000
UD_B_H	-5.12	1	0.00	0.0000
PTC_TBC_E_OUT_W	-5.09	2	0.00	0.0000
PTC_TBC_C_OUT_WO	-5.04	3	0.00	0.0000
PTC_TBC_D_MID_W	-3.02	6	0.00	0.0000
PTC_TBC_B_MID_WO	-2.29	8	0.00	0.0000
PTC_TBC_B_MID_WO:UD_B_H	2.23	9	0.00	0.0000
PTC_TBC_D_MID_W:UD_B_H	2.36	7	0.00	0.0000
PTC_TBC_E_OUT_W:UD_B_H	4.09	5	0.00	0.0000
PTC_TBC_C_OUT_WO:UD_B_H	4.1	4	0.00	0.0000
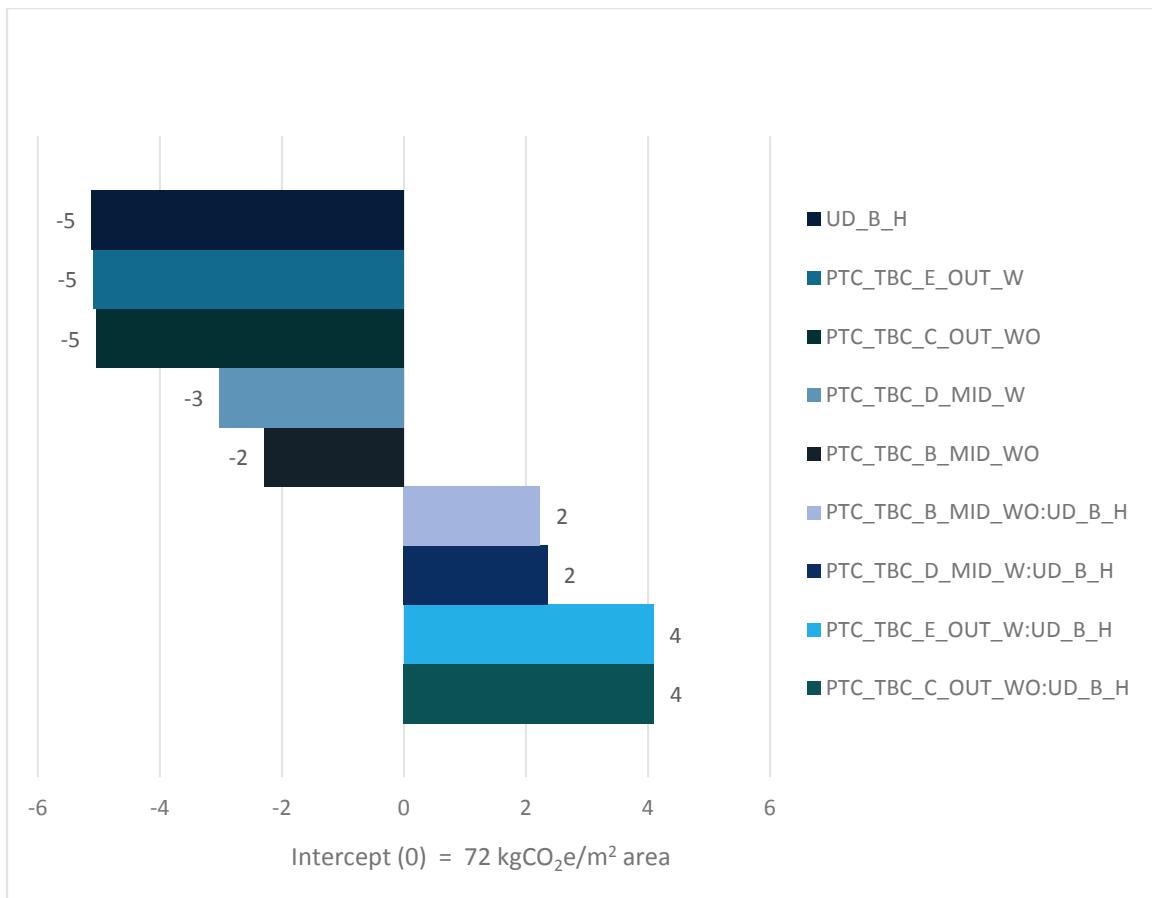
Figure 91. GLM Estimates | CO_2e Emissions (Operational) 2020. Source: the researcher
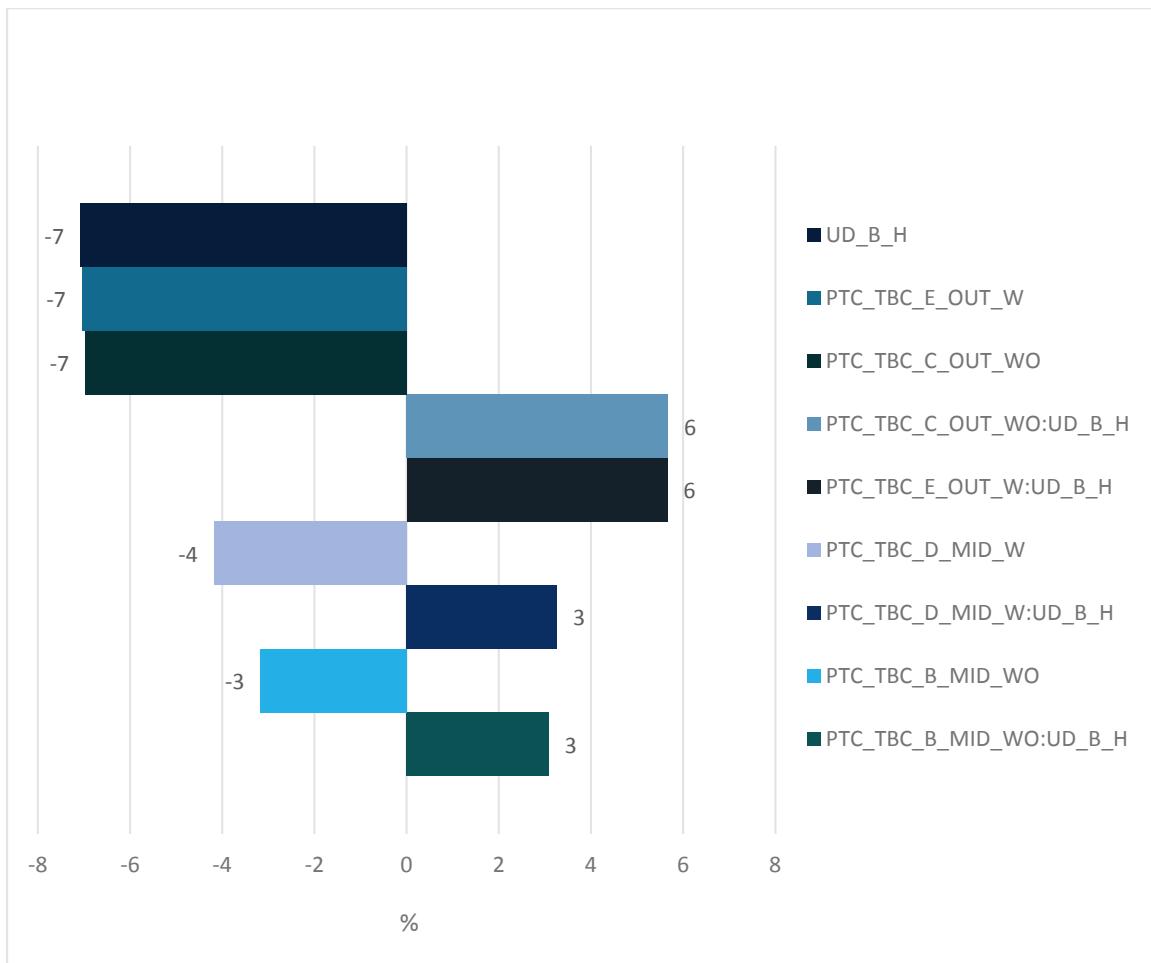
Figure 92. GLM Estimates (sorted by absolute value), in percentage compared with the intercept | CO_2e Emissions (Operational) 2020. Source: the researcher

4.1.5 Primary Energy (Operational) 2020-2050

Regarding primary energy consumption in the first thirty years of the operational phase (2020-2050), exoskeletons showed desirable main effects. From this group, the largest effect was -7% belonging to the skeletons fully exposed to the environment (OUTs) no matter if the thermal bridges were controlled or not. In the case of skeletons partly exposed to the environment (MIDs), the effect was -4% with, and -3% without controlling the thermal bridges. High density of urban tissue had a desirable main effect of -6% but the desirable effect of exoskeletons reduced in such urban contexts; 5% for OUTs, and 2% for MIDs. MIDs with controlling thermal bridges together with OUTs appeared 1% less desirable when interacting with future development of green technologies. Despite that, the technological development had by far the largest main effect and the largest desirable effect; that was -17%. It had also a desirable interaction of -2% with Global warming. Global warming showed a 4% undesirable main effect. The baseline indicated 6105 kWh/m^2 area (Table 41, Figure 93, and Figure 94).

Table 41. GLM Simplified Summary | Response Variable: Primary Energy (Operational) 2020-2050 in kWh/m^2 area. Source: the researcher

Coefficients:	Estimate	|Est.| Rank	Std. Error	t value	Pr (>|t|)
(Intercept)	6104.68	NA	14.56	419.24	0.0000
TYP_B_20_50_80	-1047.04	1	18.16	-57.65	0.0000
UD_B_H:TYP_B_20_50_80	-412.64	2	13.73	-30.06	0.0000
PTC_TBC_E_OUT_W	-405.28	3	18.80	-21.56	0.0000
PTC_TBC_C_OUT_WO	-400.69	4	18.80	-21.31	0.0000
UD_B_H	-394.55	5	16.81	-23.47	0.0000
PTC_TBC_D_MID_W	-228.64	9	18.80	-12.16	0.0000
PTC_TBC_B_MID_WO	-166.44	10	18.80	-8.85	0.0000
TYP_B_20_50_80:WDYP_B_20_50_80	-148.67	12	13.73	-10.83	0.0000
PTC_TBC_C_OUT_WO:TYP_B_20_50_80	47.92	16	21.71	2.21	0.0380
PTC_TBC_E_OUT_W:TYP_B_20_50_80	50.36	15	21.71	2.32	0.0300
PTC_TBC_D_MID_W:TYP_B_20_50_80	50.55	14	21.71	2.33	0.0295
PTC_TBC_B_MID_WO:UD_B_H	143.21	13	21.71	6.60	0.0000
PTC_TBC_D_MID_W:UD_B_H	150.23	11	21.71	6.92	0.0000
WDYP_B_20_50_80	268.82	8	9.71	27.69	0.0000
PTC_TBC_E_OUT_W:UD_B_H	300.19	7	21.71	13.83	0.0000
PTC_TBC_C_OUT_WO:UD_B_H	300.23	6	21.71	13.83	0.0000
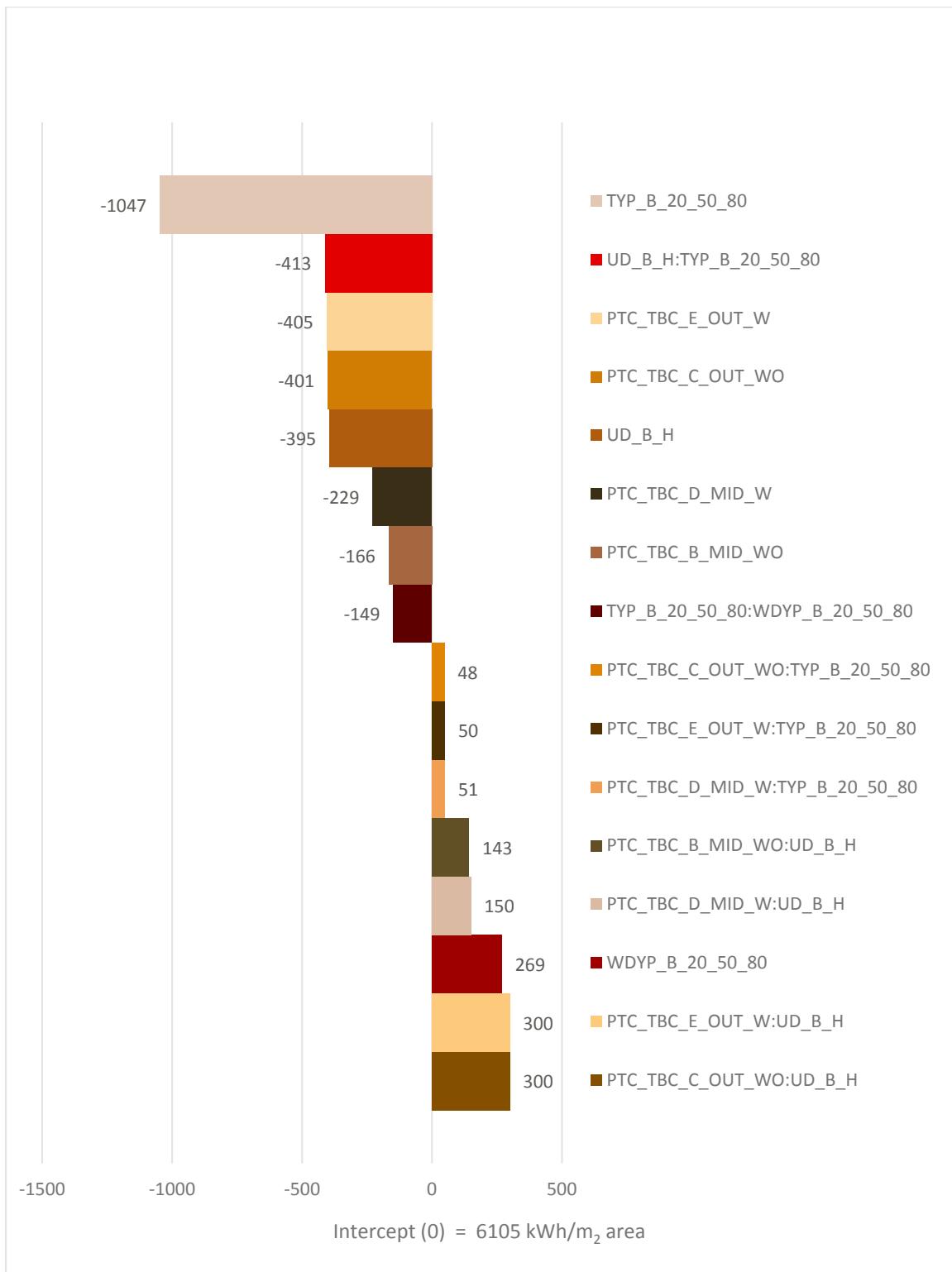
Figure 93. GLM Estimates | Primary Energy (Operational) 2020-2050. Source: the researcher
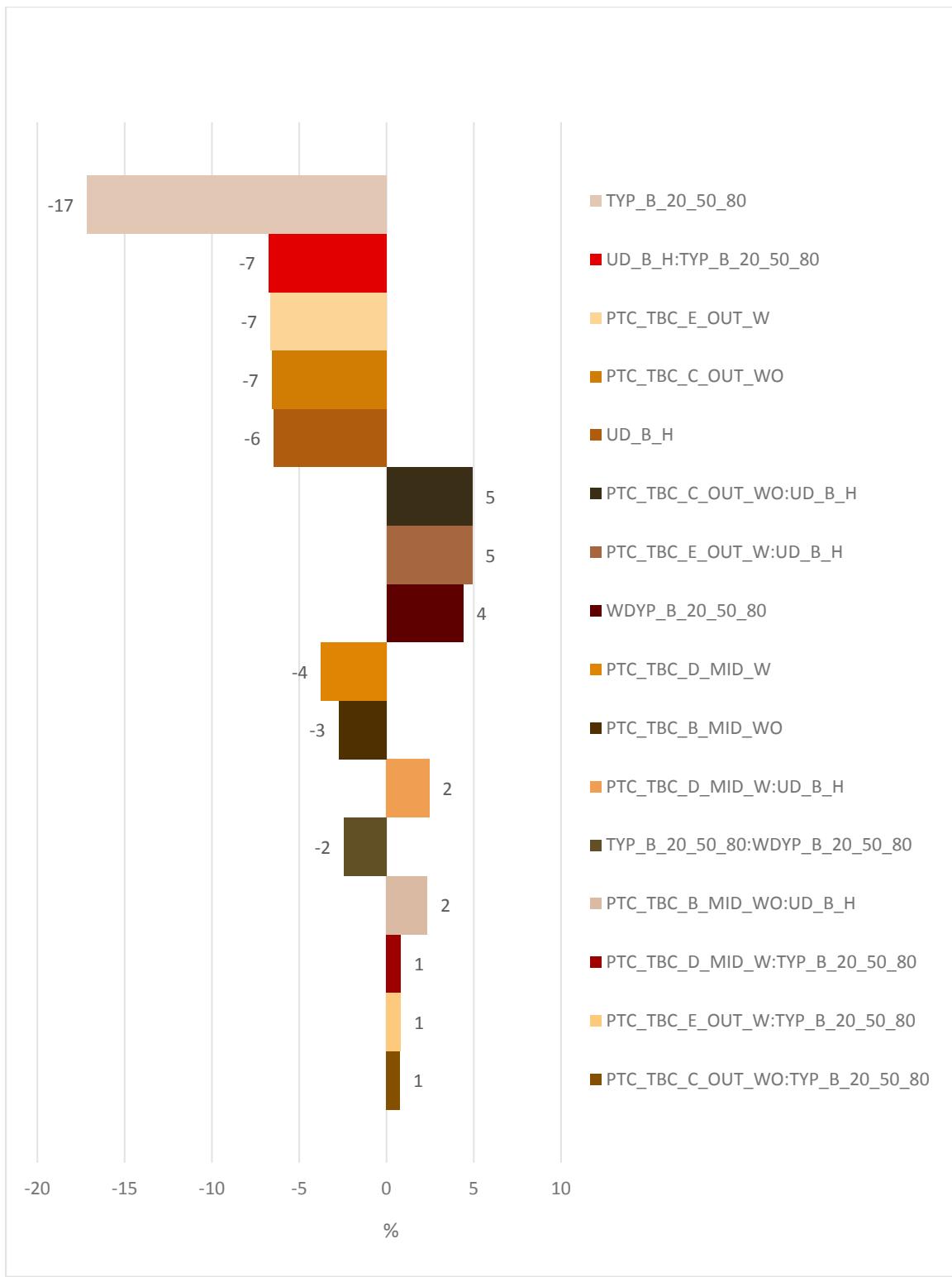
Figure 94. GLM Estimates (sorted by absolute value), in percentage compared with the intercept | Primary Energy (Operational) 2020-2050. Source: the researcher

4.1.6 CO₂e Emissions (Operational) 2020-2050

In the initial three decades of the operational phase (2020-2050), exoskeletons exhibited desirable main effects on CO₂e emissions. From this group, the largest effects were -7% and -6% belonging to the skeletons fully exposed to the environment (OUTs) with and without controlling thermal bridges respectively. In the case of skeletons partly exposed to the environment (MIDs), the effect was -4% with, and -3% without controlling the thermal bridges. High density of urban tissue had a desirable main effect of -6% but the desirable effect of exoskeletons reduced in such urban contexts; 4% for OUTs, and 2% for MIDs. MIDs with controlling thermal bridges appeared 1% less desirable when interacting with future development of green technologies. This effect was 2% in the case of OUTs. Despite that, the technological development had by far the largest main effect and the largest desirable effect; that was -41%. It had also a desirable interaction of -4% with Global warming. Global warming itself showed a 4% undesirable main effect. The baseline indicated 2161 kgCO₂e/m² area (Table 42, Figure 95, and Figure 96).

Table 42. GLM Simplified Summary | Response Variable: CO₂e Emissions (Operational) 2020-2050 in $kgCO_2/m^2$ area. Source: the researcher

Coefficients:	Estimate	|Est.| Rank	Std. Error	t value	Pr (>|t|)
(Intercept)	2161.13	NA	4.81	449.19	0.0000
TYP_B_20_50_80	-889.59	1	6.00	-148.25	0.0000
PTC_TBC_E_OUT_W	-140.72	2	6.21	-22.66	0.0000
PTC_TBC_C_OUT_WO	-139.07	3	6.21	-22.39	0.0000
UD_B_H	-138.62	4	5.56	-24.95	0.0000
TYP_B_20_50_80:WDYP_B_20_50_80	-85.82	8	4.54	-18.92	0.0000
PTC_TBC_D_MID_W	-82.44	9	6.21	-13.27	0.0000
PTC_TBC_B_MID_WO	-59.81	10	6.21	-9.63	0.0000
PTC_TBC_D_MID_W:TYP_B_20_50_80	25.46	15	7.17	3.55	0.0018
PTC_TBC_C_OUT_WO:TYP_B_20_50_80	38.59	14	7.17	5.38	0.0000
PTC_TBC_E_OUT_W:TYP_B_20_50_80	39.49	13	7.17	5.51	0.0000
PTC_TBC_B_MID_WO:UD_B_H	51.15	12	7.17	7.13	0.0000
PTC_TBC_D_MID_W:UD_B_H	53.89	11	7.17	7.51	0.0000
WDYP_B_20_50_80	96.69	7	3.21	30.15	0.0000
PTC_TBC_E_OUT_W:UD_B_H	96.86	6	7.17	13.51	0.0000
PTC_TBC_C_OUT_WO:UD_B_H	97.01	5	7.17	13.53	0.0000
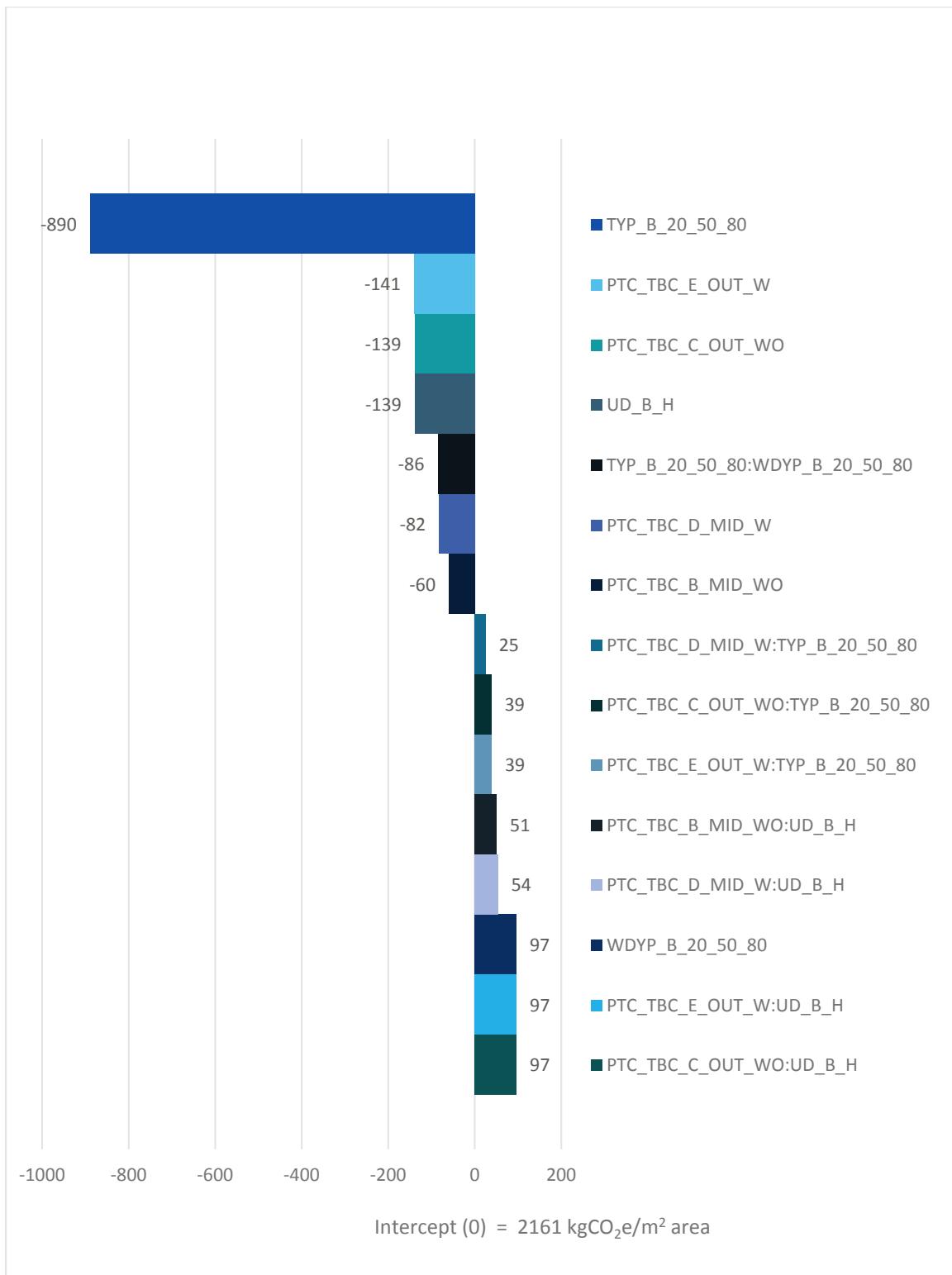
Figure 95. GLM Estimates | CO$_2$e Emissions (Operational) 2020-2050. Source: the researcher
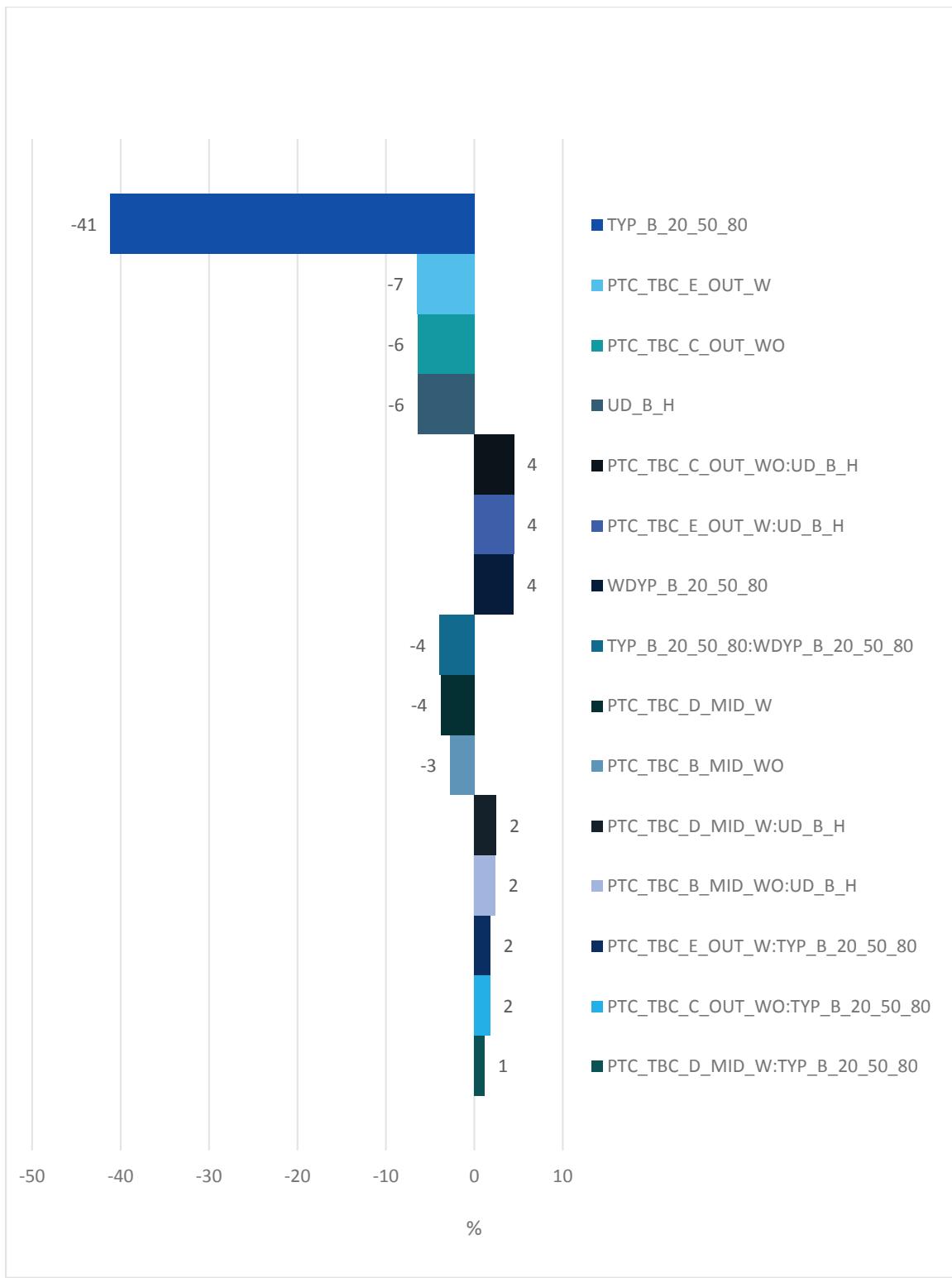
Figure 96. GLM Estimates (sorted by absolute value), in percentage compared with the intercept | CO_2e Emissions (Operational) 2020-2050. Source: the researcher

4.1.7 Primary Energy (Operational) 2020-2080

Incorporation of exoskeletons demonstrated main effects which reduced the primary energy consumption during sixty years of the operational phase (2020-2080); the effect was -6% for OUTs whether or not controlling thermal bridges, and it was -4% and -3% in the cases of MIDs with and without controlling thermal bridges respectively. OUTs and MIDs showed undesirable interactions of 4% and 2% with high-density urban contexts. OUTs (whether or not controlling thermal bridges) had an interaction of 2% with the advancement of green technologies, whereas MIDs with controlling thermal bridges showed similar but 1% smaller interaction. High-density urban tissues had a desirable main effect of -6% and interaction of -8% with green technological developments. These developments also interacted desirably with global warming at the rate of -7%. Global warming itself had an undesirable main effect of 10%. The green technological development showed by far the largest main effect as well as the largest desirable effect; that was -34%. The baseline indicated 12200 kWh/m^2 area (Table 43, Figure 97, and Figure 98).

Table 43. GLM Simplified Summary | Response Variable: Primary Energy (Operational) 2020-2080 in kWh/m^2 area. Source: the researcher

Coefficients:	Estimate	|Est.| Rank	Std. Error	t value	Pr (>|t|)
(Intercept)	12200.39	NA	41.38	294.83	0.0000
TYP_B_20_50_80	-4182.17	1	51.61	-81.03	0.0000
UD_B_H:TYP_B_20_50_80	-994.86	3	39.01	-25.50	0.0000
TYP_B_20_50_80:WDYP_B_20_50_80	-870.06	4	39.01	-22.30	0.0000
PTC_TBC_E_OUT_W	-790.72	5	53.42	-14.80	0.0000
PTC_TBC_C_OUT_WO	-780.97	6	53.42	-14.62	0.0000
UD_B_H	-763.09	7	47.78	-15.97	0.0000
PTC_TBC_D_MID_W	-441.67	10	53.42	-8.27	0.0000
PTC_TBC_B_MID_WO	-309.52	11	53.42	-5.79	0.0000
PTC_TBC_D_MID_W:TYP_B_20_50_80	171.15	16	61.69	2.77	0.0111
PTC_TBC_C_OUT_WO:TYP_B_20_50_80	192.67	15	61.69	3.12	0.0049
PTC_TBC_E_OUT_W:TYP_B_20_50_80	200.40	14	61.69	3.25	0.0037
PTC_TBC_B_MID_WO:UD_B_H	246.15	13	61.69	3.99	0.0006
PTC_TBC_D_MID_W:UD_B_H	257.85	12	61.69	4.18	0.0004
PTC_TBC_E_OUT_W:UD_B_H	542.32	9	61.69	8.79	0.0000
PTC_TBC_C_OUT_WO:UD_B_H	542.62	8	61.69	8.80	0.0000
WDYP_B_20_50_80	1269.44	2	27.59	46.01	0.0000

Intercept (0) = 12200 kWh/m² area
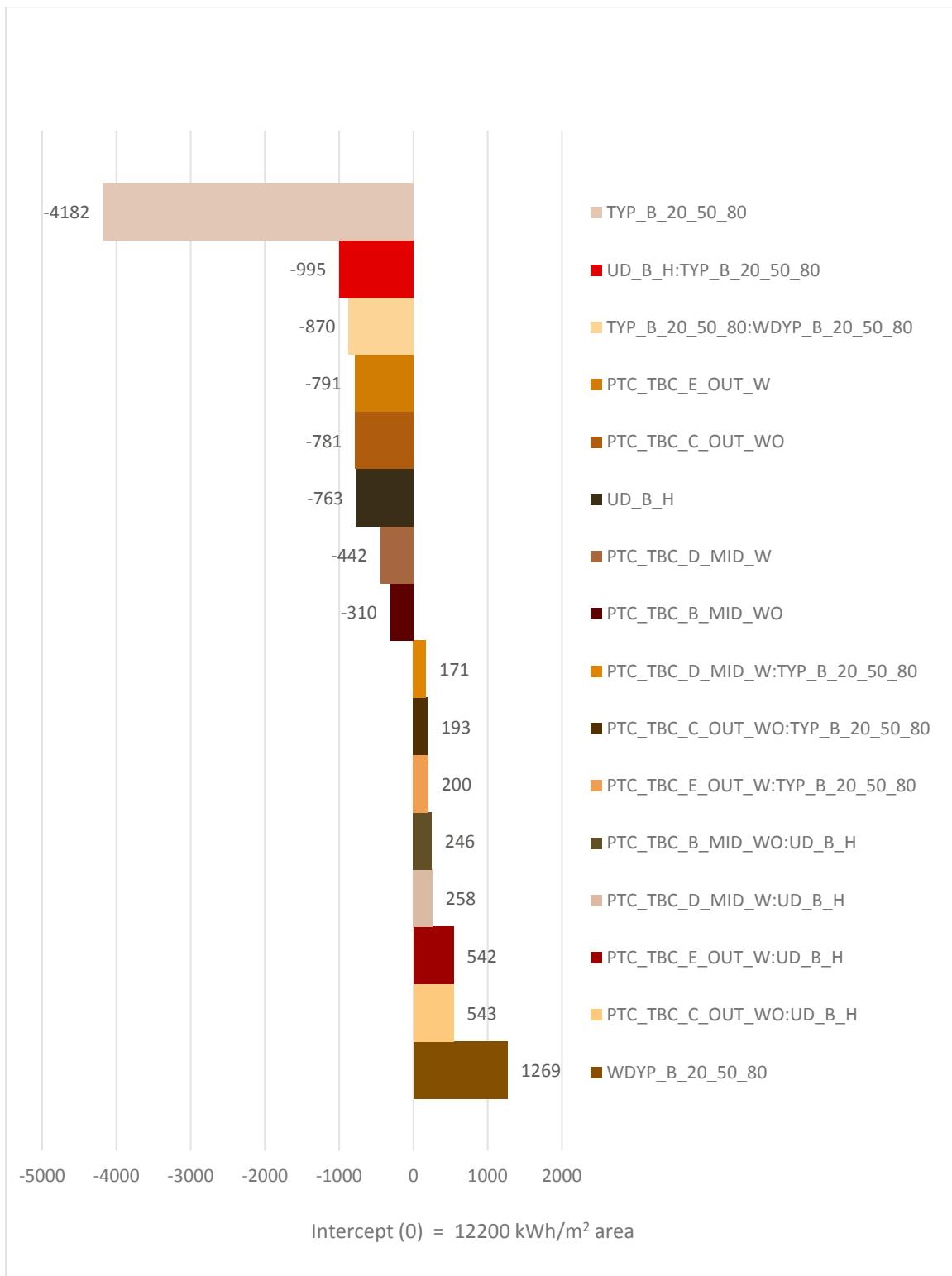
Figure 97. GLM Estimates | Primary Energy (Operational) 2020-2080. Source: the researcher
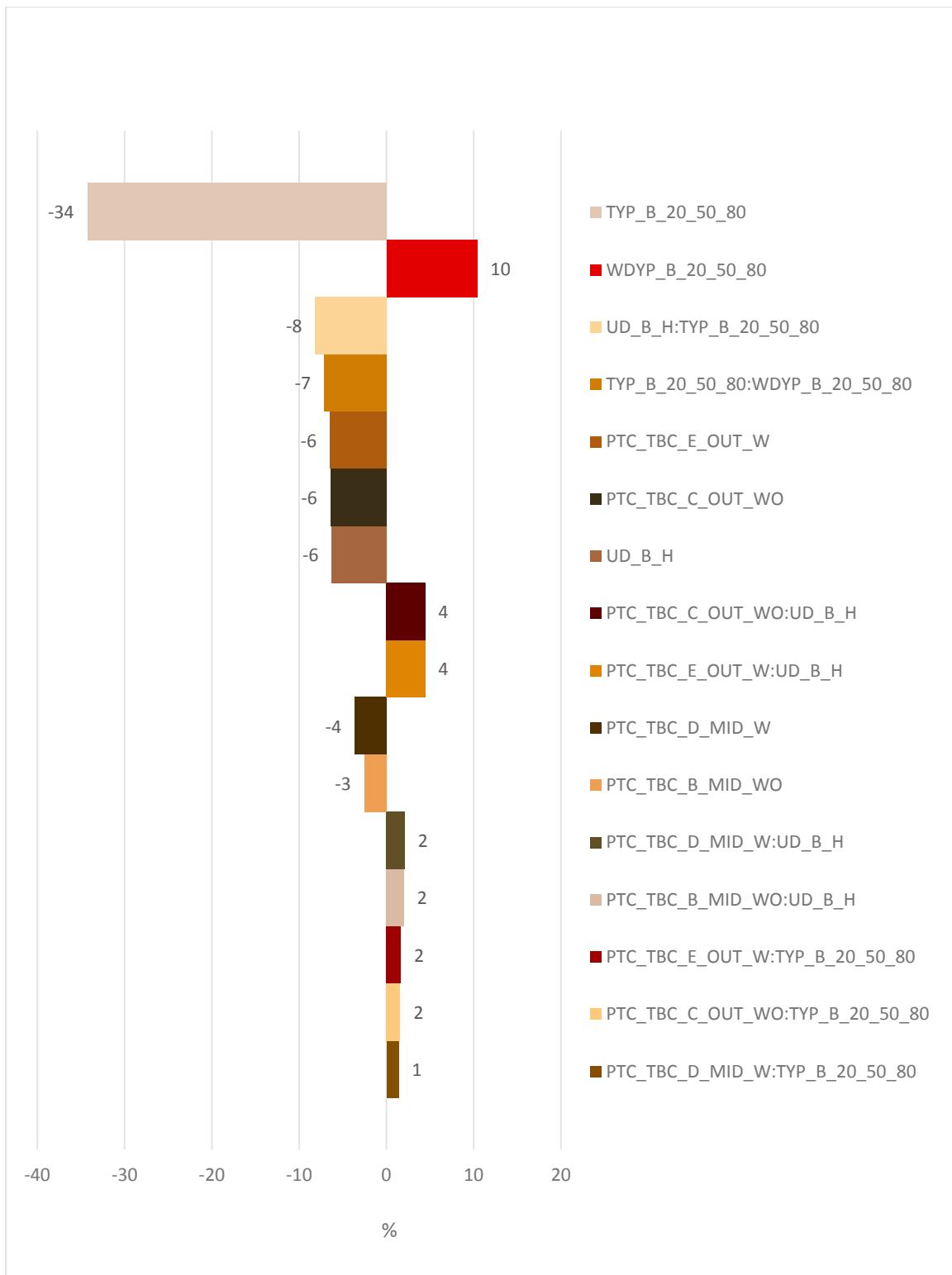
Figure 98. GLM Estimates (sorted by absolute value), in percentage compared with the intercept | Primary Energy (Operational) 2020-2080. Source: the researcher

4.1.8   CO₂ Emissions (Operational) 2020-2080

The utilization of exoskeletons showed desirable main effects resulting in a decrease in CO₂e emissions over a sixty-year operational phase (2020-2080); the effect was -6% for OUTs (whether or not controlling thermal bridges), and it was -4% and -3% in the cases of MIDs with and without controlling thermal bridges respectively. OUTs and MIDs showed undesirable interactions of 4% and 2% with high-density urban contexts. OUTs (whether or not controlling thermal bridges) had an interaction of 2% with the advancement of green technologies, whereas MIDs with controlling thermal bridges showed similar but 1% smaller interaction. High-density urban tissues had a desirable main effect of -6%. Global warming had an undesirable main effect of 11%. The green technological development showed by far the largest main effect as well as the largest desirable effect; that was -66%. These developments also interacted desirably with global warming at the rate of -10%. The baseline indicated 4317 $kgCO_2e/m^2$ area (Table 44, Figure 99, and Figure 100).

Table 44. GLM Simplified Summary | Response Variable: CO₂e Emissions (Operational) 2020-2080 in $kgCO_2e/m^2$ area. Source: the researcher

Coefficients:	Estimate	|Est.| Rank	Std. Error	t value	Pr (>|t|)
(Intercept)	4317.47	NA	15.38	280.76	0.0000
TYP_B_20_50_80	-2848.01	1	19.18	-148.49	0.0000
TYP_B_20_50_80:WDYP_B_20_50_80	-434.39	3	14.50	-29.96	0.0000
PTC_TBC_E_OUT_W	-270.69	4	19.85	-13.64	0.0000
PTC_TBC_C_OUT_WO	-267.15	5	19.85	-13.46	0.0000
UD_B_H	-264.86	6	17.76	-14.92	0.0000
PTC_TBC_D_MID_W	-159.17	9	19.85	-8.02	0.0000
PTC_TBC_B_MID_WO	-111.19	12	19.85	-5.60	0.0000
PTC_TBC_D_MID_W:TYP_B_20_50_80	80.51	15	22.92	3.51	0.0020
PTC_TBC_B_MID_WO:UD_B_H	87.83	14	22.92	3.83	0.0009
PTC_TBC_D_MID_W:UD_B_H	92.36	13	22.92	4.03	0.0006
PTC_TBC_C_OUT_WO:TYP_B_20_50_80	125.03	11	22.92	5.45	0.0000
PTC_TBC_E_OUT_W:TYP_B_20_50_80	127.91	10	22.92	5.58	0.0000
PTC_TBC_E_OUT_W:UD_B_H	165.71	8	22.92	7.23	0.0000
PTC_TBC_C_OUT_WO:UD_B_H	166.05	7	22.92	7.24	0.0000
WDYP_B_20_50_80	456.13	2	10.25	44.49	0.0000
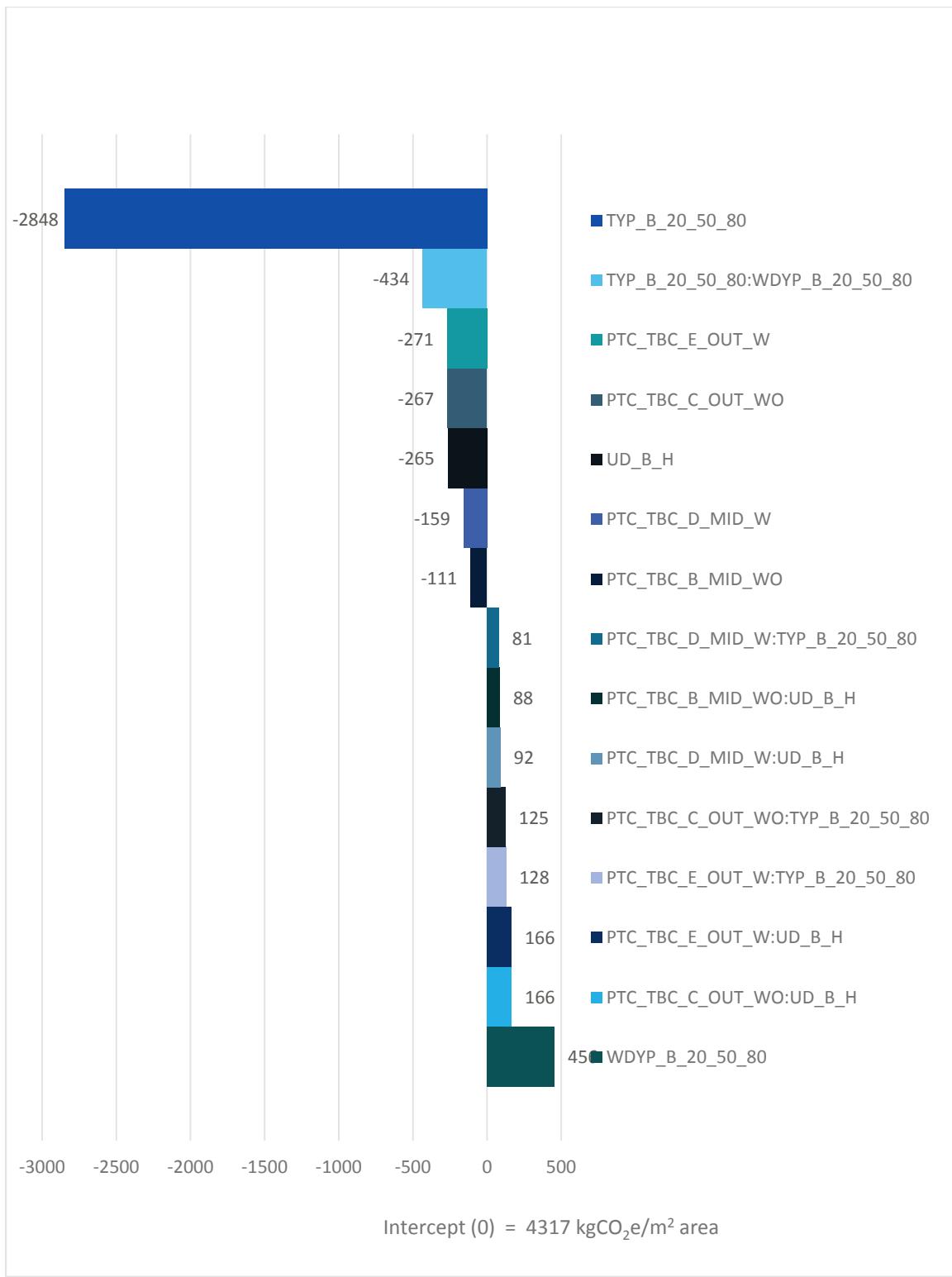
Figure 99. GLM Estimates | CO₂e Emissions (Operational) 2020-2080. Source: the researcher
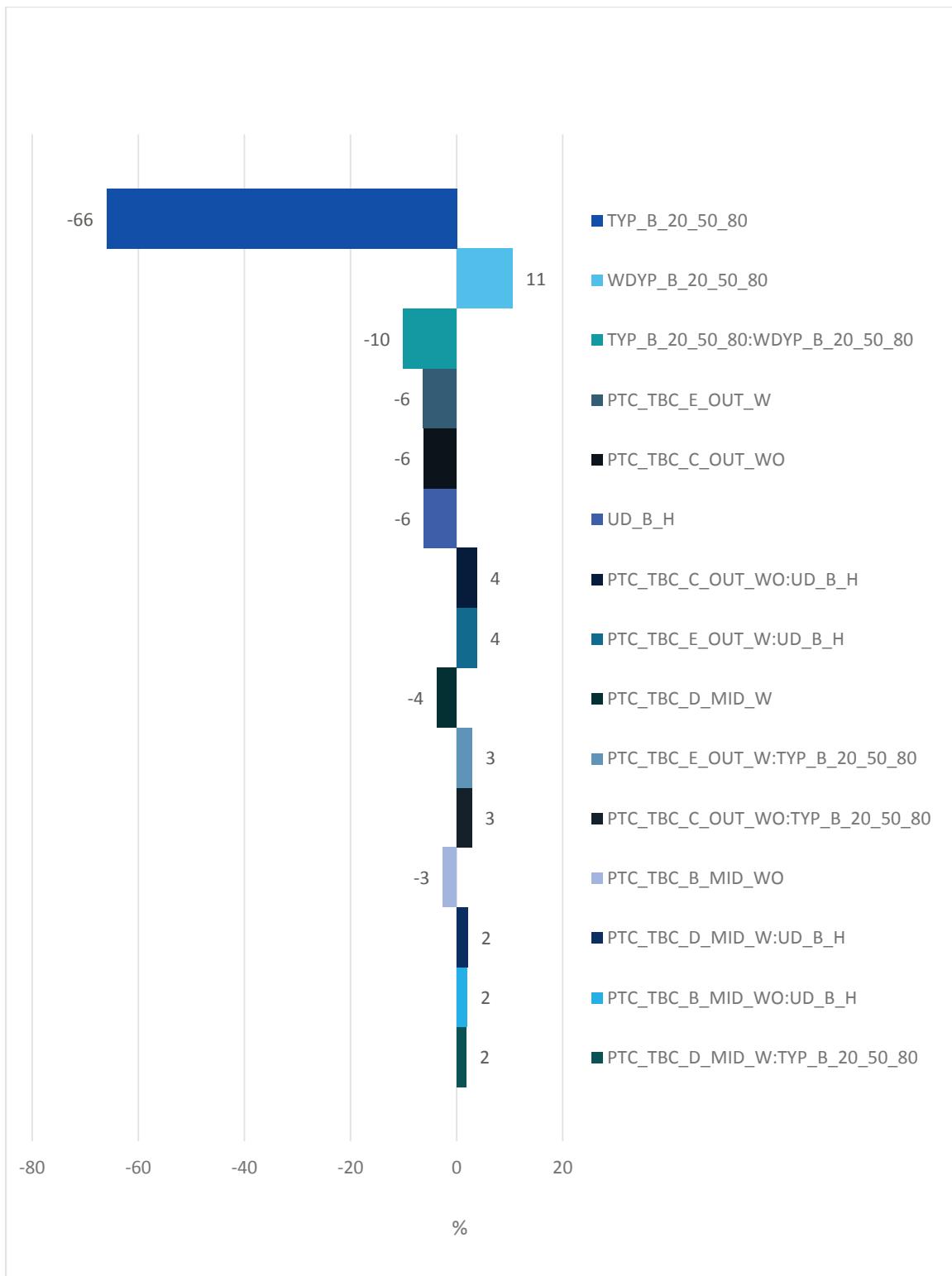
Figure 100. GLM Estimates (sorted by absolute value), in percentage compared with the intercept | CO_2e Emissions (Operational) 2020-2080. Source: the researcher

215

4.1.9   Primary Energy (Embodied + Operational) -2020-2050

Regarding cumulative primary energy consumption as the sum of EE (-2020) and the operational energy consumed during the first thirty years of the operational phase (2020-2050), exoskeletons showed desirable main effects—except for the exoskeletons partly exposed to the environment (MIDs) without controlling thermal bridges; that did not show any statistically significant main effect. From the rest of this group, the larger effect was -3% belonging to the exoskeletons fully exposed to the environment (OUTs) whether or not the thermal bridges were controlled. In the case of MIDs with controlling thermal bridges, the effect was -1%. High density of urban tissue had a desirable main effect of -6% but the desirable effect of exoskeletons reduced in such urban contexts by 4% for OUTs, and 2% for MIDs (these were even larger than their main effects). MIDs with controlling thermal bridges together with OUTs appeared 1% less desirable when interacting with future development of green technologies. Despite that, the technological development had by far the largest main effect and the largest desirable effect; that was -15%. It had also desirable interactions of -2% with Global warming, and -6% in cases in high-density urban context. Global warming showed a 4% undesirable main effect. The baseline indicated 6862 kWh/m^2 area (Table 45, Figure 101, and Figure 102).

Table 45. GLM Simplified Summary | Response Variable: Primary Energy (Embodied + Operational) - 2020-2050 in kWh/m^2 area. Source: the researcher

Coefficients:	Estimate	|Est.| Rank	Std. Error	t value	Pr (>|t|)
(Intercept)	6861.54	NA	2.95	2329.16	0.0000
TYP_B_20_50_80	-1047.04	1	2.14	-488.99	0.0000
UD_B_H:TYP_B_20_50_80	-412.64	2	1.62	-254.93	0.0000
UD_B_H	-398.96	3	2.14	-186.32	0.0000
PTC_TBC_C_OUT_WO	-193.30	7	4.05	-47.77	0.0000
PTC_TBC_E_OUT_W	-188.60	8	4.05	-46.61	0.0000
TYP_B_20_50_80:WDYP_B_20_50_80	-148.67	10	1.62	-91.85	0.0000
PTC_TBC_D_MID_W	-65.98	14	4.05	-16.30	0.0000
CR_D_GGBFS50	-61.39	15	2.56	-23.99	0.0000
PTC_TBC_C_OUT_WO:TYP_B_20_50_80	47.92	18	2.56	18.73	0.0000
PTC_TBC_E_OUT_W:TYP_B_20_50_80	50.36	17	2.56	19.68	0.0000
PTC_TBC_D_MID_W:TYP_B_20_50_80	50.55	16	2.56	19.75	0.0000
PDWPRC	73.40	13	2.22	33.12	0.0000
PTSAU	83.31	12	2.22	37.59	0.0000
PTC_TBC_B_MID_WO:UD_B_H	143.21	11	2.56	55.96	0.0000
PTC_TBC_D_MID_W:UD_B_H	150.22	9	2.56	58.70	0.0000
WDYP_B_20_50_80	276.20	6	2.14	128.99	0.0000
PTC_TBC_E_OUT_W:UD_B_H	300.19	5	2.56	117.29	0.0000
PTC_TBC_C_OUT_WO:UD_B_H	300.22	4	2.56	117.31	0.0000
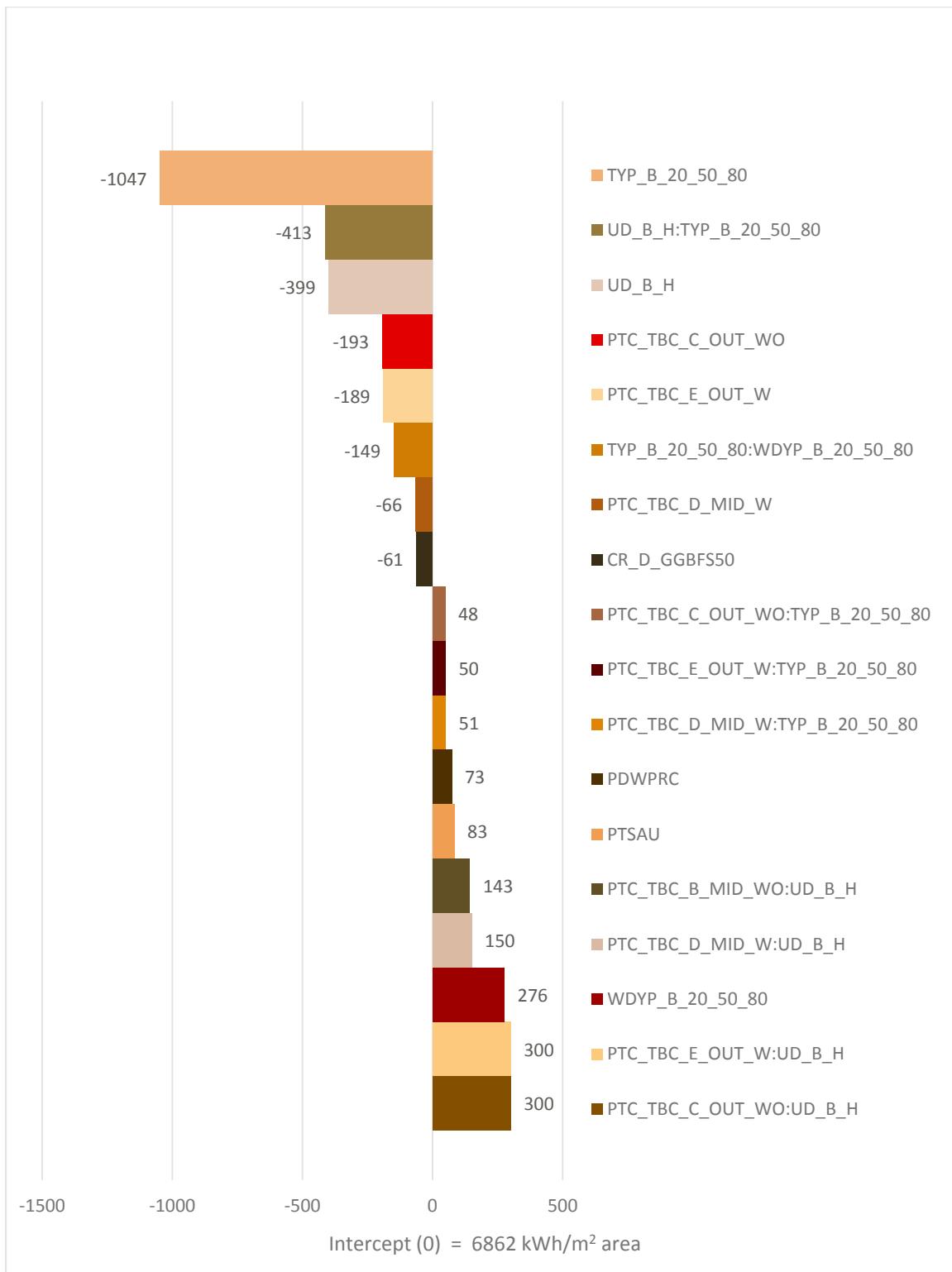
Figure 101. GLM Estimates | Primary Energy (Embodied + Operational) -2020-2050
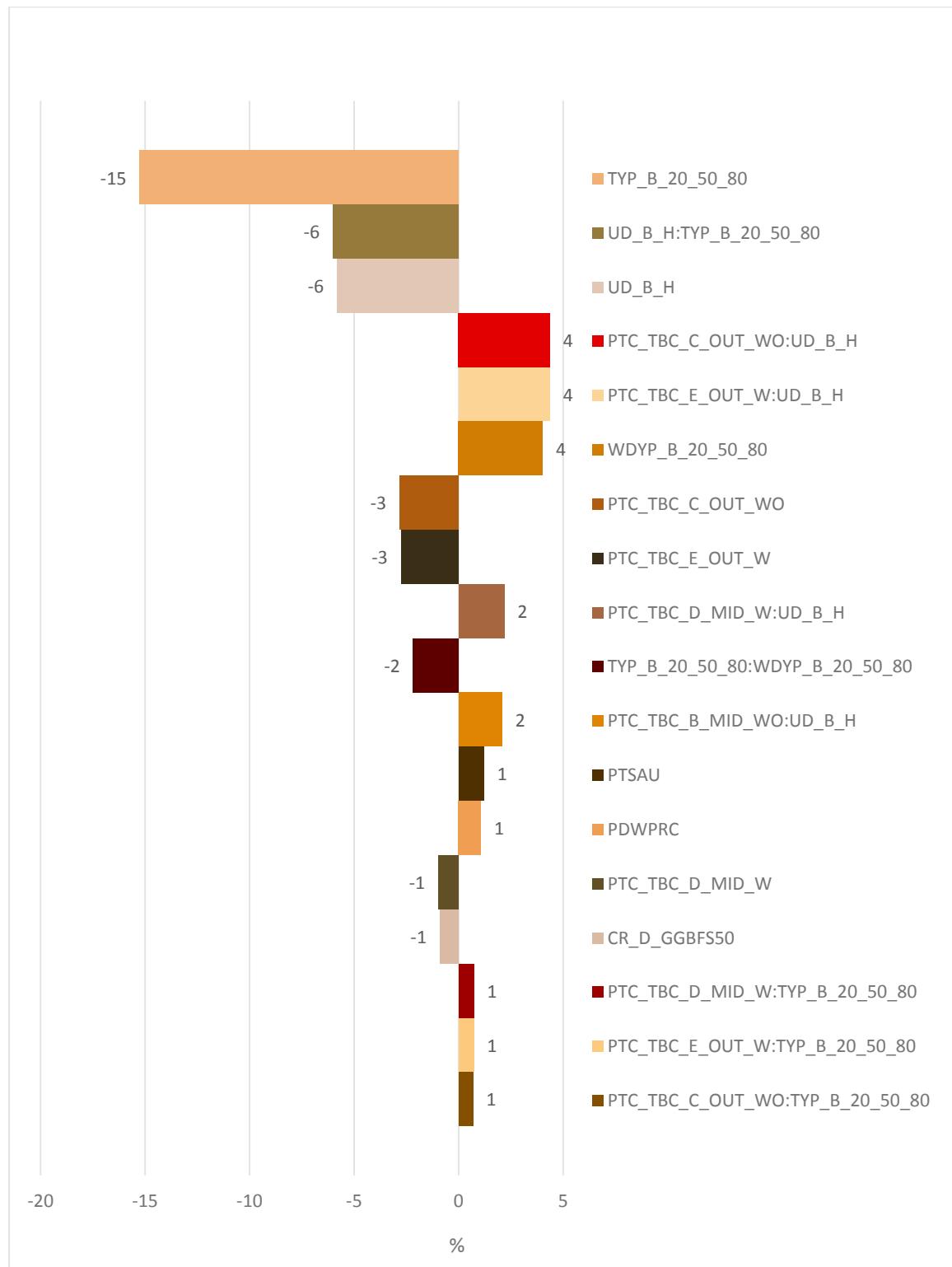
Figure 102. GLM Estimates (sorted by absolute value), in percentage compared with the intercept | Primary Energy (Embodied + Operational) -2020-2050

4.1.10 CO₂e Emissions (Embodied + Operational) -2020-2050

In terms of cumulative CO_2e emissions as the sum of embodied emissions (-2020) and operational emissions during the first thirty years of the operational phase (2020-2050), exoskeletons exhibited desirable main effects—except for the exoskeletons partly exposed to the environment (MIDs) without controlling thermal bridges; that did not show any statistically significant main effect. From the rest of this group, the larger effect was -2% belonging to the exoskeletons fully exposed to the environment (OUTs) whether or not the thermal bridges were controlled. In the case of MIDs with controlling thermal bridges, the effect was -1%. High density of urban tissue had a desirable main effect of -6% but the desirable effect of exoskeletons reduced in such urban contexts by 4% for OUTs, and 2% for MIDs (these were even larger than their main effects). OUTs and MIDs appeared 2% and 1% less desirable when interacting with future development of green technologies. Despite that, the technological development had by far the largest main effect and the largest desirable effect; that was -36%. It had also a desirable interaction of -4% with Global warming. Global warming and high-density urban contexts showed undesirable and desirable main effects of 4% and -6% respectively. CR (50% GGBFS) showed a desirable main effect of -2% as well as desirable interactions of -1% in the cases of OUTs. Long distance transportation of sand had a main effect that increased the emissions by 1%. The baseline indicated 2452 $kgCO_2e/m^2$ area (Table 46, Figure 103, and Figure 104).

Table 46. GLM Simplified Summary | Response Variable: CO_2e Emissions (Embodied + Operational) -2020-2050 in $kgCO_2e/m^2$ area. Source: the researcher

Coefficients:	Estimate	|Est.| Rank	Std. Error	t value	Pr (>|t|)
(Intercept)	2451.69	NA	0.96	2541.32	0.0000
TYP_B_20_50_80	-889.59	1	0.75	-1181.91	0.0000
UD_B_H	-138.62	2	0.70	-198.93	0.0000
TYP_B_20_50_80:WDYP_B_20_50_80	-85.81	6	0.57	-150.83	0.0000
PTC_TBC_E_OUT_W	-60.48	7	1.31	-46.12	0.0000
PTC_TBC_C_OUT_WO	-60.27	8	1.31	-45.96	0.0000
CR_D_GGBFS50	-56.87	9	0.90	-63.21	0.0000
PTC_TBC_D_MID_W	-26.81	14	1.31	-20.44	0.0000
PTC_TBC_E_OUT_W:CR_D_GGBFS50	-14.35	17	1.27	-11.28	0.0000
PTC_TBC_C_OUT_WO:CR_D_GGBFS50	-14.35	18	1.27	-11.28	0.0000
PTC_TBC_B_MID_WO:TYP_B_20_50_80	14.18	19	0.90	15.76	0.0000
PTSAU	20.46	16	0.78	26.26	0.0000
PTC_TBC_D_MID_W:TYP_B_20_50_80	25.46	15	0.90	28.30	0.0000
PTC_TBC_C_OUT_WO:TYP_B_20_50_80	38.59	13	0.90	42.89	0.0000
PTC_TBC_E_OUT_W:TYP_B_20_50_80	39.49	12	0.90	43.89	0.0000
PTC_TBC_B_MID_WO:UD_B_H	51.15	11	0.90	56.86	0.0000
PTC_TBC_D_MID_W:UD_B_H	53.89	10	0.90	59.90	0.0000
PTC_TBC_E_OUT_W:UD_B_H	96.86	5	0.90	107.67	0.0000
PTC_TBC_C_OUT_WO:UD_B_H	97.01	4	0.90	107.84	0.0000
WDYP_B_20_50_80	97.88	3	0.70	140.47	0.0000
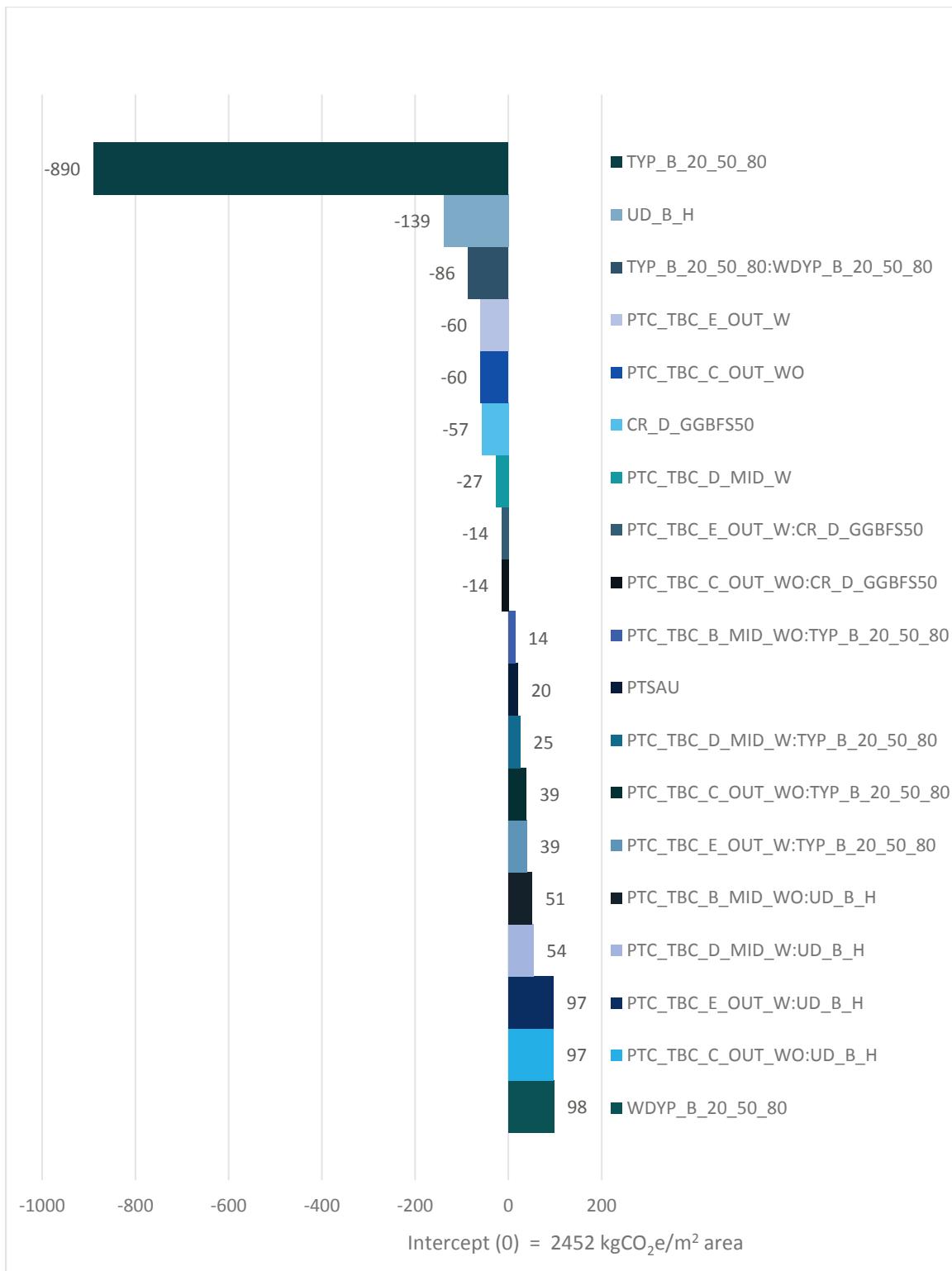
Figure 103. GLM Estimates | CO$_2$e Emissions (Embodied + Operational) -2020-2050. Source: the researcher
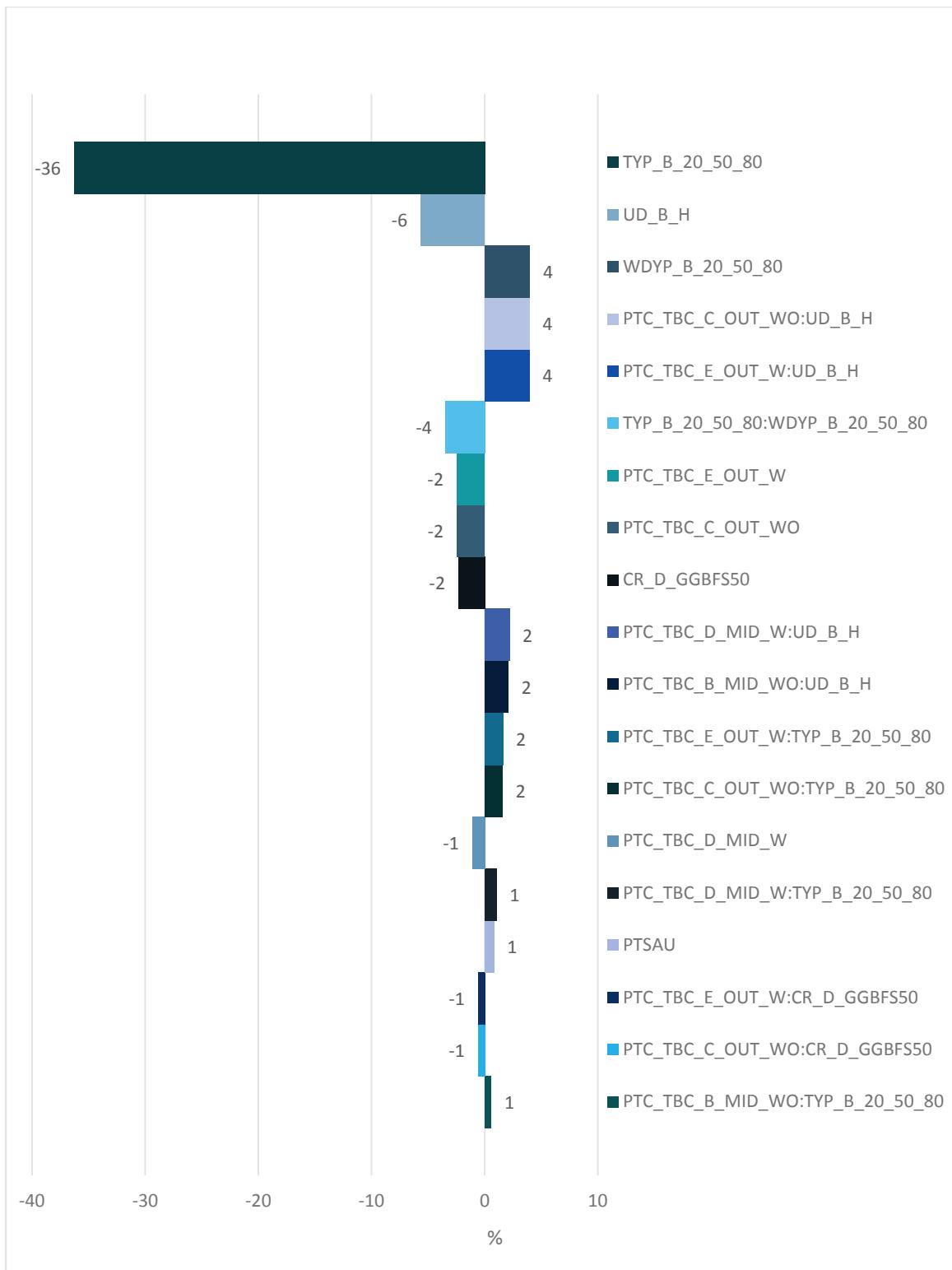
Figure 104. GLM Estimates (sorted by absolute value), in percentage compared with the intercept | CO_2e Emissions (Embodied + Operational) -2020-2050. Source: the researcher

4.1.11 Primary Energy (Embodied + Operational) -2020-2080

All exoskeletons showed desirable main effects on the cumulative primary energy consumption as the sum of the EE (-2020) and the operational energy consumed during sixty years of operational phase (2020-2080). In this group, skeletons fully exposed to the environment (OUTs, whether or not the thermal bridges were controlled) had the largest main effect that was -4%. In the case of skeletons partly exposed to the environment (MIDs) with and without controlling thermal bridges, the effect was -2% and -1% respectively. All exoskeletons showed interactions with high-density urban context; these effects were as large as the aforementioned main effects but undesirable (4%, 4%, 2%, and 1%). They also had undesirable interactions with the green technological developments that was 2% in the case of OUTs with controlling thermal bridges, and 1% in other cases. MIDs with controlling thermal bridges showed a desirable interaction of -1% with global warming. Global warming itself had an undesirable main effect of 10%. Green technological developments had by far the largest main effect and the largest desirable effect; that was -32%. It also showed desirable interactions of -8% with high-density urban contexts, and -7% with global warming. High-density urban context itself had a desirable main effect of -6%. Long distance transportation of sand, and using desalinated water in production of RC had undesirable main effects of 1%. CR (50% GGBFS) showed a desirable main effect of -1%. The baseline indicated 12935 kWh/m^2 area (Table 47, Figure 105, and Figure 106).

Table 47. GLM Simplified Summary | Response Variable: Primary Energy (Embodied + Operational) -2020-2080 in kWh/m^2 area. Source: the researcher

Coefficients:	Estimate	|Est.| Rank	Std. Error	t value	Pr (>|t|)
(Intercept)	12935.12	NA	6.22	2078.01	0.0000
TYP_B_20_50_80	-4182.16	1	6.22	-671.86	0.0000
UD_B_H:TYP_B_20_50_80	-994.86	3	4.71	-211.43	0.0000
TYP_B_20_50_80:WDYP_B_20_50_80	-870.06	4	4.71	-184.90	0.0000
UD_B_H	-763.09	5	5.76	-132.41	0.0000
PTC_TBC_C_OUT_WO	-552.16	6	7.44	-74.22	0.0000
PTC_TBC_E_OUT_W	-552.14	7	7.44	-74.21	0.0000
PTC_TBC_D_MID_W	-247.72	11	7.44	-33.30	0.0000
PTC_TBC_B_MID_WO	-142.28	16	7.44	-19.12	0.0000
CR_D_GGBFS50	-72.17	20	3.33	-21.69	0.0000
PTC_TBC_D_MID_W:WDYP_B_20_50_80	-70.80	21	7.44	-9.52	0.0000
PTC_TBC_B_MID_WO:TYP_B_20_50_80	72.37	19	7.44	9.73	0.0000
PDWPRC	86.35	18	2.88	29.97	0.0000
PTSAU	97.60	17	2.88	33.87	0.0000
PTC_TBC_D_MID_W:TYP_B_20_50_80	171.15	15	7.44	23.00	0.0000
PTC_TBC_C_OUT_WO:TYP_B_20_50_80	192.67	14	7.44	25.90	0.0000
PTC_TBC_E_OUT_W:TYP_B_20_50_80	200.40	13	7.44	26.94	0.0000
PTC_TBC_B_MID_WO:UD_B_H	246.15	12	7.44	33.08	0.0000
PTC_TBC_D_MID_W:UD_B_H	257.85	10	7.44	34.66	0.0000
PTC_TBC_E_OUT_W:UD_B_H	542.32	9	7.44	72.89	0.0000
PTC_TBC_C_OUT_WO:UD_B_H	542.62	8	7.44	72.93	0.0000
WDYP_B_20_50_80	1303.46	2	5.76	226.18	0.0000
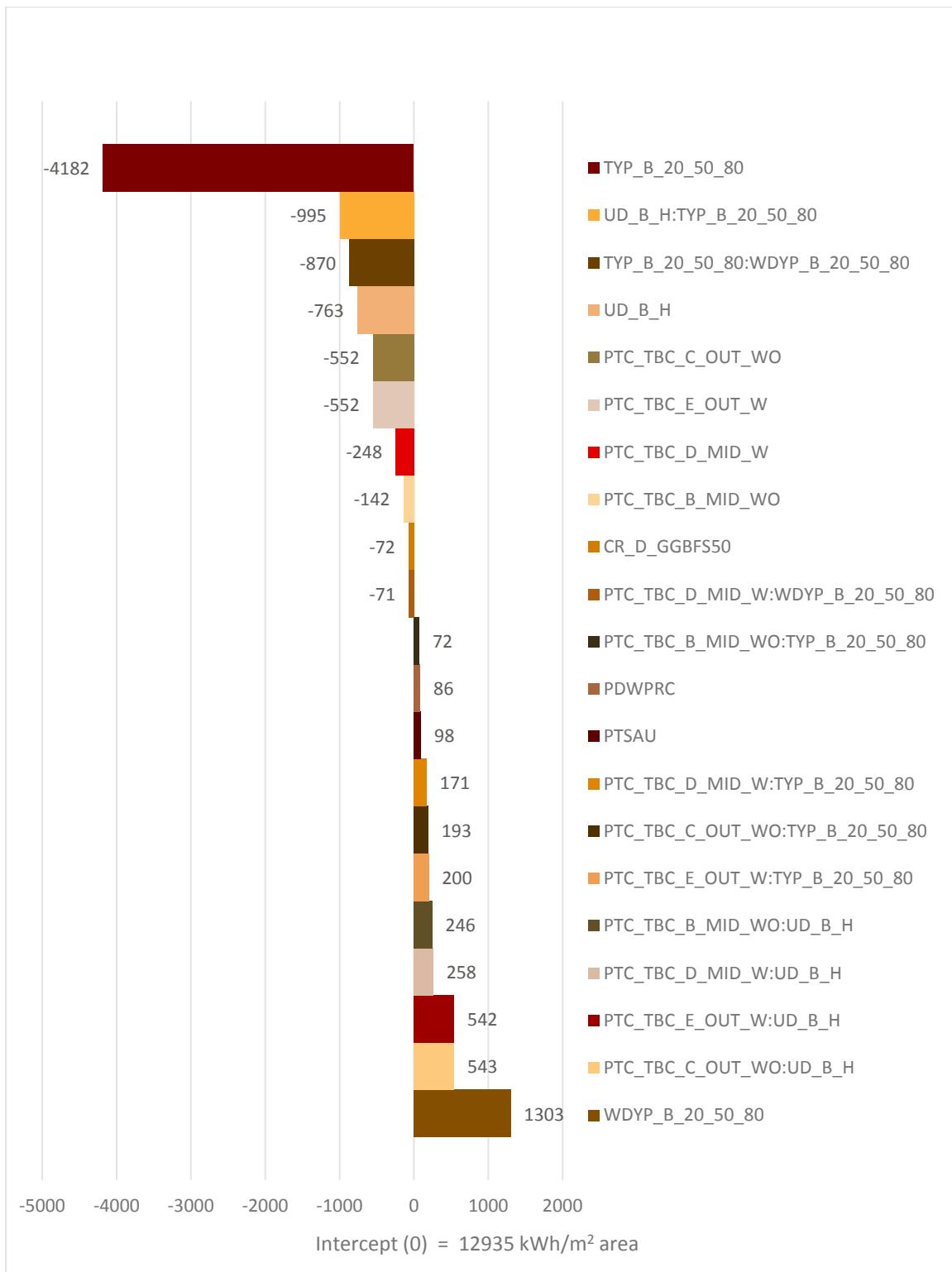
Figure 105. GLM Estimates | Primary Energy (Embodied + Operational) -2020-2080. Source: the researcher
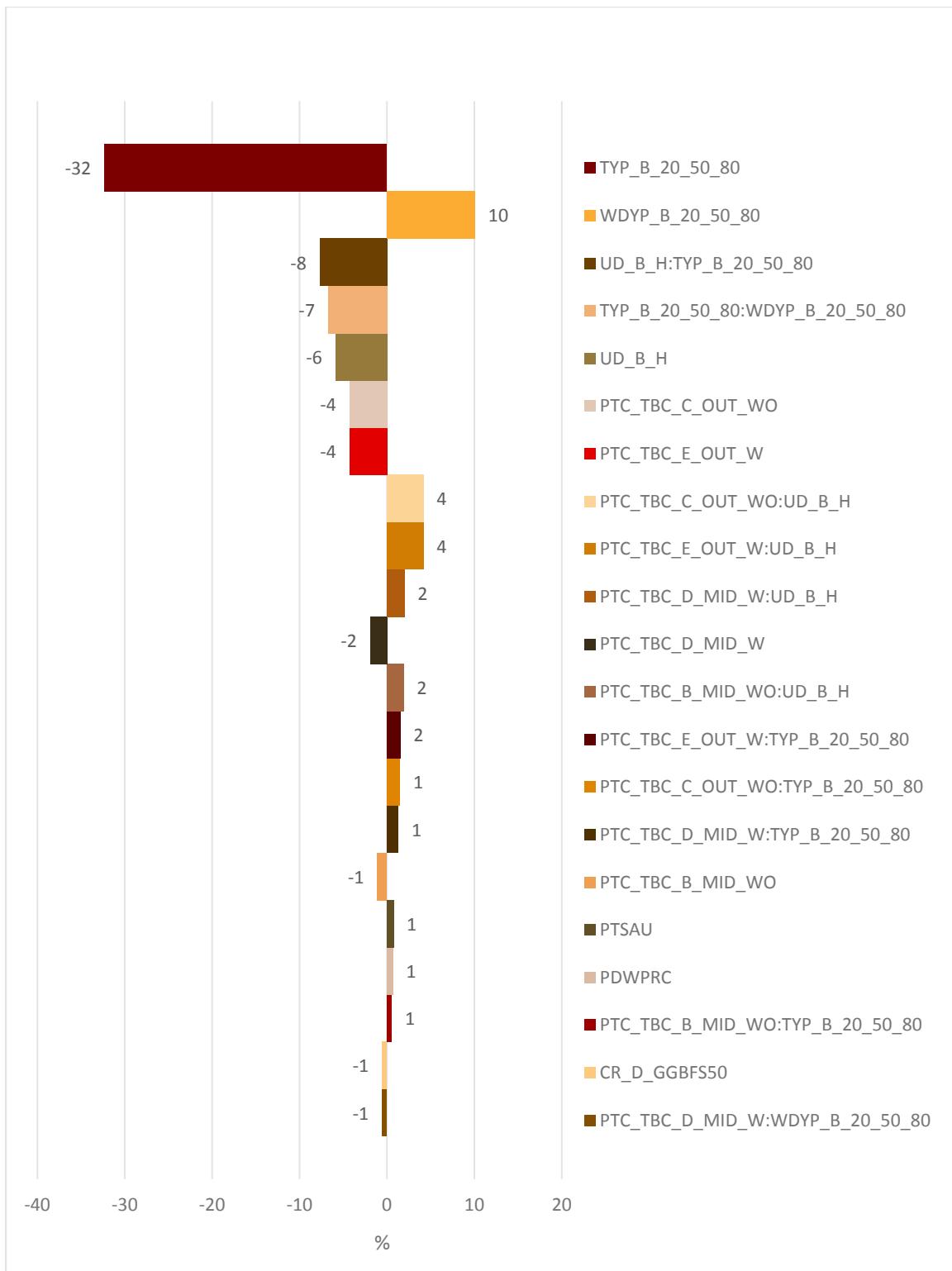
Figure 106. GLM Estimates (sorted by absolute value), in percentage compared with the intercept | Primary Energy (Embodied + Operational) -2020-2080. Source: the researcher

4.1.12   CO₂e Emissions (Embodied + Operational) -2020-2080

With respect to cumulative CO_2e emissions, encompassing both embodied emissions (-2020) and operational emissions over a period of sixty years in the operational phase (2020-2080), all exoskeletons demonstrated desirable main effects. In this group, skeletons fully exposed to the environment (OUTs, whether or not the thermal bridges were controlled) had the largest main effect that was -4%. In the case of skeletons partly exposed to the environment (MIDs) with and without controlling thermal bridges, the effect was -2% and -1% respectively. All exoskeletons showed undesirable interactions with high-density urban context; these effects were 4% for OUTs, and 2% for MIDs. They also had undesirable interactions with the green technological developments that was 3% in the case of OUTs, and 2% and 1% for MIDs with and without controlling thermal bridges. Green technological developments had by far the largest main effect and the largest desirable effect; that was -62%. It also showed desirable interactions of -9% with global warming. Global warming itself had an undesirable main effect of 10%. High-density urban context had a desirable main effect of -6%, and an undesirable interaction of 1% with high-density urban contexts. Long distance transportation of sand had an undesirable main effect of 1%. CR (50% GGBFS) showed a desirable main effect of -1%. The baseline indicated 4608 $kgCO_2e/m^2$ area (Table 48, Figure 107, and Figure 108).

Table 48. GLM Simplified Summary | Response Variable: CO_2e Emissions (Embodied + Operational) -2020-2080 in $kgCO_2e/m^2$ area. Source: the researcher

Coefficients:	Estimate	|Est.| Rank	Std. Error	t value	Pr (>|t|)
(Intercept)	4607.56	NA	2.44	1890.43	0.0000
TYP_B_20_50_80	-2848.01	1	2.39	-1189.19	0.0000
TYP_B_20_50_80:WDYP_B_20_50_80	-434.38	3	1.81	-239.94	0.0000
UD_B_H	-261.82	4	2.39	-109.32	0.0000
PTC_TBC_E_OUT_W	-191.70	5	2.86	-66.97	0.0000
PTC_TBC_C_OUT_WO	-189.77	6	2.86	-66.29	0.0000
PTC_TBC_D_MID_W	-103.70	11	2.86	-36.23	0.0000
CR_D_GGBFS50	-66.66	15	1.28	-52.07	0.0000
PTC_TBC_B_MID_WO	-61.42	16	2.86	-21.46	0.0000
PTSAU	23.97	19	1.11	21.62	0.0000
UD_B_H:TYP_B_20_50_80	29.84	18	1.81	16.48	0.0000
PTC_TBC_B_MID_WO:TYP_B_20_50_80	44.78	17	2.86	15.64	0.0000
PTC_TBC_D_MID_W:TYP_B_20_50_80	80.51	14	2.86	28.13	0.0000
PTC_TBC_B_MID_WO:UD_B_H	87.83	13	2.86	30.68	0.0000
PTC_TBC_D_MID_W:UD_B_H	92.36	12	2.86	32.27	0.0000
PTC_TBC_C_OUT_WO:TYP_B_20_50_80	125.03	10	2.86	43.68	0.0000
PTC_TBC_E_OUT_W:TYP_B_20_50_80	127.91	9	2.86	44.69	0.0000
PTC_TBC_E_OUT_W:UD_B_H	165.71	8	2.86	57.89	0.0000
PTC_TBC_C_OUT_WO:UD_B_H	166.05	7	2.86	58.01	0.0000
WDYP_B_20_50_80	462.97	2	2.39	193.31	0.0000
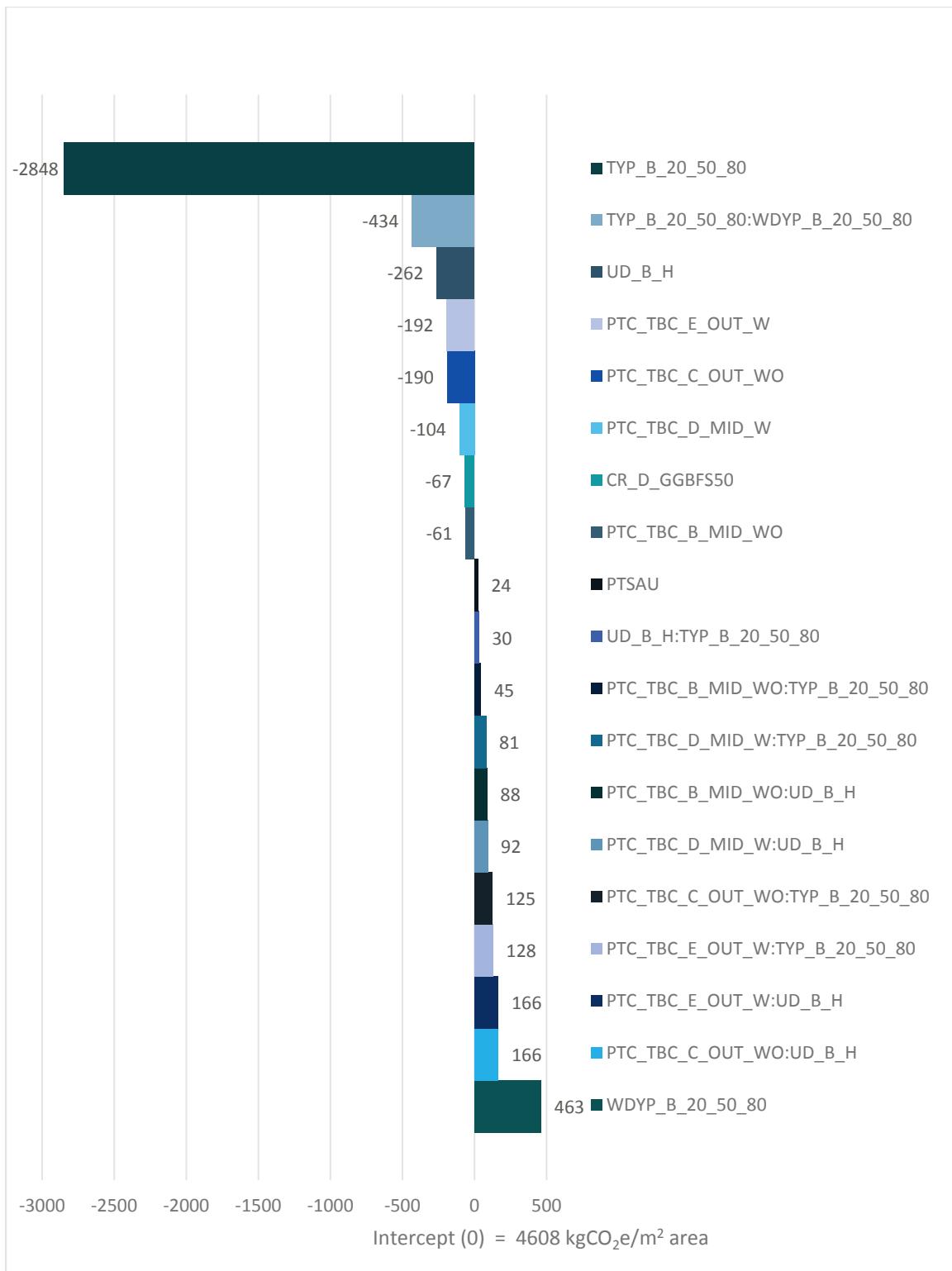
Figure 107. GLM Estimates | CO$_2$e Emissions (Embodied + Operational) -2020-2080. Source: the researcher
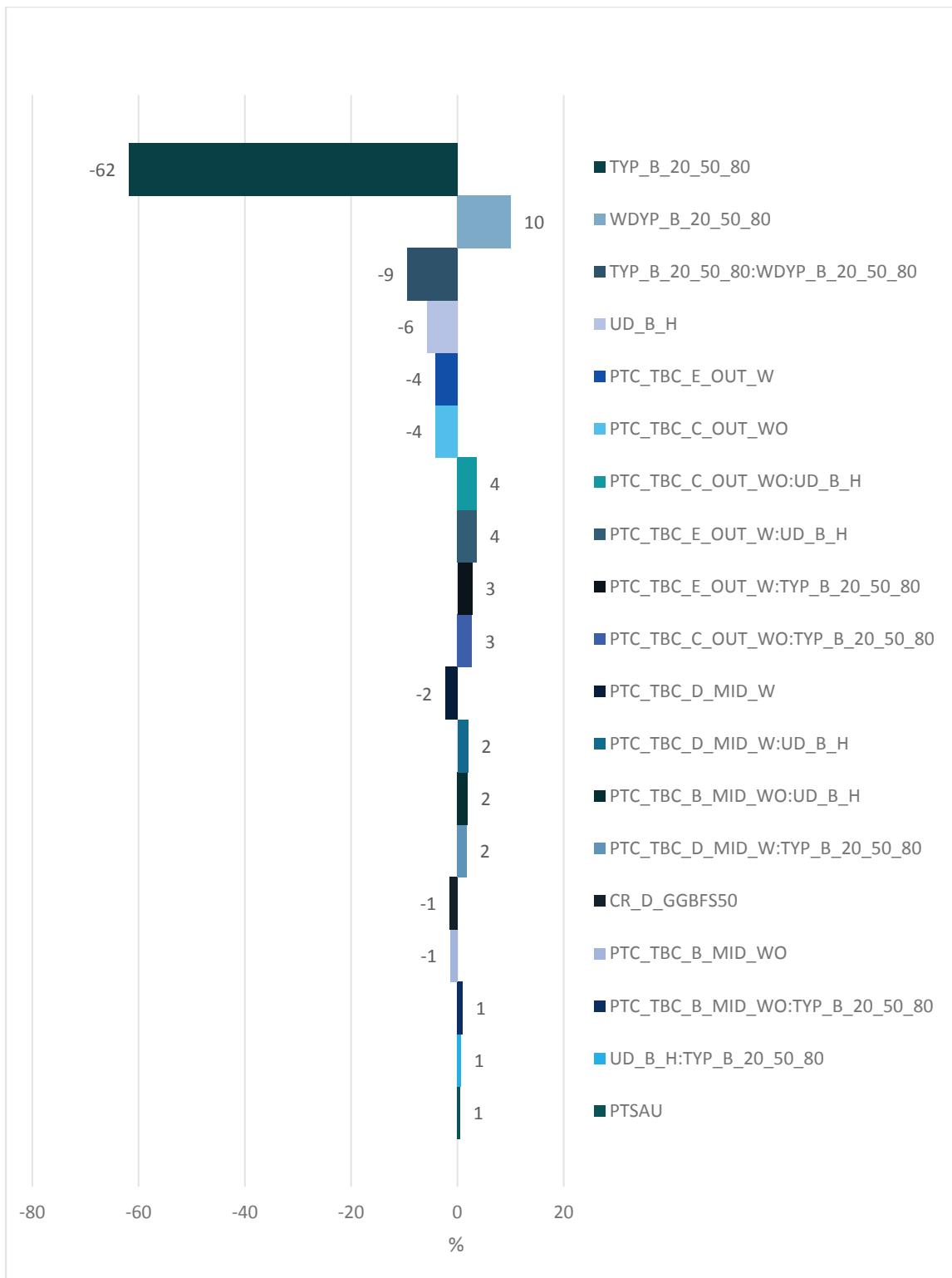
Figure 108. GLM Estimates (sorted by absolute value), in percentage compared with the intercept | CO_2e Emissions (Embodied + Operational) -2020-2080. Source: the researcher

4.2   Results of Decision Analysis

This section includes the results of decision analysis from three viewpoints of maximax criterion, maximin criterion, and minimax regret criterion. As mentioned earlier: (1) **Maximax** Criterion associates with an **optimistic/aggressive** point of view; it ranks the decision alternatives (decision options/controllable parameters—from the perspective of architectural engineers engaged in early stage of design of high-rise buildings) based on their most desirable outcomes (payoffs) in all scenarios (uncontrollable parameters); (2) **Maximin** Criterion represents a **conservative/robust** attitude where first the worst outcome of alternatives in various projected states of nature (scenarios made of combinations of uncontrollable parameters) are found, and then they (the alternatives) are ranked by their best outcomes in the aforementioned worst conditions; (3) **Minimax Regret** Criterion: it is an equivalent to a **cautious** standpoint in decision making where alternatives are first analyzed under each state of nature, the distance of their outcomes from the outcome of the best functioning alternative in that particular state of nature is listed. This distance is called regret (obviously the best functioning alternative has zero regret as it has zero distance to itself). Alternatives are ranked by their maximum corresponding regret with respect to all states of nature. The ones with the minimum of maximum regret get selected as cautious options. All these three decision analyses are suitable for conditions with deep uncertainty where probabilities/likelihoods are unknown.

The results of each criterion is illustrated in a table followed by a graph. Each table has three heat-map columns. Heat-map colors of each column is independent from other columns. First columns indicate the amounts of primary energy or CO_2e emissions prior to operational phase of buildings (short-term). Second and third columns indicate amounts of primary energy or CO_2e emissions cumulative over time including pre-operational as well as operational phase of 30 years (medium-term) and 60 years (long-term) respectively.

As introduced in earlier chapters, three factors are assumed controllable from the perspective of architectural engineers in early stage of design of tall buildings: PTC (the main factor of interest in the study at hand, that is geometrical placement of outer tube with respect to the curtain wall), TBC (thermal bridge control), and CR.

Results for four levels of CR (15% Fly Ash, 30% Fly Ash, 25% GGBFS, and 50% GGBFS) are listed in heat-map tables. For the sake of simplicity, graphs show extreme levels (15% Fly Ash, and 50% GGBFS). Numbers in tables are in functional units. Numbers in graphs are in percentage (with no decimals) relative to the best outcome in each analysis. -100% indicates the best outcome (minus sign is because of undesirability of primary energy consumption as well as CO_2e emissions). The tables are more complete while the graphs are more simplified to make comparisons more comprehendible in a glance. Both tables and graphs show the best outcomes respecting the decision option. Other outcomes, and scenarios corresponding to the decision options are not listed in the tables and graphs here (extended calculation procedures and datasets including all scenarios are available in XLSX files: MAXIMAX_18.xlsx, MAXIMIN_06.xlsx, and MINIMAX_REGRET_37.xlsx).

Die approbierte gedruckte Originalversion dieser Dissertation ist an der TU Wien Bibliothek verfügbar.
The approved original version of this doctoral thesis is available in print at TU Wien Bibliothek.

TU Bibliothek
Your knowledge hub
WIEN

Similar to the Results of GLM Analysis, results for each criterion is reported in 2 (paired) parts: one for Primary Energy, followed by another one for CO_2e Emissions. In most cases the list of factors/levels and their order of magnitude were alike and only numbers were different. Identical textual compositions and statements are used in both parts of each pair of reports wherever possible in order to make it convenient for the readers if they would like to detect these similarities and differences in the pattern of the texts too.

4.2.1 Maximax Criterion

4.2.1.1 <u>Primary Energy</u>

From the optimistic standpoint (maximax criterion), exoskeletons did not rank the highest in any of the three time-spans; the control group did. Prototypes with skeletons kept inside the curtain walls (INs) ranked first in all time-spans. Exoskeletons fully exposed to the environment (OUTs) had the worst rank in all time-spans. The difference between the best and the worst options in the time-span ending in 2020 (pre-operational), 2050 and 2080 (pre-operational + 30 and 60 years of operation, cumulative over time) were about 39%, 4%, and 2%. However, the best payoffs in 2050 and 2080 were approximately 7.1 and 10.1 times larger than the best payoff in 2020, respectively. Controlling thermal bridges slightly reduced the payoffs of exoskeletons (MIDs and OUTs) in all time-spans. CR (50% GGBFS compared with 15% Fly Ash) improved the payoffs of each option but it showed smaller effect than PTC even in short-term (Table 49).

Table 49. Maximum Payoffs. The Maximum Maximum Payoff **<u>(MaxiMax) in Bold+Underline</u>** | Primary Energy (Embodied + Operational) in kWh/m² area, cumulative over time. Note: color variations in each column are independent. Source: the researcher

PTC_TBC__CR	-2020	-2050	-2080
IN_NA__FA15	-760.56	-5022.96	-7069.71
IN_NA__FA30	-731.11	-4993.51	-7040.26
IN_NA__GGBFS25	-741.94	-5004.34	-7051.09
IN_NA__GGBFS50	**<u>-699.17</u>**	**<u>-4961.57</u>**	**<u>-7045.02</u>**
MID_WO__FA15	-891.67	-5125.42	-7134.37
MID_WO__FA30	-856.94	-5090.69	-7099.64
MID_WO__GGBFS25	-869.72	-5103.47	-7112.42
MID_WO__GGBFS50	-819.17	-5052.92	-7061.87
OUT_WO__FA15	-965.28	-5152.83	-7148.28
OUT_WO__FA30	-928.33	-5115.88	-7111.33
OUT_WO__GGBFS25	-941.67	-5129.22	-7124.67
OUT_WO__GGBFS50	-888.06	-5075.61	-7071.06
MID_W__FA15	-910.28	-5118.98	-7127.93
MID_W__FA30	-875.56	-5084.26	-7093.21
MID_W__GGBFS25	-888.33	-5097.03	-7105.98
MID_W__GGBFS50	-837.78	-5046.48	-7147.54
OUT_W__FA15	**-974.44**	**-5159.74**	**-7155.19**
OUT_W__FA30	-937.5	-5122.8	-7118.25
OUT_W__GGBFS25	-950.83	-5136.13	-7131.58
OUT_W__GGBFS50	-897.22	-5082.52	-7077.97

4.2.1.2   CO₂e Emissions

From the optimistic standpoint (maximax criterion), exoskeletons did not rank the highest in any of the three time-spans; the control group did. Prototypes with skeletons kept inside the curtain walls (INs) ranked first in all time-spans. Exoskeletons fully exposed to the environment (OUTs) had the worst rank in all time-spans. The difference between the best and the worst options in the time-span ending in 2020 (pre-operational), 2050 and 2080 (pre-operational + 30 and 60 years of operation, cumulative over time) were about 58%, 9%, and 8%. However, the best payoffs in 2050 and 2080 were approximately 5.8 and 6.4 times larger than the best payoff in 2020, respectively. Controlling thermal bridges slightly reduced the payoffs of exoskeletons (MIDs and OUTs) in the short-term but it slightly improved it in medium-term and long-term. CR (50% GGBFS compared with 15% Fly Ash) improved the payoffs of each option but it showed smaller effect than PTC even in short-term (Table 50).

Table 50. Maximum Payoffs; The Maximum Maximum Payoff **(MaxiMax) in Bold+Underline** | CO₂e Emissions (Embodied + Operational) in $kgCO_2e/m^2$ area, cumulative over time. Note: color variations in each column are independent. Source: the researcher

PTC_TBC__CR	-2020	-2050	-2080
IN_NA__FA15	-291.95	-1426.7	-1554.05
IN_NA__FA30	-273.64	-1408.39	-1535.74
IN_NA__GGBFS25	-271.71	-1406.46	-1533.81
IN_NA__GGBFS50	**-235.09**	**-1369.84**	**-1497.19**
MID_WO__FA15	-342.76	-1474.21	-1599.16
MID_WO__FA30	-321.18	-1452.63	-1577.58
MID_WO__GGBFS25	-318.91	-1450.36	-1575.31
MID_WO__GGBFS50	-275.77	-1407.22	-1532.17
OUT_WO__FA15	-368.99	-1486.34	-1610.39
OUT_WO__FA30	-346.05	-1463.4	-1587.45
OUT_WO__GGBFS25	-343.64	-1460.99	-1585.04
OUT_WO__GGBFS50	-297.77	-1415.12	-1539.17
MID_W__FA15	-345.55	-1468	-1592.95
MID_W__FA30	-323.98	-1446.43	-1571.38
MID_W__GGBFS25	-321.71	-1444.16	-1569.11
MID_W__GGBFS50	-278.56	-1401.01	-1525.96
OUT_W__FA15	**-370.39**	**-1486.84**	**-1610.89**
OUT_W__FA30	-347.45	-1463.9	-1587.95
OUT_W__GGBFS25	-345.04	-1461.49	-1585.54
OUT_W__GGBFS50	-299.17	-1415.62	-1539.67

4.2.2   Maximin Criterion

4.2.2.1   Primary Energy

In the short-term (pre-operational time-span: -2020), the control group (INs) ranked first as the most conservative/robust option group followed by the exoskeletons partly exposed to the environment (MIDs) and the exoskeletons fully exposed to the environment (OUTs). The main variable of interest (PTC) was more influential than CR (using 50% GGBFS compared to 15% Fly Ash). Controlling the thermal bridges reduced the payoffs very slightly (about 1-2%). The difference between the best and the worst option in the short-term was 37%. Medium-term and long-term results (both cumulative over time) were in contrast with the short-term ones; exoskeletons (OUTs followed by MIDs) showed better payoffs than the control group (INs). Controlling thermal bridges slightly improved the payoffs of the options incorporating the MID exoskeletons by about 1% but ineffective for OUTs. The effect of CR (using 50% GGBFS compared with 15% Fly Ash) remained desirable but its relative magnitude reduced over time. The difference between the best and the worst options in the medium-term and long-term were about 4% and 5%. However, the best payoffs in 2050 and 2080 were approximately 8.2 and 16.1 times larger than the best payoff in 2020, respectively (Table 51).

Table 51. Minimum Payoffs; The Maximum Minimum Payoff **(MaxiMin) in Bold+Underline** | Primary Energy (Embodied + Operational) in kWh/m^2 area, cumulative over time. Note: color variations in each column are independent. Source: the researcher

PTC_TBC__CR	-2020	-2050	-2080
IN_NA__FA15	-917.26	**-7315.36**	**-14478.2**
IN_NA__FA30	-887.81	-7285.91	-14448.7
IN_NA__GGBFS25	-898.65	-7296.75	-14459.6
IN_NA__GGBFS50	**-855.87**	-7253.97	-14416.8
MID_WO__FA15	-1075.9	-7283.8	-14250.4
MID_WO__FA30	-1041.17	-7249.07	-14215.7
MID_WO__GGBFS25	-1053.95	-7261.85	-14228.5
MID_WO__GGBFS50	-1003.4	-7211.3	-14177.9
OUT_WO__FA15	-1162.58	-7131.38	-13832.5
OUT_WO__FA30	-1125.64	-7094.44	-13795.5
OUT_WO__GGBFS25	-1138.97	-7107.77	-13808.9
OUT_WO__GGBFS50	-1085.36	**-7054.16**	**-13755.3**
MID_W__FA15	-1094.51	-7235.96	-14118
MID_W__FA30	-1059.78	-7201.23	-14083.2
MID_W__GGBFS25	-1072.56	-7214.01	-14096
MID_W__GGBFS50	-1022.01	-7163.46	-14045.5
OUT_W__FA15	**-1171.75**	-7135.45	-13830.7
OUT_W__FA30	-1134.8	-7098.5	-13793.8
OUT_W__GGBFS25	-1148.14	-7111.84	-13807.1
OUT_W__GGBFS50	-1094.52	-7058.22	-13753.5

4.2.2.2 CO_2e Emissions

In the short-term (pre-operational time-span: -2020), the control group (INs) ranked first as the most conservative/robust option group followed by the exoskeletons partly exposed to the environment (MIDs) and the exoskeletons fully exposed to the environment (OUTs). The main variable of interest (PTC) was more influential than CR (using 50% GGBFS compared to 15% Fly Ash). Controlling the thermal bridges reduced the payoffs very slightly (about 1%). The difference between the best and the worst option in the short-term was 54%. Medium-term and long-term results (both cumulative over time) were in contrast with the short-term ones; exoskeletons (OUTs followed by MIDs) showed better payoffs than the control group (INs). Controlling thermal bridges slightly improved the payoffs of the options incorporating the exoskeletons by about 1%. The effect of CR (using 50% GGBFS compared with 15% Fly Ash) remained desirable but its relative magnitude reduced over time. The difference between the best and the worst options in the medium-term and long-term were about 6%. However, the best payoffs in 2050 and 2080 were approximately 9.3 and 18.2 times larger than the best payoff in 2020, respectively (Table 52).

Table 52. Minimum Payoffs; The Maximum Minimum Payoff **(MaxiMin) in Bold+Underline** | CO_2e Emissions (Embodied + Operational) in $kgCO_2e/m^2$ area, cumulative over time. Note: color variations in each column are independent. Source: the researcher

PTC_TBC__CR	-2020	-2050	-2080
IN_NA__FA15	-321.51	-2590.41	-5133.66
IN_NA__FA30	-303.19	-2572.09	-5115.34
IN_NA__GGBFS25	-301.27	-2570.17	-5113.42
IN_NA__GGBFS50	**_-264.64_**	-2533.54	-5076.79
MID_WO__FA15	-377.53	-2578.03	-5050.78
MID_WO__FA30	-355.96	-2556.46	-5029.21
MID_WO__GGBFS25	-353.69	-2554.19	-5026.94
MID_WO__GGBFS50	-310.54	-2511.04	-4983.79
OUT_WO__FA15	-406.11	-2520.06	-4896.81
OUT_WO__FA30	-383.17	-2497.12	-4873.87
OUT_WO__GGBFS25	-380.76	-2494.71	-4871.46
OUT_WO__GGBFS50	-334.89	-2448.84	-4825.59
MID_W__FA15	-380.32	-2556.67	-4998.82
MID_W__FA30	-358.75	-2535.1	-4977.25
MID_W__GGBFS25	-356.48	-2532.83	-4974.98
MID_W__GGBFS50	-313.34	-2489.69	-4931.84
OUT_W__FA15	**-407.51**	-2519.66	-4894.31
OUT_W__FA30	-384.57	-2496.72	-4871.37
OUT_W__GGBFS25	-382.16	-2494.31	-4868.96
OUT_W__GGBFS50	-336.29	**_-2448.44_**	**_-4823.09_**

4.2.3 Minimax Regret Criterion

4.2.3.1 <u>Primary Energy</u>

The control group (INs) had the minimum of maximum regret merely in the short-term. In the medium-term and long-term the exoskeletons were top ranked as the cautious decisions; the best choice was OUTs followed by MIDs. CR (using 50% GGBFS compared with 15% Fly Ash) appeared effective in all time-spans and improved the results for all groups but was not as effective as the main variable of interest (PTC; i.e., IN, MID, OUT levels) in the short-term and the long-term. Controlling thermal bridges increased the maximum regrets very slightly for OUTs in all time-spans as well as MIDs in the short-term, but it improved the results of MIDs in medium-term and especially in the long-term; in the long-term it was almost as effective as the CR. The difference between the best and the worst option in the short-term, medium-term and long-term was approx. 316, 147, and 662 kWh/m^2 area respectively. Minimum of maximum regret (minimax regret) in the short-term, medium-term and long-term was approx. 0 (IN), 155 (OUT), and 103 (OUT) kWh/m^2 area. Exoskeletons became more and more desirable in the long run (Table 53, and Figure 109).

Table 53. Maximum Regret; The Minimum Maximum Regret **(MiniMax Regret) in Bold+Underline** | Primary Energy (Embodied + Operational) in kWh/m^2 area, cumulative over time. Note: color variations in each column are independent. Source: the researcher

PTC_TBC__CR	-2020	-2050	-2080
IN_NA__FA15	61.39	**301.8**	**765.29**
IN_NA__FA30	31.95	272.35	735.84
IN_NA__GGBFS25	42.78	283.18	746.67
IN_NA__GGBFS50	**<u>0</u>**	240.41	703.9
MID_WO__FA15	220.03	255.91	510
MID_WO__FA30	185.3	221.18	475.27
MID_WO__GGBFS25	198.08	233.96	488.05
MID_WO__GGBFS50	147.53	183.41	437.5
OUT_WO__FA15	306.71	231.86	180.56
OUT_WO__FA30	269.77	194.92	143.62
OUT_WO__GGBFS25	283.1	208.25	156.95
OUT_WO__GGBFS50	229.49	**<u>154.64</u>**	103.34
MID_W__FA15	238.64	244.52	448.07
MID_W__FA30	203.91	209.8	413.35
MID_W__GGBFS25	216.69	222.57	426.12
MID_W__GGBFS50	166.14	172.02	375.57
OUT_W__FA15	**315.88**	238.78	187.48
OUT_W__FA30	278.93	201.83	150.53
OUT_W__GGBFS25	292.27	215.17	163.87
OUT_W__GGBFS50	238.65	161.55	**<u>110.25</u>**

	-2020	-2050	-2080
IN_NA__FA15	61.39	301.8	765.29
IN_NA__GGBFS50	0	240.41	703.9
MID_WO__FA15	220.03	255.91	510
MID_WO__GGBFS50	147.53	183.41	437.5
OUT_WO__FA15	306.71	231.86	180.56
OUT_WO__GGBFS50	229.49	154.64	103.34
MID_W__FA15	238.64	244.52	448.07
MID_W__GGBFS50	166.14	172.02	375.57
OUT_W__FA15	315.88	238.78	187.48
OUT_W__GGBFS50	238.65	161.55	110.25
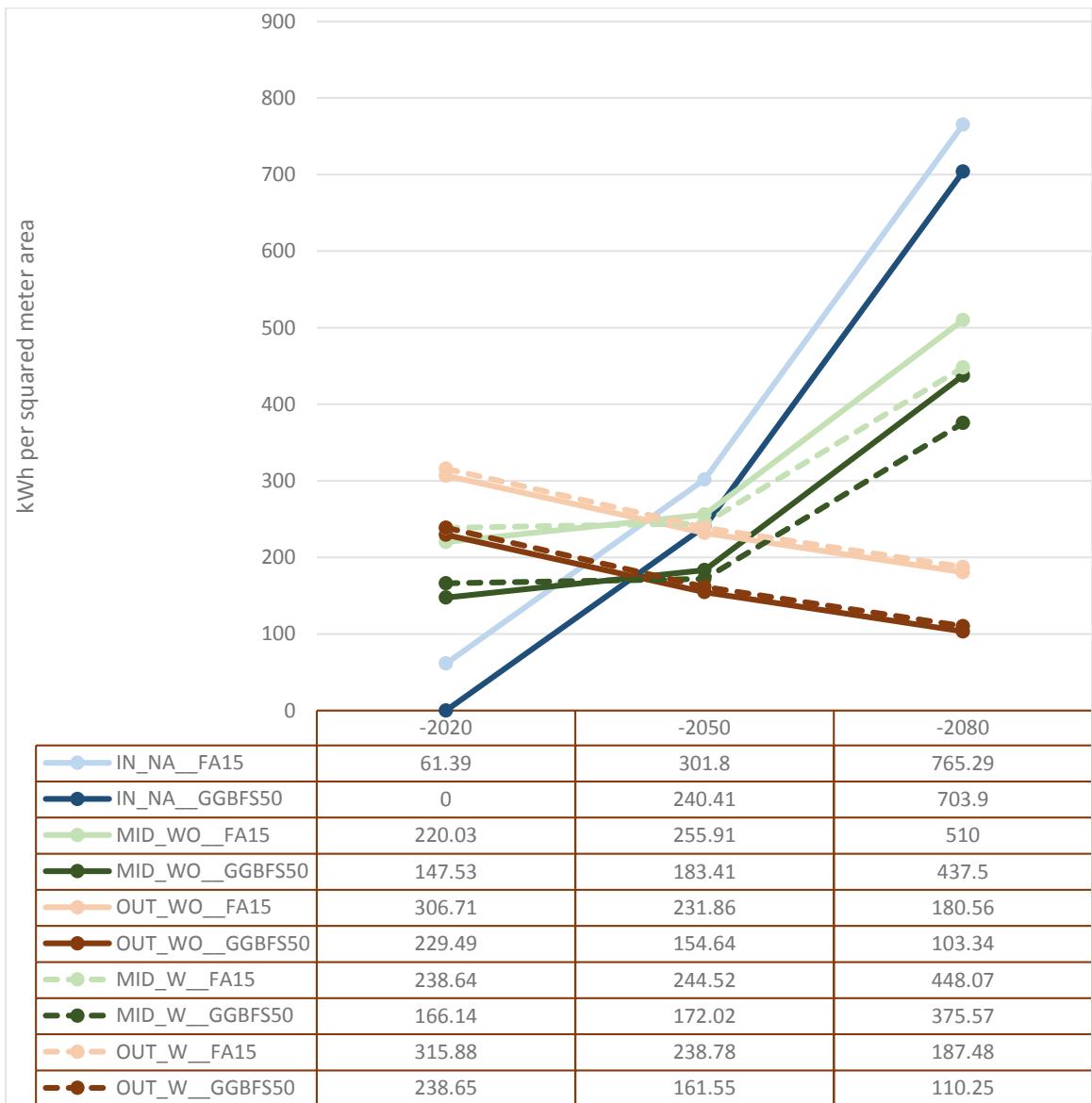
Figure 109. Maximum Regret | Primary Energy (Embodied + Operational), cumulative over time.
Source: the researcher

235

4.2.3.2   CO$_2$e Emissions

The control group (INs) had the minimum of maximum regret merely in the short-term. In the medium-term and long-term the exoskeletons were top ranked as the cautious decisions; the best choice was OUTs followed by MIDs. CR (using 50% GGBFS compared with 15% Fly Ash) appeared effective in all time-spans and improved the results for all groups but was not as effective as the main variable of interest (PTC; i.e., IN, MID, OUT levels) in the short-term and the long-term. Controlling thermal bridges increased the maximum regrets very slightly for OUTs in all time-spans as well as MIDs in the short-term, but it improved the results of MIDs in medium-term and especially in the long-term; in the long-term it was almost as effective as the CR. The difference between the best and the worst option in the short-term, medium-term and long-term was approx. 143, 106, and 269 kgCO$_2$e/m^2 area respectively. Minimum of maximum regret (minimax regret) in the short-term, medium-term and long-term was approx. 0 (IN), 44 (MID_W), and 50 (OUT) kgCO$_2$e/m^2 area. Exoskeletons became more and more desirable in the long run (Table 54, and Figure 110).

Table 54. Maximum Regret; The Minimum Maximum Regret **(MiniMax Regret) in Bold+Underline** | CO$_2$e Emissions (Embodied + Operational) in kgCO$_2$e/m^2 area, cumulative over time. Note: color variations in each column are independent. Source: the researcher

PTC_TBC__CR	-2020	-2050	-2080
IN_NA__FA15	56.87	**149.53**	**318.13**
IN_NA__FA30	38.56	131.22	299.82
IN_NA__GGBFS25	36.63	129.29	297.89
IN_NA__GGBFS50	**0**	92.67	261.27
MID_WO__FA15	112.89	131.94	230.04
MID_WO__FA30	91.32	110.36	208.46
MID_WO__GGBFS25	89.05	108.09	206.19
MID_WO__GGBFS50	45.9	64.95	163.05
OUT_WO__FA15	141.47	124.07	120.77
OUT_WO__FA30	118.53	101.13	97.83
OUT_WO__GGBFS25	116.12	98.72	95.42
OUT_WO__GGBFS50	70.25	52.85	**49.55**
MID_W__FA15	115.68	110.58	178.08
MID_W__FA30	94.11	89.01	156.51
MID_W__GGBFS25	91.84	86.74	154.24
MID_W__GGBFS50	48.7	**43.59**	111.09
OUT_W__FA15	**142.87**	124.57	121.27
OUT_W__FA30	119.93	101.63	98.33
OUT_W__GGBFS25	117.52	99.22	95.92
OUT_W__GGBFS50	71.65	53.35	50.05

	-2020	-2050	-2080
IN_NA__FA15	56.87	149.53	318.13
IN_NA__GGBFS50	0	92.67	261.27
MID_WO__FA15	112.89	131.94	230.04
MID_WO__GGBFS50	45.9	64.95	163.05
OUT_WO__FA15	141.47	124.07	120.77
OUT_WO__GGBFS50	70.25	52.85	49.55
MID_W__FA15	115.68	110.58	178.08
MID_W__GGBFS50	48.7	43.59	111.09
OUT_W__FA15	142.87	124.57	121.27
OUT_W__GGBFS50	71.65	53.35	50.05
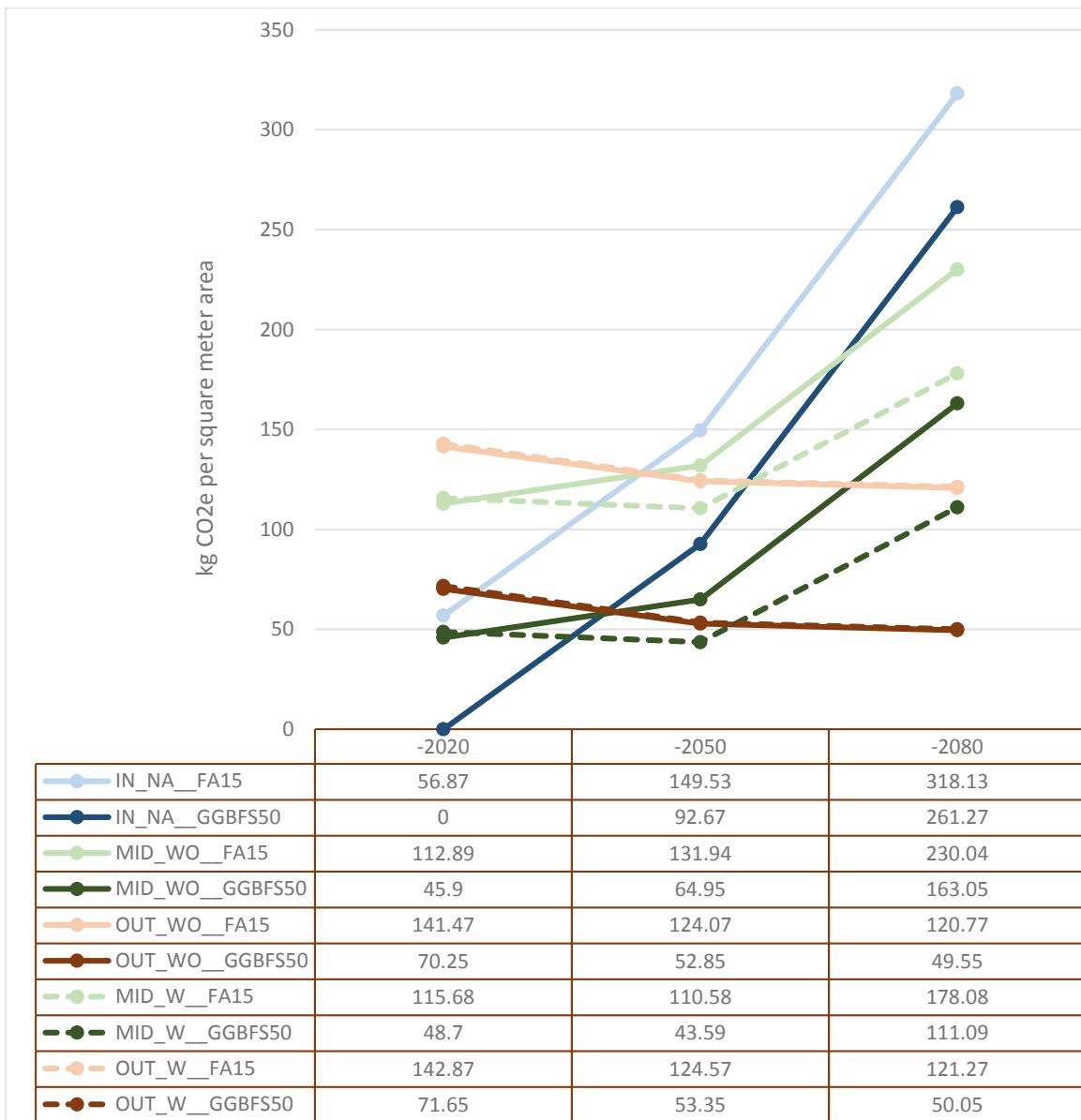
Figure 110. Maximum Regret | CO_2e Emissions (Embodied + Operational), cumulative over time.
Source: the researcher

5 Chapter No. 5

Discussion and Conclusion

5.1 Summary of Key Findings, and Answer to Research Questions

In this section, after a brief review of the preceding experimental and analytical steps, the final findings of the research are summarized and interpreted to answer the research questions.

As previously described in the first three chapters, the researcher conducted a series of computer experiments involving cylindrical 40-story office building prototypes. All these prototypes had a diagrid RC structural system, a service core, an FCU + DOAS HVAC system, and an LED electric lighting system (for a quick overview of the overall architectural and structural configuration, see Figure 57, Figure 58, Figure 59, and Figure 66). The experiments were conducted in the hot desert climate of Dubai, with a total of 1440 scenarios derived from a full factorial DoE combining various levels of different factors, as outlined below (for a quick review of the conceptual framework and full factorial DoE, see Figure 44, Figure 45, and Figure 46).

The response variables measured primary energy consumption and CO_2e emissions (refer to subsection 2.3.9 for more details). The main independent variable of interest, or the focus factor, was the PTC factor, which determined whether exoskeletons were employed (vs an endoskeleton, serving as the control group or baseline level). The factors considered in scenario planning were categorized into two groups: those affecting the pre-operational phase and those influencing the operational phase. The former included PTC, the use of insulation materials to control structural thermal bridging (TBC factor), replacements of cement (CR factor), the utilization of desalinated water in the production of RC (PDWPRC local factor), and long-distance transportation of sand (PTSAU local factor). The latter group encompassed PTC_TBC, variations in urban tissue density (UD factor), climate change and global warming (WDYP factor), and the advancement of green technologies (TYP, which comprised multiple factors such as the COP of the HVAC system, efficacy of the LED electric lighting system, and the energy mix in electricity production).

These factors were categorized as either controllable or uncontrollable, considering the perspective of architectural engineers engaged in the early stages of tall building design. PTC, TBC, and CR were identified as controllable, while the remaining factors were classified as uncontrollable. (For a comprehensive list of all factors, please refer Table 6 and Table 9).

After performing the experiments, the researcher applied statistical and mathematical analysis methods to analyze the results of the experiments (i.e., GLM analysis to answer the first research question; and objective decision analysis methods of maximax, maximin, and minimax regret to answer the second research question). These analyses were conducted both cross-sectionally and longitudinally over three time periods: one, the embodied or pre-operational phase, covering the time period up to the beginning of the operational phase (-2020), also referred to as the short term; and two time periods, each thirty years into the operational phase, -2050 and -2080 respectively (also referred to as the medium term, which includes 30 years, and the long term, which includes 60 years of operation). Here, cross-sectional means analyzing or comparing different factors or alternatives all at once, at certain points in time (at a specific point in time); and longitudinal means analyzing the results cumulatively over time.

A reminder: in the following, for brevity, the terms "desirable" and "undesirable" refer respectively to a decrease and an increase in the response variables. This is because, in general, a decrease in primary energy consumption or CO_2e emissions is considered desirable and an increase is considered undesirable.

● *First Research Question:*

What is the impact of exoskeletons (vs endoskeletons) on the life cycle primary energy consumption and CO_2e emissions of tall buildings? I.e., how effective and desirable is it compared to and in interaction with some other controllable and uncontrollable factors from the perspective of architectural engineers in the early stage of design?

A note prior to answering the first research question:

The results expressed as percentages concerning the primary energy consumption were in most cases quite to somewhat similar to those of CO_2e emissions. All detailed numbers are available in the previous chapter. Here, for the sake of briefness, only the smallest and the largest numbers are mentioned in the text; they are meant to give the audience general estimates and ease their ability to stay on track with the key findings.

● *Answer to the First Research Question:*

The first section of the previous chapter (4.1 Results of GLM Analysis) replied to the first research question in detail. Below is a summarized version with interpretations where relevant:

• All factors in this study demonstrated: (1) a statistically significant impact, whether large or small, on the response variables, and (2) an interaction with the main variable of interest, i.e., the employment of exoskeletons (vs endoskeletons).

• The main effect of the variable of interest in the short term (17 to 28 %): The employment of exoskeletons increased primary energy consumption and CO_2e emissions in the pre-operational phase (i.e., embodied primary energy and carbon), because it required additional structural materials (this is explained in greater detail in the answer to the second research question).

• The main effect of the variable of interest in the medium term and long term (up to -7 %): The employment of exoskeletons reduced primary energy consumption and CO_2e emissions during the operational phase, as well as during the sum of pre- and operational phases. This indicates the desirable effect of shading on space cooling in the hot climate, which was more crucial than its minor undesirable effect on space heating and electric lighting.

• The uncontrollable factor of improvement of green technologies (i.e., the optimistic level of the TYP factor) proved to have by far the largest desirable main effect among all factors (-15 to -66 %)—both in the operational phase and in the sum of pre- and operational phases (it was more effective on CO_2e emissions, and unsurprisingly during the second 30 years of the operational phase where in the optimistic scenarios there is a decrease in emissions from electricity production). However, the desirable effect of the employment of exoskeletons diminished as it interacted with optimistic future scenarios projecting an advanced context of green technologies (where HVAC and electric lighting systems are highly energy-efficient and powered by an eco-friendly electricity production system with an energy mix of sources with low to zero GHG emissions). In other words, the employment of exoskeletons becomes relatively more advantageous if the pessimistic technological scenario (no further green development) takes place.

• Global warming (i.e., the pessimistic level of the WDYP factor) showed an undesirable main effect (4 to 11 %) both during the operational phase and during the sum of the pre- and operational phases. The employment of exoskeletons had small desirable or negligible interactions with global warming (-1 % up to zero). One noteworthy observation in the results, although not directly related to the research question, is the significant and positive interaction between global warming and the improvement of green technologies (-2 to -10%); this finding confirms the effectiveness of local adaptation to climate change: the enhancement of green technologies in the local construction industry and electricity production can partially reduce the adverse effects of global warming on a local scale.

• Shading + glare effect of high-density urban context (i.e., the high-density level of the UD factor) showed a desirable main effect (-6 to -7%), indicating that the magnitude of the effect of its desirable shading effect on space cooling was larger than the undesirable effects of it, and that of glare on space heating and electric lighting. The magnitude of the desirability of exoskeletons' shading effect reduced in high-density urban contexts (2 to 6 %). In other words, the employment of exoskeletons becomes relatively more advantageous when the tall building is not surrounded (overshadowed) by other tall buildings in the hot desert climate.

• Thermal bridging control (i.e., the "W" or "con" level of the TBC factor) had a small undesirable effect in the pre-operational phase (1 to 3%), and a small to

negligible effect (<= 1%) both during the operational phase and during the sum of the pre- and operational phases. Since the exoskeletons partly exposed to the environment (MID) had long thermal bridging areas (as the entire length of diagrid elements was located at the boundary between the interior and exterior space), thermal bridging control had a relatively larger, but still small, desirable effect in the operational phase.

• In the short term, both local factors of long-distance transportation of sand (i.e., the PTSAU factor), and the use of desalinated water in RC production (i.e., the PDWPRC factor) had undesirable main effects (3 to 10 %) and undesirable interactions with the employment of exoskeletons (up to 3 %)—proportionate to their extra weight of structural materials. The legacy of these effects gradually diminished (to 1 down to 0 %) in the medium term and long term. Similarly but in the opposite direction, in the short term, the replacements of cement (i.e., the CR factor) showed desirable main effect (-8 to -19 %) and undesirable interactions with the employment of exoskeletons (-1 to -5 %)—proportionate to their extra weight of structural materials. The legacy of these effects gradually diminished (to -1 up to 0 %) in the medium term and long term.

• In conclusion, up to this point, the main effect of using exoskeletons (vs endoskeletons) on primary energy consumption and CO_2e emissions proved to be inconsistent throughout the life cycle of tall buildings (in the hot desert climate of Dubai); exoskeletons increased these metrics during the pre-operational phase, but reduced them during both the operational phase and the sum of the pre- and operational phases.

All factors studied showed statistically significant main effects and interactions with the main variable of interest, i.e., use of exoskeletons (vs endoskeletons), regardless of their magnitude, which in several cases was not considerably large. In the short term, CR proved to have a desirable main effect and interaction with the main variable of interest, proportionate to the extra amounts of structural materials; similar but in the opposite direction of this was true in respect of long-distance transportation of sand, and the use of desalinated water in the production of RC. These three factors remained effective but their magnitude decreased in the medium term and almost faded out in the long term.

Some uncontrollable factors, from the perspective of architectural engineers involved in the early design stage of tall buildings, had major effects on the operational phase greater than that of the use of exoskeletons (vs endoskeletons):

(1) The improvement of green technologies (i.e., the COP of HVAC systems, the efficacy of electric lighting systems, thermal bridge control, and the energy mix in electricity production) proved to have by far the largest and most desirable main effect; however, it also revealed an undesirable interaction with the employment of exoskeletons; this implies that the use of exoskeletons becomes relatively more advantageous in pessimistic technological scenarios where further development of green technologies is unlikely in the future;

(2) The main effect of shading and glare in high-density urban contexts proved to be desirable and slightly larger than that of the employment of

exoskeletons; however, it interacted undesirably with exoskeletons, largely neutralizing their desirable effect; this suggests that the employment of exoskeletons is more beneficial for relatively isolated tall buildings, those located far from the agglomeration of other tall buildings;

(3) Global warming showed a relatively large undesirable main effect in the long term but had small or negligible interactions with the main variable of interest.

● *Second Research Question:*

What would be the optimal decision or decisions about the controllable factors, made objectively (based on quantitative data), by architectural engineers considering such uncontrollable circumstances?

A few notes prior to answering the second research question:

To answer the second research question, the researcher applied three decision analysis methods to analyze the outcomes of the experiments and objectively find the optimal decisions: the maximax criterion, which represents an optimistic point of view; the maximin criterion, a conservative/robust point of view; and the minimax regret criterion, which looks from a cautious perspective.

The decision analyses were aimed at selecting the optimal levels of controllable factors (from the perspective of architectural engineers involved in the early design stage of tall buildings), which were: (1) use of exoskeletons (levels: IN as the endoskeleton that was the control group; MID, and OUT, representing exoskeletons partially and fully exposed to the environment, both with or without TBC); and (2) CRs.

Even before performing the statistical analysis, it was quite clear that for the particular CR factor, the optimal level would be GGBFS50; simply because ceteris paribus: (1) it had the least EE and EC among the levels of this factor, and (2) this factor could have no interaction with factors in the operational phase, i.e., HVAC or electric lighting systems. The main reason for including this generally known factor in this question was to give some tangible sense of scale to compare with it to better understand the relative magnitude of the effect of the other controllable factor, which was the main variable of interest in the study; i.e., the use of exoskeletons (vs endoskeletons).

● *Answer to the Second Research Question:*

The second section of the previous chapter (4.2 Results of Decision Analysis) replied to the second research question in detail. A summarized version is presented below with interpretation where applicable:

• With respect to the response variables, the results for primary energy consumption were similar to those for CO_2e emissions in terms of the ranking of the main alternatives (IN, MID, OUT)— therefore, for the sake of brevity, the terms 'primary energy consumption' or 'CO_2e emissions' are sometimes not mentioned in the following paragraphs—yet, (1) in general there was a greater relative contrast between the CO_2e emissions' results compared to the results of primary energy consumption; (2) in the long-term optimistic scenarios, CO_2e emissions reduced more significantly than primary energy consumption.

• The prototypes employing the endoskeleton (the main control group; i.e., IN), proved to be optimal in the pre-operational phase (time-spans ending in 2020), regardless of the decision criterion applied (optimistic/conservative/cautious). This was because the prototypes employing the endoskeleton used a smaller amount of structural materials (concrete and steel rebars), and had no insulation materials to control the structural thermal bridging (as they had none). The former was more crucial. Several interrelated reasons can be listed to explain the increased usage of structural materials in the prototypes employing the exoskeletons: (1) wind loads were larger on the exoskeletons because of larger spans and roughness of the exterior tube; (2) the radial beams connecting the cores to the exoskeletons had larger spans; and larger spans required deeper cross-sections; (3) in order to intensify the shading effect of the exoskeletons, the cross-sections of their diagrid elements were assumed wider than in the endoskeleton (in which the cross-sections were assumed to be neutral; i.e., perfect square); this intentional structural over-design of the cross-sections of the diagrid elements of the exoskeletons resulted in the absorption of higher forces in the diagrid elements and thus required wider beams connecting them to the core; (4) additional spandrel/ring beams were incorporated into the exoskeletons fully exposed to the environment (OUT) to connect the diagrid elements together (in addition to the ring beams at the perimeter boundary of the slabs). Similar to the reason above, this could increase the stiffness of the outer tube and thus result in larger beams connecting to the core. Larger beams that would withstand greater forces when connecting to the core also required thicker core walls. The exoskeletons turned out to be stiffer, but also heavier (by requiring larger amounts of structural materials). This resulted in higher EE and EC. Two local factors, the use of desalinated water in RC production (PDWPRC) and the long-distance transport of sand from Australia (PTSAU), also affected exoskeletons more than endoskeletons, again due to the larger amounts of concrete and reinforcement in the former than in the latter. Thus, the endoskeleton proved to incorporate less primary energy and CO_2e emissions in all scenarios in the preoperational phase. However, it is important to remember that, due to the long lifetime of tall buildings, more attention needs to be paid to long-term records than to relatively short-term records. As already mentioned in the previous chapter (Figure 81, and Figure 82), the baselines/intercepts of long-term primary energy and CO_2e emissions were 15-17 times greater than the short-term ones.

• Regarding the medium-term (up to 30 years of operational phase) and long-term (up to 60 years of operational phase) time periods, the answers to the second research question were different from the answers regarding the short-term time period (pre-operational phase). Prototypes employing the endoskeleton performed better in the medium and long term, compared to those with exoskeletons, only with respect to the optimistic scenarios (i.e., the maximax criterion). The use of exoskeletons was optimal in the medium and long term when conservative/robust or cautious criteria (i.e.,

243

maximin criterion and minimax regret criterion) were applied. One of the reasons was that the desirable effect of exoskeleton shading on facades in the hot desert climate became more crucial in harsher conditions or pessimistic scenarios: during the operational phase, when there is no significant shading of the urban context protecting the facades; and no future ecological technological improvements, namely those crucial for space cooling in the hot desert climate, i.e., COP of HVAC systems and energy mix in electricity production.

• From an optimistic perspective (maximax criterion), the relative difference between the best and the worst alternative decreased in a longitudinal order (cumulative over time). An interpretation for this is that in the medium term and the long term, the electric lighting and the HVAC systems become less energy consuming and at the same time, the carbon footprint of electricity production becomes smaller due to the advances in the energy mix. The following two items indicate the relative reduction: (1) concerning the maximum payoffs of primary energy (Embodied /+ Operational) cumulative over time; in the short term, the best alternative was 39% better than the worst; 'the difference between the best and the worst alternative' in the medium term, and 'that' in the long term, relative to 'that' in the short term was 72%, and 40% respectively. (2) concerning the maximum payoffs of CO_2e emissions (Embodied /+ Operational) cumulative over time; in the short term, the best alternative was 58% better than the worst; 'the difference between the best and the worst alternative' in the medium term, and 'that' in the long term, relative to 'that' in the short term was 87%, and 84% respectively.

• From both a conservative/robust perspective (maximin criterion) and a cautious standpoint (minimax regret criterion), the relative difference between the best and worst alternatives decreased, shaping break-even points in the medium-term, and then increased in the long-term, cumulatively over time. The general interpretation is that in the long term, the desirable shading effect becomes crucial in pessimistic scenarios, especially when no further development of green technologies occurs, particularly for tall buildings located in low-density urban contexts, where their facades are not overshadowed by other buildings. This shading effect compensates for and surpasses the undesirable effect of consuming extra structural (and insulation) materials observed in the short term. The following 2(×2) items indicate this relative reduction followed by an increase: (1-1) the minimum payoffs of primary energy (Embodied /+ Operational) cumulatively over time: In the short term, the best alternative was 37% better than the worst. The difference between the best and worst alternative in the medium term and long term, relative to that in the short term, was 83% and 229%, respectively. (1-2) the minimum payoffs of CO_2e emissions (Embodied /+ Operational) cumulatively over time: In the short term, the best alternative was 54% better than the worst. The difference between the best and worst alternative in the medium term and long term, relative to that in the short term, was 99% and 217%, respectively. (2-1) the maximum regret of primary energy (Embodied /+ Operational) cumulatively over time: In the short term, the best alternative was 316 kWh/m^2 area better than the worst. The difference between the best and worst alternative in the medium term and long term, relative to that in the short term, was 47% and 207%, respectively. (2-2) the maximum regret of CO_2e emissions (Embodied /+ Operational) cumulatively over time: In the short term, the best alternative was 143 kgCO$_2$e/m^2 area better than the worst. The difference between the best and worst alternative in the medium term and long term, relative to that in the short term, was 74% and 188%, respectively.

• In conclusion, the endoskeletons (i.e., the control group) required less amount of structural materials (and insulation) and thus proved to be optimal in the short term, regardless of the decision criterion used. Yet, given the long lifetimes of tall buildings and the significantly higher baselines for long-term primary energy and CO_2e emissions compared to the short-term, it is advisable to prioritize the long-term records over the short-term ones. In the medium and long term, however, endoskeletons continued to prove optimal only from an optimistic perspective (maximax criterion) in which optimistic future scenarios dominated. From this point of view, the difference between the best alternative (endoskeleton) and the worst (exoskeleton fully exposed to the environment) decreased over time.

In contrast, exoskeletons proved to be the optimal alternatives in the medium to long term if pessimistic scenarios were prioritized (i.e., maximin criterion analyzing from a robust/conservative point of view) or if a balanced or cautious perspective was made decisive using the minimax regret criterion. The use of exoskeletons proved to be able to exceed break-even points in the medium term and convert their effects on life-cycle primary energy consumption and CO_2e emissions (cumulative over time) from undesirable in the short term to desirable (with almost twice the relative magnitude) in the long term.

5.2   Significance, Contribution and Impact

This section answers the following questions:

1. *Why is this research and its results significant?*
2. *Who can benefit from the present investigation and its results? And how?*
3. *How does this research and its results relate to the literature?*
4. *How reliable, valid, and replicable are the results?*
5. *How could the results be generalized or extended?*

Here the researcher begins with answering the first three questions briefly in a concise paragraph, and then unfolds it in more detail below (note: the answers to the three questions were inseparable from one another, so they come with and in combination with each other):

The significant original contribution of this research to the interdisciplinary field of architectural engineering is that it represents the first comprehensive scientific study of its own kind, dedicated to illuminating the impact of utilizing exoskeletons vs endoskeletons on the life-cycle primary energy consumption and CO2e emissions of tall buildings; by employing a replicable quantitative methodology, without oversimplifying critical interacting factors (including multiple controllable factors influencing design choices and uncontrollable factors associated with urban, technological, and climatic contexts that evolve over time).

Architectural engineers involved in the early stages of designing high-rise buildings benefit not only from the results of the study at hand but also from its research design, methods, and workflow applied during its process. For the first time, this study investigated the environmental impact of using exoskeletons (vs endoskeletons) in tall buildings by calculating and estimating two major metrics: emissions of GHGs and the consumption of primary energies during the most influential time spans in the life cycle of tall buildings (pre-operational and operational phases). To the best of the researcher's knowledge, there has never been such a case in the literature before. Although exoskeletons have been used in the design of several prominent high-rise buildings—from the super-tall John Hancock Center in Chicago and IBM Tower in Pittsburgh in the middle of the twentieth century to recent examples like O-14 tower in Dubai, One Thousand Museum tower in Miami, and Morpheus Hotel at City of Dreams, Macau—and some of their architects, engineers, or researchers had claimed environmental benefits of their design, they did not publish comprehensive scientific quantitative evidence-based reports about the environmental impacts of the employment of exoskeletons. Thus, a gap in the academic and scientific literature existed prior to this research. Given the global climate crisis and the depletion of available resources on the one hand, and the very long service life of tall buildings' PSEs, including exoskeletons (e.g., for buildings taller than 150 m, it would be in the scale of centuries or arguably infinite time-span), and the large amounts of structural materials spent in it, and the potential for interaction with rapidly evolving HVAC and electric lighting systems,

energy mix in electricity production, urban and climate contexts in the long run, it has been crucial to assess the environmental effect of such decisions (i.e., whether or not to employ exoskeletons) before implementing them. Needless to say, this alone would not solve the aforementioned global crises but enables architectural engineers to make better-informed decisions and improve the situation as much as they possibly could by better understanding and assessing the life cycle impacts of tall building exoskeletons vs endoskeletons, which was previously understudied.

Even the relatively closest studies to the current study in terms of focusing on the life cycle impacts of tall building exoskeletons, i.e., the papers by Felkner et al. [11] and Weber et al. [13], were unable to address the research questions of this dissertation. The former ([11]), although shared similar objectives, could not provide estimates for GHG emissions or primary energy, as it did not calculate the EE and EC of the structural system. More significantly, it did not estimate site energy (i.e., electricity or fuel) consumption related to HVAC and electric lighting systems or consider the primary energies needed to generate and deliver electricity or fuel for operating these systems, thus preventing estimates of primary energy and GHG emissions. The latter ([13]) did not have these limitations, but it lacked an apple-to-apple comparison, as it compared exoskeletons with endoskeletons of different structural types. It had an advantage over the former in that it considered a couple of medium-term future scenarios for electricity production. In the current study, these limitations were addressed, and, as mentioned earlier, various combinations of different controllable design factors and uncontrollable context factors were used to create multiple future scenarios, enabling the analysis of the potential environmental impact of employing exoskeletons (vs endoskeletons). Beyond these two papers, other papers in the relevant literature on tall building structural systems (e.g., see the papers by Trabucco et al. [4][5], and Foraboschi et al. [6]) did not address the potential interactions between structural systems and other building systems, such as HVAC and electric lighting, placing this topic outside the scope of their research. In the study by Moussavi and Akbarnezhad [8], despite conducting an LCA comparing different structural systems, including exterior bracings and shear walls, and considering the thermal mass effect of structural elements on operational space heating and cooling energy and carbon footprint, they did not explore the possibility of overshadowing the facade by the structural elements. Furthermore, these studies did not develop scenarios related to the surrounding urban context or consider future scenarios involving changes in climate, the energy mix in electricity production, or other time-dependent variables. The scope of previous research by K S Moon et al., which focused on reducing the quantities of structural materials through geometric optimization of layouts of different structural systems and materials (e.g., [146][148][149][150][151][153]), did not extend to exploring possible interactions between the structural system and HVAC and electric lighting systems. While the researcher found all the aforementioned literature sources valuable and inspiring, this dissertation constitutes a substantial advance by effectively addressing the above limitations and filling a crucial gap in its specific research niche.

Another set of contributions of this research is its attention to the nature of early stages in the design process, where major decisions are made while many details remain undefined. It also deals with numerous trivial parameters, which can overly complicate calculations, make them lengthy, and difficult to comprehend. This issue was addressed throughout the present investigation, drawing insights from the literature. Some of these insights might have been applied in architectural engineering in unique ways that

previous researchers may not be aware of. These insights can expedite and simplify future research by directing focus towards key factors, thus saving time and effort for researchers and architectural engineers involved in the early design stages of tall buildings. Several significant findings include:

    (1) The cradle-to-gate embodied primary and CO2e emissions of structural materials are the dominant factors in the entire life cycle of structural systems, as previously noted [6] and confirmed [4][5] in the literature;

    (2) In contrast, in the HVAC [238][239][240][8] and electric lighting systems [241, pp. 49–52][242], by far, the highest amount of primary energy consumption and CO2e emissions is attributed to the operational phase. Effects from other life-cycle phases, such as pre-operational and end-of-life primary energy and emissions, are marginal;

    (3) Including future improvement scenarios in the energy mix of electricity production, the efficacy of electric lighting systems, and the COP of the HVAC systems allowed for the development of more optimistic scenarios alongside the conventional 'business as usual' scenarios, which may sound rather pessimistic when considering the progress of these technologies in recent centuries.

For professional practice of tall building design projects in reality with more or less similar parameters (e.g., dimensions, climate, and other characteristics) to those in the prototypes in this research, architectural engineers may refer to or directly use the results to improve initial scientific conjecture or design decisions. In other words, this research, through its experiments, prototypes, and results on numerous variables and their interactions, provides a set of transparent reference points that did not exist before this investigation. Therefore, the results of this research enhance the conjecture of architectural engineers in similar projects. Since the results are presented in detail in the previous chapter and briefly at the beginning of this chapter, the researcher does not repeat them here. However, it is highly recommended that readers review them before proceeding with this section.

Last but not least, the research design, statistical and mathematical approach to the analysis (specifically, the factorial DoE followed by the application of GLM, and finally, the three objective decision analyses of the maximax criterion, maximin criterion, and minimax regret), represents a novel and suitable combination within the context of LCA for exoskeletons (vs endoskeletons). This approach effectively addressed the conditions and requirements of the study, enabling the researcher to address the research questions. The researcher highly recommends this approach for further research and practice in similar topics. Similarly, this research could serve as a reference in relevant engineering mathematics and statistics articles or books (e.g., [369] or [175]) as an example of an interdisciplinary experimental study with multiple controllable and uncontrollable factors and categorical levels varying over different time spans. It identifies their magnitude of influence and desirability at each point in time (cross-sectional) and throughout time spans (longitudinal), followed by ranking (design/decision) alternatives based on objective analysis of plausible future outcomes from different standpoints (i.e., optimistic, conservative/robust, and cautious) to find optimal solutions for each perspective.

- How reliable, valid, and replicable are the results?

The researcher meticulously executed each stage of building modeling and simulations using valid software programs and methods and by employing data with the highest possible accuracy level. Based on the reasons and explanations in the following paragraphs, it can be concluded that the results of this research have a reasonable degree of validity and reliability—given the time and budget constraints of the research, the real-world conditions in terms of the unavailability or absence of some comprehensive local databases, and also the scenario-based nature of LCA in which uncertainty is an inherent aspect. The replicability of the results was certified by a detailed explanation of the methods and materials, as well as the inclusion of all technical files and open-source algorithms and scripts developed by the researcher as attachments to this dissertation.

As discussed earlier in detail (in 3.3.2.6 Embodied Primary Energy and Carbon of Superstructures, and CR Effect), due to the absence of country-specific LCI databases in the UAE, the ICE database v.2.0 (2011) [47] and v.3.0 (2019) [48] were considered for estimating the embodied primary energy and CO_2e emissions of construction materials (occurring before 2020, assumed as the first year of the operational phase). Using databases from other countries, like ICE, is common in such situations; and the ICE database's global usage and reliability, adhering to standards EN 15804 [68] and EN 15978 [164], add to its credibility [286][287][288][289][290][291][292]. UAE's mix of energy in electricity production in 2020 resembled the UK's in 2011, both having less than 5% renewables, making ICE version 2.0 a more reasonable choice compared to version 3.0, especially concerning CO_2e emissions [295][296]. This alignment with older databases is often observed in developing countries where the industries share similarities with older industries in developed countries [281][292][291][289][283]. Further support came from newer EPDs in Dubai, aligning closely with UK's 2011 figures, confirming ICE 2.0's relevance [300][302][47]. The selection of the LCI database, despite limitations, remained a pragmatic and valid choice considering the research context and available data. Nevertheless, inclusion and assessment of the impact of the two local factors of PDWPRC and PTSAU were also done to minimize the aforementioned limitation and to increase the reliability and validity of the results.

Similarly, with regard to operational primary energy and CO_2e emissions, one might question the validity and the effects of the PEFs and CO_2e emission coefficients on the results, since those coefficients were partially originated from the USA or international databases (revisit Table 34 and Table 35). First, those coefficients in different countries are not so different that they could drastically change the results of this study (especially in terms of relative percentages and rankings) because, for instance, the differences between the results of primary energy consumption and CO_2e emissions of the different alternatives in this study are rooted in operational electricity and natural gas delivered energy demands, which are independent of the aforementioned coefficients. Second, the ratio of the magnitude of the effect of the most impactful factors (i.e., advancement of green technologies) to those of the main variable of interest (i.e., employment of exoskeletons vs endoskeletons) is so large (e.g., more than 1000%, in the case of operational CO_2e emissions 2020-2080) that relatively small variations in the aforementioned coefficients cannot have a considerable consequence on the results.

A key point to remember and consider here is that the present investigation neither did aim to address a specific actual and real building project in Dubai, nor did aim to be limited by a group of local audience in that area. All the modelings, simulations and calculations was to bring about an example for holistic and generic research purposes addressing the early stage of design of tall buildings, to provide a research report useful for a large global audience group of architectural engineers. Certainly in the construction projects that are really going to be implemented, the numbers need to be prepared more accurately according to the specific case and local standards and legal frameworks. As a disclaimer statement, the researcher finds it necessary to mention that in no way does this research claim to be an alternative to specific studies of any project in reality.

The choice of years with round numbers (i.e., 2020, 2050, and 2080) simplifies the replication of the study at hand, as data for these years are easier to obtain. It also improves communication with a broader audience, who can use these years as benchmarks to compare with other future predictions often aligned with decades starting in round numbers. Governments and international agencies often formulate strategic targets at such junctures; e.g., the European Union's 2050 climate neutrality strategy [370] and policies for 2020, 2030, and 2050 [371]; similarly, Saudi Arabia [372] and the UAE [373] have undertaken initiatives with the goal of reducing greenhouse gas emissions to net zero by 2060 and 2050, respectively. In addition, these round years facilitate technical simulations using software; specifically, the free software used to generate future weather data based on climate change (CCWorldWeatherGen V 1.9 [252]) only addressed the years 2050 and 2080. Although it was technically feasible to extrapolate the results to other years (e.g., 2053, 2083), avoiding this approach improves the accessibility and replicability for the audience. Given the holistic and general approach of this research, the researcher intentionally avoided such projection processes.

Building modelings and simulations in the present investigation (architectural, structural, HVAC, daylighting, etc.) has been done with significant care and accuracy in comparison to typical researches in similar fields. For instance, in the structural analysis and design in this research, valid standard methods and all wind loads and seismic loads (both dynamic and static) were applied meeting actual building codes, e.g., International Building Code (IBC), Eurocode, etc. As mentioned earlier, a literature review study by James Helal et al. in 2020 found, the absence or lack of appliance of lateral loads or standard structural analysis and design methods could end up in underestimation of up to over 20% of GHG emissions in structural systems for tall buildings [174]. Many existing literature sources on LCA of tall buildings structural systems are subject to this problem; e.g., it is not indicated in the study by Zhao and Haojia [374] whether wind or seismic loads were at all considered, whereas Moussavi Nadoushani and Akbarnezhad [8] only considered seismic loads; in studies by Foraboschi et al. [6], Cho et al. [375], Felkner et al. [11], and Weber et al. [13] only wind loads were applied, and in the study by Trabucco et al. [4][5], it is not clear what methods or codes has been used in structural analysis and design with respect to wind and seismic loads.

As indicated earlier, the technical procedures carried out and the tools employed in the experiments and analyses are thoroughly documented in the third chapter and

included as a complete archive of files attached to this dissertation. The researcher has thoroughly verified all components, conducted random checks with alternative versions of the software, and ensured complete agreement in the results. Consequently, it is deduced that any researcher or professional using similar methods, tools, and programs would be capable of replicating this research.

- How could the results be generalized or extended?

Contrary to some superficial assumptions implying that the generalizability of results is a prerequisite of all good research, this is an ideal and it is generally not the case in either quantitative or qualitative research [376]; "When we give proper weight to local conditions, any generalization is a working hypothesis, not a conclusion" [377, p. 125] [376]. In fact it is a highly subject- and case-sensitive issue, and it requires a deep understanding of the subject matter, aims and objectives and the context of a research.

As for this particular research, it exhibits relatively minor potential for 'statistical' generalization at the present time, while demonstrating major 'transferability' and 'analytic' generalizability. Projects with variables within reasonable limits of the parameters in this research may closely relate to the study at hand and derive considerations and evidence-based scientific conjecture from its results as a base point with caution as initial guidance and reference of approximation (*'transferability'*), but it is important to consider that the results of this research, similar to the results of other building LCA studies, may not be universally applicable to all cases (*'statistical' generalization*), because many other potential factors and scenarios can affect the results including variations in geometry, design, materials, function, industrial, natural (namely climate, soil, wind and earthquake), urban and other context parameters among others. The philosophy underlying LCA is based on the fact that such results cannot and should not be unreasonably generalized, and that separate assessments should be conducted for different products, services, or decisions at different times and locations. However, over time and with the replication of several similar studies to increase the number and diversity of samples, the cumulative results of this research and those of other studies will allow statistical generalizability. As a result, it will be possible to reasonably predict the environmental impacts of various types of exoskeletons in tall buildings with different shapes, heights, materials, and under varying climatic and contextual conditions worldwide. '*Transferability*' requires relevant architectural and engineering experience and expertise to distinguish the extent to which a new high-rise building project or study can relate to the results of the present investigation; nevertheless, in writing this dissertation, the researcher has attempted to explain each step or parameter as clearly as possible to enhance future references and replications. Some scholars have truly emphasized these important facts about the limitations of generalizability in their research articles and reports with topics close to this study (e.g., see [8][4][5]), and others have not done so for some reasons (possibly because they assume it is obvious, or due to the limitations of the number of pages of some journal articles, etc.).

The extensibility of the conceptual and methodological frameworks in this research (*'analytic' generalization*) are significant; (1) its research design and objective approach in finding key drivers in terms of life cycle stages of different building

systems, and in analyzing multiple parameters from different disciplines—in relation to the architectural engineering question—while using the applied statistical procedures and methods (including the combination of factorial DoE and GLMs, as well as the decision criteria); and (2) the free and open-source parametric building geometry generator, BIM solution, performance simulation, and quantity estimation tools (i.e. the GH/Python scripts/algorithms and workflow pipelines) that the researcher developed during and for this research are widely extensible and open for integration with new research and practice projects on similar topics. Many experts in building design and whole building LCA have called for unified tools and methods for both purposes at the same time [378]. In response to this need, it is expected that the use and extension of the research design, frameworks and algorithms of the study at hand will save time and energy for the benefit of such experts, making it possible to conduct several similar studies on tall buildings with different heights, structural systems, materials, etc. in different climates and locations around the world much faster than this research.

5.3   Recommendations for Further Research and Action

It is worth recalling the scope and delimitations of the study before moving on to the recommendations for future work. As already explained (in the first and second chapters), some experiment parameters were intentionally fixed and did not vary across experiments. This practice, known as delimiting and defining the scope and focus area of the research variables (i.e., control variables in the conceptual framework), was used. In other words, all experiments concerned prototypes that had the following properties in common: a 40-story cylindrical office building with an RC diagrid structural system in a hot desert climate (Dubai, UAE). This allowed the researcher to investigate accurate and reliable building simulations and estimations or include several other moderating variables (i.e., the studied factors/levels) from different disciplines and time spans with which to interact and put into perspective the main variable of interest in this research (employment of exoskeletons vs endoskeletons), similar to reality.

Nevertheless, some of the control variables in this study remain possibilities for future investigation as moderating variables. These include other locations/climates, structural materials and systems, overall forms, heights, and shapes of high-rise exoskeleton cross-sections. Using methods and workflows similar to the present investigation, valuable computer simulation-based experimental projects are recommended for future exploration. These projects can compare the effects of exoskeletons (vs endoskeletons) in different:

1. Locations/climates (e.g., hot desert vs temperate vs cold).
2. Structural materials (e.g., RC vs steel vs timber vs composites).
3. Structural systems (e.g., diagrid vs braced tube).
4. Overall forms (e.g., cylindrical vs box with different orientations; also vertical extrusion vs tapered vs twisted vs free-form).
5. Heights (e.g., 20 vs 40 vs 60 stories).
6. Shapes of cross-sections of exoskeleton elements (e.g., full vs hollow core; perpendicular to facade vs parallel vs in-line with facade)

Similarly, the study at hand focused on superstructures. Substructures (i.e., foundations, basement floors and walls), were intentionally excluded from the experiments, not only in this study but also in several other prior literature sources that concentrated on LCA or early design optimization of tall building structures (e.g., see [4][5][6][11][13]). This exclusion was deliberate and aimed at facilitating direct comparisons between the results of this research and the closest literature sources in the past. However, it would be advantageous in the future to expand the scope of such studies to incorporate the impact of exoskeletons on tall building substructures, particularly when considering various soil classes. For instance, a hypothesis in this context could be as follows: given that superstructure alternatives with exoskeletons have proven to be more massive than those with endoskeletons, it is conceivable that the foundations supporting the former would also be relatively more massive, potentially resulting in larger environmental impacts, ceteris paribus.

The unavailability of sufficient and reliable local or country-specific data, particularly inventory data related to electricity and embodied primary energy from building materials, as well as emission characterization factors in Dubai, UAE, caused an unavoidable limitation. This limitation was partially addressed by employing approximations and alternative sources, such as the inclusion of the local factors of PDWPRC and PTSAU in the assessment. However, despite careful considerations, it may still introduce some uncertainties and biases into the analysis. To fully address this limitation, which unfortunately is a general issue in many countries, especially developing ones, extensive research, raising stakeholders' awareness, and receiving special attention and support from governments and national and international organizations are required, as indicated by prior research (e.g., see [281][282][283][284][288]).

Regarding the three pillars of sustainability (environmental, social, and economic), this research assessed two major environmental metrics as response variables: primary energy consumption (reflecting the resource depletion impact category) and CO_2e emissions (reflecting the climate change impact category) assumed as the most relevant and familiar to the global audience of this research. Other environmental impact categories (ozone depletion, acidification, and pollution of water and soil, etc.) sounded too advanced and detailed for the present investigation (taking into account the many dimensions that architectural engineers have to analyze and decide about at the early stage of design of tall buildings) but anyway, it remains as a topic for future research. So were the economic and social aspects of exoskeletons (which were not in the scope of this research). The former can be a topic for local research as costs, especially costs of energy, differ a lot from place to place, and from time to time (predicting weighing factors of environmental costs for long-term scenarios e.g., predicting 2080 at present time seemed too uncertain and unclear). The latter is also a highly subjective aspect of exoskeletons that, for instance, has to do with aesthetics and has been partially investigated in the literature. A general topic worth highlighting for future research is to compare occupants' behavior with respect to exoskeletons (vs endoskeletons) of tall buildings.

Since any future environmentally friendly action needs to be supported by research, and any further investigation can (and should) be updated by the practical results in reality, the researcher attempted to make the research design, conceptual framework, methods, and the workflow of the study at hand reusable and extensible for both further research and practical purposes. Even the digital tools that the researcher developed during the process will be available to support future studies (that was why the researcher tried to integrate different techniques in an extensible parametric setup wherever possible).

It is expected that the architectural engineers involved in the early stage of the design of tall buildings use this research material as a significant base point to improve their scientific conjecture about the impact of exoskeletons (vs endoskeletons) on the life cycle primary energy consumptions and CO_2e emissions of tall buildings.

Appendix:

List of Attached Technical Files and Algorithms

This appendix includes a comprehensive list of the most important technical files and algorithms employed throughout the research. These resources cover a broad spectrum of domains and procedures, from general architectural and geometric modeling to structural analysis and design, HVAC and electric lighting simulations, LCI and LCIA, mathematical and statistical analysis, and more.

Some of these files contain multiple integrated visual programming and Python algorithms developed by the researcher, mostly as GH components or setups.

Table 55 presents the list of these files, which are included with the dissertation as digital attachments for transparency and detail on all methodologies and analyses applied in this research. The table rows include the heading numbers of the corresponding sections or subsections and some keywords to facilitate the search of the files.

All these files will be available to the board of examiners to support the evaluation of the dissertation.

In addition, these files will also be made available to the general audience of this dissertation upon reasonable request. Requests from the audience should be sent by email to the following address:
aryan_shahabian@yahoo.com
.

Table 55. List of attached technical files with corresponding section/subsection references and keywords. Source: the researcher

Sections/Subsections	File Names	Some Related Keywords
3.2	Diagrid_Tall_Building_Geometry_Generator.gh	Overall Architecture, Generative Geometrical Model, Diagrid Tall Building Model, PTC
3.3, 3.3.1	Wind_and_Seismic.gh	Wind Loads, Seismic Loads, Balancing Base Shear Forces, PTC
3.3, 3.3.1, 3.3.2	NEW_IN_015.EDB NEW_MID_020.EDB NEW_OUT_013.EDB	Structural Analysis, Dead and Live Loads and Load Combinations (Gravity, Wind, Seismic), Final Structural Design (Diagrid Columns, Core Shear Walls, Floor Slabs, Beams), PTC
3.3.2	Pre_Operational_Inventory_and_Impact.gh	Embodied (Pre-Operational) Primary Energy and CO_2e emissions, LCI, LCIA, Structural Elements (Diagrid Columns, Core Shear Walls, Floor Slabs, Beams), PTC, TBC, CR, PDWPRC, PTSAU
3.3.2, 3.4.1	Thermal_bridges_geometry.3dm U_values_calculation.gh	TBC, PTC
3.4.1, 3.4.2	-_Dubai_2020.epw -_Dubai_HadCM3-A2-2050.epw -_Dubai_HadCM3-A2-2080.epw	EPW, WDYP, WDY
3.4, 3.4.1, 3.4.2	HVAC_ElectricLighting.3dm HVAC_ElectricLighting.gh	HVAC, Electric Lighting, Operational Energy Modeling, Fuel, Electricity, Zones, Adjacencies, Constructions, Shading/Context, COP, Air Details, FCU + DOAS, Daylight, LED, EPW, PTC, TBC, TYP, WDYP, WDY, UD
3.4.3, 3.3.2	Characterization_Factors.gh	Electricity Primary Energy and CO_2e emissions, PEF, TYP
3.4.3	Operational_Inventory_and_Impact_Key_Years.xlsx	Operational Primary Energy and CO_2e emissions, LCI, LCIA, PTC, TBC, TYP, WDYP, WDY, UD
3.4.3, 3.3.2, 3.5	results03_EmbodiedAndOperational_ary031_ALL.csv (All 1440 Scenarios)	Embodied (Pre-Operational) and Operational Primary Energy and CO_2e emissions, LCIA, PTC, TBC, CR, PDWPRC, PTSAU, TYP, WDYP, UD
3.5, 3.5.1, 4.1	GLM_all_ary016.R GLM_all_ary017_01.pdf (61 Pages)	Answer to First Research Question, Results of GLM Analysis, Statistical Analysis, Embodied (Pre-Operational) and Operational Primary Energy and CO_2e emissions, PTC, TBC, CR, PDWPRC, PTSAU, TYP, WDYP, UD
3.5, 3.5.2, 4.2	MAXIMAX_18.xlsx MAXIMIN_06.xlsx MINIMAX_REGRET_37.xlsx	Answer to Second Research Question, Results of Decision Analysis, Maximax, Maximin, Minimax Regret, Embodied (Pre-Operational) and Operational Primary Energy and CO_2e emissions, PTC, TBC, CR, PDWPRC, PTSAU, TYP, WDYP, UD

References

[1]   A. Shahabian, "Internet of Things and the Future of Life-Cycle Assessment in Smart World," in *Vienna young Scientists Symposium VSS2018*, Vienna: Vienna University of Technology (TU Wien), 2018, pp. 40–41. [Online]. Available: https://www.researchgate.net/publication/325871906_Internet_of_Things_and_the_Future_of_Life-Cycle_Assessment_in_Smart_World

[2]   I. Rusi, "The Contemporary Trend of Perforation. Case of Exoskeleton Concrete Shells," *Int. J. Sci. Res.*, 2019, [Online]. Available: https://iris.unife.it/bitstream/11392/2409398/1/Rusi_IJSR.pdf

[3]   C. Besjak and A. Thewis, "Shenzhen Rural Commercial Bank Headquarters: an Iconic Tower Defined by the Integration of Architecture, Structure and Sustainability Goals," *Int. J. High-Rise Build.*, 2022, doi: 10.21022/IJHRB.2022.11.1.31.

[4]   D. Trabucco, A. Wood, O. Vassart, N. Popa, and D. Davies, *Life Cycle Assessment of Tall Building Structural Systems*. Chicago: Council on Tall Buildings and Urban Habitat, 2015. [Online]. Available: https://store.ctbuh.org/research-reports/48-life-cycle-assessment-2015.html

[5]   D. Trabucco, A. Wood, O. Vassart, and N. Popa, "A Whole LCA of the Sustainable Aspects of Structural Systems in Tall Buildings," *Int. J. High-Rise Build.*, vol. 5, no. 2, pp. 71–86, 2016, doi: 10.21022/IJHRB.2016.5.2.71.

[6]   P. Foraboschi, M. Mercanzin, and D. Trabucco, "Sustainable structural design of tall buildings based on embodied energy," *Energy Build.*, vol. 68, no. PARTA, pp. 254–269, 2014, doi: 10.1016/j.enbuild.2013.09.003.

[7]   A. Fadai, W. Winter, and M. Gruber, "Wood Based Construction for Multi-Storey Buildings . the Potential of Cement Bonded Wood Composites As Structural Sandwich Panels," *World Conf. Timber Eng.*, 2012.

[8]   Z. S. Moussavi Nadoushani and A. Akbarnezhad, "Effects of structural system on the life cycle carbon footprint of buildings," *Energy Build.*, vol. 102, pp. 337–346, 2015, doi: 10.1016/j.enbuild.2015.05.044.

[9]   M. Lamperti Tornaghi, A. Loli, and P. Negro, "Balanced evaluation of structural and environmental performances in building design," *Buildings*, 2018, doi: 10.3390/buildings8040052.

[10]   N. Huberman, D. Pearlmutter, E. Gal, and I. A. Meir, "Optimizing structural

roof form for life-cycle energy efficiency," *Energy Build.*, 2015, doi: 10.1016/j.enbuild.2015.07.008.

[11]   J. Felkner, J. Schwartz, and E. Chatzi, "Framework for Balancing Structural Efficiency and Operational Energy in Tall Buildings," *J. Archit. Eng.*, 2019, doi: 10.1061/(ASCE)AE.1943-5568.0000355.

[12]   A. Shahabian, "Integration of solar-climatic vision and structural design in architecture of tall buildings," in *Proceedings of International Conference CISBAT 2015 Future Buildings and Districts Sustainability from Nano to Urban Scale*, J.-L. Scartezzini, Ed., Lausanne: Lausanne, LESO-PB, EPFL, 2015, pp. 179–184. doi: 10.5075/epfl-cisbat2015-179-184.

[13]   R. E. Weber, C. Mueller, and C. Reinhart, "Solar exoskeletons–An integrated building system combining solar gain control with structural efficiency," *Sol. Energy*, no. 240, pp. 301–314, 2022.

[14]   H. L. Pesonen *et al.*, "Framework for scenario development in LCA," *International Journal of Life Cycle Assessment*. 2000. doi: 10.1007/BF02978555.

[15]   Skyscrapercenter.com, "Tallest Buildings - Demolished," *CTBUH*, 2023. https://www.skyscrapercenter.com/buildings?status=demolished&material=all &function=all&location=world&year=2023 (accessed Aug. 28, 2023).

[16]   P. Oldfield, "Embodied carbon and high-rise," in *CTBUH 9th World Congress*, Shanghai, China, 2012.

[17]   J. Wolf, "0-14 Tower, Dubai (photograph - licensed under CC BY-ND 2.0: https://creativecommons.org/licenses/by-nd/2.0/)," *Flickr*, 2011. https://www.flickr.com/photos/joebehr/5516576932 (accessed Apr. 25, 2023).

[18]   Störfix, "Morpheus at City of Dreams, Hotel in Macau (photograph - licensed under CC BY-SA 3.0 DE: https://creativecommons.org/licenses/by-sa/3.0/de/deed.en)," *Wikimedia*, 2018. https://commons.wikimedia.org/wiki/File:Macau-Morpheus-02.jpg (accessed May 15, 2023).

[19]   J. Ravi, "John Hancock Center in Chicago, Illinois, USA (photograph - licensed under CC BY-SA 3.0: https://creativecommons.org/licenses/by-sa/3.0/deed.en)," *Wikimedia*, 2011. https://commons.wikimedia.org/wiki/File:John_Hancock_Center_2.jpg (accessed Apr. 25, 2023).

[20]   Cbaile19, "United Steelworkers Building, Pittsburgh (photograph - licensed under CC0 1.0: https://creativecommons.org/publicdomain/zero/1.0/deed.en)," *Wikimedia*, 2023. https://commons.m.wikimedia.org/wiki/File:United_Steelworkers_Building,_2 023-01-04,_01.jpg (accessed Apr. 25, 2023).

[21]   J. Basbagill, F. Flager, M. Lepech, and M. Fischer, "Application of life-cycle assessment to early stage building design for reduced embodied environmental

impacts," *Build. Environ.*, vol. 60, pp. 81–92, 2013, doi: 10.1016/j.buildenv.2012.11.009.

[22] R. Ghattas, J. Gregory, T. R. Miller, and R. Kirchain, "The decision-making process in the design of residential structures," *MIT Concr. Sustain. Hub*, 2015.

[23] J. Gregory, "Building life cycle assessment to support building design," *MIT CSHub Webinar*, 2017. https://www.youtube.com/watch?v=5JDcccCxhuE (accessed Mar. 11, 2023).

[24] M. A. Zanni, R. Soetanto, and K. Ruikar, "Defining the sustainable building design process: Methods for BIM execution planning in the UK," *Int. J. Energy Sect. Manag.*, 2014, doi: 10.1108/IJESM-04-2014-0005.

[25] The British Standards Institution, "Specification for information management for the capital/delivery phase of construction projects using building information modelling: PAS 1192-2:2013," *BSI Stand. Publ.*, 2013.

[26] A. H. Blackwell and E. Manar, "Prototype," *UXL Encyclopedia of Science(3rd ed.)*. Gale, part of Cengage Group, 2015. [Online]. Available: https://go.gale.com/ps/i.do?p=SCIC&u=dclib_main&id=GALE%7CENKDZQ 347975681&v=2.1&it=r&sid=SCIC&asid=0c8f739d

[27] M. Koechlin and É. Nouguier, "Eiffel Tower early sketch by Maurice Koechlin (photograph - licensed under Public Domain: https://en.wikipedia.org/wiki/Public_domain)," *Wikimedia*, 1884. https://commons.wikimedia.org/wiki/File:Maurice_koechlin_pylone.jpg (accessed Apr. 29, 2023).

[28] Myrabella, "Eiffel Tower (photograph - licensed under CC BY-SA 3.0: https://creativecommons.org/licenses/by-sa/3.0/)," *Wikimedia*, 2012. https://commons.wikimedia.org/wiki/File:Eiffel_tower_from_Cite_Architectur e_Chaillot.jpg (accessed Apr. 29, 2023).

[29] Biso, "BMW 1 Series Coupé, clay model, BMW Museum, Munich, Germany (photograph - licensed under CC BY 3.0: https://creativecommons.org/licenses/by/3.0/deed.en)," *Wikimedia*, 2009. https://commons.m.wikimedia.org/wiki/File:BMW_1_Series_model.jpg (accessed Apr. 29, 2023).

[30] M 93, "BMW 1er M Coupé E82 (photograph - licensed under CC BY-SA 3.0 DE: https://creativecommons.org/licenses/by-sa/3.0/de/deed.en)," *Wikimedia*, 2013. https://commons.m.wikimedia.org/wiki/File:BMW_1er_M_Coupé_(E82)_–_Heckansicht,_1._Juni_2013,_Düsseldorf.jpg (accessed Apr. 29, 2023).

[31] CTBUH, "Cities by Number of 150m+ Buildings," 2023. https://www.skyscrapercenter.com/cities (accessed Apr. 29, 2023).

[32] A. Shahabian and A. Fadai, "Intelligent Parametric BIM Solution and Optimizer for Diagrid High-rise Structures," in *5th Vienna young Scientists Symposium (VSS2019)*, Vienna: TU Wien, 2019, pp. 42–43. [Online].

Available:
https://vss2019.abstracts.eu/90ea968553ba92845e363c9848b7e168.html

[33] B. Durakovic, "Design of experiments application, concepts, examples: State of the art," *Period. Eng. Nat. Sci.*, 2017, doi: 10.21533/pen.v5i3.145.

[34] A. Schlueter and P. Geyer, "Linking BIM and Design of Experiments to balance architectural and technical design factors for energy performance," *Autom. Constr.*, 2018, doi: 10.1016/j.autcon.2017.10.021.

[35] T. Whalen and G. Churchill, "Decisions under uncertainty." Robinson College of Business Georgia State University, 1971.

[36] K. Al-Kodmany, "The sustainability of tall building developments: A conceptual framework," *Buildings*. 2018. doi: 10.3390/buildings8010007.

[37] M. M. Ali and K. Al-Kodmany, "Tall buildings and Urban habitat of the 21st century: A global perspective," *Buildings*, 2012, doi: 10.3390/buildings2040384.

[38] P. Oldfield, D. Trabucco, and A. Wood, "Five energy generations of tall buildings: An historical analysis of energy consumption in high-rise buildings," *J. Archit.*, 2009, doi: 10.1080/13602360903119405.

[39] P. Oldfield, D. Trabucco, and A. Wood, "Five energy generations of tall buildings," in *The Sustainable Tall Building*, 2019. doi: 10.4324/9781315695686-3.

[40] K. Al-Kodmany, "Sustainability and the 21st century vertical city: A review of design approaches of tall buildings," *Buildings*. 2018. doi: 10.3390/buildings8080102.

[41] M. M. Ali and K. S. Moon, "Advances in structural systems for tall buildings: Emerging developments for contemporary urban giants," *Buildings*. 2018. doi: 10.3390/buildings8080104.

[42] M. M. Ali and K. S. Moon, "Structural Developments in Tall Buildings: Current Trends and Future Prospects," *Archit. Sci. Rev.*, vol. 50, no. 3, pp. 205–223, 2007, doi: 10.3763/asre.2007.5027.

[43] "Architectural engineer," *McGraw-Hill Dictionary of Scientific & Technical Terms, 6E.*, 2003. https://encyclopedia2.thefreedictionary.com/Architectural+engineer (accessed Mar. 10, 2023).

[44] American Society of Civil Engineers (ASCE), "Architectural Engineering Institute (AEI)," 2022. https://www.asce.org/communities/institutes-and-technical-groups/architectural-engineering-institute (accessed Mar. 10, 2023).

[45] The University of Texas at Austin, "What is Architectural Engineering?," 2019. https://www.caee.utexas.edu/architectural/whatisarche (accessed May 05, 2019).

[46]   Merriam-Webster, "Architectural engineering," 2023. https://www.merriam-webster.com/dictionary/architectural engineering (accessed Mar. 10, 2023).

[47]   G. Hammond and C. Jones, *Inventory of Carbon and Energy (ICE) Version 2.0*. Sustainable Energy Research Team (SERT), University of Bath, 2011.

[48]   C. Jones and G. Hammond, *Inventory of Carbon and Energy (ICE) Version 3.0*. Circular Ecology and University of Bath, 2019.

[49]   Lhzss8, "Shenzhen Rural Commercial Bank Headquarters (photograph - licensed under CC BY-SA 4.0: https://creativecommons.org/licenses/by-sa/4.0/deed.en)," *Wikimedia*, 2022. https://commons.wikimedia.org/wiki/File: 深圳农商银行大厦.jpg (accessed May 01, 2023).

[50]   Simsalabimbam, "Former Wholesale Market Hall (view from east) and constructsite of the new ECB building, in Frankfurt am Main, Germany (photograph - licensed under CC BY-SA 3.0: https://creativecommons.org/licenses/by-sa/3.0/deed.en)," *Wikimedia*, 2012. https://commons.m.wikimedia.org/wiki/File:European_Central_Bank_-_new_building_under_construction_-_Frankfurt_-_Germany_-_16.jpg (accessed May 01, 2023).

[51]   N. Nagel, "New building of the European Central Bank in Frankfurt Main, Germany (photograph - licensed under CC BY-SA 3.0: https://creativecommons.org/licenses/by-sa/3.0/deed.en)," *Wikimedia*, 2014. https://commons.m.wikimedia.org/wiki/File:European_Central_Bank_-_building_under_construction_-_Frankfurt_-_Germany_-_14.jpg (accessed May 01, 2023).

[52]   O. P. Gbenebor, S. O. Adeosun, A. A. Adegbite, and C. Akinwande, "Organic and mineral acid demineralizations: effects on crangon and Liocarcinus vernalis–sourced biopolymer yield and properties," *J. Taibah Univ. Sci.*, 2018, doi: 10.1080/16583655.2018.1525845.

[53]   C. Molnar and J. Gair, "19.1 Types of Skeletal Systems," *NSCC Academic Biology 1050*, 2022. https://pressbooks.nscc.ca/biology1050/chapter/19-1-types-of-skeletal-systems/ (accessed Aug. 29, 2023).

[54]   Y. Akmal *et al.*, "A comprehensive description of the exoskeleton of six Lobster species (Genus Panulirus) in Aceh Province, Indonesia," *Fish. Res.*, 2023, doi: 10.1016/j.fishres.2023.106731.

[55]   L. Melton, "Noma: from grasshopper brews to age-old 'garum,'" *Nature biotechnology*. 2022. doi: 10.1038/s41587-022-01622-6.

[56]   M. Mahboub, M. Hassan, A. Bream, A. Mohamed, and M. Abdel-Samad, "Preparation, Characterization and Anticancer Activity of Chitosan Prepared from the American Cockroach, Periplaneta americana," *Egypt. Acad. J. Biol. Sci. A, Entomol.*, 2021, doi: 10.21608/eajbsa.2021.185450.

[57]   F. Sado, H. J. Yap, R. A. R. Ghazilla, and N. Ahmad, "Design and control of a

wearable lower-body exoskeleton for squatting and walking assistance in manual handling works," *Mechatronics*, 2019, doi: 10.1016/j.mechatronics.2019.102272.

[58]   C. Siviy *et al.*, "Opportunities and challenges in the development of exoskeletons for locomotor assistance," *Nature Biomedical Engineering*. 2023. doi: 10.1038/s41551-022-00984-1.

[59]   A. López-González, J. Tejada, and J. López-Romero, "Review and Proposal for a Classification System of Soft Robots Inspired by Animal Morphology," *Biomimetics*, 2023, doi: 10.3390/biomimetics8020192.

[60]   H. Hillewaert, "Liocarcinus vernalis (Risso, 1816) (photograph - licensed under CC BY-SA 4.0: https://creativecommons.org/licenses/by-sa/4.0/deed.en)," *Wikimedia*, 2004. https://commons.wikimedia.org/wiki/File:Liocarcinus_vernalis.jpg (accessed May 01, 2023).

[61]   Wikipedian Prolific and Wilfredor, "Morphology and Locomotive system of Equus ferus caballus (a common horse) (image - licensed under CC BY-SA 3.0: https://creativecommons.org/licenses/by-sa/3.0/deed.en)," *Wikimedia*, 2015. https://commons.m.wikimedia.org/wiki/File:Horse_anatomy.svg (accessed May 01, 2023).

[62]   T. Quine, "Tortoise skeleton cross-section (photograph - licensed under CC BY-SA 4.0: https://creativecommons.org/licenses/by-sa/4.0/deed.en)," *Wikimedia*, 2017. https://commons.m.wikimedia.org/wiki/File:Turtle_skeleton_cross-section_(28053263449).jpg (accessed May 01, 2023).

[63]   DARPA, "DARPA Exoskeleton (photograph - licensed under Public Domain: https://commons.m.wikimedia.org/wiki/Commons:Licensing#Material_in_the_public_domain)," *Wikimedia*, 2007. https://commons.m.wikimedia.org/wiki/File:DARPA_Exoskeleton.tiff#mw-jump-to-license (accessed May 01, 2023).

[64]   S. Jurvetson, "An electrically powered exoskeleton suit currently in development by Tsukuba University of Japan (photograph - licensed under CC BY 2.0: https://creativecommons.org/licenses/by/2.0/deed.en)," *Wikimedia*, 2005. https://commons.m.wikimedia.org/wiki/File:Hybrid_Assistive_Limb.jpg (accessed May 01, 2023).

[65]   CTBUH, *CTBUH Height Criteria for Measuring & Defining Tall Buildings*. CTBUH, 2023. [Online]. Available: https://cloud.ctbuh.org/CTBUH_HeightCriteria.pdf

[66]   Skyscrapercenter.com, "Commerzbank Tower, Frankfurt am Main," 2023. https://www.skyscrapercenter.com/building/commerzbank-tower/780 (accessed Aug. 18, 2023).

[67]   International Organization for Standardization (ISO), *ISO 14025:2006*

Environmental labels and declarations — Type III environmental declarations — Principles and procedures. International Organization for Standardization (ISO), 2006. [Online]. Available: https://www.iso.org/standard/38131.html

[68]   BSI, "BS EN 15804:2012+A2:2019 - Standards Publication Sustainability of construction works — Environmental product declarations — Core rules for the product category of construction products," 2019.

[69]   Worldometer, "Hong Kong Population," 2023. https://www.worldometers.info/world-population/china-hong-kong-sar-population/ (accessed Mar. 11, 2023).

[70]   Worldometer, "Population Density of Vienna," 2023. https://worldpopulationreview.com/world-cities/vienna-population (accessed Mar. 11, 2023).

[71]   L. K. P. Lau, W. C. L. Lai, and C. W. D. Ho, "Quality of life in a 'high-rise lawless slum': A study of the 'Kowloon Walled City,'" *Land use policy*, 2018, doi: 10.1016/j.landusepol.2018.04.047.

[72]   CTBUH, "Makkah Royal Clock Tower," 2023. https://www.skyscrapercenter.com/building/makkah-royal-clock-tower/84#tab-research (accessed Mar. 12, 2023).

[73]   K. Al-Kodmany and M. M. Ali, *The future of the city: tall buildings and urban design*, vol. 50, no. 12. Southampton, UK: WIT press, 2013. doi: 10.5860/choice.50-6573.

[74]   H. Ritchie and M. Roser, "Urbanization," *Our World Data*, 2018, [Online]. Available: https://ourworldindata.org/urbanization

[75]   Department of Economic and Social Affairs Population Division, "World Population Prospects 2022 Summary of Results," United Nations, New York, 2022. [Online]. Available: https://www.un.org/development/desa/pd/sites/www.un.org.development.desa.pd/files/wpp2022_summary_of_results.pdf

[76]   M. F. Neves, "The food business environment and the role of China and Brazil building a 'food bridge,'" *China Agric. Econ. Rev.*, 2010, doi: 10.1108/17561371011017478.

[77]   CTBUH, "Petronas Towers Kuala Lumpur," 2023. https://www.skyscrapercenter.com/complex/154 (accessed Mar. 11, 2023).

[78]   CTBUH, *CTBUH Video Interview - Adrian Smith*, (2015). [Online]. Available: https://www.youtube.com/watch?v=OZAR2CQ2FiI

[79]   D. B. Audretsch, "Agglomeration and the location of innovative activity," *Oxford Rev. Econ. Policy*, 1998, doi: 10.1093/oxrep/14.2.18.

[80]   S. Jang, J. Kim, and M. von Zedtwitz, "The importance of spatial agglomeration in product innovation: A microgeography perspective," *J. Bus.*

Res., 2017, doi: 10.1016/j.jbusres.2017.05.017.

[81] Y. M. Yeung, "High-rise, high-density housing: Myths and reality," *Habitat Int.*, 1977, doi: 10.1016/0197-3975(77)90031-5.

[82] M. Andersson and H. Lööf, "Agglomeration and productivity: Evidence from firm-level data," *Ann. Reg. Sci.*, 2011, doi: 10.1007/s00168-009-0352-1.

[83] G. K. Dreicer, S. B. Landau, and C. W. Condit, "The Rise of the New York Skyscraper, 1865-1913," *Technol. Cult.*, 1997, doi: 10.2307/3106882.

[84] R. Kavilkar and S. Patil, "Study of High Rise Residential Buildings in Indian Cities (A Case Study –Pune City)," *Int. J. Eng. Technol.*, 2014, doi: 10.7763/ijet.2014.v6.671.

[85] R. Tavernor, "Visual and cultural sustainability: The impact of tall buildings on London," *Landsc. Urban Plan.*, 2007, doi: 10.1016/j.landurbplan.2007.05.010.

[86] E. Zaidan, "Cultural-based challenges of the westernised approach to development in newly developed societies," *Dev. Pract.*, 2019, doi: 10.1080/09614524.2019.1598935.

[87] W. K. E. Osterhaus, "Office lighting: A review of 80 years of standards and recommendations," in *Conference Record - IAS Annual Meeting (IEEE Industry Applications Society)*, 1993. doi: 10.1109/ias.1993.299211.

[88] Government of Dubai and Dubai Municipality, *Al Sa'fat - Dubai Green Building System - Version 2.0*, Version 2. Dubai: Dubai Municipality, 2020.

[89] European Standards, *BS EN 12464-1:2021 Light and lighting. Lighting of work places Indoor work places–Part 1: Indoor Work Places*. European Standards, 2021. [Online]. Available: https://www.en-standard.eu/bs-en-12464-1-2021-light-and-lighting-lighting-of-work-places-indoor-work-places/

[90] Chicago Architectural Photographing Company, "Home Insurance Building (photograph - licensed under Public Domain: https://en.wikipedia.org/wiki/Public_domain)," *Wikimedia*. https://en.wikipedia.org/wiki/File:Home_Insurance_Building.JPG (accessed May 03, 2023).

[91] AlexanderUtz, "The Fine Arts Building on Michigan Avenue (photograph - licensed under CC BY-SA 4.0: https://creativecommons.org/licenses/by-sa/4.0/deed.en)," *Wikimedia*, 2023. https://commons.wikimedia.org/wiki/File:Fine_Arts_Building_Facade,_2023.png (accessed May 03, 2023).

[92] T. Hisgett, "Manhattan Municipal Building (photograph - licensed under CC BY 2.0: https://creativecommons.org/licenses/by/2.0/deed.en)," *Wikimedia*, 2011. https://en.wikipedia.org/wiki/File:Manhattan_Municipal_Building_(6215147594).jpg (accessed May 03, 2023).

[93]   M. A. Weiss, "Skyscraper zoning: New york's pioneering role," *J. Am. Plan. Assoc.*, 1992, doi: 10.1080/01944369208975794.

[94]   R. Obermaier, "Chrysler Building from the SUMMIT at One Vanderbilt (photograph - licensed under CC BY-SA 4.0: https://creativecommons.org/licenses/by-sa/4.0/deed.en)," *Wikimedia*, 2021. https://commons.wikimedia.org/wiki/File:Chrysler_Building_Nov_2021.jpg (accessed May 06, 2023).

[95]   J. Ravi, "Chicago Board of Trade Building in Chicago, Illinois, USA (photograph - licensed under CC BY-SA 3.0: https://creativecommons.org/licenses/by-sa/3.0/deed.en)," *Wikimedia*, 2011. https://commons.wikimedia.org/wiki/File:Chicago_Board_Of_Trade_Building _%28altered_filtration_version%29.jpg (accessed May 06, 2023).

[96]   E. W. Wolner, "Form Follows Finance: Skyscrapers and Skylines in New York and Chicago Carol Willis Here's the Deal: The Buying and Selling of a great American City Ross Miller," *J. Soc. Archit. Hist.*, 1996, doi: 10.2307/991152.

[97]   M. Pauken, "Sleeping soundly on summer nights: A history of air conditioning in the home," *ASHRAE J.*, 1999.

[98]   Chicago Daily Tribune, "Air Conditioning for the Tribune Tower," p. 14, Jun. 10, 1934.

[99]   P. Marquis *et al.*, "Window wall and curtain wall: An objective review," in *6th CSCE-CRC International Construction Specialty Conference 2017 - Held as Part of the Canadian Society for Civil Engineering Annual Conference and General Meeting 2017*, 2017.

[100] C. Schittich, G. Staib, D. Balkow, M. Schuler, and W. Sobek, *Glass construction manual*. Walter de Gruyter, 2012.

[101] K. Ohyama, "Seagram Building (photograph - licensed under CC BY-SA 2.0: https://creativecommons.org/licenses/by-sa/2.0/deed.en)," *Wikimedia*, 2017. https://commons.wikimedia.org/wiki/File:Seagram_Building_%283509830711 6%29.jpg (accessed May 08, 2023).

[102] Rs1421, "Shinjuku Mitsui Building. From the observatory floor of Tokyo Metropolitan Government Building (photograph - licensed under CC BY-SA 3.0: https://creativecommons.org/licenses/by-sa/3.0/deed.en)," *Wikimedia*, 2012. https://commons.wikimedia.org/wiki/File:Shinjuku-Mitsui-Building-01.jpg (accessed May 08, 2023).

[103] T. E. Johnson, "Low-e glazing design guide," *Archit. Press*, 1991.

[104] I. P. Knight and G. Dunn, "Evaluation of heat gains in UK office environments," in *Worldwide CIBSE/ASHRAE Gathering of the Building Services Industry*, 2003.

[105] IPCC, "Change, Intergovernmental Panel On Climate. Climate Change 2007: The physical science basis, summary for policy makers," 2007.

[106] A. Wood, "Green or grey? The aesthetics of tall building sustainability," in *CTBUH 2008, 8th World Congress - Tall and Green: Typology for a Sustainable Urban Future, Congress Proceedings*, 2008.

[107] Cmglee, "Mesiniaga Tower viewed from the Subang–Kelana Jaya Link (photograph - licensed under CC BY-SA 4.0: https://creativecommons.org/licenses/by-sa/4.0/deed.en)," *Wikimedia*, 2020. https://commons.wikimedia.org/wiki/File:Cmglee_Mesiniaga_Tower.jpg (accessed May 08, 2023).

[108] T. Wolf, "Commerzbank Tower Frankfurt (photograph - licensed under CC BY-SA 3.0 DE: https://creativecommons.org/licenses/by-sa/3.0/de/deed.de)," *2019*. https://commons.wikimedia.org/wiki/File:Commerzbank_Tower_Frankfurt.jpg (accessed May 08, 2023).

[109] D. Trabucco, "Historical Evolution of the Service Core," *CTBUH J.*, no. 1, pp. 42–47, 2010.

[110] D. Trabucco, "An analysis of the relationship between service cores and the embodied/running energy of tall buildings," in *Structural Design of Tall and Special Buildings*, 2008. doi: 10.1002/tal.477.

[111] D. Gissen, "Bigness vs. 'Green-ness': The Shared Global Ideology of the Big and the Green," *Thresholds*, 2003, doi: 10.1162/thld_a_00358.

[112] K. Yeang and R. Powell, "Designing the ecoskyscraper: Premises for tall building design," *Struct. Des. Tall Spec. Build.*, 2007, doi: 10.1002/tal.414.

[113] K. Al-kodmany, *The vertical city: a sustainable development model*. WIT press, 2018.

[114] K. Al-kodmany, *Eco-towers: Sustainable cities in the sky*. WIT press, 2015.

[115] A. Mahdavi, "What is the one true sustainable building?," *TEDxTUWien 2022 (https://repositum.tuwien.at/handle/20.500.12708/154399)*, 2022. https://www.youtube.com/watch?v=4GgkDMxVG7w (accessed Sep. 09, 2023).

[116] A. Mahdavi, "On the global planetary crisis: Are buildings the solution?," *Emerging Fields in Architecture*, 2021. https://www.youtube.com/watch?v=BIeNH80Aw4w&t=1753s (accessed Mar. 13, 2023).

[117] K. Al-kodmany and M. M. Ali, *The future of the city: Tall buildings and urban design*. WIT press, 2013.

[118] A. David, T. Bednar, M. Leeb, and H. Schöberl, "Planung, Ausführung und Betriebserfahrung eines Plus Energie Bürohochhauses," in *Bauphysik Kalender*, 2023. doi: 10.1002/9783433611289.ch16.

[119] J. Eberhardsteiner, "TU UniverCity," 2023. https://www.tuwien.at/tu-

wien/campus/tu-univercity (accessed Mar. 13, 2023).

[120] M. Samimi and F. Nasrollahi, *Intelligent Design using Solar-Climatic Vision: Energy and Comfort Improvement in Architecture and Urban Planning using SOLARCHVISION*. Berlin: Universitätsverlag der TU Berlin, 2014.

[121] M. Samimi, "Weather Data and Solar Orientations," in *Future City Architecture for Optimal Living*, Cham: Springer, 2015, pp. 221–240.

[122] R. Legg, "Room Heat Gains, Air Diffusion, and Air Flow Rates," in *Air Conditioning System Design*, 2017. doi: 10.1016/b978-0-08-101123-2.00005-4.

[123] CTBUH, "PIF Tower," 2023. https://www.skyscrapercenter.com/building/pif-tower/8774 (accessed Mar. 13, 2023).

[124] CTBUH, "KfW Westarkade," 2023. https://www.skyscrapercenter.com/building/kfw-westarkade/12268 (accessed Mar. 13, 2023).

[125] A. Drainville, "CBD - Doha, Qatar (photograph - licensed under CC BY-NC 2.0: https://creativecommons.org/licenses/by-nc/2.0/)," *Flickr*, 2015. https://www.flickr.com/photos/axelrd/16215359572 (accessed May 09, 2023).

[126] Marc.desbordes, "Burj Qatar, Doha, Qatar (photograph - licensed under CC BY-NC 2.0: https://creativecommons.org/licenses/by-nc/2.0/)," *Flickr*, 2014. https://www.flickr.com/photos/27294603@N05/12985873975 (accessed May 08, 2023).

[127] Dead.rabbit, "Salesforce Tower from Salesforce Park (photograph - licensed under CC BY-SA 4.0: https://creativecommons.org/licenses/by-sa/4.0/deed.en)," *Wikimedia*, 2021. ttps://commons.wikimedia.org/wiki/File:Salesforce_Tower_from_Salesforce_Park.jpg (accessed May 08, 2023).

[128] F. Ding and A. Kareem, "Tall Buildings with Dynamic Facade Under Winds," *Engineering*, 2020, doi: 10.1016/j.eng.2020.07.020.

[129] Inhabitat, "Al Bahr Towers by AEDAS (photograph - licensed under CC BY-NC-ND 2.0: https://creativecommons.org/licenses/by-nc-nd/2.0/)," *Flickr*, 2014. https://www.flickr.com/photos/inhabitat/12331034465 (accessed May 11, 2023).

[130] M. Posch, "Erste Campus - mehr als nur ein Arbeitsplatz," in *Innovationsinkubator Industriebau : Industrial Building as Innovation Incubator*, C. M. Achammer and I. Kovacic, Eds., Eigenverlag Wien, 2019. doi: 10.34726/969x-sr53.

[131] ERSTE Group, "Erste Campus," 2023. https://www.erstegroup.com/en/about-us/erste-campus (accessed Mar. 13, 2023).

[132] Henke Schreieck Architekten, "Erste Campus," 2023. https://www.henkeschreieck.at/index.php/projects/buero/erste-campus/

(accessed Mar. 13, 2023).

[133] CTBUH, "GSW Hauptverwaltung," 2023.
https://www.skyscrapercenter.com/building/gsw-hauptverwaltung/9331
(accessed Mar. 13, 2023).

[134] J. D. Holmes, *Wind Loading of Structure*. CRC press, 2018.

[135] P. Irwin *et al.*, "Wind and Tall Buildings – Negatives and Positives," *Struct. Des. Tall Spec. Build.*, pp. 915–928, 2008.

[136] K. Al-kodmany and M. M. Ali, "An overview of structural and aesthetic developments in tall buildings using exterior bracing and diagrid systems," *Int. J. High-Rise Build.*, pp. 271–291, 2016.

[137] S. Stephens, "0-14 Tower," *Architectural Record*, 2011.
https://www.architecturalrecord.com/articles/7866-0-14-tower (accessed May 12, 2023).

[138] K. Minner, "COR / Oppenheim Architecture + Design," *ArchDaily*, 2010.
https://www.archdaily.com/87063/cor-oppenheim-architecture-design (accessed May 12, 2023).

[139] ArchDaily, "170 Amsterdam / Handel Architects," *ArchDaily*, 2015.
https://www.archdaily.com/642475/170-amsterdam-handel-architects (accessed May 12, 2023).

[140] I. Block, "Zaha Hadid Architects unveils Morpheus hotel in Macau," *Dezeen*, 2018. https://www.dezeen.com/2018/06/15/zaha-hadid-architects-morpheus-hotel-in-macau-architecture/amp/ (accessed May 12, 2023).

[141] P. Pintos, "Brunel Building / Fletcher Priest Architects," *ArchDaily*, 2020.
https://www.archdaily.com/949559/brunel-building-fletcher-priest-architects (accessed May 12, 2023).

[142] R. S. Aouf, "SOM unveils 'breathing' Shenzhen bank tower enclosed in diagrid," *Dezeen*, 2022. https://www.dezeen.com/2022/01/06/som-rural-commercial-bank-headquarters-shenzhen-architecture/ (accessed May 12, 2023).

[143] CTBUH, "875 North Michigan Avenue," 2023.
https://www.skyscrapercenter.com/building/875-north-michigan-avenue/345 (accessed Mar. 13, 2023).

[144] CTBUH, "Willis Tower," 2023.
https://www.skyscrapercenter.com/building/willis-tower/169 (accessed Mar. 13, 2023).

[145] A. Astaneh-Asl, "Progressive collapse prevention in new and existing buildings," in *9th Arab Structural Engineering Conference*, Abu Dhabi, UAE, 2003.

[146] K. S. Moon, J. J. Connor, and J. E. Fernandez, "Diagrid structural systems for tall buildings: Characteristics and methodology for preliminary design," *Struct. Des. Tall Spec. Build.*, 2007, doi: 10.1002/tal.311.

[147] *Minimum Design Loads for Buildings and Other Structures, SEI/ASCE 7-02*. American Society of Civil Engineers (ASCE), 1996. doi: 10.1061/9780784406243.

[148] K. S. Moon, "Optimal grid geometry of diagrid structures for tall buildings," *Archit. Sci. Rev.*, 2008, doi: 10.3763/asre.2008.5129.

[149] K. S. Moon, "Sustainable structural engineering strategies for tall buildings," *Struct. Des. Tall Spec. Build.*, vol. 17, no. 5, pp. 895–914, 2008, doi: 10.1002/tal.475.

[150] K. S. Moon, "Stiffness-based design methodology for steel braced tube structures: A sustainable approach," *Eng. Struct.*, 2010, doi: 10.1016/j.engstruct.2010.06.004.

[151] K. S. Moon, "Diagrid Systems for Structural Design of Complex-Shaped Tall Buildings," *Int. J. High-Rise Build.*, 2016, doi: 10.21022/ijhrb.2016.5.4.243.

[152] K. S. Moon, "Outrigger Systems for Structural Design of Complex-Shaped Tall Buildings," *Int. J. High-Rise Build.*, 2016, doi: 10.21022/ijhrb.2016.5.1.13.

[153] K. Moon, "Comparative evaluation of diagrid and braced tube structures for tall buildings," in *Structures and Architecture - Proceedings of the 3rd International Conference on Structures and Architecture, ICSA 2016*, 2016. doi: 10.1201/b20891-176.

[154] K. S. Moon, "Studies on various structural system design options for twisted tall buildings and their performances," *Struct. Des. Tall Spec. Build.*, 2014, doi: 10.1002/tal.1038.

[155] K. S. Moon, "Comparative evaluation of structural systems for tapered tall buildings," *Buildings*, 2018, doi: 10.3390/buildings8080108.

[156] K. S. Moon, "Structural performance of superframed conjoined towers," *Struct. Des. Tall Spec. Build.*, 2021, doi: 10.1002/tal.1857.

[157] K. S. Moon, "Developments of structural systems toward mile-high towers," *Int. J. High-Rise Build.*, 2018, doi: 10.21022/IJHRB.2018.7.3.197.

[158] Austrian Standards International, *ÖNORM EN 15643:2021 - Sustainability of construction works - Framework for assessment of buildings and civil engineering works*. 2021. [Online]. Available: https://shop.austrian-standards.at/action/en/public/details/709936/OENORM_EN_15643_2021_12_15

[159] Austrian Standards International, *ÖNORM EN 1990:2021-10 - Eurocode - Basis of structural and geotechnical design*. 2021. [Online]. Available: https://shop.austrian-

standards.at/action/en/public/details/707080/OENORM_EN_1990_2021_10_0
1

[160] S. Suh *et al.*, "System Boundary Selection in Life-Cycle Inventories Using Hybrid Approaches," *Environmental Science and Technology*. 2004. doi: 10.1021/es0263745.

[161] A. Zamagni, P. Buttol, P. P.L., B. R., and M. P., "Critical review of the current research needs and limitations related to ISO-LCA practice," *Deliv. D7 Work Packag. 5 CALCAS Proj.*, 2008.

[162] International Organization for Standardization, *ISO 14040 + Amd 1:2020-Environmental management - Life Cycle Assessment - Principles and Framework*. 2020. doi: 10.1016/j.ecolind.2011.01.007.

[163] International Organization for Standardization, *ISO 14044:2006 + Amd 1:2017; Environmental management — Life cycle assessment — Requirements and guidelines*. International Organization for Standardization, 2017. [Online]. Available: https://www.iso.org/standard/38498.html

[164] Austrian Standards International, *ÖNORM EN 15978-1 - Sustainability of construction works — Methodology for the assessment of performance of buildings — Part 1: Environmental Performance*. European Committee for Standardization, 2021.

[165] K. Young, *LIFE CYCLE ASSESSMENT (LCA) OF ISOLATEK INTERNATIONAL PASSIVE FIRE PROTECTION PRODUCTS*. Sustainable Minds, 2019. [Online]. Available: https://transparencycatalog.com/assets/uploads/pdf/Isolatek_Products_Public_Verified_LCA_Aprl2019.pdf

[166] D. P. Bentz, C. F. Ferraris, and K. A. Snyder, "Best Practices Guide for High-Volume Fly Ash Concretes : Assuring Properties and Performance," 2013. doi: 10.6028/NIST.TN.1812.

[167] A. P. Fantilli and B. Chiaia, "Eco-mechanical performances of cement-based materials: An application to self-consolidating concrete," *Constr. Build. Mater.*, 2013, doi: 10.1016/j.conbuildmat.2012.09.075.

[168] ASCE, "ASCE 2019 Best Paper Award," 2023. https://ascelibrary.org/jaeied/best_paper_awards (accessed Mar. 15, 2023).

[169] J. H. Holland, *Adaptation in natural and artificial systems : an introductory analysis with applications to biology, control, and artificial intelligence*. 1975.

[170] X.-S. Yang, *Nature-Inspired Optimization Algorithms*, 2nd ed. Elsevier, 2020. [Online]. Available: https://www.elsevier.com/books/nature-inspired-optimization-algorithms/yang/978-0-12-821986-7

[171] K. Miettinen, *Nonlinear Multiobjective Optimization*. Elsevier, 1998. [Online]. Available: https://link.springer.com/book/10.1007/978-1-4615-5563-6

270

[172] K. Deb, *Multi-Objective Optimization using Evolutionary Algorithms*. Wiley, 2001. [Online]. Available: https://www.wiley.com/en-us/Multi+Objective+Optimization+using+Evolutionary+Algorithms-p-9780471873396

[173] R. Lapisa, "The effect of building geometric shape and orientation on its energy performance in various climate regions," *Int. J. GEOMATE*, 2019, doi: 10.21660/2019.53.94984.

[174] J. Helal, A. Stephan, and R. H. Crawford, "The influence of structural design methods on the embodied greenhouse gas emissions of structural systems for tall buildings," *Structures*, 2020, doi: 10.1016/j.istruc.2020.01.026.

[175] D. C. Montgomery, *Design and analysis of experiments*, Ninth Edit. John Wiley & Sons, 2017.

[176] BotMultichill and Elekhh, "30 St Mary Axe, 'Gherkin' (photograph - licensed under Public Domain: https://en.wikipedia.org/wiki/Public_domain)," *Wikimedia*, 2007. https://commons.wikimedia.org/wiki/File:30_St_Mary_Axe,_%27Gherkin%27 .JPG (accessed May 15, 2023).

[177] Fastily, "30 St Mary Axe 7 (photograph - licensed under CC BY-SA 3.0: https://creativecommons.org/licenses/by-sa/3.0/deed.en)," *Wikimedia*, 2012. https://commons.wikimedia.org/wiki/File:30_St_Mary_Axe_7_2012-07-03.jpg (accessed May 15, 2023).

[178] M. Hillary, "View from the Gherkin (photograph - licensed under CC BY 2.0: https://creativecommons.org/licenses/by/2.0/)," *Flickr*, 2009. https://www.flickr.com/photos/markhillary/3930474913 (accessed May 15, 2023).

[179] Godsfriendchuck, "One Thousand Museum seen on 20 March 2019 (photograph – licensed under CC BY-SA 4.0: https://creativecommons.org/licenses/by-sa/4.0/deed.en)," *Wikimedia*, 2019. https://commons.wikimedia.org/wiki/File:One_Thousand_Museum_March_20 19.jpg (accessed May 15, 2023).

[180] Government of Dubai, "Al Sa'fat - Dubai Green Building Evaluation System," 2016, [Online]. Available: https://www.dm.gov.ae/en/Business/DubaiCentralLaboratory/ProductCertificat ionServices/Documents/Green Building Certification/AL-SA%27FAT.pdf

[181] Government of Dubai, *Green Building Regulations & Specifications*. Dubai: Dubai Electricity and Water Authority, 2016. [Online]. Available: https://www.dewa.gov.ae/~/media/Files/Consultants and Contractors/Green Building/Greenbuilding_Eng.ashx

[182] B. Bolker, "How do you deal with factors, in factorial design, when some or all levels of a factor are meaningless for one or some levels of another factor?," 2019. https://stats.stackexchange.com/q/424666 (accessed May 03, 2020).

[183] S. A. Miller, "Supplementary cementitious materials to mitigate greenhouse gas emissions from concrete: can there be too much of a good thing?," *J. Clean. Prod.*, 2018, doi: 10.1016/j.jclepro.2018.01.008.

[184] M. Amran, S. Debbarma, and T. Ozbakkaloglu, "Fly ash-based eco-friendly geopolymer concrete: A critical review of the long-term durability properties," *Construction and Building Materials*. 2021. doi: 10.1016/j.conbuildmat.2020.121857.

[185] T. Y. Duvallet, M. Mahmoodabadi, A. E. Oberlink, T. L. Robl, and R. B. Jewell, "Production of α′H-belite-CSA cement at low firing temperatures," *Cem. Concr. Compos.*, 2022, doi: 10.1016/j.cemconcomp.2022.104820.

[186] R. Xiao, B. Huang, H. Zhou, Y. Ma, and X. Jiang, "A state-of-the-art review of crushed urban waste glass used in OPC and AAMs (geopolymer): Progress and challenges," *Cleaner Materials*. 2022. doi: 10.1016/j.clema.2022.100083.

[187] E. Samariddin Sadriddin O'g'li, A. Hilola, S. Qizi, J. Yigitali, and J. ' Ra O'g'li, "INGREDIENT OF PORTLAND CEMENT," *Int. Bull. Appl. Sci. Technol.*, 2022, [Online]. Available: https://www.researchcitations.com/index.php/ibast/article/view/60

[188] A. Bosoaga, O. Masek, and J. E. Oakey, "CO2 Capture Technologies for Cement Industry," in *Energy Procedia*, 2009. doi: 10.1016/j.egypro.2009.01.020.

[189] R. M. Andrew, "Global CO2 emissions from cement production, 1928-2018," *Earth System Science Data*. 2019. doi: 10.5194/essd-11-1675-2019.

[190] V. M. Malhotra, "Making concrete 'greener' with fly ash," *Concr. Int.*, vol. 5, no. 21, pp. 61–66, 1999.

[191] A. A. Phul, M. J. Memon, S. N. R. Shah, and A. R. Sandhu, "GGBS And Fly Ash Effects on Compressive Strength by Partial Replacement of Cement Concrete," *Civ. Eng. J.*, 2019, doi: 10.28991/cej-2019-03091299.

[192] M. P. Kumar, V. Srinivas, and M. Z. Nawaz, "Experimental investigation on high strength concrete using GGBS, FLYASH & Sp-430 Super Plasticizer," *Int. J. Civ. Eng. Technol.*, 2017.

[193] C. Fan and S. A. Miller, "Reducing greenhouse gas emissions for prescribed concrete compressive strength," *Constr. Build. Mater.*, 2018, doi: 10.1016/j.conbuildmat.2018.02.092.

[194] Z. Giergiczny, "Fly ash and slag," *Cement and Concrete Research*. 2019. doi: 10.1016/j.cemconres.2019.105826.

[195] Government of Dubai, *Dubai Building Code*, 2021st ed. Government of Dubai, 2021. [Online]. Available: https://dm.gov.ae/wp-content/uploads/2021/12/Dubai Building Code_English_2021 Edition_compressed.pdf

[196] A. N. Angelakis *et al.*, "Desalination: From ancient to present and future," *Water (Switzerland)*. 2021. doi: 10.3390/w13162222.

[197] X. Jia, J. J. Klemeš, P. S. Varbanov, and S. R. W. Alwi, "Analyzing the energy consumption, GHG emission, and cost of seawater desalination in China," *Energies*, 2019, doi: 10.3390/en12030463.

[198] A. S. Bello, N. Zouari, D. A. Da'ana, J. N. Hahladakis, and M. A. Al-Ghouti, "An overview of brine management: Emerging desalination technologies, life cycle assessment, and metal recovery methodologies," *Journal of Environmental Management*. 2021. doi: 10.1016/j.jenvman.2021.112358.

[199] P. Peduzzi, "Sand, rarer than one thinks," *Environ. Dev.*, vol. 11, pp. 208–218, 2014, doi: 10.1016/j.envdev.2014.04.001.

[200] M. Gucwa and A. Schäfer, "The impact of scale on energy intensity in freight transportation," *Transp. Res. Part D Transp. Environ.*, vol. 23, pp. 41–49, 2013, doi: 10.1016/j.trd.2013.03.008.

[201] X. Yin *et al.*, "China's transportation energy consumption and CO2 emissions from a global perspective," *Energy Policy*, vol. 82, no. 1, pp. 233–248, 2015, doi: 10.1016/j.enpol.2015.03.021.

[202] DB Group, "Facts and figures 2017," *Deutsche Bahn*. https://www.deutschebahn.com/en/group/ataglance/facts_figures-1776344 (accessed Aug. 30, 2018).

[203] carboncare, "CO2 Emissions Calculator for transport and logistics," 2023. https://www.carboncare.org/en/co2-emissions-calculator (accessed Oct. 09, 2023).

[204] G. P. Hammond and C. I. Jones, "Embodied energy and carbon in construction materials," no. May, pp. 87–98, 2008, doi: 10.1680/ener.2008.161.2.87.

[205] A. García-Olivares, J. Solé, and O. Osychenko, "Transportation in a 100% renewable energy system," *Energy Convers. Manag.*, vol. 158, no. August 2017, pp. 266–285, 2018, doi: 10.1016/j.enconman.2017.12.053.

[206] J. Schoof, "Built on sand: Is the construction boom depleting supplies?," *Detail*. https://www.detail-online.com/article/built-on-sand-is-the-construction-boom-depleting-supplies-16825/# (accessed Oct. 10, 2019).

[207] W. Goetzler, M. Guernsey, J. Young, and J. Fuhrman, "The Future of Air Conditioning for Buildings," 2016.

[208] Deep (https://physics.stackexchange.com/users/122958/deep), "Is there some theoretical maximum coefficient of performance (COP) for heat pumps and chillers?," *Physics Stack Exchange*, 2017. https://physics.stackexchange.com/a/350906 (accessed Sep. 19, 2023).

[209] M. Pattison *et al.*, *Solid-State Lighting 2017 - Suggested Research Topics Supplement: Technology and Market Context*. U.S. Department of Energy -

Energy Efficiency & Renewable Energy - Building Technologies Program, 2017. [Online]. Available: https://www.energy.gov/sites/prod/files/2017/09/f37/ssl_supplement_suggested-topics_sep2017_0.pdf

[210] Schoeck, "Thermal insulation (Isokorb®)," 2023. https://www.schoeck.com/en/isokorb (accessed Sep. 19, 2023).

[211] Schoeck, "Schöck Sconnex®," 2023. https://www.schoeck.com/en/sconnex (accessed Sep. 19, 2023).

[212] Farrat, "STRUKTRA^TM - Structural Thermal Breaks," 2023. https://farrat.com/category/structural-thermal-breaks/ (accessed Sep. 19, 2023).

[213] S. E. Belcher, J. N. Hacker, and D. S. Powell, "Constructing design weather data for future climates," *Build. Serv. Eng. Res. Technol.*, 2005, doi: 10.1191/0143624405bt112oa.

[214] F. Mostafavi, M. Tahsildoost, and Z. S. Zomorodian, "Energy efficiency and carbon emission in high-rise buildings: A review (2005-2020)," *Building and Environment*. 2021. doi: 10.1016/j.buildenv.2021.108329.

[215] R. Giridharan, S. Ganesan, and S. S. Y. Lau, "Daytime urban heat island effect in high-rise and high-density residential developments in Hong Kong," *Energy Build.*, 2004, doi: 10.1016/j.enbuild.2003.12.016.

[216] R. Priyadarsini, W. N. Hien, and C. K. Wai David, "Microclimatic modeling of the urban thermal environment of Singapore to mitigate urban heat island," *Sol. Energy*, 2008, doi: 10.1016/j.solener.2008.02.008.

[217] S. T. Mansouri and E. Zarghami, "Investigating the effect of the physical layout of the architecture of high-rise buildings, residential complexes, and urban heat islands," *Energy Built Environ.*, 2023, doi: 10.1016/j.enbenv.2023.07.004.

[218] A. Aboelata and S. Sodoudi, "Evaluating urban vegetation scenarios to mitigate urban heat island and reduce buildings' energy in dense built-up areas in Cairo," *Build. Environ.*, 2019, doi: 10.1016/j.buildenv.2019.106407.

[219] Z. A. Rahaman *et al.*, "Assessing the impacts of vegetation cover loss on surface temperature, urban heat island and carbon emission in Penang city, Malaysia," *Build. Environ.*, 2022, doi: 10.1016/j.buildenv.2022.109335.

[220] Bbrannon4 (UnmetHours.com), "What software can integrally simulate CFD and energy?," 2018. https://unmethours.com/question/29072/what-software-can-integrally-simulate-cfd-and-energy/ (accessed Feb. 03, 2023).

[221] C. Mackey, "PET evaluation problem," 2016. https://discourse.ladybug.tools/t/pet-evaluation-problem/1157/6 (accessed Sep. 09, 2023).

[222] Ladybug Tools LLC, "What is Dragonfly?"

https://www.ladybug.tools/dragonfly.html (accessed Sep. 13, 2023).

[223]   B. Bueno, "Urban Weather Generator (UWG)," *Ladybug Tools*, 2023. https://github.com/ladybug-tools/uwg (accessed Sep. 13, 2023).

[224]   L. Khalidi, "The Destruction of Yemen and Its Cultural Heritage," *Int. J. Middle East Stud.*, 2017, doi: 10.1017/S0020743817000691.

[225]   M. M. AlAttar, D. M. Sadek, and S. Ali Ayoub, "Recycling of Industrial and Agricultural Wastes in Compressed Stabilized Earth Blocks for Sustainable Development," *Int. J. Adv. Eng. Bus. Sci.*, vol. 4, no. 2, pp. 199–221, 2023, doi: 10.21608/ijaebs.2023.164929.1052.

[226]   A. A. Baeissa, "Mud-Brick High-Rise Buildings Architectural Linkages for Thermal Comfort in Hadhramout Valley, Yemen," *Int. Trans. J. Eng. Manag. Appl. Sci. Technol.*, 2014, [Online]. Available: https://tuengr.com/V05/0167.pdf

[227]   Dan, "Shibam Hadramawt, Yemen (photograph - licensed under CC BY-SA 2.0: https://creativecommons.org/licenses/by-sa/2.0/)," *Flickr*, 2008. https://www.flickr.com/photos/twiga_swala/2286377195/in/photostream/ (accessed Sep. 09, 2023).

[228]   CTBUH, "DC Towers," 2023. https://www.skyscrapercenter.com/complex/468 (accessed Mar. 27, 2023).

[229]   CTBUH, "DC Tower I." https://www.skyscrapercenter.com/building/dc-tower-i/1245 (accessed Mar. 27, 2023).

[230]   CTBUH, "DC Tower II." https://www.skyscrapercenter.com/building/dc-tower-ii/2858 (accessed Mar. 27, 2023).

[231]   J. Lin, H. Wan, and Y. Cui, "Analyzing the spatial factors related to the distributions of building heights in urban areas: A comparative case study in Guangzhou and Shenzhen," *Sustain. Cities Soc.*, 2020, doi: 10.1016/j.scs.2019.101854.

[232]   K. Al-Kodmany, "The Logic of Vertical Density: Tall Buildings in the 21st Century City High-Rise Buildings," *Orig. Publ. Int. J. High-Rise Build.*, 2012, [Online]. Available: https://www.academia.edu/download/58068059/2012_INtJourHigRiseBuil_TheLogicofVerticalDensity.pdf

[233]   J. Qu, Z. Wang, and P. Du, "Comparative Study on the Development Trends of High-rise Buildings Above 200 Meters in China, the USA and the UAE," *Int. J. High-Rise Build.*, 2021, doi: 10.21022/IJHRB.2021.10.1.63.

[234]   J. Bolleter, *Desert paradises: Surveying the landscapes of dubai's urban model*. 2019. doi: 10.4324/9781351129763.

[235]   Prasanaik, "Sheikh Zayed Road in 1990 (photograph - licensed under CC BY 3.0: https://creativecommons.org/licenses/by/3.0/)," *Wikipedia*, 2008.

https://en.wikipedia.org/wiki/File:Sheikh_Zayed_Road_in_1990.jpg (accessed Sep. 11, 2023).

[236] T. Reckmann, "Dubai Skyline mit Burj Khalifa (photograph - licensed under CC BY 2.0: https://creativecommons.org/licenses/by/2.0/deed.en)," *Wikimedia*, 2015. https://commons.wikimedia.org/wiki/File:Dubai_Skyline_mit_Burj_Khalifa_(18241030269).jpg (accessed Sep. 11, 2023).

[237] Tehran Times, "110 hectares of gardens destroyed in Tehran in 3 years," 2018. https://www.tehrantimes.com/news/422101/110-hectares-of-gardens-destroyed-in-Tehran-in-3-years (accessed Mar. 27, 2023).

[238] N. Hassan and S. Javed, "NIET GE Comparative life-cycle assessment of constant air volume, variable air volume and active climate beam systems for a Swedish office building," in *40th AIVC Conference*, 2019.

[239] S. Chen, K. Zhang, and S. Setunge, "Comparison of three HVAC systems in an office building from a life cycle perspective," 2011.

[240] S. Chen and G. Zhang, "Life cycle assessment of HVAC systems in office buildings," in *Proceedings of 2011 lnternational Conference on Renewable Energy and Energy Efficiency*, Pactoconvex Indonesia, 2011, pp. 1–7.

[241] M. J. Scholand and H. E. Dillon, *Life-Cycle Assessment of Energy and Environmental Impacts of LED Lighting Products - Part 2: LED Manufacturing and Performance*. U.S. Department of Energy - Energy Efficiency & Renewable Energy - Building Technologies Program, 2012. [Online]. Available: https://www.pnnl.gov/main/publications/external/technical_reports/PNNL-21443.pdf

[242] P. Principi and R. Fioretti, "A comparative life cycle assessment of luminaires for general lighting for the office - Compact fluorescent (CFL) vs Light Emitting Diode (LED) - A case study," *J. Clean. Prod.*, vol. 83, pp. 96–107, 2014, doi: 10.1016/j.jclepro.2014.07.031.

[243] Dubai Electricity & Water Authority (PJSC), "Renewable energy shaping the future of sustainability," 2020. https://www.dewa.gov.ae/en/about-us/media-publications/latest-news/2020/01/renewable-energy-shaping-the-future-of-sustainability (accessed Mar. 27, 2023).

[244] "Rhinoceros®," *Robert McNeel & Associates (TLM, Inc.)*, 2023. https://www.rhino3d.com/ (accessed Oct. 02, 2023).

[245] David Rutten at Robert McNeel & Associates, "Grasshopper® - ALGORITHMIC MODELING FOR RHINO," 2023. https://www.grasshopper3d.com/ (accessed Oct. 02, 2023).

[246] "ETABS®," *Computers and Structures, Inc.*, 2023. https://www.csiamerica.com/products/etabs (accessed Oct. 02, 2023).

[247] D. Rutten, "Evolutionary Principles applied to Problem Solving using Galapagos," *Grasshopper*, 2010. https://www.grasshopper3d.com/profiles/blogs/evolutionary-principles (accessed Oct. 02, 2023).

[248] "Ladybug," *Ladybug Tools® LLC*, 2023. https://www.ladybug.tools/ladybug.html (accessed Oct. 02, 2023).

[249] "Honeybee," *Ladybug Tools® LLC*, 2023. https://www.ladybug.tools/honeybee.html (accessed Oct. 02, 2023).

[250] "EnergyPlus™," *U.S. Department of Energy (DOE), National Renewable Energy Laboratory (NREL), and Collaborators*, 2023. https://energyplus.net/ (accessed Oct. 02, 2023).

[251] "OpenStudio®," *Alliance for Sustainable Energy, LLC (OpenStudio® is developed in collaboration by NREL, ANL, LBNL, ORNL, and PNNL)*, 2023. https://openstudio.net/ (accessed Oct. 02, 2023).

[252] "Climate Change World Weather File Generator for World-Wide Weather Data – CCWorldWeatherGen," *University of Southampton, Energy & Climate Change*, 2023. https://energy.soton.ac.uk/ccworldweathergen/ (accessed Oct. 02, 2023).

[253] Lawrence Berkeley National Laboratory (LBNL), "THERM - Two-Dimensional Building Heat-Transfer Modeling," 2023. https://windows.lbl.gov/software-tools (accessed Oct. 02, 2023).

[254] RFritz and AMcneil, "About Radiance," 2019. https://www.radiance-online.org/about (accessed Oct. 02, 2023).

[255] "DAYSIM," *daysim.ning.com*, 2023. https://github.com/MITSustainableDesignLab/Daysim (accessed Oct. 02, 2023).

[256] "Python™," *Python Software Foundation*, 2023. https://www.python.org/ (accessed Oct. 02, 2023).

[257] "Microsoft Excel," *Microsoft*, 2023. https://www.microsoft.com/en-us/microsoft-365/excel (accessed Oct. 02, 2023).

[258] "R (The R Project for Statistical Computing)," *The R Foundation*. https://www.r-project.org/ (accessed Oct. 02, 2023).

[259] CTBUH, "Dubai Full Building List." http://www.skyscrapercenter.com/compare-data/submit?type%5B%5D=building&status%5B%5D=COM&status%5B%5D=UC&status%5B%5D=UCT&status%5B%5D=STO&status%5B%5D=PRO&base_city=630&base_height_range=0&base_company=All&base_min_year=1900&base_max_year=9999&skip_compa (accessed Jun. 29, 2020).

[260] CTBUH, "CTBUH Tall Building Height Calculator."

heightcalculator.ctbuh.org (accessed Oct. 06, 2019).

[261] KONE, "KONE Quick Traffic." https://eritrea.kone.com/downloads-tools/ (accessed Oct. 06, 2019).

[262] S. Mirniazmandan, M. Alaghmandan, F. Barazande, and E. Rahimianzarif, "Mutual effect of geometric modifications and diagrid structure on structural optimization of tall buildings," *Archit. Sci. Rev.*, 2018, doi: 10.1080/00038628.2018.1477043.

[263] K. Jani and P. V Patel, "Analysis and Design of Diagrid Structural System for High Rise Steel Buildings," *Procedia Eng.*, vol. 51, pp. 92–100, 2013, doi: 10.1016/j.proeng.2013.01.015.

[264] . N. B. P., "DIAGRID STRUCTURAL SYSTEM: STRATEGIES TO REDUCE LATERAL FORCES ON HIGH-RISE BUILDINGS," *Int. J. Res. Eng. Technol.*, 2014, doi: 10.15623/ijret.2014.0304067.

[265] A. G. Shah and V. B. Patel, "A Parametric Study of Tall Structures with Diagrid," *IUP J. Struct. Eng.*, vol. 13, no. 1, 2020.

[266] F. Fu, *Design and Analysis of Tall and Complex Structures*. 2018. doi: 10.1016/c2015-0-06071-3.

[267] N. B. Panchal, V. Patel, and D. Pandya, "Optimum angle of diagrid structural system," *Int. J. Eng. Tech. Res.*, vol. 2, no. 6, pp. 150–157, 2014.

[268] C. Nayak, S. Walke, and S. Kokare, "Optimal Structural Design of Diagrid Structure for Tall Structure," in *ICRRM 2019 – System Reliability, Quality Control, Safety, Maintenance and Management*, 2020. doi: 10.1007/978-981-13-8507-0_39.

[269] American Concrete Institute, "Standards Adoption." https://www.concrete.org/publications/standards/standardsadoption.aspx (accessed May 08, 2020).

[270] International Code Council, *International Building Code (IBC) 2018*. International Code Council, 2018.

[271] I. C. C. (ICC), "Overview of the International Building Code® (IBC®)," 2018. https://www.iccsafe.org/products-and-services/i-codes/2018-i-codes/ibc/ (accessed Jun. 21, 2020).

[272] ACI Committee 318, *Building Code Requirements for Structural Concrete (ACI 318-19) and Commentary (ACI 318R-19) - SI Units*. American Concrete Institute (ACI), 2019. doi: 10.14359/51716937.

[273] American Society of Civil Engineers (ASCE), *Minimum Design Loads and Associated Criteria for Buildings and Other Structures*. American Society of Civil Engineers (ASCE), 2017. doi: https://doi.org/10.1061/9780784414248.

[274] Dubai Municipality, *Dubai wind code*. Dubai Municipality, 2013.

[275] British Standards Institution, *Eurocode 1: Actions on structures - Part 1-4: General actions - Wind actions (BS EN 1991-1-4:2005+A1:2010)*. British Standards Institution, 2010.

[276] Austrian Standards International, *ÖNORM B 1991-1-4:2019, Eurocode 1: Actions on structures — Part 1-4: General actions — Wind actions —National specifications concerning ÖNORM EN 1991-1-4 and national supplements*. 2019.

[277] Austrian Standards International, *ÖNORM B 1991-1-4:2023, Eurocode 1: Actions on structures — Part 1-4: General actions — Wind actions — National specifications concerning ÖNORM EN 1991-1-4 and national supplements*. 2023.

[278] Dubai Municipality, *Seismic Design Code for Dubai*. Dubai Municipality, 2013.

[279] United Arab Emirates Ministry of Interior Gen. Command of Civil Defense, *UAE Fire and Life Safety Code of Practice*, 2018 Editi. United Arab Emirates Ministry of Interior Gen. Command of Civil Defense, 2018. [Online]. Available: https://www.dcd.gov.ae/portal/eng/UAEFIRECODE_ENG_SEPTEMBER_2018.pdf

[280] International Code Council, "2018 International Building Code (IBC) - Sixth Version: Nov 2021," 2021. https://codes.iccsafe.org/content/IBC2018P6 (accessed Sep. 25, 2023).

[281] A. Ciroth, C. Di Noi, S. Syed Burhan, and M. Srocka, "LCA database creation: Current challenges and the way forward," *IjoLCAS*, 2019.

[282] M. Shaukat, "LCA in Saudi Arabia: a critical review," *Int. J. Life Cycle Assess.*, 2023, doi: 10.1007/s11367-023-02197-3.

[283] I. A. Amarasinghe, D. Soorige, and D. Geekiyanage, "Comparative study on Life Cycle Assessment of buildings in developed countries and Sri Lanka," *Built Environ. Proj. Asset Manag.*, 2020, doi: 10.1108/BEPAM-10-2019-0090.

[284] M. H. Alzard, H. El-hassan, and T. El-maaddawy, "Environmental and economic life cycle assessment of recycled aggregates concrete in the United Arab Emirates," *Sustain.*, 2021, doi: 10.3390/su131810348.

[285] A. Rauf, D. E. Attoye, and R. Crawford, "Embodied and Operational Energy of a Case Study Villa in UAE with Sensitivity Analysis," *Buildings*, 2022, doi: 10.3390/buildings12091469.

[286] Y. Saadah and B. AbuHijleh, "Decreasing CO2 emissions and embodied energy during the construction phase using sustainable building materials," *Int. J. Sustain. Build. Technol. Urban Dev.*, vol. 1, no. 2, pp. 115–120, 2010.

[287] Z. S. Zomorodian and M. Tahsildoost, "Energy and carbon analysis of double skin façades in the hot and dry climate," *J. Clean. Prod.*, 2018, doi:

10.1016/j.jclepro.2018.06.178.

[288] A. Shahabian, A. Fadai, and T. Peruzzi, "Future of Life-Cycle Assessment in a Smart and/or Sustainable World," in *Interdisciplinary Approaches to Public Policy and Sustainability*, R. Das and N. Mandal, Eds., Pennsylvania, USA: IGI Global, 2020, pp. 177–207. doi: 10.4018/978-1-7998-0315-7.ch009.

[289] S. A. K. A. Uda, R. Waluyo, W. Nuswantoro, V. H. Puspasari, and A. B. P. Gawei, "Embodied energy consumption in flexible pavement materials: A case study in Yogyakarta, Indonesia," in *AIP Conference Proceedings*, 2023. doi: 10.1063/5.0111156.

[290] N. Atmaca, A. Atmaca, and A. İ. Özçetin, "The impacts of restoration and reconstruction of a heritage building on life cycle energy consumption and related carbon dioxide emissions," *Energy Build.*, 2021, doi: 10.1016/j.enbuild.2021.111507.

[291] P. Muñoz, D. Dominguez, R. Sánchez-Vázquez, V. Letelier, and O. Gencel, "Building decarbonization by means of ancient techniques. Assessment of environmental impact, energy performance and mechanical safety," *J. Build. Eng.*, 2023, doi: 10.1016/j.jobe.2023.106896.

[292] M. S. M. Almulhim, D. V. L. Hunt, and C. D. F. Rogers, "A resilience and environmentally sustainable assessment framework (RESAF) for domestic building materials in Saudi Arabia," *Sustain.*, 2020, doi: 10.3390/SU12083092.

[293] CTBUH, "Philip Oldfield - City Committee Member," 2023. https://www.ctbuh.org/people-profile/philip-oldfield (accessed Apr. 09, 2023).

[294] The British University in Dubai, "Faculty of Engineering and IT - Professor Bassam Abu-Hijleh," 2023. https://www.buid.ac.ae/programmes/academics-faculty-of-engineering-it/ (accessed Apr. 09, 2023).

[295] The Conversation, "Britain's electricity since 2010: wind surges to second place, coal collapses and fossil fuel use nearly halves," 2023. https://theconversation.com/britains-electricity-since-2010-wind-surges-to-second-place-coal-collapses-and-fossil-fuel-use-nearly-halves-129346 (accessed Mar. 27, 2023).

[296] Energy Dubai, "Analysis of UAE Energy mix targets for 2030," 2014. https://www.energydubai.com/uae-energy-mix-targets-for-2030/ (accessed Mar. 27, 2023).

[297] G. Hammond and C. Jones, *A BSRIA guide - Embodied Carbon - The Inventory of Carbon and Energy (ICE)*. University of Bath and BSRIA, 2011.

[298] E. Miebach, "Renewables deliver more electricity for the first time," *Deutsche Welle*, 2019. https://www.dw.com/en/german-renewables-deliver-more-electricity-than-coal-and-nuclear-power-for-the-first-time/a-49606644 (accessed Mar. 27, 2023).

[299] oekobaudat.de, "Process Data set: Beton der Druckfestigkeitsklasse C 45/55,"

2018.
https://oekobaudat.de/OEKOBAU.DAT/datasetdetail/process.xhtml?uuid=a366
2e98-9dc9-412f-9603-
47f653f3db7f&version=00.03.000&stock=OBD_2020_II&lang=en (accessed
Mar. 28, 2023).

[300] Golden Readymix (GRM), "EPD for concrete produced at Golden Readymix
LLC concrete plant located in Dubai, United Arab Emirates," 2017. [Online].
Available: https://www.nrmca.org/wp-
content/uploads/2019/10/GoldenReadymixEPD.pdf

[301] CEN (European Committee For Standardization), *EN 15804:2012+A1:2013
Sustainability of Construction works - Environmental Product declarations -
Core rules for the product category of construction Products*. 2014.

[302] Building Research Establishment (BRE), "EPD on Carbon Steel Reinforcing
Bar," 2015. [Online]. Available:
https://www.greenbooklive.com/pdfdocs/en15804epd/BREGENEPD000038.pd
f

[303] L. S. M. de Silva, Diogo Aparecido Lopes Nunes, Andréa Oliveira Piekarski,
Cassiano Moro Silva Moris, Virgínia Aparecida da Souza and T. O. Rodrigues,
"Why using different Life Cycle Assessment software tools can generate
different results for the same product system? A cause–effect analysis of the
problem," *Sustain. Prod. Consum.*, vol. 20, pp. 304–315, 2019, [Online].
Available:
https://www.sciencedirect.com/science/article/pii/S2352550919301733

[304] Everything-about-concrete.com, "Concrete mixing ratios," 2023.
https://www.everything-about-concrete.com/concrete-mixing-ratios.html
(accessed Apr. 09, 2023).

[305] P. W. Gerbens-Leenes, A. Y. Hoekstra, and R. Bosman, "The blue and grey
water footprint of construction materials: Steel, cement and glass," *Water
Resour. Ind.*, 2018, doi: 10.1016/j.wri.2017.11.002.

[306] T. Zimmermann and D. Lehký, "Fracture parameters of concrete C40/50 and
C50/60 determined by experimental testing and numerical simulation via
inverse analysis," *Int. J. Fract.*, 2015, doi: 10.1007/s10704-015-9998-0.

[307] International Water Summit, "Energy Efficient Desalination; Meeting the
GCC's water needs in an environmentally sustainable way,"
internationalwatersummit.com, 2018.

[308] Ladybug Tools LLC, "Is Ladybug Tools validated?," 2023.
https://www.ladybug.tools/about.html#7 (accessed Jan. 18, 2023).

[309] A. Mahdavi and H. Shirdel, "Iterative building optimization via sequential
local optimization operations on distinct attribute clusters of design variants,"
in *Building Simulation Conference Proceedings*, 2019. doi:
10.26868/25222708.2019.210116.

[310] M. Vellei *et al.*, "Documenting occupant models for building performance simulation: a state-of-the-art," *Journal of Building Performance Simulation*. 2022. doi: 10.1080/19401493.2022.2061050.

[311] M. Rashani and A. Mahdavi, "Energy retrofit alternatives for three apartment buildings in Kosovo," *Pollack Period.*, 2023, doi: 10.1556/606.2022.00745.

[312] P. G. Ellis and P. A. Torcellini, "Simulating tall buildings using energyplus," in *IBPSA 2005 - International Building Performance Simulation Association 2005*, 2005.

[313] C. Mackey, "Energy modeling of a cylindrical tall building with diagrid structural thermal mass," 2016. https://discourse.ladybug.tools/t/energy-modeling-of-a-cylindrical-tall-building-with-diagrid-structural-thermal-mass/1218/3 (accessed Feb. 08, 2023).

[314] C. Mackey, "Ladybug 0.0.65 & Honeybee 0.0.62 Release," 2017. https://discourse.ladybug.tools/t/ladybug-0-0-65-honeybee-0-0-62-release/1990 (accessed Feb. 08, 2023).

[315] ASHRAE, *ASHRAE handbook: Fundamentals*. American Society of Heating, Refrigerating and Air-Conditioning Engineers (ASHRAE), 2001. [Online]. Available: https://sovathrothsama.files.wordpress.com/2016/03/ashrae-hvac-2001-fundamentals-handbook.pdf

[316] ASHRAE, *ASHRAE Handbook Fundamentals*. American Society of Heating, Refrigerating and Air-Conditioning Engineers, 2017.

[317] Lawrence Berkeley Nation Laboratory, *THERM 7 / WINDOW 7 NFRC Simulation Manual*, no. July. National Fenestration Rating Council, Inc., 2017. [Online]. Available: https://windows.lbl.gov/sites/default/files/Downloads/NFRCSim7-July2017.pdf

[318] C. Mackey, "Any suggestions for 3D U-value calculation?," 2017. https://discourse.ladybug.tools/t/any-suggestions-for-3d-u-value-calculation/2119/2?u=aryanshahabian (accessed Apr. 25, 2020).

[319] C. Mackey, "2D Vs 3D Thermal Bridging Modelling," 2018. https://discourse.ladybug.tools/t/2d-vs-3d-thermal-bridging-modelling/3363/6?u=aryanshahabian (accessed Apr. 24, 2020).

[320] C. Klee and A. Love, "Thermal performance of facades," 2012. https://www.payette.com/wp-content/uploads/archive/uploads/research_project/1416244116-0d52d646c2431daf2/2012_AIA UPJOHN GRANT_Thermal Performance of Facades_Payette Final Report.pdf (accessed Apr. 24, 2020).

[321] International Organization for Standardization, *ISO 15099:2003(en) Thermal performance of windows, doors and shading devices — Detailed calculations*. International Organization for Standardization, 2003. [Online]. Available: https://www.iso.org/obp/ui/#iso:std:iso:15099:ed-1:v1:en

[322] BBSR, "Nutzungsdauern von Bauteilen für Lebenszyklusanalysen nach Bewertungssystem Nachhaltiges Bauen (BNB) (English: Service lives of building components for life cycle assessments according to the Sustainable Building Assessment System)," *Bundesinstitut für Bau-, Stadt- und Raumforschung (BBSR) (English: The Federal Institute for Research on Building, Urban Affairs and Spatial Developmen)*, 2011. https://www.nachhaltigesbauen.de/fileadmin/pdf/baustoff_gebauededaten/BNB_Nutzungsdauern_von_Bauteilen__2011-11-03.pdf (accessed Sep. 23, 2022).

[323] J. Sierra-Pérez, J. Boschmonart-Rives, and X. Gabarrell, "Environmental assessment of façade-building systems and thermal insulation materials for different climatic conditions," *J. Clean. Prod.*, 2016, doi: 10.1016/j.jclepro.2015.11.090.

[324] L. Aditya *et al.*, "A review on insulation materials for energy conservation in buildings," *Renewable and Sustainable Energy Reviews*. 2017. doi: 10.1016/j.rser.2017.02.034.

[325] Morrison Hershfield Limited, *Building Envelope Thermal Bridging Guide v1.6*, Version 1. Vancouver, BC: BC Hydro Power Smart, 2021. [Online]. Available: https://www.bchydro.com/content/dam/BCHydro/customer-portal/documents/power-smart/builders-developers/building-envelope-thermal-bridging-guide-v1-6.pdf

[326] J. Lstiburek, "Moisture control for buildings," *ASHRAE Journal*. American Society of Heating, Refrigerating and Air-Conditioning Engineers, 2002.

[327] A. Nash, *Permeability of Common Building Material to Water Vapor*. University of Alaska Fairbanks, Cooperative Extension Service, 2017.

[328] X. Ma, R. Tu, X. Cheng, S. Zhu, J. Ma, and T. Fang, "Experimental study of thermal behavior of insulation material rigid polyurethane in parallel, symmetric, and adjacent building façade constructions," *Polymers (Basel).*, 2018, doi: 10.3390/polym10101104.

[329] M. Holladay, "Is closed-cell spray foam fire resistant or does it spread fire?," *Fire Barrier - Green Building Advisor*, 2012. https://www.greenbuildingadvisor.com/question/is-closed-cell-spray-foam-fire-resistant-or-does-it-spread-fire (accessed May 07, 2020).

[330] J. Le Dréau, R. L. Jensen, and K. Kolding, "Thermal behaviour of a gypsum fibre board associated with rigid polyurethane foam under standard fire conditions," in *Energy Procedia*, 2015. doi: 10.1016/j.egypro.2015.11.615.

[331] Certainteed, "What is fire rated gypsum?," 2023. https://www.certainteed.com/drywall/what-fire-rated-gypsum-board/ (accessed Aug. 14, 2023).

[332] M. A. Sultan, "Fire resistance of wood stud wall assemblies," *Fire Mater.*, 2021, doi: 10.1002/fam.2918.

[333] Dubai Central Laboratory Department, "Specific Rules for Type 1 Certification

of Glazed Glass as per Clause {501.01B] of the Al Sa'fat Dubai Green Building Evaluation System," 2019. https://www.dm.gov.ae/en/Business/DubaiCentralLaboratory/ProductCertificat ionServices/Documents/Type1 Product Certification/DM-DCLD-RD-DP32-5103 %28IC%29.pdf (accessed Apr. 25, 2020).

[334] B. Anderson, *Conventions for U-value calculations 2006 edition*. Watford, UK: BRE, 2006. [Online]. Available: www.brepress.com

[335] The Official Website of the City of New York, "Commercial Districts - NYC Department of City Planning," 2023. https://www.nyc.gov/site/planning/zoning/districts-tools/commercial-districts-c1-c8.page (accessed Mar. 05, 2023).

[336] JALOXA, "BS8206-2 Glazing Calculator for Radiance," 2022. http://www.jaloxa.eu/resources/radiance/bs8206_glazing.shtml (accessed Feb. 14, 2023).

[337] British Standards Institution, *Lighting for buildings –Part 2: Code of practice for daylighting*. 2008.

[338] A. Jacobs, *Radiance Cookbook*, Revision: axel AT jaloxa DOT eu, 2014. [Online]. Available: http://www.jaloxa.eu/resources/radiance/documentation/docs/radiance_cookbo ok.pdf

[339] M. Dahlhausen, "What is the most efficient (or most common) HVAC system for tall office building in tropical desert climate?," 2019. https://unmethours.com/question/30973/what-is-the-most-efficient-or-most-common-hvac-system-for-tall-office-building-in-tropical-desert-climate/ (accessed Feb. 14, 2023).

[340] C. Mackey, "Fan Coil Units + DOAS vs VAV w/ Reheat," 2019. https://discourse.ladybug.tools/t/fan-coil-units-doas-vs-vav-w-reheat/4871/2?u=aryanshahabian (accessed Sep. 19, 2023).

[341] S. Chen and G. Zhang, "Comparison of Three HVAC systems in Commercial Buildings from a Life Cycle Perspective," *2011 Int. Conf. Futur. Manag. Sci. Eng. (Icfmse 2011), Vol 1*, 2011.

[342] Dubai Municipality, "Electric heaters are frequently used with winter's low temperatures," *Twitter*, 2022. https://twitter.com/DMunicipality/status/1487727537694380037?s=20 (accessed Sep. 19, 2023).

[343] EnergyPlus, "Weather Data," 2023. https://energyplus.net/weather (accessed Mar. 07, 2023).

[344] "Meteonorm Software." https://meteonorm.com/ (accessed Sep. 30, 2023).

[345] M. F. Jentsch, P. A. B. James, L. Bourikas, and A. B. S. Bahaj, "Transforming existing weather data for worldwide locations to enable energy and building

performance simulation under future climates," *Renew. Energy*, 2013, doi: 10.1016/j.renene.2012.12.049.

[346] IPCC, "Data Distribution Centre - Intergovernmental Panel on Climate Change." https://www.ipcc-data.org/sim/gcm_clim/SRES_TAR/hadcm3_download.html (accessed Oct. 01, 2023).

[347] "WeatherShift^TM." http://www.weather-shift.com/ (accessed Oct. 01, 2023).

[348] "Where to find epw files associated with the future climate scenarios?" https://unmethours.com/question/35064/where-to-find-epw-files-associated-with-the-future-climate-scenarios/ (accessed Jun. 20, 2020).

[349] "2013 ASHRAE Handbook - Fundamentals (SI)," no. 1, p. 2013, 2013.

[350] T. Hoyt, E. Arens, and H. Zhang, "Extending air temperature setpoints: Simulated energy savings and design considerations for new and retrofit buildings," *Build. Environ.*, 2015, doi: 10.1016/j.buildenv.2014.09.010.

[351] C. F. Reinhart and O. Walkenhorst, "Validation of dynamic RADIANCE-based daylight simulations for a test office with external blinds," *Energy Build.*, 2001, doi: 10.1016/S0378-7788(01)00058-5.

[352] L. Akimov, G. De Michele, U. Filippi Oberegger, V. Badenko, and A. G. Mainini, "Evaluation of EN15193-1 on energy requirements for artificial lighting against Radiance-based DAYSIM," *J. Build. Eng.*, 2021, doi: 10.1016/j.jobe.2021.102698.

[353] L. Pompei, L. Blaso, S. Fumagalli, and F. Bisegna, "The impact of key parameters on the energy requirements for artificial lighting in Italian buildings based on standard EN 15193-1:2017," *Energy Build.*, 2022, doi: 10.1016/j.enbuild.2022.112025.

[354] schorsch.com, "Trans Material Types," *Rayfront 1.0 User Manual*. https://www.schorsch.com/en/software/rayfront/manual/transdef.html (accessed Dec. 30, 2022).

[355] A. Shahabian, "Trans Material components (problem with colour)," *discourse.ladybug.tools*, 2019. https://discourse.ladybug.tools/t/trans-material-components-problem-with-colour/4977 (accessed Dec. 30, 2022).

[356] J. A. Jakubiec, "Spectral Materials Database," *Design for Climate & Comfort Lab - University of Toronto*, 2019. http://spectraldb.com/materials/1423 (accessed Jun. 01, 2019).

[357] P. Maleetipwan-Mattsson and T. Laike, "Optimal office lighting use: A swedish case study," *Facilities*, 2015, doi: 10.1108/F-01-2014-0004.

[358] C. Kofod, "Solid State Lighting Annex: Task 7: Smart Lighting – New Features Impacting Energy Consumption; First Status Report, Energy Efficient End-Use Equipment (4E)," 2016. [Online]. Available: https://www.iea-

4e.org/wp-content/uploads/publications/2022/11/SSL-Annex-Task-7-Smart-Lighting-–-New-Features-Impacting-Energy-Consumption_second-report_final.pdf

[359] M. Deru and P. Torcellini, "Source Energy and Emission Factors for Energy Use in Buildings (Revised; No. NREL/TP-550-38617)," Golden, CO (United States), 2018.

[360] I. Ustadi, T. Mezher, and M. R. M. Abu-Zahra, "The Effect of the Carbon Capture and Storage (CCS) Technology Deployment on the Natural Gas Market in the United Arab Emirates," in *Energy Procedia*, 2017. doi: 10.1016/j.egypro.2017.03.1773.

[361] A. Hindley and J. Bishop, "The GCC Power & Desalination 2012 Report," in *An in-depth Outlook of the GCC Power& Desalination Market up to 2020*, MEED Insight, 2012.

[362] The UAE Government Portal, "Dubai Clean Energy Strategy," 2019. https://u.ae/en/more/uae-future/2030-2117 (accessed Mar. 10, 2023).

[363] IPCC, "Average life-cycle carbon dioxide-equivalent emissions for different electricity generators," 2018. https://www.world-nuclear.org/nuclear-essentials/how-can-nuclear-combat-climate-change.aspx (accessed Mar. 31, 2023).

[364] J. A. Nelder and R. W. Wedderburn, "Generalized linear models," *J. R. Stat. Soc. Ser. A*, vol. 135, no. 3, pp. 370–384, 1972.

[365] RDocumentation, "glm: Fitting Generalized Linear Models," 2023. https://www.rdocumentation.org/packages/stats/versions/3.6.2/topics/glm (accessed Mar. 27, 2023).

[366] L. Wang, Q. Li, M. Sun, and G. Wang, "Robust optimisation scheduling of CCHP systems with multi-energy based on minimax regret criterion," *IET Gener. Transm. Distrib.*, 2016, doi: 10.1049/iet-gtd.2015.1344.

[367] W. C. Ling, V. Andiappan, Y. K. Wan, and D. K. S. Ng, "A systematic decision analysis approach to design biomass combined heat and power systems," *Chem. Eng. Res. Des.*, 2018, doi: 10.1016/j.cherd.2018.07.016.

[368] russellpierce (https://stats.stackexchange.com/users/196/russellpierce), "Interpreting summary function for lm model in R," *Cross Validated*, 2013. https://stats.stackexchange.com/questions/49939/interpreting-summary-function-for-lm-model-in-r/49941#49941 (accessed Mar. 27, 2023).

[369] M. L. Pannier, P. Schalbart, and B. Peuportier, "Comprehensive assessment of sensitivity analysis methods for the identification of influential factors in building life cycle assessment," *J. Clean. Prod.*, 2018, doi: 10.1016/j.jclepro.2018.07.070.

[370] European Commission, "2050 long-term strategy," *Climate strategies & targets*, 2023. https://climate.ec.europa.eu/eu-action/climate-strategies-

targets/2050-long-term-strategy_en (accessed Aug. 29, 2023).

[371] G. Amanatidis, *European policies on climate and energy towards 2020, 2030 and 2050*. European Parliament, 2019. [Online]. Available: https://www.europarl.europa.eu/RegData/etudes/BRIE/2019/631047/IPOL_BRI(2019)631047_EN.pdf

[372] A. Batrawy, "Saudi Arabia pledges 2060 target of net-zero emissions," *apnews.com*, 2021. https://apnews.com/article/climate-business-middle-east-dubai-united-arab-emirates-1335e47922965f7db43f5e7057cf7265 (accessed Aug. 28, 2023).

[373] J. Gnana and S. Pradhan, "Dubai plans to slash emissions by 30% by 2030," *spglobal.com*, 2022.

[374] X. Zhao and M. A. Haojia, "Structural System Embodied Carbon Analysis for Super Tall Buildings," in *Procedia Engineering*, 2015. doi: 10.1016/j.proeng.2015.08.420.

[375] Y. S. Cho, J. H. Kim, S. U. Hong, and Y. Kim, "LCA application in the optimum design of high rise steel structures," *Renewable and Sustainable Energy Reviews*. 2012. doi: 10.1016/j.rser.2012.01.076.

[376] D. F. Polit and C. T. Beck, "Generalization in quantitative and qualitative research: Myths and strategies," *Int. J. Nurs. Stud.*, 2010, doi: 10.1016/j.ijnurstu.2010.06.004.

[377] E. G. Guba, "Toward a Methodology of Naturalistic Inquiry in Educational Evaluation. CSE Monograph Series in Evaluation, 8.," *ERIC*, 1978.

[378] T. Bruce-Hyrkäs, P. Pasanen, and R. Castro, "Overview of Whole Building Life-Cycle Assessment for Green Building Certification and Ecodesign through Industry Surveys and Interviews," in *Procedia CIRP*, 2018. doi: 10.1016/j.procir.2017.11.127.

.

List of Tables

List of Figures

Curriculum Vitae (CV)

Aryan SHAHABIAN

Doctoral Candidate in Architectural Sciences and Technology (2018-present), Faculty of Architecture and Planning, TU Wien (Vienna University of Technology), Vienna, Austria

b. 1980 , he/him
Extended CV: **http://aryan-sh.blogspot.com/p/about-me.html**
Email: **aryan_shahabian@yahoo.com**

Professional Activities

- **2018-present| Member of Editorial Advisory Board / Peer Reviewer** at multiple international scientific journals, books, and conferences in architecture, urban planning, engineering, and design, including:
  - Journal of Urban Planning and Development, **American Society of Civil Engineers: ASCE**, (USA, Since Dec 2022);
  - Journal of Construction Engineering and Management (**ASCE**, USA, Since Nov 2022);
  - Annual and seasonal conferences run by the **Association of Collegiate Schools of Architecture: ACSA** (USA, Since Oct 2022) in partnership with the **American Institute of Architects (AIA)**, University of Massachusetts Amherst, and the University of British Columbia, Canada;
  - International Journal of Urban Planning and Smart Cities (IJUPSC, Since 2019);
  - International Journal of Digital Innovation in the Built Environment (IJDIBE, Since 2021);
  - Journal of Engineering and Applied Science (JEAS, Since 2021);
  - Book chapters published by IGI Global (USA, Since 2018);
  - More info available on ORCID
- **2003-present|** Pasargad Consulting Architects & Planners, (2003-) Partner and Founding Member, (2007-) Member of Board of Directors, and Head of Architecture Section
- 2022-2023| TEDxTUWien, Co-Organizer (co-curator and designer), TEDx Talks at TU Wien
- 2018-2021| Vienna young Scientists Symposium (VSS) organization team member, Vienna
- 2011| Coop Himmelb(l)au, Architecture Team, Vienna
- 2009-2018| SOLARCHVISION, Project Partner
- 2003-2005| Fluid Motion Architects, Design Associate
- 1998-2002| Shahabian & Associates, Architectural Design Assistant

Education & Qualification

- 2019| Extended Study on Innovation, Innovation Incubation Center (i²c), TU Wien, Vienna
- 2011| **MSc in Urban Strategies**, Institute of Architecture, University of Applied Arts Vienna (die Angewandte)
- 2007| **MSc in Architectural Engineering** (Nationally Awarded Diploma Project), Iran University of Science & Technology (IUST)
- 1998| High school diploma, Mathematics & Physics, Allameh Helli high school (affiliated to National Organization for Development of Exceptional Talents), Tehran

Publications, Research & Educational Activities

- 2020| The book chapter "Future of Life-Cycle Assessment in a Smart and/or Sustainable World" in the book "Interdisciplinary Approaches to Public Policy and Sustainability", with Prof. Alireza Fadai, and Thomas Peruzzi, IGI Global, USA, ISBN:

299

9781799803157, DOI: 10.4018/978-1-7998-0315-7.ch009

- 2019| The paper "Impact of Exoskeletons on Life-Cycle Primary Energy Consumption and CO_2e Emissions of Tall Buildings" in the book "Innovationsinkubator Industriebau: Industrial Building as Innovation Incubator. Praxisreport 2019", Editors: Achammer, Christoph M.; Kovacic, Iva, TU Wien, Vienna, ISBN: 978-3-200-06660-1, DOI: 10.34726/969x-sr53

- 2019| The paper "Intelligent Parametric BIM Solution and Optimizer for Diagrid High-Rise Structures" (with Prof. Fadai). In Proceedings of Vienna young Scientists Symposium VSS2019. TU Wien, Vienna

- 2018| The paper "Internet of Things and the Future of Life-Cycle Assessment in Smart World". In Proceedings of Vienna young Scientists Symposium VSS2018. TU Wien, Vienna

- 2017| "An algorithm generates numerous interlocking objects"(developed by Aryan Shahabian). Architecture and design news published in 5 languages worldwide: Chinese, English, French, Persian, and Spanish.

- 2015| The paper: "Integration of solar-climatic vision and structural design in architecture of tall buildings", CISBAT-2015, Conference on "Future Buildings and Districts; Sustainability from Nano to Urban Scale" at EPFL, Lausanne, Switzerland

- 2014| The paper "Towards the parametric integration of climatic elements into structures", Architecture & Construction Magazine, with Mojtaba Samimi

- 2011| Coop Himmelb(l)au, Sustainable Architecture Research Team, Vienna

- 2010| The paper of "A Strategy to Regulate & Design Urban Tissues Façades by Applying Digital Parametric Scripts Covering Flexible 3D Geometric Structures", the Congress for Building Façades & the Image of the City, Tehran Municipality

- 2009| The paper of "The relationship between Historical art & architecture & conceptual & minimalist art", Abadi Architecture Quarterly Journal

- 2009| The paper of "deDeformation", Abadi Architecture Quarterly Journal

- 2008| Selected & honored Diploma Project (Master of Architecture), Architecture & Planning Faculty, IUST

- 2005| Interview with Bahram Shirdel, Architecture Students' Scientific Association, Architecture & Planning Faculty, IUST

- 2003-2005| Secretary of Architecture Students' Scientific Association, Architecture & Planning Faculty, IUST

- 2003| Selected published work in International Competition of Design "Kooshk", Architecture & Urbanism Magazine, Tehran

- 2003| Founding & teaching the Computer Aided Design Workshop. Architecture & Planning Faculty, IUST

Lectures & Teaching Experiences

- 2020| Group discussion on the "Definition of PhD by Design", at the online conference "Mapping, reflecting, developing PhD by Design" (Sep. 27, 2020), organized by the Institute of Architecture and Planning, University of Liechtenstein

- 2019| Lecture "Impact of Topological Relationship between Outer Primary Structural Elements and Curtain Walls on Life-Cycle Efficiency of Tall Buildings in Hot Climates", PhD Day of the 24th Industrial Building Seminar, Institute of Interdisciplinary Construction Process Management, Faculty of Civil Engineering, TU Wien, Vienna

- 2018| Lecture "Internet of Things and the Future of Life-Cycle Assessment in Smart World", Vienna young Scientists Symposium, TU Wien, Vienna

- 2018| Lecture "Doctoral Research Progress, and Higher Education in Austria vs Iran" for doctoral candidates of Urban Planning and Architecture, IAU, Kish International Branch

- 2017| Lecture "Algorithmic Thinking for Architects and Designers", University of Applied Arts Vienna

- 2016| Lecture "Sustainability, Comfort and Energy Considerations in Design of Building Façade and Urban Tissue", Conference on Building Façade and Urbanscape, 22nd District, Tehran Municipality

- 2015| Panel discussion "Nature of Architectural Thought" with N. Saboori, Gh. Cont and Sh. Yaghini. Iranian Artists Forum, Tehran

- 2015| Lecture "Save as Structure 3", University of Applied Arts Vienna, with M Samimi

- 2015| Lecture "Magic in Art & Architecture", University of Applied Arts Vienna

- 2014| Lecture "Save as Structure 2", University of Applied Arts Vienna

- 2011| Intensive Workshop on Applying Digital Parametric Tools in Urban Strategies, Institute of Architecture, University of Applied Arts Vienna

- 2009| Founding & teaching the Digital Architecture Workshop, Syndicate of Consulting Architects & Planners of Iran

- 2008| Teaching the module "Architectural Design 3", Azad University, Roodehen, Iran

- 2006-2008| Teaching Assistant, Architectural Design in B.A. & M.A. levels, Architecture & Planning Faculty, IUST

301